

THESE POUR OBTENIR LE GRADE DE DOCTEUR DE
L'ÉCOLE NATIONALE SUPERIEURE DE CHIMIE DE MONTPELLIER

En Ingénierie Biomoléculaire

École doctorale Sciences Chimiques Balard

Unité de recherche Institut des biomolécules Max Mousseron

Bioreductive Activated Prodrugs to Target Tumour Hypoxia

Présentée par **Emilie Anduran**

le 2 Novembre 2022

Sous la direction de **Pr. Jean-Yves WINUM, Pr. Philippe Lambin**
et **Dr. Ludwig Dubois**

Devant le jury composé de

Prof. Nicolaas SCHAPER, Professeur, CARIM, Maastricht, Pays-Bas	Président du jury
Prof. Sébastien CLEMENT, Professeur, ICGM, Montpellier, France	Rapporteur
Prof. Guido HAENEN, Professeur, NUTRIM/CARIM, Maastricht, Pays-Bas	Rapporteur
Prof. Sébastien THIBAUDEAU, Professeur, IC2MP, Poitiers, France	Rapporteur
Prof. Raivis ŽALUBOVSKIS, Professeur, IOS, Riga, Lettonie	Rapporteur
Dr. Ludwig DUBOIS, Professeur associé, GROW, Maastricht, Pays-Bas	Co-encadrant de thèse
Prof. Philippe LAMBIN, Professeur, GROW, Maastricht, Pays-Bas	Co-directeur de thèse
Prof. Jean-Yves WINUM, Professeur, IBMM, Montpellier, France	Co-directeur de thèse



UNIVERSITÉ DE
MONTPELLIER

BIOREDUCTIVE ACTIVATED PRODRUGS TO TARGET TUMOUR HYPOXIA

© 2022 Emilie Anduran

Cover design: the University of Maastricht

Print by: Imprimerie Castay – www.imprimerie-castay.com

ISBN: 979-10-415-0322-3

BIOREDUCTIVE ACTIVATED PRODRUGS TO TARGET TUMOUR HYPOXIA

DISSERTATION

to obtain the degree of Doctor at Maastricht University,
on the authority of the Rector Magnificus, Prof. dr. Pamela Habıboviç and
to obtain the degree of Docteur de l'Ecole Nationale Supérieure de Chimie de Montpellier
on the authority of Le Directeur Pascal Dumy
in accordance with the decision of the Board of Deans,
to be defended in public on Wednesday November, the 2nd 2022, at 10:00 hours

by

Emilie Anduran

Supervisors:

Prof. dr. P. Lambin

Prof. dr. J.-Y. Winum

Co-supervisors:

Dr. L. J. Dubois

Assessment Committee:

Prof. dr. T. Hackeng (chair)

Prof. dr. S. Clément (University of Montpellier, Montpellier, France)

Prof. dr. G. Haenen

Prof. dr. S. Thibaudeau (University of Poitiers, Poitiers, France)

Prof. dr. R. Žalubovskis (Technical university of Riga, Riga, Latvia)

TABLE OF CONTENTS

Chapter 1.	General Introduction	9
Chapter 2.	Hypoxia-activated prodrug derivatives of anti-cancer drugs: a patent review 2006 – 2021	27
Chapter3.	Hypoxia-activated prodrug derivatives of carbonic anhydrase inhibitors in benzenesulfonamide series: synthesis and biological evaluation	45
Chapter 4.	Design, synthesis and biological evaluations of toll-like receptor 7 & 8 agonist HAP (Imiquimod / Resiquimod) and Bruton’s tyrosine kinase inhibitor (ibrutinib) HAPs for Immunotherapy	65
Chapter 5.	Design and synthesis of new hypoxia-activated prodrug antibody-conjugated derivative of the toll-like receptor agonist Resiquimod: a proof-of-concept study to increase tumour uptake	91
Chapter 6.	General Discussion and future perspectives	115
	Summary	125
	Résumé	129
	Impact paragraph	133
	Acknowledgements	137
	Curriculum Vitae	141
	List of publications	143

List of abbreviations:

ADC	antibody-drug conjugate
AE	anion exchanger
APC	antigen-presenting cell
ARNT	aryl hydrocarbon receptor nuclear translocator
BNC	bicarbonate transporter
BTK	Bruton's tyrosine kinase
CA	carbonic anhydrase
CDI	carbonyl diimidazole
DAMP	damage-associated molecular pattern
DAR	drug-to-antibody ratio
DCM	dichloromethane
DIC	diisopropylcarbodiimide
DIEA	diisopropylethylamine
DMA	dimethylacetamide
DMAP	dimethylaminopyridine
DMEM	Dulbecco's Modified Eagle Medium
DMSO	dimethyl formamide
DNA	deoxyribonucleic acid
DSC	disuccinimidyl carbonate
EDC	1-Ethyl-3-(3-dimethylaminopropyl)carbodiimide
EGFR	endothelial growth factor receptor
ESI	electrospray ionization
FDA	food and drug administration
HAP	hypoxia-activated prodrug
HATU	hexafluorophosphate azabenzotriazole tetramethyl uronium
HER2	human epidermal growth factor receptor 2
HIF 1 α and 1 β	hypoxia-inducible factor 1 α and 1 β
HOBt	1-Hydroxybenzotriazole hydrate
HRMS	high resolution mass spectrometry
HPLC	high performance liquid chromatography
HRE	hypoxia-responsive element
LC-MS	liquid chromatography-mass spectroscopy
MALDI	matrix-assisted laser desorption/ionization
MMC	mitomycin C
MsCl	mesyl chloride
M-W	micro-wave
NMR	nuclear magnetic resonance
PAMP	pathogen-associated molecular pattern
PHD	prolyl hydroxylase
PNPC	<i>p</i> -nitrophenyl chloroformate
RPMI	Roswell Park Memorial Institute
rt	room temperature

TFA	trifluoroacetic acid
THF	tetrahydrofuran
TLC	thin layer chromatography
TLR	toll like receptor
TOF	time of flight
TPG	triphosgen
Ub	ubiquitin ligase
UPLC	ultra performance liquid chromatography
VHL	Von Hippel-Lindau protein

Chapter 1

General Introduction & Thesis Outline

CANCER

Nowadays, cancer is one of the main causes of mortality worldwide, in 2020 it was the second cause of death after ischemic heart disease with 10 million death cases and could continue rising with an estimation of 13.2 million deaths in 2030.¹ According to the World Health Organization, in 2020 approximately 10 million cancer-related deaths were reported, nearly 1 death in 6 all over the world. The most common types of cancer were the breast (2.26 million cases), lung (2.21 million cases), colon and rectal (1.93 million cases), prostate (1.41 million cases), skin (non-melanoma, 1.20 million cases) and stomach (1.09 million cases) cancers. The types of cancer with the highest mortality rates were lung (1.80 million deaths), colon and rectum (916 000 deaths), liver (830 000 deaths), stomach (769 000 deaths) and breast (685 000 deaths) cancers, but these rates are still increasing every year. Today, tobacco use, alcohol consumption, unhealthy diet, physical inactivity, air pollution and infections are the major risk factors explaining the rise in cancer incidence.^{2,3}

Cancer is a general term referring to a large group of diseases which can be characterized by an uncontrollable and rapid proliferation of abnormal cells able to spread and invade adjoining parts of the body, usually named as metastasis. Cancer arises from the transformation of normal cells in tumour cells through a multi-step process due to genetic mutations occurring during DNA replication each time that cells divide.⁴ The accumulation of these mutations after several duplications allows these abnormal cells to become aggressive and to develop ability to adapt to arch conditions. The tumour microenvironment is constituted out of different type of cells such as fibroblasts, various immune cells and blood and lymphatic cells embedded in tightly packed extracellular matrices. The second characteristic associated to harsh metabolic microenvironment results in an imbalance of positive and negative regulators of processes in activating and deregulating angiogenesis, desmoplasia, and inflammation.⁵ Thus, enabling tumour progression and resistance to conventional therapies. Today these characteristics are well known as "cancer hallmarks", they comprise sustaining proliferative signalling, evading growth suppressors, resisting cell death, enabling replicative immortality, inducing angiogenesis, activating invasion and metastasis, reprogramming of energy metabolism and evading immune destruction. Currently, the biology of cancer remains to be understood through the finding of new traits in order to develop and improve treatments.⁶

All cancers are different depending on their type or their advanced stage, thereby each treatment differ. The main objective of cancer treatments is to offer to patients a complete cure of cancer, to diminish adverse effects and/or to offer a better quality of life. In order to achieve this, the different treatment options currently used are surgery, chemotherapy, radiation therapy or hormonal therapy. However, nowadays cancer research focuses more on targeted therapies with the aim to decrease patient side effects by allowing a better control of the drug delivery to the tumour environment. Immunotherapy has also emerged as promising treatment, by stimulating or reactivating patient immune system to eradicate cancer.^{7,8}

TUMOUR HYPOXIA

Hypoxia has been studied since the 1930s and is known, nowadays, to be a common feature of solid tumours, characterised by a very low oxygen content, typically less than 1%.^{9,10} This poor oxygen levels are principally caused by an abnormal blood vascularisation development in rapidly growing tumours. The resulting diffusion limitations prevent a homogeneous oxygen, but also nutrient diffusion into tumours cells (Figure 1) which leads to a high scale adaptative reprogramming, making tumours more aggressive, proliferative and resistant to conventional treatments.¹¹⁻¹⁶ However, hypoxia is an extremely valuable target to be exploited for certain anti-cancer therapy strategies.¹⁷

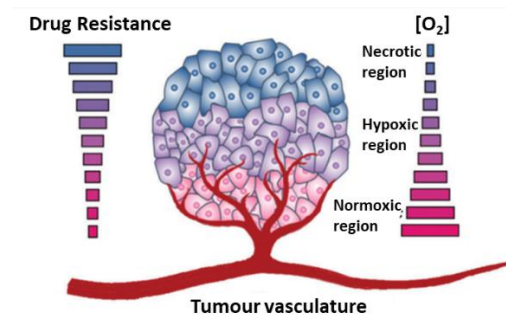


Figure 1: Hypoxia heterogenous tumour microenvironment.¹⁸

THE HIF PATHWAY

Adaptation of cancer cells to an anaerobic environment is achieved by the transcriptional induction of genes that are involved in several mechanisms driven by the activation of hypoxia-inducible factor 1 α (HIF-1 α).¹⁹⁻²¹ Three HIF- α have been identified till date, HIF-1 α , a well-known transcriptional nucleoprotein targeting several genes, HIF-2 α and HIF-3 α , two other analogues less expressed in tissues.²² HIF-1 comprises two subunits, HIF-1 α , present in the cytoplasm in every tissue, is oxygen sensitive and its level increases in hypoxic conditions due to stabilisation (Figure 2) and HIF-1 β , also known as ARNT, which is located in the nucleus and binds to HIF-1 α to promote angiogenesis mechanisms amongst others, helping cells to adjust hypoxia.²³⁻²⁶ In normoxic conditions, HIF-1 α undergoes degradation by ubiquitylation.²⁷ Prolyl hydroxylase (PHD) enzymes hydroxylate proline residues of HIF-1 α molecules enabling the binding of the E3 ubiquitin ligase complex containing the Von Hippel-Lindau (VHL) protein and leading to recognition by a protease enzyme and degradation of HIF-1 α .²⁸ However, in hypoxic environment, the hydroxylation step is inhibited, thereby the HIF-1 α protein is not degraded and accumulates in the cytoplasm. Then, HIF-1 α enters in the cell nucleus and dimerizes with HIF-1 β to form the HIF-1 complex. This complex interacts with the P300 co-factor and binds to the hypoxia-responsive element (HRE) regions present in the promotor region of multiple genes, resulting in their transcription to enable the survival of cells in hypoxia.²⁹⁻³¹

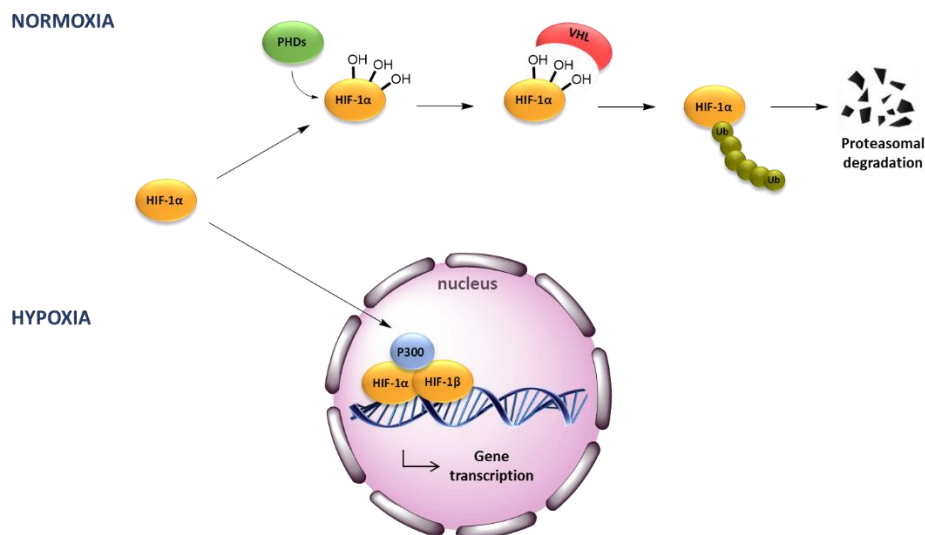


Figure 2: Schematic representation of the HIF pathway in normoxic and hypoxic environment.

Abbreviations: hypoxia-inducible factor 1 α and 1 β (HIF-1 α and HIF-1 β), prolyl hydroxylase (PHD), Von Hippel-Lindau protein (VHL), E3 ubiquitin ligase (Ub), co-factor (P300). Adapted from ³¹

Among the different mechanisms involved in cancer cell survival in the harsh hypoxic environment, the HIF transcriptional activation enables the glycolytic energy production in tumour cells. Today, it is well known that hypoxic cells need to maintain a stable glucose metabolism, described as the Warburg effect.^{32,33} Indeed, because of their important proliferation, glucose metabolism plays a key role in hypoxic tumour cell development, upregulating several metabolic pathways essential for cancer cells survival.³⁴ Nevertheless, contrarily to aerobic cancer cells, under hypoxic conditions this essential glycolysis process produces lactate as by-product which is excreted to prevent intracellular acidification.^{35,36} Moreover, glycolysis results as well in the production of carbon dioxide which can diffuse passively across the membrane and requires the action of another protein, carbonic anhydrase IX (CAIX), which is transcriptionally upregulated upon hypoxia via the HIF pathway, to counteract its effects.

CARBONIC ANHYDRASE IX

CAIX is a zinc metallo-enzyme, member of the carbonic anhydrase (CA) family which catalyse efficiently the reversible hydration reaction of carbon dioxide in bicarbonate and a proton. Carbonic anhydrases are categorised in 8 classes: α , β , γ , δ , ζ , η , θ and ι .^{37,38} The human carbonic anhydrases belong all to the α class and are present in 15 different isoforms, of which 12 are catalytically active. These active isoforms differ from each other for their kinetic properties, response to inhibitors and subcellular localization. Indeed, CAs I, II, III, VII and XIII are cytosolic, CAs IV, IX, XII and XIV are membrane bound, CAs Va and Vb are mitochondrial and CAVI is secreted principally in saliva. CA are involved in several physiological processes, such as the maintenance of pH and bicarbonate homeostasis, respiration, bone metabolism, and tumorigenesis.³⁹⁻⁴¹ However, in recent years CAIX has received a lot of attention from scientists because of its high catalytical potency and its highest production of protons among the other CAs. Indeed, the expression of CAIX is transcriptionally regulated *via* the HIF stabilisation

pathway in cancer cells.⁴² It is a transmembrane glycoprotein with the majority of its CA domain exposed to the extracellular environment. Based on these facts, it has been proposed that CAIX may contribute to tumour proliferation by acidification of the extracellular pH in response to hypoxia or loss of the negative regulation by von Hippel-Lindau protein.⁴²⁻⁴⁵ The protons produced after hydration of the carbon dioxide by the catalytic activity of CAIX accumulate in the extracellular space causing its acidification. This stimulates the degradation of the extracellular matrix, thereby promoting tumour invasion. The bicarbonate formed is transported back into cells by sodium bicarbonate transporters (NBCs) or anion exchangers (AEs). The CAII, forming a metabolon with CAIX, catalyses the conversion of bicarbonate back to water and carbon dioxide using intracellular produced protons.^{46,47} These bicarbonate concentrations cause a slightly alkaline intracellular pH, which promotes tumour cell survival and proliferation in a hostile acidic environment. Therefore, CAIX is involved in the regulation of the balance between the intracellular alkaline pH and the extracellular pH of tumour cells (Figure 3).⁴⁸ Moreover, it has been determined that CAIX was involved in other metabolic mechanisms needed for cancer cells survival. Indeed, meta-analysis studies showed clearly that high CAIX expression represents an adverse prognostic marker in solid tumours, for this reason, it has been proven that CAIX represented an attractive target for anticancer treatment.⁴⁹

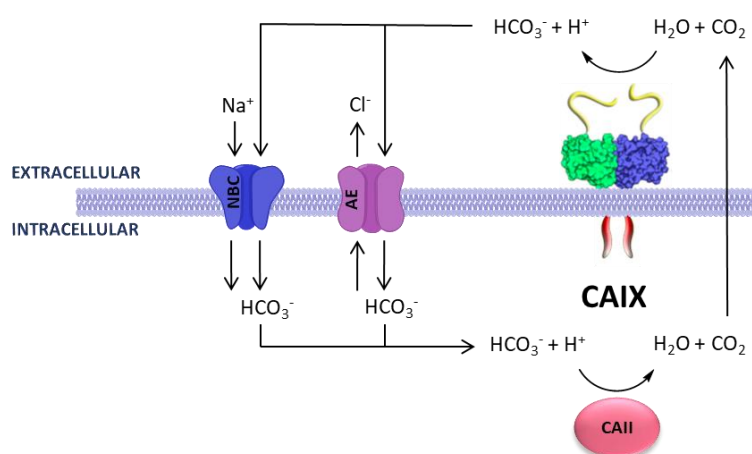


Figure 3: CAIX metabolism pathway involved in cellular pH regulation.

Abbreviations: Sodium-bicarbonate co-transporter (NBC), Anion exchanger (AE), carbonic anhydrase IX (CAIX), carbonic anhydrase II (CAII). Adapted from ^{44,48,50}

CARBONIC ANHYDRASE IX INHIBITORS

Many transmembrane-specific carbonic anhydrase inhibitors (CAIs) have been designed to induce an increase of the intracellular pH leading to the cell death. Generally, CAIs are designed to bind to the zinc central atom in the active site of the enzyme enabling its inhibition, however, some other inhibitors have been designed, to bind to the enzyme by anchoring to the zinc-coordinated water/hydroxide ion.^{36,51-53} When potent and selective inhibitors block e.g. CAIX activity, extracellular pH increases to a more physiological range and causes an increase in intracellular pH resulting in cell death.^{44,47} The sulfonamide/sulfamate class of inhibitors have been used for decades for different types of pathologies but although encountered large reversed-effects, this compound family still is the most studied one till date. Among the newer

generation of sulfonamide inhibitors, few of them were investigated on *in vivo* animal models and so far, only one, SLC-0111 (also known as WBI-5111) progressed to clinical trials for the treatment of advanced, metastatic hypoxic tumours overexpressing CAIX/XII and showed promising preclinical anticancer action leading to reduction of primary tumour growth, inhibition of invasion and metastasis, and a reduction in the cancer stem cell population.⁵⁴ Moreover, SLC-0111 has been used as a lead molecule for designing other analogues with improved selective CAIX inhibitory activity.⁵⁵ Promising results have also been obtained with the use of CAIX inhibitor conjugates combining small molecule CAIX inhibitors to cytotoxic agents with a moiety possessing further antitumour actions such as specifically direct the therapeutic agent to CAIX expressing cells.⁵⁶ This is the so-called dual targeting approach, to promote a higher tumour specific targeting, an increase of concentration of the payload in the tumour environment and a decrease of toxicity on normal tissues.

HYPOXIA-ACTIVATED PRODRUGS

In order to take advantage of the difference of oxygen concentration between hypoxic tumours and healthy tissues, in the last 30 years, researchers focused their efforts in the development of bio-reducible prodrugs, named later hypoxia-activated prodrugs (HAPs) to exploit the unique microenvironment of hypoxic tumours for personalized cancer medicine. The HAP purpose is to generate a cytotoxic effector selectively in the hypoxic environment by undergoing a biotransformation following reductive metabolism by oxidoreductase enzymes, upregulated in tumour cells. Moreover, after released, these effectors might partially diffuse back into the surrounding aerobic areas of the tumour to produce a cytotoxic effect on rapidly proliferating cells, as bystander effect.⁵⁷ HAPs require enzymatic activation, typically by 1 or 2 electron oxidoreductases. In the mono-electron reduction pathway, the HAP is reduced to form a fleeting radical anion. In presence of oxygen, this radical will be rapidly back oxidised in the initial form of the prodrug with generation of superoxide radicals quenched by superoxide dismutase, thus preventing cytotoxic effects on normal cells. Under hypoxic conditions, this reduction of HAP cannot be reversed. The cytotoxic payload is generated either by fragmentation or by further reduction, disproportionation followed by subsequent reduction of the radical. In the two-electrons reduction pathway, contrarily to the mono-electron one, the HAP activation pathway is not oxygen dependent, thereby the cytotoxic species are directly released following the enzymatic reduction. Thus, this pathway can also occur in normoxic tissues and causes dose-limiting toxicity (Figure 4).⁵⁸

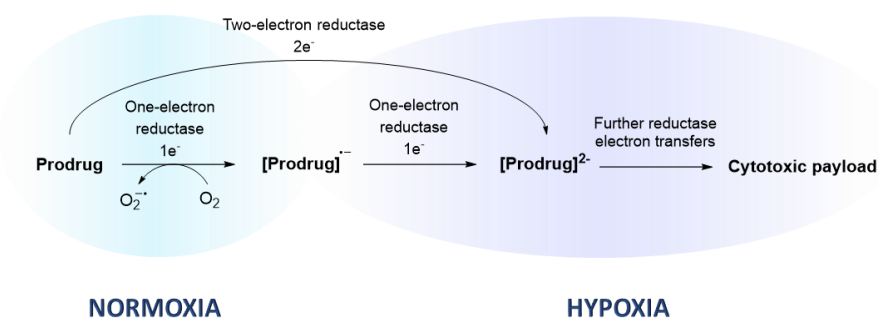


Figure 4: general activation mechanism of hypoxia-activated prodrugs. Adapted from ⁵⁹

HAPs generally comprise three moieties, a payload, a linker and a trigger. The payload is the cytotoxic compound which has to be released in the hypoxic tumour environment to kill cells after enzymatic activation. The linker has to be able to deactivate the payload until its activation and the chemical trigger should be susceptible to enzymatic activation under hypoxic conditions. The trigger group plays a key role, it has to determine the prodrug activation in hypoxic cells to allow the payload release at certain hypoxic levels depending on their reductive potential.^{60,61} A range of different chemical triggers have been identified to enable the selective targeting of hypoxic cells and can be grouped into 5 main categories: nitro compounds, aromatic *N*-oxides, aliphatic *N*-oxides, quinones, and transition metal complexes. Among them, three chemical classes have been extensively studied even up to the clinical stage, quinones, *N*-oxides, and more particularly nitro-aromatics such as the 2-nitroimidazole scaffold.

Quinones

Quinone-based prodrugs are the earliest developed HAPs, exemplified with the quinone mitomycin C, but however with limited effects in clinical trials. Quinone HAPs can be activated by the one electron or the two electron reduction pathways through cytochrome reductases or DT-diaphorase activation respectively.^{18,62} The first quinone-based HAP, mitomycin C (MMC) was developed in the 1960s and proposed to induce hypoxia selective cytotoxicity by DNA alkylation through a reductive mechanism. MMC however did not show high hypoxia selective activation, therefore, in order to improve the hypoxia activation, other quinone compounds have been developed such as porfiromycin (POR) or apaziquone (EO9) having a greater hypoxia selectivity. However, clinical studies demonstrated that POR did not show sufficient cytotoxicity compared to MMC and EO9 showed poor pharmacokinetic properties. In addition, structural modifications of EO9 have been achieved leading to pharmacokinetic and tissue penetration improvement.^{59,63–65}

Aromatic/aliphatic *N*-oxides

The *N*-oxides compound family represents the most potential hypoxia-activated class of prodrugs because of their low cytotoxicity under normoxic conditions, but selective reduction to effective therapeutic compounds in hypoxic environments. These features make *N*-oxides valuable for the synthesis of highly potent HAPs. Two drugs, tirapazamine (TPZ) and AQ4N represent this compound family.

TPZ, an aromatic *N*-oxide developed in the 1980s, is one of the best-characterized HAPs. It undergoes a one-electron enzymatic reduction by, for example cytochrome P450 (CP450) to generate, after further spontaneous reactions in hypoxic environment, its active metabolites, a DNA-damaging agent or benzotriazinyl radicals.⁶⁶ TPZ can undergo, as well, a two-electron reduction pathway in aerobic conditions bypassing the formation of the radical intermediate, generating a non-toxic metabolite.^{62,63} This feature reflects the high hypoxia-selectivity of this prodrug. TPZ entered clinical trials, combined with cisplatin, etoposide and/or radiotherapy for several cancer types. Promising results were observed on different type of cancers, showing

anticancer effects.⁶⁷⁻⁶⁹ However, TPZ did not show enough efficacy because of a too rapid metabolism.^{18,70} SN30000, the optimised derivative of TPZ and currently in clinical trials, has been designed to overpass this issue⁵⁹.

AQ4N is an aliphatic N-oxide metabolized under hypoxia to AQ4, by CP450 or inducible nitric oxide synthase enzymes (iNOS). AQ4 is a high affinity DNA intercalator inhibiting topoisomerase II after activation following a two-electron reduction pathway selectively in hypoxic environment. This activation step is inhibited in presence of oxygen.^{58,59,63} Clinical trials demonstrated significant activity of the AQ4N metabolite and also its ability to diffuse in surrounding tumour hypoxic cells exerting a bystander effect.^{58,71-74}

Nitro-aromatics

Nitro-aromatic HAPs were amongst the first oxygen-sensitive prodrugs to have been developed. Metronidazole and misonidazole were first designed as radiosensitizers for radiotherapy to mimic the oxygen effect in normoxic tissue. With the aim to improve these compounds, other radiosensitizer prodrugs such as pimonidazole, etanidazole and nimorazole have been synthesized.⁷⁵⁻⁷⁹ Later, hypoxia-selective HAPs have been developed exemplified with PR-104 and TH-302.

PR-104 is phosphate ester pre-prodrug that undergoes a hydrolysis step by phosphatases to generate the prodrug PR-104A, which is converted after oxidoreductase activation following one-electron or two-electron reduction into two cytotoxic metabolites acting both as DNA interstrand cross-linkers.^{59,62,63} It has been shown in *in vitro* study that PR-104 could be activated in hypoxic environment by CP450, but also in aerobic conditions in an oxygen-insensitive manner by the aldo-keto reductase 1C3.^{58,80-82} In addition, PR-104 showed toxic effect on clinical trials, which limits its use as a HAP in solid tumours.⁸³ CP-506 is a second generation of PR-104, resistant to aerobic activation by aldo-keto reductases. In hypoxic environment, CP-506 undergoes one-electron bioreduction to form, after further reduction, cytotoxic metabolites acting, similar to PR-104, as DNA interstrand cross-linkers. This analogue of PR-104 is expected to enter in clinical trials in 2022.^{5,84-86}

Another promising nitro-aromatic prodrug is evofosfamide (TH-302), a 2-nitroimidazole-based nitrogen mustard prodrug. The activation of TH-302 occurs via one-electron oxidoreductases in hypoxic cells, leading to the fragmentation of the nitroimidazole trigger and release of bromoisophosphoramidate mustard acting, as in the case of PR-104, as a DNA cross-linking agent.⁸⁷ Evofosfamide has been shown, when combined with other cytotoxic treatments, to enhance anticancer targeted therapeutic or radiotherapy effects.⁸⁸⁻⁹³ TH-302 showed a high selectivity for hypoxic cells, which enabled it to progress into clinical trials.⁹⁴⁻⁹⁸ However, in two phase 3 trials, TH-302 did not show any improvement on overall survival compared to standard of care, halting its further clinical development.⁹⁹

OUTLINES OF THE THESIS

The hypoxic microenvironment is a well-known feature of solid tumours causing treatment resistance, increasing tumour aggressiveness and proliferation. Tumour hypoxia is a promising therapeutic target in cancer treatment which has attracted researchers since many decades with the aim to develop prodrugs enabling to target hypoxic tumours in order to deliver cytotoxic compounds directly in the hypoxic environment. Today several hypoxia-activated prodrugs have been developed. Several HAPs have been tested in advanced clinical trials as monotherapy but also in combination with radiotherapy or chemotherapy and have proven some benefit in phase 2 trials, but all failed in phase 3 trials. **Chapter 2** summarizes the progress achieved over the last 15 years through investigation of key patents claiming the development of new generations of HAPs which can preferentially release chemotherapeutic agents within hypoxic tumours. Within this PhD thesis, several strategies will be investigated exploiting the concept of hypoxia-activated prodrugs. **Chapter 3** describes the design, synthesis and evaluations of carbonic anhydrase IX inhibitors combining different hypoxia triggers with two benzenesulfonamide analogues. **Chapter 3** also describes the different biological evaluations performed on these compounds in terms of inhibition potency, cytotoxicity toward different human cancer cell lines in normoxic and in anoxic conditions and toxicity on zebrafish larvae model. This in order to determine the efficacy of the prodrugs. Today, immunotherapy is the most rapidly growing treatment class and has a major impact in oncology, but lacks efficacy in the hypoxic tumour microenvironment. In order to improve the efficacy of this drug family, we synthesized immunotherapeutic HAPs to target the hypoxic tumour environment. The design and synthesis of these HAPs comprising either a nitroimidazole, nitrofuran and nitrothiophene hypoxia trigger coupled through a carbamate link to two toll-like receptor agonists and a Bruton's tyrosine kinase inhibitor as immunotherapeutics is described in **Chapter 4**. Biological evaluations are detailed as well, achieved by viability assay on two selected prodrugs of the series to test their ability to be activated and to release the cytotoxic payload under anoxic condition. Antibody-drug conjugates (ADCs) have been intensively studied as promising biotherapeutic strategies to specifically target cancer cells and allowing the release of highly potent drugs directly in the tumour microenvironment. In addition, already 12 ADCs have been approved by the Food and Drug Administration (FDA). Therefore, **Chapter 5** describes the synthesis of new drug-antibody conjugates combining a toll-like receptor agonist, Resiquimod, as cytotoxic payload, a nitroimidazole moiety as hypoxia trigger both connected to Cetuximab, an antibody specific to the EGFR receptor highly expressed on tumour cells. This concept will improve targeting the hypoxic tumour environment, increase the payload efficiency and potentially decrease normal tissues adverse effect. Finally, **chapter 6** provides a general discussion of the work outlined in this thesis. Future directions and perspective of HAP development within this work are discussed.

References

1. Mattiuzzi, C.; Lippi, G. Current Cancer Epidemiology. *Journal of Epidemiology and Global Health* **2019**, *9* (4), 217–222. <https://doi.org/10.2991/jegh.k.191008.001>.
2. Hiatt, R. A.; Beyeler, N. Cancer and Climate Change. *Lancet Oncol.* **2020**, *21* (11), 519–527. [https://doi.org/10.1016/s1470-2045\(20\)30448-4](https://doi.org/10.1016/s1470-2045(20)30448-4).
3. de Martel, C.; Georges, D.; Bray, F.; Ferlay, J.; Clifford, G. M. Global Burden of Cancer Attributable to Infections in 2018: A Worldwide Incidence Analysis. *The Lancet Global Health* **2020**, *8* (2), 180–190. [https://doi.org/10.1016/S2214-109X\(19\)30488-7](https://doi.org/10.1016/S2214-109X(19)30488-7).
4. Graham, T. A.; Sottoriva, A. Measuring Cancer Evolution from the Genome. *Journal of Pathology* **2017**, *241* (2), 183–191. <https://doi.org/10.1002/path.4821>.
5. Fu, Z.; Mowday, A. M.; Smail, J. B.; Hermans, I. F.; Patterson, A. v. Tumour Hypoxia-Mediated Immunosuppression: Mechanisms and Therapeutic Approaches to Improve Cancer Immunotherapy. *Cells* **2021**, *10* (5), 1006. <https://doi.org/10.3390/cells10051006>.
6. Hanahan, D.; Weinberg, R. A. Hallmarks of Cancer: The next Generation. *Cell* **2011**, *144* (5), 646–674. <https://doi.org/10.1016/j.cell.2011.02.013>.
7. Wang, J.-J.; Lei, K.-F.; Han, F. Tumor Microenvironment: Recent Advances in Various Cancer Treatments. *Eur Rev Med Pharmacol Sci.* **2018**, *22* (12), 3855–3864. https://doi.org/10.26355/eurev_201806_15270.
8. Yin, W.; Wang, J.; Jiang, L.; James Kang, Y. Cancer and Stem Cells. *Experimental Biology and Medicine* **2021**, *246*, 1791–1801. <https://doi.org/10.1177/15353702211005390>.
9. Ebbesen, P.; Pettersen, E. O.; Gorr, T. A.; Jobst, G.; Williams, K.; Kieninger, J.; Wenger, R. H.; Pastorekova, S.; Dubois, L.; Lambin, P.; Wouters, B. G.; van den Beucken, T.; Supuran, C. T.; Poellinger, L.; Ratcliffe, P.; Kanopka, A.; Grlach, A.; Gasmann, M.; Harris, A. L.; Maxwell, P.; Scozzafava, A. Taking Advantage of Tumor Cell Adaptations to Hypoxia for Developing New Tumor Markers and Treatment Strategies. *Journal of Enzyme Inhibition and Medicinal Chemistry* **2009**, *24* (1), 1–39. <https://doi.org/10.1080/14756360902784425>.
10. Anduran, E.; Dubois, L. J.; Lambin, P.; Winum, J. Y. Hypoxia-Activated Prodrug Derivatives of Anti-Cancer Drugs: A Patent Review 2006–2021. *Expert Opinion on Therapeutic Patents* **2022**, *32* (1), 1–12. <https://doi.org/10.1080/13543776.2021.1954617>.
11. Wilson, W. R.; Hay, M. P. Targeting Hypoxia in Cancer Therapy. *Nature Reviews Cancer* **2011**, *11*, 393–410. <https://doi.org/10.1038/nrc3064>.
12. Peng, X.; Gao, J.; Yuan, Y.; Liu, H.; Lei, W.; Li, S.; Zhang, J.; Wang, S. Hypoxia-Activated and Indomethacin-Mediated Theranostic Prodrug Releasing Drug On-Demand for Tumor Imaging and Therapy. *Bioconjugate Chemistry* **2019**, *30* (11), 2828–2843. <https://doi.org/10.1021/acs.bioconjchem.9b00564>.
13. Liu, J. N.; Bu, W.; Shi, J. Chemical Design and Synthesis of Functionalized Probes for Imaging and Treating Tumor Hypoxia. *Chemical Reviews* **2017**, *177* (9), 6160–6224. <https://doi.org/10.1021/acs.chemrev.6b00525>.
14. Vilaplana-Lopera, N.; Besh, M.; Moon, E. J. Targeting Hypoxia: Revival of Old Remedies. *Biomolecules* **2021**, *11* (11), 1604. <https://doi.org/10.3390/biom11111604>.
15. Lindsay, D.; Garvey, C. M.; Mumenthaler, S. M.; Foo, J. Leveraging Hypoxia-Activated Prodrugs to Prevent Drug Resistance in Solid Tumors. *PLoS Comput Biol* **2016**, *12* (8), 1–25. <https://doi.org/10.1371/journal.pcbi.1005077>.
16. Kang, D.; Cheung, S. T.; Wong-Rolle, A.; Kim, J. Enamine N-Oxides: Synthesis and Application to Hypoxia-Responsive Prodrugs and Imaging Agents. *ACS Central Science* **2021**, *7* (4), 631–640. <https://doi.org/10.1021/acscentsci.0c01586>.

17. Sun, Z.; Zhang, H.; Zhang, H.; Wu, J.; Gao, F.; Zhang, C.; Hu, X.; Liu, Q.; Wei, Y.; Wei, Y.; Zhuang, J.; Zhuang, J.; Huang, X. A Novel Model System for Understanding Anticancer Activity of Hypoxia-Activated Prodrugs. *Molecular Pharmaceutics* **2020**, *17* (6), 2072–2082. <https://doi.org/10.1021/acs.molpharmaceut.0c00232>.
18. Sharma, A.; Arambula, J. F.; Koo, S.; Kumar, R.; Singh, H.; Sessler, J. L.; Kim, J. S. Hypoxia-Targeted Drug Delivery. *Chemical Society Reviews* **2019**, *48*, 771–813. <https://doi.org/10.1039/c8cs00304a>.
19. Denko, N. C. Hypoxia, HIF1 and Glucose Metabolism in the Solid Tumour. *Nat Rev Cancer* **2008**, *8* (9), 705–713. <https://doi.org/10.1038/nrc2468>.
20. Ivan, M.; Kondo, K.; Yang, H.; Kim, W.; Valiando, J.; Ohh, M.; Salic, A.; Asara, J. M.; Lane, W. S.; Kaelin, J. HIF α Targeted for VHL-Mediated Destruction by Proline Hydroxylation: Implications for O₂ Sensing. *Science* **2001**, *292* (5516), 464–468. <https://doi.org/10.1126/science.1059817>.
21. Teicher, B. A. *Tumor Models in Cancer Research*, 1st ed.; Cancer Drug Discovery and Development Series Editor; Springer, 2011.
22. Jing, X.; Yang, F.; Shao, C.; Wei, K.; Xie, M.; Shen, H.; Shu, Y. Role of Hypoxia in Cancer Therapy by Regulating the Tumor Microenvironment. *Molecular Cancer* **2019**, *18* (157), 1–15. <https://doi.org/10.1186/s12943-019-1089-9>.
23. Fallah, J.; Rini, B. I. HIF Inhibitors: Status of Current Clinical Development. *Current Oncology Reports* **2019**, *21* (6), 1–10. <https://doi.org/10.1007/s11912-019-0752-z>.
24. Yu, A. Y.; Frid, M. G.; Shimoda, L. A.; Wiener, C. M.; Stenmark, K.; Semenza, G. L.; Se, G. L. Temporal, Spatial, and Oxygen-Regulated Expression of Hypoxia-Inducible Factor-1 in the Lung. *Am J Physiol.* **1998**, *275* (4), 818–826.
25. Luo, X.; Li, A.; Chi, X.; Lin, Y.; Liu, X.; Zhang, L.; Su, X.; Yin, Z.; Lin, H.; Gao, J. Hypoxia-Activated Prodrug Enabling Synchronous Chemotherapy and HIF-1 α Downregulation for Tumor Treatment. *Bioconjugate Chemistry* **2021**, *32* (5), 983–990. <https://doi.org/10.1021/acs.bioconjchem.1c00131>.
26. Patiar, S.; Harris, A. L. Role of Hypoxia-Inducible Factor-1 α as a Cancer Therapy Target. *Endocrine-Related Cancer* **2006**; *13*, 62–75. <https://doi.org/10.1677/erc.1.01290>.
27. Harris, A. L. Hypoxia - A Key Regulatory Factor in Tumour Growth. *Nature Reviews Cancer* **2002**, *2*, 38–47. <https://doi.org/10.1038/nrc704>.
28. Semenza, G. L. Hydroxylation of HIF-1: Oxygen Sensing at the Molecular Level. *Physiology* **2004**, *19* (4), 176–182. <https://doi.org/10.1152/physiol.00001.2004>.
29. Shibata, T.; Giaccia, A. J.; Martin Brown, J. Hypoxia-Inducible Regulation of a Prodrug-Activating Enzyme for Tumor-Specific Gene Therapy. *Neoplasia* **2002**, *4* (1), 40–48. <https://doi.org/10.1038/sj/neo/7900189>.
30. Baran, N.; Konopleva, M. Molecular Pathways: Hypoxia-Activated Prodrugs in Cancer Therapy. *Clinical Cancer Research* **2017**, *23* (10), 2382–2391. <https://doi.org/10.1158/1078-0432.CCR-16-0895>.
31. Wigerup, C.; Pålman, S.; Bexell, D. Pharmacology & Therapeutics Therapeutic Targeting of Hypoxia and Hypoxia-Inducible Factors in Cancer. *Pharmacology and Therapeutics* **2016**, *164*, 152–169. <https://doi.org/10.1016/j.pharmthera.2016.04.009>.
32. Warburg, O. *SCIENCE Injuring of Respiration On the Origin of Cancer Cells* **1956**, *123* (3191), 309–314.
33. vander Heiden, M. G.; Cantley, L. C.; Thompson, C. B. Understanding the Warburg Effect: The Metabolic Requirements of Cell Proliferation. *Science* **2009**, *324* (5930), 1029–1033. <https://dx.doi.org/10.1126/science.1160809>
34. Park, J. H.; Pyun, W. Y.; Park, H. W. Cancer Metabolism: Phenotype, Signaling and Therapeutic Targets. *Cells* **2020**, *9* (10), 2308. <https://doi.org/10.3390/cells9102308>.
35. Parks, S. K.; Chiche, J.; Pouyssegur, J. PH Control Mechanisms of Tumor Survival and Growth. *Journal of Cellular Physiology* **2011**, *226* (2), 299–308. <https://doi.org/10.1002/jcp.22400>.

Chapter 1

36. Buabeng, E. R.; Henary, M. Developments of Small Molecules as Inhibitors for Carbonic Anhydrase Isoforms. *Bioorganic and Medicinal Chemistry* **2021**, *39*, 1–23. <https://doi.org/10.1016/j.bmc.2021.116140>.
37. Supuran, C. T. Novel Carbonic Anhydrase Inhibitors. *Future Medicinal Chemistry* **2021**, *13* (22), 1935–1937. <https://doi.org/10.4155/fmc-2021-0222>
38. Supuran, C. T. Emerging Role of Carbonic Anhydrase Inhibitors. *Clin Sci (Lond)* **2021**, *135* (10), 1233–1249. <https://doi.org/10.1042/cs20210040>
39. Lomelino, C.; McKenna, R. Carbonic Anhydrase Inhibitors: A Review on the Progress of Patent Literature (2011–2016). *Expert Opinion on Therapeutic Patents* **2016**, *26* (8), 947–956. <https://doi.org/10.1080/13543776.2016.1203904>.
40. Monti, S. M.; Supuran, C. T.; de Simone, G. Anticancer Carbonic Anhydrase Inhibitors: A Patent Review (2008–2013). *Expert Opinion on Therapeutic Patents* **2013**, *23* (6), 737–749. <https://doi.org/10.1517/13543776.2013.798648>.
41. Rami, M.; Dubois, L.; Parvathaneni, N. K.; Alterio, V.; van Kuijk, S. J. A.; Monti, S. M.; Lambin, P.; de Simone, G.; Supuran, C. T.; Winum, J. Y. Hypoxia-Targeting Carbonic Anhydrase IX Inhibitors by a New Series of Nitroimidazole-Sulfonamides/Sulfamides/Sulfamates. *Journal of Medicinal Chemistry* **2013**, *56* (21), 8512–8520. <https://doi.org/10.1021/jm4009532>.
42. Švastová, E.; Hulíková, A.; Rafajová, M.; Zat’Ovičová, M.; Gibadulinová, A.; Casini, A.; Cecchi, A.; Scozzafava, A.; Supuran, C. T.; Pastorek, J.; Pastoreková, S. Hypoxia Activates the Capacity of Tumor-Associated Carbonic Anhydrase IX to Acidify Extracellular PH. *FEBS Letters* **2004**, *577* (3), 439–445. <https://doi.org/10.1016/j.febslet.2004.10.043>.
43. Bartoov, M.; Parkkila, S.; Pohlodek, K.; Karttunen, T. J.; Galbav, T.; Mucha, V.; Harris, A. L.; Pastorek, J.; Pastorek, S. Expression of Carbonic Anhydrase IX in Breast Is Associated with Malignant Tissues and Is Related to Overexpression of C-ErbB2. *Journal of Pathology* **2002**, *197* (3), 314–321. <https://doi.org/10.1002/path.1120>.
44. Becker, H. M. Carbonic Anhydrase IX and Acid Transport in Cancer. *British Journal of Cancer* **2020**, *122*, 157–167. <https://doi.org/10.1038/s41416-019-0642-z>.
45. Cecchi, A.; Hulikova, A.; Pastorek, J.; Pastoreková, S.; Scozzafava, A.; Winum, J. Y.; Montero, J. L.; Supuran, C. T. Carbonic Anhydrase Inhibitors. Design of Fluorescent Sulfonamides as Probes of Tumor-Associated Carbonic Anhydrase IX That Inhibit Isozyme IX-Mediated Acidification of Hypoxic Tumors. *Journal of Medicinal Chemistry* **2005**, *48* (15), 4834–4841. <https://doi.org/10.1021/jm0501073>.
46. van Kuijk, S. J. A.; Yaromina, A.; Houben, R.; Niemans, R.; Lambin, P.; Dubois, L. J. Prognostic Significance of Carbonic Anhydrase IX Expression in Cancer Patients: A Meta-Analysis. *Frontiers in Oncology* **2016**, *6* (69), 1–16. <https://doi.org/10.3389/fonc.2016.00069>.
47. Lee, S. H.; Griffiths, J. R. How and Why Are Cancers Acidic? Carbonic Anhydrase IX and the Homeostatic Control of Tumour Extracellular Ph. *Cancers* **2020**, *12* (6), 1–23. <https://doi.org/10.3390/cancers12061616>.
48. Pastorekova, S.; Gillies, R. J. The Role of Carbonic Anhydrase IX in Cancer Development: Links to Hypoxia, Acidosis, and Beyond. *Cancer and Metastasis Reviews* **2019**, *38*, 65–77. <https://doi.org/10.1007/s10555-019-09799-0>.
49. Angeli, A.; Carta, F.; Nocentini, A.; Winum, J. Y.; Zalubovskis, R.; Akdemir, A.; Onnis, V.; Eldehna, W. M.; Capasso, C.; Simone, G. de; Monti, S. M.; Carradori, S.; Donald, W. A.; Dedhar, S.; Supuran, C. T. Carbonic Anhydrase Inhibitors Targeting Metabolism and Tumor Microenvironment. *Metabolites* **2020**, *10* (10), 1–21. <https://doi.org/10.3390/metabo10100412>.
50. Nocentini, A.; Supuran, C. T. Carbonic Anhydrase Inhibitors as Antitumor/Antimetastatic Agents: A Patent Review (2008–2018). *Expert Opinion on Therapeutic Patents* **2018**, *28* (10), 729–740. <https://doi.org/10.1080/13543776.2018.1508453>.

51. Maresca, A.; Temperini, C.; Vu, H.; Pham, N. B.; Poulsen, S.-A.; Scozzafava, A.; Quinn, R. J.; Supuran, C. T. Non-Zinc Mediated Inhibition of Carbonic Anhydrases: Coumarins Are a New Class of Suicide Inhibitors. *J. Am. Chem. Soc.* **2009**, *131* (8), 3057–3062. <https://doi.org/10.1021/ja809683v>.
52. Touisni, N.; Maresca, A.; McDonald, P. C.; Lou, Y.; Scozzafava, A.; Dedhar, S.; Winum, J.-Y.; Supuran, C. T.; Fiorentino, S.; Florence, I. Glycosyl Coumarin Carbonic Anhydrase IX and XII Inhibitors Strongly Attenuate the Growth of Primary Breast Tumors. *J. Med. Chem.* **2011**, *54* (24), 8271–8277. <https://doi.org/10.1021/jm200983e>.
53. Maresca, A.; Temperini, C.; Pochet, L.; Masereel, B.; Scozzafava, A.; Supuran, C. T. Deciphering the Mechanism of Carbonic Anhydrase Inhibition with Coumarins and Thiocoumarins. *J. Med. Chem.* **2010**, *53*, 335. <https://doi.org/10.1021/jm901287j>.
54. Frost, S. C., McKenna, R. *Carbonic Anhydrase: Mechanism, Regulation, Links to Disease, and Industrial Applications*, 1st ed.; Subcellular Biochemistry, Vol. 75; Springer Netherlands: Dordrecht, 2014. <https://doi.org/10.1007/978-94-007-7359-2>.
55. Ilies, M. A.; Winum, J. Y. *Carbonic Anhydrase Inhibitors for the Treatment of Tumors: Therapeutic, Immunologic, and Diagnostic Tools Targeting Isoforms IX and XII*, 1st ed.; Carbonic Anhydrases: Biochemistry and Pharmacology of an Evergreen Pharmaceutical Target Vol. 16; Elsevier, **2019**; pp 331–365. <https://doi.org/10.1016/B978-0-12-816476-1.00016-2>.
56. Supuran, C. T. Experimental Carbonic Anhydrase Inhibitors for the Treatment of Hypoxic Tumors. *Journal of Experimental Pharmacology* **2020**, *2020* (12), 603–617. <https://doi.org/10.2147/JEP.S265620>.
57. Denny, W. A.; Wilson, W. R.; Hay, M. P. Recent Developments in the Design of Bioreductive Drugs. *Br J Cancer Suppl.* **1996**, *27*, 32–38.
58. Phillips, R. M. Targeting the Hypoxic Fraction of Tumours Using Hypoxia-Activated Prodrugs Cytotoxic Reviews Godefridus J. Peters and Eric Raymond. *Cancer Chemotherapy and Pharmacology* **2016**, *77*, 441–457. <https://doi.org/10.1007/s00280-015-2920-7>.
59. Mistry, I. N.; Thomas, M.; Calder, E. D. D.; Conway, S. J.; Hammond, E. M. Clinical Advances of Hypoxia-Activated Prodrugs in Combination With Radiation Therapy. *Radiation Oncology Biology* **2017**, *98* (5), 1183–1196. <https://doi.org/10.1016/j.ijrobp.2017.03.024>.
60. Connor, L. J. O.; Cazares-körner, C.; Saha, J.; Evans, C. N. G.; Stratford, M. R. L.; Hammond, E. M.; Conway, S. J. Design, Synthesis and Evaluation of Molecularly Targeted Hypoxia-Activated Prodrugs. **2016**, *11* (4), 781–794. <https://doi.org/10.1038/nprot.2016.034>.
61. Liang, D.; Miller, G. H. and Tranmer, G. K. Hypoxia Activated Prodrugs Factors Influencing Design and Development. *Curr Med Chem.* **2015**, *22* (37), 4313–4325. <https://doi.org/10.2174/0929867322666151021111016>
62. Zeng, Y.; Ma, J.; Zhan, Y.; Xu, X.; Zeng, Q.; Liang, J.; Chen, X. Hypoxia-Activated Prodrugs and Redox-Responsive Nanocarriers. *International Journal of Nanomedicine* **2018**, *2018* (13), 6551–6574. <https://doi.org/10.2147/IJN.S173431>.
63. Guise, C. P.; Mowday, A. M.; Ashoorzadeh, A.; Yuan, R.; Lin, W. H.; Wu, D. H.; Smail, J. B.; Patterson, A. v; Ding, K. Bioreductive Prodrugs as Cancer Therapeutics: Targeting Tumor Hypoxia. *Chin J Cancer.* **2014**, *33* (2), 80–86. <https://doi.org/10.5732/cjc.012.10285>.
64. Phillips, R. M.; Hendriks, H. R.; Peters, G. J. EO9 (Apaziquone): From the Clinic to the Laboratory and Back Again. *British Journal of Pharmacology* **2013**, *168* (1), 11–18. <https://doi.org/10.1111/j.1476-5381.2012.01996.x>.
65. Brown, J. M.; Wilson, W. R. EXPLOITING TUMOUR HYPOXIA IN CANCER TREATMENT. Exploiting tumour hypoxia in cancer treatment. *Nature Reviews Cancer* **2004**, *4*, 437–447. <https://doi.org/10.1038/nrc1367>.

Chapter 1

66. Shinde, S. S.; Hay, M. P.; Patterson, A. v.; Denny, W. A.; Anderson, R. F. Spin Trapping of Radicals Other than the $\cdot\text{OH}$ Radical upon Reduction of the Anticancer Agent Tirapazamine by Cytochrome P450 Reductase. *J Am Chem Soc* **2009**, *131* (40), 14220–14221. <https://doi.org/10.1021/ja906860a>.
67. Le, Q. T. X.; Moon, J.; Redman, M.; Williamson, S. K.; Lara, P. N.; Goldberg, Z.; Gaspar, L. E.; Crowley, J. J.; Moore, D. F.; Gandara, D. R. Phase II Study of Tirapazamine, Cisplatin, and Etoposide and Concurrent Thoracic Radiotherapy for Limited-Stage Small-Cell Lung Cancer: SWOG 0222. *Journal of Clinical Oncology* **2009**, *27* (18), 3014–3019. <https://doi.org/10.1200/JCO.2008.21.3868>.
68. Rischin, D.; Peters, L.; Fisher, R.; Macann, A.; Denham, J.; Poulsen, M.; Jackson, M.; Kenny, L.; Penniment, M.; Carry, J.; Lamb, D.; McClure, B. Tirapazamine, Cisplatin, and Radiation versus Fluorouracil, Cisplatin, and Radiation in Patients with Locally Advanced Head and Neck Cancer: A Randomized Phase II Trial of the Trans-Tasman Radiation Oncology Group (TROG 98.02). *Journal of Clinical Oncology* **2005**, *23* (1), 79–87. <https://doi.org/10.1200/JCO.2005.01.072>.
69. Treat, J.; Johnson, E.; Langer, C.; Belani, C.; Haynes, B.; Greenberg, R.; Rodriguez, R.; Drobins, P.; Miller, W.; Meehan, L.; Mckeon, A.; Devin, J.; von Roemeling, R.; Viallet, J. Tirapazamine With Cisplatin in Patients With Advanced Non-Small-Cell Lung Cancer: A Phase II Study. *J Clin Oncol.* **1998**, *16* (11), 3524–3527. <https://doi.org/10.1200/jco.1998.16.11.3524>
70. Hicks, K. O.; Pruijn, F. B.; Sturman, J. R.; Denny, W. A.; Wilson, W. R. Multicellular Resistance to Tirapazamine Is Due to Restricted Extravascular Transport: A Pharmacokinetic/Pharmacodynamic Study in HT29 Multicellular Layer Cultures. *Cancer Res.* **2003**, *63* (18), 5970–5977.
71. Friery, O. P.; Gallagher, R.; Murray, M. M.; Hughes, C. M.; Galligan, E. S.; McIntyre, I. A.; Patterson, L. H.; Hirst, D. G.; McKeown, S. R. Enhancement of the Anti-Tumour Effect of Cyclophosphamide by the Bioreductive Drugs AQ4N and Tirapazamine. *British Journal of Cancer* **2000**, *82* (8), 1469–1473. <https://doi.org/10.1054/bjoc.1999.1132>.
72. McKeown, S. R.; Hejmadi, M. v.; McIntyre, I. A.; McAleer, J.; Patterson, L. H. AQ4N: An Alkylaminoanthraquinone N-Oxide Showing Bioreductive Potential and Positive Interaction with Radiation in Vivo. *British Journal of Cancer* **1995**, *72* (1), 76–81.
73. Trédan, O.; Garbens, A. B.; Lalani, A. S.; Tannock, I. F. The Hypoxia-Activated Prodrug AQ4N Penetrates Deeply in Tumor Tissues and Complements the Limited Distribution of Mitoxantrone. *Cancer Research* **2009**, *69* (3), 940–947. <https://doi.org/10.1158/0008-5472.CAN-08-0676>.
74. Ming, L.; Byrne, N. M.; Camac, S. N.; Mitchell, C. A.; Ward, C.; Waugh, D. J.; McKeown, S. R.; Worthington, J. Androgen Deprivation Results in Time-Dependent Hypoxia in LNCaP Prostate Tumours: Informed Scheduling of the Bioreductive Drug AQ4N Improves Treatment Response. *International Journal of Cancer* **2013**, *132* (6), 1323–1332. <https://doi.org/10.1002/ijc.27796>.
75. Overgaard, J. Clinical Evaluation of Nitroimidazoles as Modifiers of Hypoxia in Solid Tumors. *Oncol Res.* **1994**, *6* (10-11), 509–518.
76. Grigsby, P. W.; Winter, K.; Wasserman, T. H.; Marcial, V.; Rotman, M.; Cooper, J.; Keys, H.; Asbell, S. O.; Phillips, T. L. Irradiation with or without misonidazole for patients with stages IIIB and IVA carcinoma of the cervix: final results of RTOG 80-05. Radiation Therapy Oncology Group. *Int J Radiat Oncol Biol Phys.* **1999**, *44* (3), 513–517. [https://doi.org/10.1016/s0360-3016\(99\)00054-1](https://doi.org/10.1016/s0360-3016(99)00054-1)
77. Curie, M.; Wing, R. Clinical Results of Hypoxic Cell Radiosensitisation from Hyperbaric Oxygen to Accelerated Radiotherapy, Carbogen and Nicotinamide M Saunders and S Dische. *Br J Cancer Suppl.* **1996**, *27*, 271–278.
78. Overgaard, J.; Hansen, H. S.; Overgaard, M.; Bastholt, L.; Berthelsen, A.; Specht, L.; Lindeløv, B.; Jørgensen, K. A Randomized Double-Blind Phase III Study of Nimorazole as a Hypoxic Radiosensitizer of Primary Radiotherapy in Supraglottic Larynx and Pharynx Carcinoma. Results of the Danish Head and Neck Cancer Study (DAHANCA) Protocol 5-85. *Radiother Oncol.* **1998**, *46* (2), 135–146.

79. Grau Eriksen, J.; Nordmark, M.; Alsner, J.; Horsman, M. R.; Overgaard, J.; Grau Eriksen, J.; Nordmark, M.; Alsner, J.; Horsman, M. R. Plasma osteopontin, hypoxia, and response to the hypoxia sensitiser nimorazole in radiotherapy of head and neck cancer: results from the DAHANCA 5 randomised double-blind placebo-controlled trial. *Lancet Oncol.* **2005**, *6* (10), 757-764. [https://doi.org/10.1016/S1470-2045\(05\)](https://doi.org/10.1016/S1470-2045(05)).
80. Guise, C. P.; Abbattista, M. R.; Singleton, R. S.; Holford, S. D.; Connolly, J.; Dachs, G. U.; Fox, S. B.; Pollock, R.; Harvey, J.; Guilford, P.; Doñate, F.; Wilson, W. R.; Patterson, A. v. The Bioreductive Prodrug PR-104 Is Activated under Aerobic Conditions by Human Aldo-Keto Reductase 1C3. *Cancer Research* **2010**, *70* (4), 1573-1584. <https://doi.org/10.1158/0008-5472.CAN-09-3237>.
81. Patterson, A. v.; Ferry, D. M.; Edmunds, S. J.; Gu, Y.; Singleton, R. S.; Patel, K.; Pullen, S. M.; Hicks, K. O.; Syddall, S. P.; Atwell, G. J.; Yang, S.; Denny, W. A.; Wilson, W. R. Mechanism of Action and Preclinical Antitumor Activity of the Novel Hypoxia-Activated DNA Cross-Linking Agent PR-104. *Clinical Cancer Research* **2007**, *13* (13), 3922-3932. <https://doi.org/10.1158/1078-0432.CCR-07-0478>.
82. Mckeage, M. J.; Jameson, M. B.; Ramanathan, R. K.; Rajendran, J.; Gu, Y.; Wilson, W. R.; Melink, T. J.; Tchekmedyan, S. PR-104 a Bioreductive Pre-Prodrug Combined with Gemcitabine or Docetaxel in a Phase Ib Study of Patients with Advanced Solid Tumours. *BMC Cancer* **2012**, *12* (496), 1-10. <http://www.biomedcentral.com/1471-2407/12/496>.
83. Abou-Alfa, G. K.; Chan, S. L.; Lin, C. C.; Chiorean, E. G.; Holcombe, R. F.; Mulcahy, M. F.; Carter, W. D.; Patel, K.; Wilson, W. R.; Melink, T. J.; Gutheil, J. C.; Tsao, C. J. PR-104 plus Sorafenib in Patients with Advanced Hepatocellular Carcinoma. *Cancer Chemotherapy and Pharmacology* **2011**, *68* (2), 539-545. <https://doi.org/10.1007/s00280-011-1671-3>.
84. van der Wiel, A. M. A.; Jackson-Patel, V.; Niemans, R.; Yaromina, A.; Liu, E.; Marcus, D.; Mowday, A. M.; Lieuwes, N. G.; Biemans, R.; Lin, X.; Fu, Z.; Kumara, S.; Jochems, A.; Ashoorzadeh, A.; Anderson, R. F.; Hicks, K. O.; Bull, M. R.; Abbattista, M. R.; Guise, C. P.; Deschoemaeker, S.; Thiolloy, S.; Heyerick, A.; Solivio, M. J.; Balbo, S.; Smaill, J. B.; Theys, J.; Dubois, L. J.; Patterson, A. v.; Lambin, P. Selectively Targeting Tumor Hypoxia with the Hypoxia-Activated Prodrug CP-506. *Molecular Cancer Therapeutics* **2021**, *20* (12), 2372-2383. <https://doi.org/10.1158/1535-7163.MCT-21-0406>.
85. Solivio, M. J.; Stornetta, A.; Gilissen, J.; Villalta, P. W.; Deschoemaeker, S.; Heyerick, A.; Dubois, L.; Balbo, S. In Vivo Identification of Adducts from the New Hypoxia-Activated Prodrug CP-506 Using DNA Adductomics. *Chemical Research in Toxicology* **2022**, *35* (2), 275-282. <https://doi.org/10.1021/acs.chemrestox.1c00329>.
86. Jackson-Patel, V.; Liu, E.; Bull, M. R.; Ashoorzadeh, A.; Bogle, G.; Wolfram, A.; Hicks, K. O.; Smaill, J. B.; Patterson, A. v. Tissue Pharmacokinetic Properties and Bystander Potential of Hypoxia-Activated Prodrug CP-506 by Agent-Based Modelling. *Frontiers in Pharmacology* **2022**, *13*, 1-17. <https://doi.org/10.3389/fphar.2022.803602>.
87. Meng, F.; Evans, J. W.; Bhupathi, D.; Banica, M.; Lan, L.; Lorente, G.; Duan, J. X.; Cai, X.; Mowday, A. M.; Guise, C. P.; Maroz, A.; Anderson, R. F.; Patterson, A. v.; Stachelek, G. C.; Glazer, P. M.; Matteucci, M. D.; Hart, C. P. Molecular and Cellular Pharmacology of the Hypoxia-Activated Prodrug TH-302. *Molecular Cancer Therapeutics* **2012**, *11* (3), 740-751. <https://doi.org/10.1158/1535-7163.MCT-11-0634>.
88. Hu, J.; van Valckenborgh, E.; Xu, D.; Menu, E.; de Raeve, H.; de Bryune, E.; Xu, S.; van Camp, B.; Handisides, D.; Hart, C. P.; Vanderkerken, K. Synergistic Induction of Apoptosis in Multiple Myeloma Cells by Bortezomib and Hypoxia-Activated Prodrug TH-302, in Vivo and in Vitro. *Molecular Cancer Therapeutics* **2013**, *12* (9), 1763-1773. <https://doi.org/10.1158/1535-7163.MCT-13-0123>.
89. Liapis, V.; Labrinidis, A.; Zinonos, I.; Hay, S.; Ponomarev, V.; Panagopoulos, V.; DeNichilo, M.; Ingman, W.; Atkins, G. J.; Findlay, D. M.; Zannettino, A. C. W.; Evdokiou, A. Hypoxia-Activated pro-Drug TH-302 Exhibits Potent Tumor Suppressive Activity and Cooperates with Chemotherapy against Osteosarcoma. *Cancer Letters* **2015**, *357* (1), 160-169. <https://doi.org/10.1016/j.canlet.2014.11.020>.
90. Meng, F.; Bhupathi, D.; Sun, J. D.; Liu, Q.; Ahluwalia, D.; Wang, Y.; Matteucci, M. D.; Hart, C. P. Enhancement of Hypoxia-Activated Prodrug TH-302 Anti-Tumor Activity by Chk1 Inhibition. *BMC Cancer* **2015**, *15* (1), 1-17. <https://doi.org/10.1186/s12885-015-1387-6>.

Chapter 1

91. Peeters, S. G. J. A.; Zegers, C. M. L.; Biemans, R.; Lieuwes, N. G.; van Stiphout, R. G. P. M.; Yaromina, A.; Sun, J. D.; Hart, C. P.; Windhorst, A. D.; van Elmpt, W.; Dubois, L. J.; Lambin, P. TH-302 in Combination with Radiotherapy Enhances the Therapeutic Outcome and Is Associated with Pretreatment [18F]HX4 Hypoxia PET Imaging. *Clinical Cancer Research* **2015**, *21* (13), 2984–2992. <https://doi.org/10.1158/1078-0432.CCR-15-0018>.
92. Sagar, J. K.; Tannock, I. F. Chemotherapy Rescues Hypoxic Tumor Cells and Induces Their Reoxygenation and Repopulation - An Effect That Is Inhibited by the Hypoxia-Activated Prodrug TH-302. *Clinical Cancer Research* **2015**, *21* (9), 2107–2114. <https://doi.org/10.1158/1078-0432.CCR-14-2298>.
93. Sun, J. D.; Liu, Q.; Ahluwalia, D.; Li, W.; Meng, F.; Wang, Y.; Bhupathi, D.; Ruprell, A. S.; Hart, C. P. Efficacy and Safety of the Hypoxia-Activated Prodrug TH-302 in Combination with Gemcitabine and Nab-Paclitaxel in Human Tumor Xenograft Models of Pancreatic Cancer. *Cancer Biology and Therapy* **2015**, *16* (3), 438–449. <https://doi.org/10.1080/15384047.2014.1003005>.
94. Ganjoo, K. N.; Cranmer, L. D.; Butrynski, J. E.; Rushing, D.; Adkins, D.; Okuno, S. H.; Lorente, G.; Kroll, S.; Langmuir, V. K.; Chawla, S. P. A Phase I Study of the Safety and Pharmacokinetics of the Hypoxia-Activated Prodrug TH-302 in Combination with Doxorubicin in Patients with Advanced Soft Tissue Sarcoma. *Oncology* **2011**, *80* (1–2), 50–56. <https://doi.org/10.1159/000327739>.
95. Weiss, G. J.; Infante, J. R.; Chiorean, E. G.; Borad, M. J.; Bendell, J. C.; Molina, J. R.; Tibes, R.; Ramanathan, R. K.; Lewandowski, K.; Jones, S. F.; Lacouture, M. E.; Langmuir, V. K.; Lee, H.; Kroll, S.; Burris, H. A. Phase 1 Study of the Safety, Tolerability, and Pharmacokinetics of TH-302, a Hypoxia-Activated Prodrug, in Patients with Advanced Solid Malignancies. *Clinical Cancer Research* **2011**, *17* (9), 2997–3004. <https://doi.org/10.1158/1078-0432.CCR-10-3425>.
96. Chawla, S. P.; Cranmer, L. D.; van Tine, B. A.; Reed, D. R.; Okuno, S. H.; Butrynski, J. E.; Adkins, D. R.; Hendifar, A. E.; Kroll, S.; Ganjoo, K. N. Phase II Study of the Safety and Antitumor Activity of the Hypoxia-Activated Prodrug TH-302 in Combination with Doxorubicin in Patients with Advanced Soft Tissue Sarcoma. *Journal of Clinical Oncology* **2014**, *32* (29), 3299–3306. <https://doi.org/10.1200/JCO.2013.54.3660>.
97. Weiss, G. J.; Lewandowski, K.; Oneall, J.; Kroll, S. Resolution of Cullen's Sign in Patient with Metastatic Melanoma Responding to Hypoxia-Activated Prodrug TH-302. *Dermatology Reports* **2011**, *3* (3), 1–2. <https://doi.org/10.4081/dr.2011.e56>.
98. Borad, M. J.; Reddy, S. G.; Bahary, N.; Uronis, H. E.; Sigal, D.; Cohn, A. L.; Schelman, W. R.; Stephenson, J.; Chiorean, E. G.; Rosen, P. J.; Ulrich, B.; Dragovich, T.; del Prete, S. A.; Rarick, M.; Eng, C.; Kroll, S.; Ryan, D. P. Randomized Phase II Trial of Gemcitabine plus TH-302 versus Gemcitabine in Patients with Advanced Pancreatic Cancer. *Journal of Clinical Oncology* **2015**, *33* (13), 1475–1481. <https://doi.org/10.1200/JCO.2014.55.7504>.
99. Tap, W. D.; Papai, Z.; van Tine, B. A.; Attia, S.; Ganjoo, K. N.; Jones, R. L.; Schuetze, S.; Reed, D.; Chawla, S. P.; Riedel, R. F.; Krarup-Hansen, A.; Toulmonde, M.; Ray-Coquard, I.; Hohenberger, P.; Grignani, G.; Cranmer, L. D.; Okuno, S.; Agulnik, M.; Read, W.; Ryan, C. W.; Alcindor, T.; del Muro, X. F. G.; Budd, G. T.; Tawbi, H.; Pearce, T.; Kroll, S.; Reinke, D. K.; Schöffski, P. Doxorubicin plus Evofosfamide versus Doxorubicin Alone in Locally Advanced, Unresectable or Metastatic Soft-Tissue Sarcoma (TH CR-406/SARCO21): An International, Multicentre, Open-Label, Randomised Phase 3 Trial. *The Lancet Oncology* **2017**, *18* (8), 1089–1103. [https://doi.org/10.1016/S1470-2045\(17\)30381-9](https://doi.org/10.1016/S1470-2045(17)30381-9).

Chapter 2

Hypoxia-activated prodrug derivatives of anti-cancer drugs: a patent review 2006 – 2021

Emilie Anduran, Ludwig J Dubois, Philippe Lambin & Jean-Yves Winum

Published in Expert Opinion on Therapeutic Patents, Volume 32, 2022 - Issue 1

Abstract

Introduction: The hypoxic tumour microenvironment represents a persistent obstacle in the treatment of most solid tumours. In the past years, significant efforts have been made to improve the efficacy of anti-cancer drugs. Therefore, hypoxia-activated prodrugs (HAPs) have attracted widespread interest as a therapeutic means to treat hypoxic tumour.

Areas covered: This updated review paper covers patents published between 2014 and 2020 on the developments of HAP derivatives of anti-cancer compounds.

Expert Opinion: Despite significant achievements in the development of HAP derivatives of anti-cancer compounds and although many clinical trials have been performed or are ongoing both as monotherapies and as part of combination therapies, there has currently no HAP anti-cancer agent been commercialized into the market. Unsuccessful clinical translation is partly due to the lack of patient stratification based on reliable biomarkers that are predictive of a positive response to hypoxia-targeted therapy.

Keywords:

hypoxia, tumour, anti-cancer compounds, hypoxia-activated prodrug, bioreductive prodrug.

Article highlights

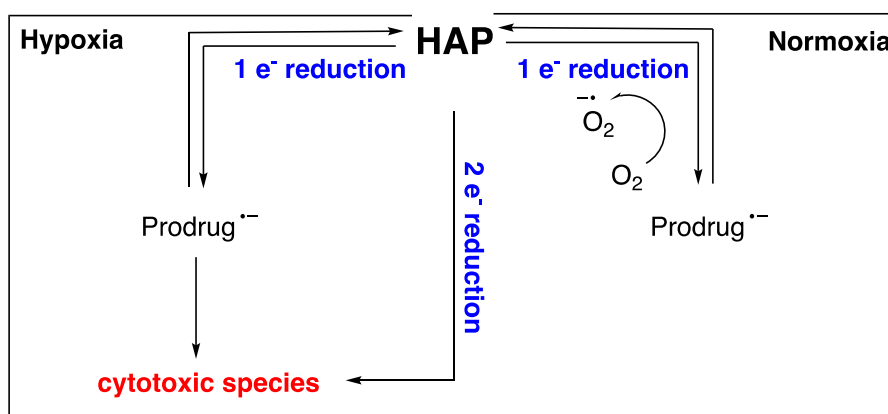
- Hypoxia is a common feature of most solid tumours and has been associated with poor patient outcome and aggressive metastatic phenotypes.
- Hypoxia-Activated Prodrugs (HAPs) are based on the selective release of toxic species upon reduction by reductive enzymes upon hypoxia.
- HAPs with tumour targeting properties have a better safety profile and anti-tumour activity.
- Failure of HAPs in clinical trials is due to the lack of reliable biomarkers that are predictive of the hypoxia-status of the tumour.
- In line with a personalized medicine approach, hypoxia-based biomarkers for patient selection are needed for translation from bench to bedside.

Introduction

With almost 9.6 million deaths per year, cancer is one of the leading causes of mortality worldwide.¹ Solid malignancies, which make up most of all human cancers, still challenge the best endeavours of researchers in the quest for the most effective treatment. One of fundamental features of solid tumours is intratumoural heterogeneity, which has multifactorial origins including genetic, epigenetic and microenvironmental factors.² Hypoxia, defined as a state of lowered oxygen tension (typically less than 1%), is a prevalent characteristic of the tumour microenvironment and one of the most important factors in negative clinical outcomes for cancer therapies.³ Through multiple mechanisms regulated, predominantly by the transcription factors HIFs (hypoxia-inducible factors), hypoxia drives tumorigenesis and contributes to aggressive proliferation, metastatic invasiveness and recurrence of tumour cells.^{4,5} It also allows tumour to evade the immune system,⁶⁻⁸ and mediates resistance to conventional chemo-, radio- and immunotherapy.⁹ In lieu of the critical role of hypoxia in anti-cancerous treatment failures, there has been significant interest to find therapeutic opportunities in exploiting intra-tumoural hypoxia in cancer therapy.¹⁰ Two main strategies could be considered in hypoxia-directed cancer therapy by making use of either the hypoxia-reducible conditions,¹¹ or key molecular targets that enable hypoxic tumour cells to proliferate and survive (HIF-1, HIF-2,¹² and their downstream targets such as CA IX for example^{13,14}).

Taking advantage of the redox potential difference between hypoxic and normoxic areas became a significant direction for researchers in the last 20 years to develop bioreductive prodrugs, named as hypoxia-activated prodrugs (HAP), to improve the efficacy of drugs that are ineffective against tumour cells in hypoxic microenvironments.¹⁵⁻¹⁸ Two decades of research have allowed to build a large overview within the HAPs landscape.¹⁵⁻¹⁸ The selectivity of HAPs with regard to hypoxia relies on a preferential activation in hypoxic versus well-oxygenated tissues, an easy diffusion within the hypoxic tumour areas, and the release of their active anti-neoplastic warhead which diffuses partially back into the aerobic fraction of the tumour to produce a cytotoxic effect on rapidly proliferating cells, creating a bystander effect.

The backbone for the design of HAP is a molecular motif used as cleavable entity which is susceptible to bioreduction. Deciphering the molecular mechanism of the different HAP classes suggests a mono- or di-electronic reduction activation process carried out by endogenous oxidoreductases. In the mono-electron reduction pathway, the HAP is reduced in an anion radical. Under normoxic conditions, the process is instantly quenched by oxygen leading to back-oxidation to the parent HAP with generation of superoxide radicals. Under hypoxic conditions, the reduction of HAP cannot be reversed, or further reduction reactions and fragmentation continue until the active effector is released.¹⁵⁻¹⁸ In contrast to mono-electronic reduction, the two-electron reduction pathway is an oxygen-independent activation pathway of the prodrug that leads directly or indirectly to the cytotoxic species. This pathway can also occur in normoxic tissue and causes dose-limiting toxicity (Scheme 1).



Scheme 1: General scheme for the reductive activation of HAP by one or two electrons

Among the five different chemical triggers susceptible to be enzymatically reduced under hypoxic conditions (nitro groups, quinones, aromatic and aliphatic *N*-oxides, or transition metals), three classes have been extensively studied up to the clinical stage such quinones, *N*-oxides and more particularly nitro-aromatics such as the 2-nitroimidazole scaffold.¹⁵ Depending on the hypoxic threshold needed for their activation, two subclasses of HAP have been defined. Class I are HAPs that required mild hypoxic condition (10 mmHg or less) to be activated (for example *N*-oxides HAP) and class II HAPs that are activated only under extreme hypoxic conditions (<5 mmHg) producing stable cytotoxic species which can enhance bystander effect¹⁹. On the characteristics of their design and activation mechanisms, these families and classes of HAPs have been discussed in details in some very recent review papers.¹⁵⁻¹⁸ Some representative HAPs (Figure 1) were subject to advanced clinical trials as monotherapy, but also in combination with radiotherapy or chemotherapy and have proven some benefit in phase 2 trials but all failed in phase 3 trials.

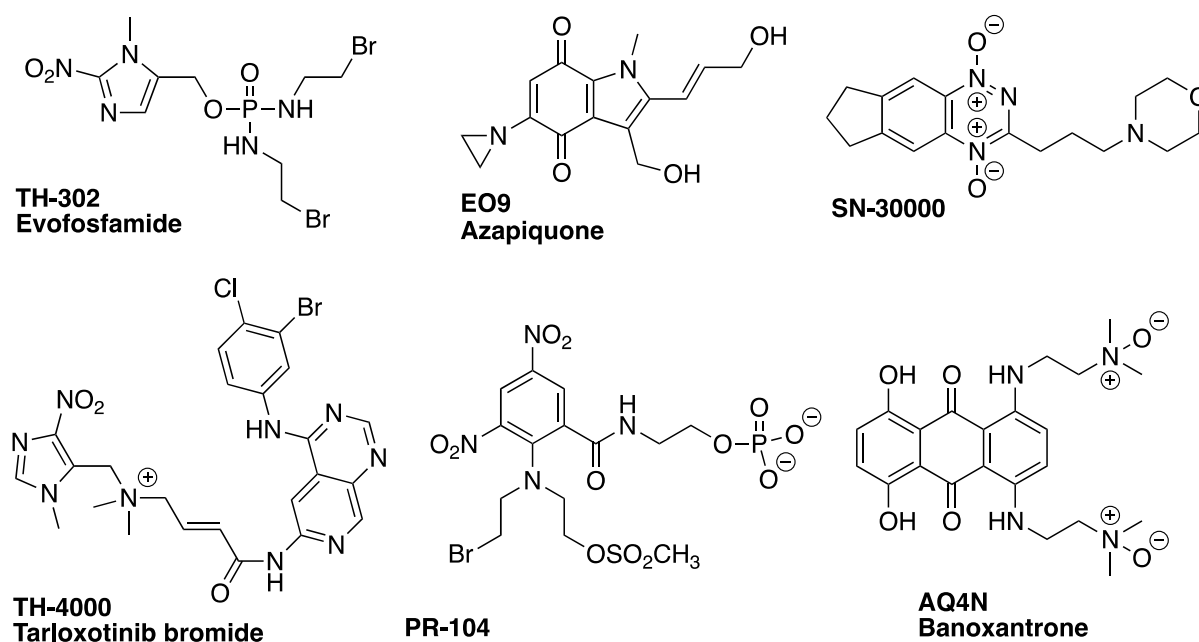


Figure 1: Structures of some representatives HAPs

Upon selective activation in hypoxic tissues, most of HAPs reported a release of cytotoxic species damaging the DNA. Nevertheless, HAPs of enzyme inhibitors with anti-cancer targets have been described in the last years.²⁰⁻²⁷ Although a major review paper on HAPs was published in 2019,¹⁵ the last patent overview related to HAPs has been reported in 2005 by Denny W.²⁸ This review summarizes patents claimed in recent years (2014-2020) regarding new generation of HAPs targeting critical component of hypoxic tumours.

Patent applications related to HAP

The patents on HAP have been retrieved by multiple search engines including Espacenet, Free patents online, Google patents and SciFinder. This section is only focusing on new HAP structures constituted of a hypoxia trigger linked to an anti-cancerous agent. Patent applications related to administration of a combination of known HAPs with anti-cancer drugs, or known HAPs encapsulated inside nanoparticles, are not considered.

In a patent of 2014 filed by Jinan Trio Pharmatech Co Ltd, hypoxia-activated prodrugs of *p*-nitroarylmethylcrizotinib (Figure 2) are reported as anti-tumour drugs against hepatocellular carcinoma.²⁹

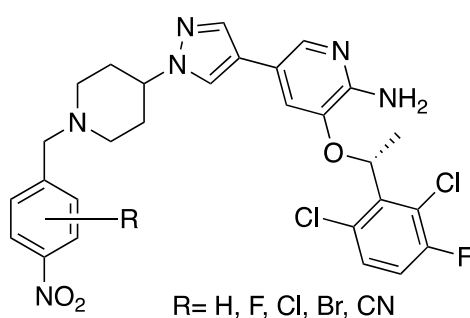


Figure 2: HAPs of *p*-nitroarylmethylcrizotinib

Exemplified with *p*-nitrobenzylcrizotinib (R=H), this compound was shown to display better water solubility, bioavailability, and biological stability compared to crizotinib, a multikinase inhibitor able to inhibit the growth of liver cancer tumours by targeting the activity of the hepatocyte growth factor receptor (c-MET, HGFR). The *in vivo* efficacy of *p*-nitrobenzylcrizotinib on the growth of Hep3B liver cancer tumours with low expression of c-MET and on the growth of MHCC97-H liver cancer tumours with high expression of c-MET was comparable between crizotinib and *p*-nitrobenzylcrizotinib. The beneficial effects of *p*-nitrobenzylcrizotinib are characterized by a better tissue distribution with selectivity for tumour tissue and by significant lower toxic adverse effects, mainly manifested in low damage to the intestinal mucosa and the degree of diarrhea, low weight loss after treatment, and low damage to liver function.²⁹

In 2017, Fei et al. disclosed HAP derivatives of Lenvatinib (Figure 3), a tyrosine kinase inhibitor (TKI) targeting vascular endothelial growth factor (VEGF) receptors VEGFR1 (FLT1), VEGFR2 (KDR), and VEGFR3 (FLT4). Different HAP derivatives are claimed in nitrofurane, nitrothiophene and nitrophenyl series.³⁰ These HAP compounds have been found to be not degraded under

normoxic conditions and to have low tyrosine kinase inhibitory activity. Target compounds demonstrated an inhibitory effect on the growth of human liver cancer HepG2 cell transplanted subcutaneously.

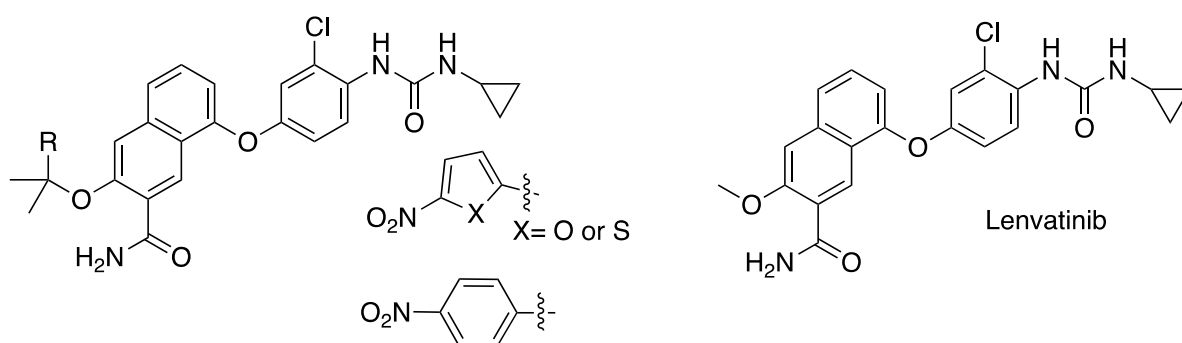


Figure 3: HAPs of Lenvatinib

In patent CN107417672A, Univ East China Normal claimed HAP derivatives based on 2,2-dimethyl-3-(2-nitroimidazolyl) propionic acid, that they exemplified with HAPs of paclitaxel (Figure 4).³¹ Good stability was observed in human plasma and *in vitro* nitroreductase experiments showed that paclitaxel can be quickly released. *In vitro* cytotoxicity assays reported moderate selectivity toward hypoxic H460 and HT29 tumour cells with selective ratios ranging from 1.1 to 2.2. toward hypoxic tumour cells.³²

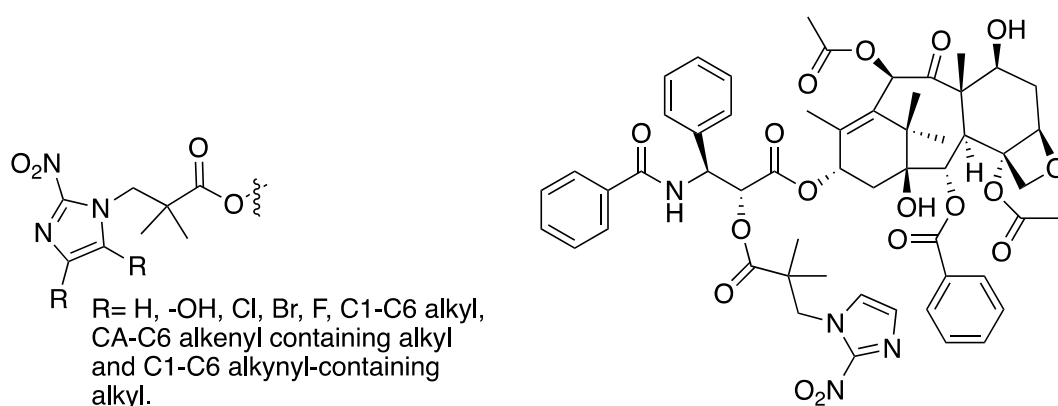


Figure 4: HAPs of Paclitaxel

In two patents from 2018, [33-34] Jiangsu Qianzhikang Biomedical Tech Co Ltd, reported HAP derivatives of the nucleoside anti-tumour drug gemcitabine, based on the structure of the phosphoramidate gemcitabine ProTide prodrug NUC-1031.³⁵ Compounds were designed by modifying the phenyl and/or benzyl group in NUC-1031, by R₁ and/or R₂ groups which can be either benzyl, alkyl or alkenyl residues, or a nitroaryl or heteroaryl bioreducible moiety. On the 21 compounds described in the patent applications, all HAPs, as exemplified by compound **1** (Figure 5), were shown to present a stronger *in vitro* cytotoxicity than gemcitabine or NUC-1031. Significant *in vivo* growth inhibition effects of these compounds on orthotopic or subcutaneous transplanted BxPC3 human pancreatic cancer cells in nude mice were demonstrated.

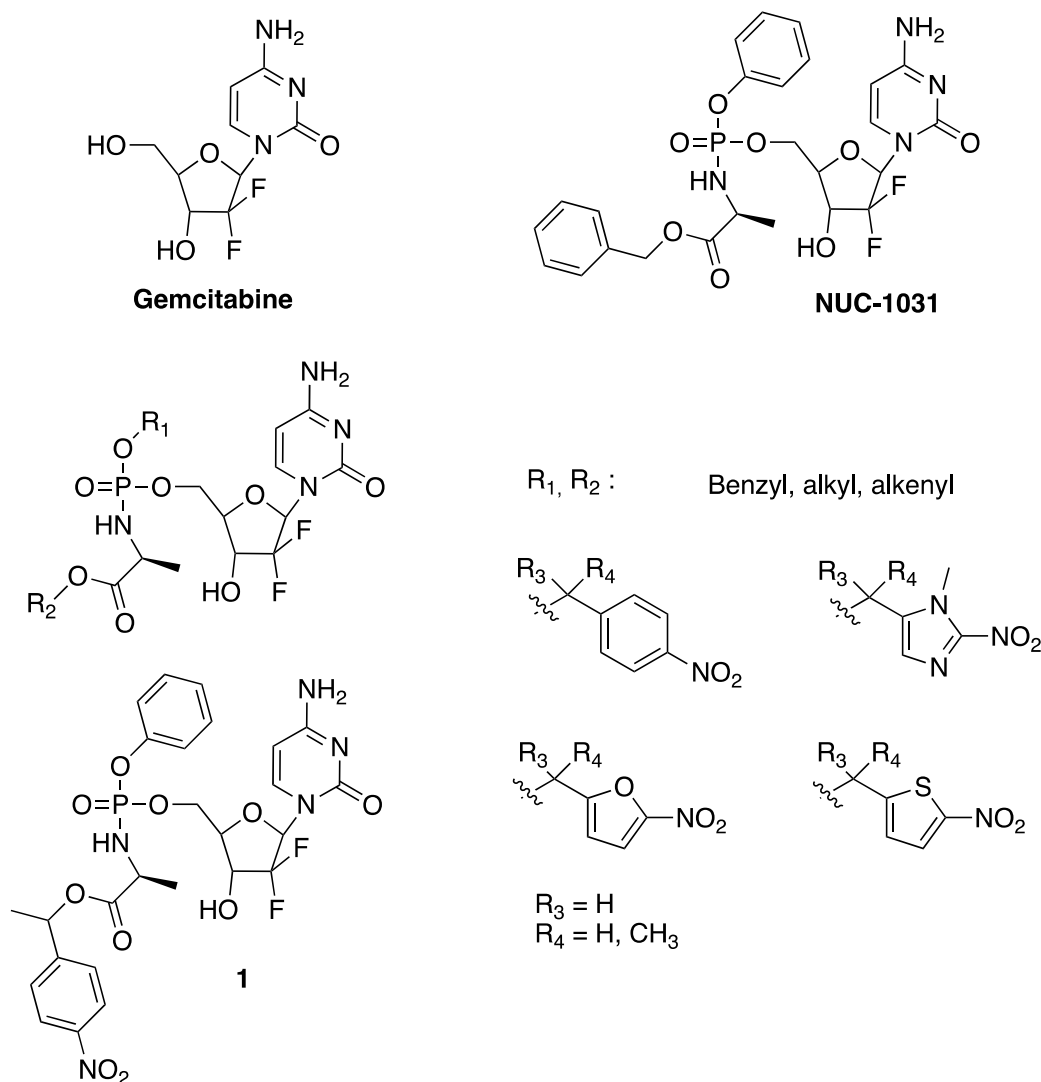


Figure 5: HAPs of gemcitabine prodrug.

In 2018, a patent application from Univ Guangzhou Medical reported the HAP derivative of doxorubicin where modification of the amino group located at the 3' position of doxorubicin is linked to a nitrogen mustard, at the para-position of phenyl bis(chloroethyl)amine), via a the bioreducible azo bond (Figure 6).³⁶ The authors demonstrated in B16 melanoma and 4T1 breast cancer cells, as well as in fibroblasts, that doxorubicin is released under hypoxic conditions and accumulates in the nucleus whereas under normoxic conditions, the prodrugs are mainly distributed in the lysosomes of the cells. These results indicate that the doxorubicin prodrug may enter the cell through endocytosis, and can be effectively transferred to the nucleus after activation by hypoxia, confirming the properties of hypoxia-induced nuclear targeted enrichment. Moreover, compared with normoxic conditions, this doxorubicin prodrug has higher and concentration-dependent cytotoxicity to both 4T1 and B16 cells under hypoxic conditions.³⁶

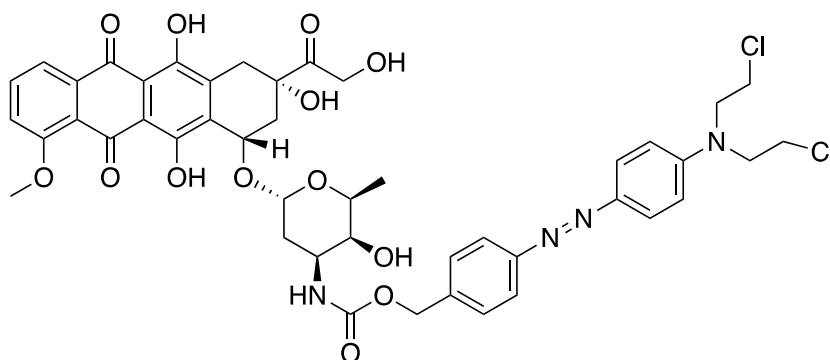


Figure 6: HAP of doxorubicin

In patents CN109721603 (A) and CN111925371 (A), Univ. Beijing Technology disclosed respectively in 2019 and 2020 the synthesis of quinone derivatives and 4-nitrophenyl derivative of O6-3-aminomethyl benzyl guanine (Figure 7) with the aim to target the DNA repair enzyme MGMT in hypoxic solid tumour cells and to overcome MGMT-mediated drug resistance, while reducing toxic adverse effects on normal tissues.³⁷⁻³⁸ The *in vitro* results show that upon treatment of SF767 and SF763 human brain glioma cells under hypoxia and normoxia, the prodrug system preferentially released active MGMT inhibitors upon hypoxia. No *in vivo* results are provided in the two patent applications.

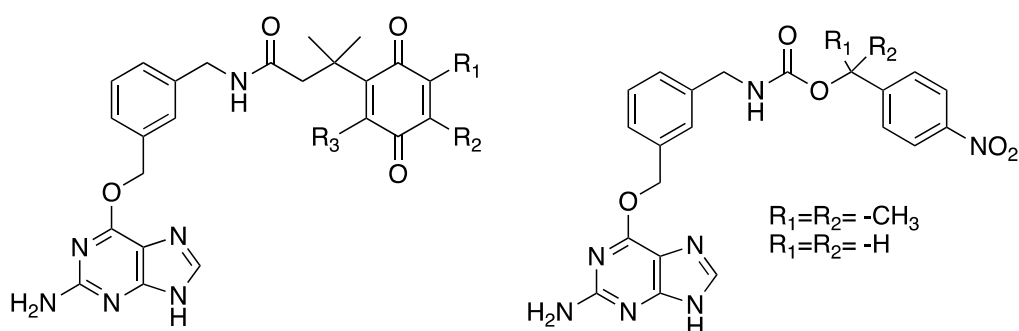


Figure 7: HAPs of O6-3-aminomethyl benzyl guanine

Univ. Shenyang Pharmaceutica disclosed in 2020 a patent application related to integrated prodrugs constituted for the exemplified compounds (Figure 8), of a photosensitizer (pyropheophorbide) and the nitrogen mustard prodrug activated by hypoxia PR104A, connected all together with a linker having a thioether, a monothioether or an ethyl group.³⁹ PR104A is connected to the linker via a carbonate bond and the photosensitizer, *via* an ester bond. This compound is able to give, in presence of 1, 2-Distearoyl-sn-glycero-3-phosphoethanolamine-poly(ethylene glycol) (DSPE-PEG), self-assembled nanometer drug delivery system. The main objective of this work is to elaborate on a safe and effective nano-drug delivery system for the combined delivery of hypoxia-activated prodrugs and photosensitizers. The dual mode of photo-induced electron transfer and reactive oxygen species under laser irradiation triggers selective drug release at the tumour site. Photodynamic therapy aggravates the hypoxia state of the tumour site and promotes hypoxia activation of the prodrug leading to an improved

synergistic therapeutic effect. Through an easy one step nano-precipitation process, easily scalable, authors obtained 100nm uniformly spherical nanoparticles having good colloidal stability. Nanoparticles with a thioketal derivative showed higher synergistic cytotoxicity than nanoparticles with a thio-ether derivative or with direct connection via ethyl group. The three prodrug nanoparticles showed higher cellular uptake efficiency than the pyropheophorbide solution. Pharmacokinetic studies showed that PEG-modified prodrug self-assembled nanoparticles have a significant prolonged plasma half-life compared to PR104A. The tissue distribution experiment of PEG-modified prodrug self-assembled nanoparticles revealed that the three type of nanoparticles accumulate in the tumour site through the EPR effect, with an increase of the fluorescent signal with time due to the prolonged blood circulation time. The *in vivo* anti-tumour experiment of PEG-modified prodrug self-assembled nanoparticles showed an inhibition of tumour growth to a certain extent under non-light. In contrast, laser-treated nanoparticles with thioketal derivative showed the best anti-tumour effect which can be attributed to their good stability, high tumour accumulation, and the fastest release of the light-triggered dual-mode PR104A.³⁹

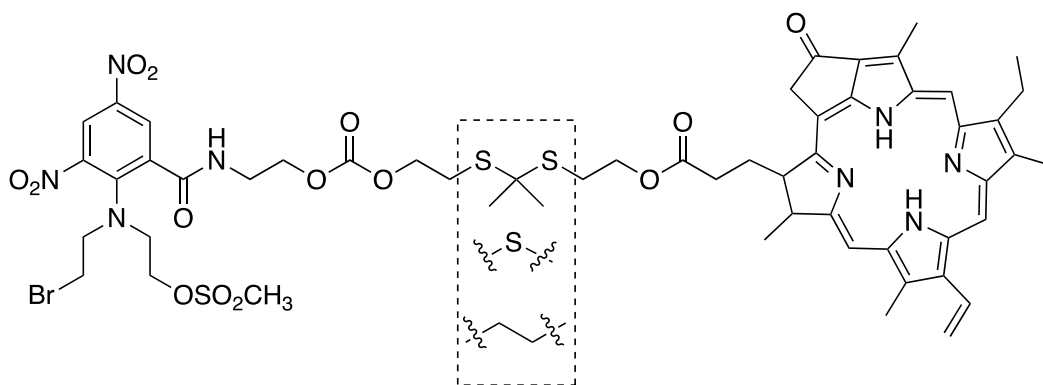


Figure 8: PR104A HAP conjugated with pyropheophorbide.

Conclusion

This review mainly focuses on hypoxia-activated prodrug related patents from 2014 to 2020. Tumour hypoxia poses a formidable challenge to therapeutic intervention. The last years, several patent applications have been delivered, showing that pharmaceutical companies and academic groups, essentially from China, were and are still very active in this field (Table 1). On the large number of HAP compounds described, the nitro (hetero)aromatic triggers are always considered as the best structural feature to achieve bioreductive properties. The majority of reported HAP compounds demonstrated better pharmacological properties compared to the parent anti-cancer compounds. Several *in vitro* and *in vivo* studies indicate hypoxia selectivity and therapeutic efficacy. To the best of our knowledge, none of these HAP derivatives are currently in clinical trials and it remains to be shown if these compounds are safe and effective. Companion diagnostics remain important for proper patient selection and to provide evidence of drug efficacy at early time points utilizing window-of-opportunity trials. By essence, the

number of patent applications in the field of HAP emphasize the hope that the exploitation of tumour hypoxia is still a promising area.

Table 1: Selected patent applications about HAP published during 2014-present

Patent Number (publication date)	Applicants	HAP trigger	Cytotoxic species / target
CN103570689A (2014-02-12)	Jinan Trio Pharmatech Co Ltd	Nitro-aromatic	Crizotinib / Tyrosine kinase c-MET
CN107513057A (2017-12-26)	Univ Nanjing Medica	Nitro-aromatic	Lenvatinib / Tyrosine kinase
CN107417672A (2017-12-01)	Univ East China Normal.	Nitro-aromatic	Paclitaxel / Tubulin
WO 2018028494A1 (2018-02-15)	Jiangsu Qianzhikang Biological Medicine Science And Tech Co Ltd	Nitro-aromatic	Gemcitabin / DNA
CN107698639A (2018-02-16)	Jiangsu Qianzhikang Biological Medicine Science and Tech Co Ltd	Nitro-aromatic	Gemcitabin / DNA
CN108395460A (2018-08-14)	Univ Guangzhou Medical	Diaryl-diazene	Doxorubicin – nitrogen mustard / DNA
CN109721603A (2019-05-07)	Univ Beijing Technology	Quinone	O6-3-aminomethyl benzyl guanine / DNA repair enzyme MGMT
CN111135299A (2020-05-12)	Univ Shenyang Pharmaceutica	Nitro-aromatic	PR104-A – Photosensitizer / DNA
CN111925371A (2020-11-13)	Univ Beijing Technology	Nitro-aromatic	O6-3-aminomethyl benzyl guanine / DNA repair enzyme MGMT

Expert opinion

Even if HAPs were successful *in vitro* and *in vivo*, they are yet to achieve successful results in clinical setting largely. This is due in clinical studies to the lack of reliable biomarkers that are predictive of a positive response to hypoxia-targeted therapy which implies to identify and select patients with hypoxic tumours prior to enrolment.⁴⁰⁻⁴³ Although the increasing number of patent applications (Table 1) within the field of hypoxia-activated prodrugs, it remains utmost important to develop companion diagnostics in parallel already in preclinical settings to proof targeting efficacy, i.e reduction in hypoxic target expression or hypoxic fraction itself, at early time points after treatment start. Furthermore, proper executed preclinical toxicity studies need to be executed to proof absence of off-target effects. These strategies will expedite successful clinical trials. Despite the difficulties and roadblocks, HAPs remain powerful tools and a

Chapter 2

promising therapeutic strategy in cancer research in particular in combination with immunotherapy.⁴⁴ There is indeed converging evidence indicating that hypoxia can cause tumor resistance to immunotherapy by several mechanisms, including high concentration of ADP a very immunosuppressive molecule, accumulation of Treg, tumor associated macrophages (M2-like phenotype), IL10, and VEGF.⁴⁵ Using novel delivery strategies might further improve the selectivity and efficiency of hypoxia-targeted therapies and should therefore be taken into consideration for future therapeutic design.

References

Papers of special note have been highlighted as:

* of interest

** of considerable interest

1. World Health Organisation Home Page. <https://www.who.int/news-room/fact-sheets/detail/cancer>
2. Dagogo-Jack, I.; Shaw, A. T. Tumor heterogeneity and resistance to cancer therapies. *Nat. Rev. Clin. Oncol.* **2018**, *15* (2), 81-94. <https://doi.org/10.1038/nrclinonc.2017.166>.
3. Vaupel, P. Hypoxia and aggressive tumor phenotype: implications for therapy and prognosis. *Oncologist* **2008**, *3*, 21–26. <https://doi.org/10.1634/theoncologist.13-s3-21>.
4. Jing, X.; Yang, F.; Shao, C. et al. Role of hypoxia in cancer therapy by regulating the tumor microenvironment. *Mol. Cancer* **2019**, *18* (1), 157. <https://doi.org/10.1186/s12943-019-1089-9>.
5. Harris, A. L. Hypoxia: a key regulatory factor in tumour growth. *Nat. Rev. Cancer* **2002**, *2* (1), 38–47. <https://doi.org/10.1038/nrc704>.
6. You, L.; Wu, W.; Wang, X., et al. The role of hypoxia-inducible factor 1 in tumor immune evasion. *Med. Res. Rev.* **2020**, *41* (3), 1622–1643. <https://doi.org/10.1002/med.21771>.
7. Pietrobon, V.; Marincola, F. M. Hypoxia and the phenomenon of immune exclusion. *J. Transl. Med.* **2021**, *19* (1), 9. <https://doi.org/10.1186/s12967-020-02667-4>.
8. Abou Khouzam, R.; Brodaczewska, K.; Filipiak, A. et al. Tumor Hypoxia Regulates Immune Escape/Invasion: Influence on Angiogenesis and Potential Impact of Hypoxic Biomarkers on Cancer Therapies. *Front. Immunol.* **2021**, *11*, 613114. <https://doi.org/10.3389/fimmu.2020.613114>.
9. Luo, W.; Wang, Y. Hypoxia Mediates Tumor Malignancy and Therapy Resistance. in *Hypoxia and Cancer Metastasis, Advances in Experimental Medicine and Biology*, D. M. Gilkes ed., vol. 1136; Springer, Cham, **2019**; pp 1-18. https://doi.org/10.1007/978-3-030-12734-3_1.
10. Brown, J. M.; Wilson, W. R. Exploiting tumour hypoxia in cancer treatment. *Nat. Rev. Cancer* **2004**, *4* (6), 437-447. <https://doi.org/10.1038/nrc1367>.
* A comprehensive summary about treatment strategy exploiting tumor hypoxia
11. Jackson, R. K.; Liew, L. P.; Hay, M. P. Overcoming Radioresistance: Small Molecule Radiosensitisers and Hypoxia-activated Prodrugs. *Clin. Oncol. (R. Coll. Radiol.)* **2019**, *31* (5), 290-302. <https://doi.org/10.1016/j.clon.2019.02.004>.
12. Wigerup, C.; Pålman, S.; Bexell, D. Therapeutic targeting of hypoxia and hypoxia-inducible factors in cancer. *Pharmacol. Ther.* **2016**, *164*, 152-169. <https://doi.org/10.1016/j.pharmthera.2016.04.009>.
13. Dubois, L. J.; Niemans, R.; van Kuijk, S. J. et al. New ways to image and target tumour hypoxia and its molecular responses. *Radiother Oncol.* **2015**, *116* (3), 352-357. <https://doi.org/10.1016/j.radonc.2015.08.022>.
14. Supuran, C. T. Experimental Carbonic Anhydrase Inhibitors for the Treatment of Hypoxic Tumors. *J. Exp. Pharmacol.* **2020**, *12*, 603-617. <http://doi.org/10.2147/JEP.S265620>.
15. Sharma, A.; Arambula, J. F.; Koo, S. et al. Hypoxia-targeted drug delivery. *Chem. Soc. Rev.* **2019**, *48* (3), 771-813. <https://doi.org/10.1039/C8CS00304A>.
** A comprehensive review on Hypoxia-targeted drug delivery
16. Su, M. X.; Zhang, L. L.; Huang, Z. J. et al. Investigational Hypoxia-Activated Prodrugs: Making Sense of Future Development. *Curr. Drug Targets* **2019**, *20* (6), 668-678. <https://doi.org/10.2174/1389450120666181123122406>.
17. Baran, N.; Konopleva, M. Molecular Pathways: Hypoxia-Activated Prodrugs in Cancer Therapy. *Clin. Cancer Res.* **2017**, *23* (10), 2382-2390. <https://doi.org/10.1158/1078-0432.ccr-16-0895>.

Chapter 2

18. Phillips, R. M. Targeting the hypoxic fraction of tumours using hypoxia-activated prodrugs. *Cancer Chemother. Pharmacol.* **2016**, 77 (3), 441-457. <https://doi.org/10.1007/s00280-015-2920-7>.
19. Foehrenbacher, A.; Secomb, T. W.; Wilson, W. R. et al. Design of optimized hypoxia-activated prodrugs using pharmacokinetic/pharmacodynamic modelling. *Front Oncol* **2013**, 3, 314. <https://doi.org/10.3389/fonc.2013.00314>.
20. Dickson, B. D.; Wong, W. W.; Wilson, W. R. et al. Studies Towards Hypoxia-Activated Prodrugs of PARP Inhibitors. *Molecules* **2019**, 24 (8), 1559. <https://doi.org/10.3390/molecules24081559>.
21. Liew, L. P.; Singleton, D. C.; Wong, W. W. et al. Hypoxia-Activated Prodrugs of PERK Inhibitors. *Chem. Asian. J.* **2019**, 14 (8), 1238-1248. <https://doi.org/10.1002/asia.201801826>.
22. Bielec, B.; Schueffl, H.; Terenzi, A. et al. Development and biological investigations of hypoxia-sensitive prodrugs of the tyrosine kinase inhibitor crizotinib. *Bioorg. Chem.* **2020**, 99, 103778. <https://doi.org/10.1016/j.bioorg.2020.103778>.
23. de Simone, G.; Vitale, R. M.; di Fiore, A. et al. Carbonic anhydrase inhibitors: Hypoxia-activatable sulfonamides incorporating disulfide bonds that target the tumor-associated isoform IX. *J. Med. Chem.* **2006**, 49, 5544-5551. <https://doi.org/10.1021/jm060531j>.
24. Nocentini, A.; Trallori, E.; Singh, S. et al. 4-Hydroxy-3-nitro-5-ureido-benzenesulfonamides Selectively Target the Tumor-Associated Carbonic Anhydrase Isoforms IX and XII Showing Hypoxia-Enhanced Antiproliferative Profiles. *J. Med. Chem.* **2018**, 61, 10860-10874. <https://doi.org/10.1021/acs.jmedchem.8b01504>.
25. Aspatwar, A.; Parvathaneni, N. K.; Barker, H. et al. Design, synthesis, in vitro inhibition and toxicological evaluation of human carbonic anhydrases I, II and IX inhibitors in 5-nitroimidazole series. *J. Enzyme Inhib. Med. Chem.* **2020**, 35, 109-117. <https://doi.org/10.1080/14756366.2019.1685510>.
26. van Kuijk, S. J. A.; Parvathaneni, N. K.; Niemans, R. et al. New approach of delivering cytotoxic drugs towards CAIX expressing cells: A concept of dual-target drugs. *Eur. J. Med. Chem.* **2017**, 127, 691-702. <https://doi.org/10.1016/j.ejmech.2016.10.037>.
27. Aspatwar, A.; Becker, H. M.; Parvathaneni, N. K. et al. Nitroimidazole-based inhibitors DTP338 and DTP348 are safe for zebrafish embryos and efficiently inhibit the activity of human CA IX in *Xenopus* oocytes. *J. Enzyme Inhib. Med. Chem.* **2018**, 33, 1064-1073. <https://doi.org/10.1080/14756366.2018.1482285>.
28. Denny, W. A. Hypoxia-activated anticancer drugs. *Expert. Opin. Ther. Pat.* **2005**, 15 (6), 635-646. <http://dx.doi.org/10.1517/13543776.15.6.635>.
29. Yinjie, H.; Wanhu, L.; Fang, Q. et al. Para-nitro aromatic methyl crizotinib hypoxia-activated prodrug for anticancer drugs. CN103570689A, **2014**.
30. Fei, L.; Dongyin, C.; Lei, Y. et al. Hypoxia-activated prodrug of lenvatinib and application of hypoxia activated prodrug. CN107513057A, **2017**.
31. Wei, L.; Chen, J.; Shuai, W. et al. Hypoxic activation prodrug based on 2,2-dimethyl-3-(2-nitroimidazolyl) propionic acid. CN107417672A, **2017**.
32. Qiumeng, Z.; Chen, J.; Yu, J. et al. Synthesis of New Branched 2-Nitroimidazole as a Hypoxia Sensitive Linker for Ligand-Targeted Drugs of Paclitaxel. *ACS Omega* **2018**, 3 (8), 8813-8818. <https://doi.org/10.1021/acsomega.8b01208>.
33. Fei, L.; Xinji, Z.; Yi, Z. N-formate hypoxic activation prodrug of gemcitabine phosphate and application of prodrug. CN107698639A, **2018**.
34. Fei, L. Gemcitabine prodrug and application thereof. WO2018028494A1, **2018**.
35. Slusarczyk, M.; Lopez, M. H.; Balzarini, J. et al. Application of ProTide technology to gemcitabine: a successful approach to overcome the key cancer resistance mechanisms leads to a new agent (NUC-1031) in clinical development. *J. Med. Chem.* **2014**, 57 (4), 1531-1542. <https://doi.org/10.1021/jm401853a>.
36. Shiyang, L.; Xueyan, J.; Hong, C. et al. Hypoxia activation doxorubicin prodrug and preparation method thereof. CN108395460A, **2018**.

37. Guohui, S.; Weinan, X.; Xiaodong, S. et al. Inhibitor of low-oxygen targeted tumor cell DNA repair enzyme methylguanine methyl transferase (MGMT), and preparation method and application of inhibitor. CN109721603A, **2019**.
 38. Guohui, S.; Yaxin, H.; Zhaoqi, H. et al. Nitrobenzene substituted O6-3-aminomethylbenzylguanine, and preparation method and application thereof. CN111925371A, **2020**.
 39. Zhonggui, H.; Jin, S.; Dongyang, Z. et al. Construction of photosensitizer-hypoxia activated prodrug integrated prodrug self-assembled nanoparticles. CN111135299A, **2020**.
 40. Lindner, L. H. Hypoxia-activated prodrug: an appealing preclinical concept yet lost in clinical translation. *Lancet Oncol.* **2017**, *18* (8), 991–993. [https://doi.org/10.1016/s1470-2045\(17\)30401-1](https://doi.org/10.1016/s1470-2045(17)30401-1).
 41. Spiegelberg, L.; Houben, R.; Niemans, R. et al. Hypoxia-activated prodrugs and (lack of) clinical progress: the need for hypoxia-based biomarker patient selection in phase III clinical trials. *Clin. Transl. Radiat. Oncol.* **2019**, *15*, 62–69. <https://doi.org/10.1016/j.ctro.2019.01.005>.
 42. Yang, L.; West, C. M. L. Hypoxia gene expression signatures as predictive biomarkers for personalising radiotherapy. *Br. J. Radiol.* **2019**, *92* (20180036), 1–9. <https://doi.org/10.1259/bjr.20180036>.
 43. Sanduleanu, S.; Jochems, A.; Upadhaya, T. et al. Non-invasive imaging prediction of tumor hypoxia: A novel developed and externally validated CT and FDG-PET-based radiomic signatures. *Radiother. Oncol.* **2020**, *153*, 97-105. <https://doi.org/10.1016/j.radonc.2020.10.016>.
 44. Salem, A.; Asselin, M. C.; Reymen, B. et al. Targeting Hypoxia to Improve Non-Small Cell Lung Cancer Outcome. *J. Natl. Cancer Inst.* **2018**, *110* (1), 14–30. <https://doi.org/10.1093/jnci/djx160>.
 45. Wang, B.; Zhao, Q.; Zhang, Y.; Liu, Z.; Zheng, Z.; Liu, S.; Meng, L.; Xin, Y.; Jiang, X. Targeting hypoxia in the tumor microenvironment: a potential strategy to improve cancer immunotherapy. *J. Exp. Clin. Cancer Res.* **2021**, *40* (1), 24. <https://doi.org/10.1186/s13046-020-01820-7>.
 46. Spiegelberg, L.; Van Hoof, S. J.; Biemans, R. et al. Evofosfamide sensitizes esophageal carcinomas to radiation without increasing normal tissue toxicity. *Radiother. Oncol.* **2019**, *141*, 247–255. <https://doi.org/10.1016/j.radonc.2019.06.034>.
 47. Nytko, K. J.; Grgic, I.; Bender, S. et al. The hypoxia-activated prodrug evofosfamide in combination with multiple regimens of radiotherapy *Oncotarget* **2017**, *8* (14), 23702–23712. <https://doi.org/10.18632/oncotarget.15784>.
 48. Meng, F.; Evans, J. W.; Bhupathi, D. et al. Molecular and cellular pharmacology of the hypoxia-activated prodrug TH-302. *Mol. Cancer Ther.* **2012**, *11* (3), 740–751. <https://doi.org/10.1158/1535-7163.mct-11-0634>.
 49. Hong, C. R.; Dickson, B. D.; Jaiswal, J. K. et al. Cellular pharmacology of evofosfamide (TH-302): a critical re-evaluation of its bystander effects. *Biochem. Pharmacol.* **2018**, *156*; 265–280. <https://doi.org/10.1016/j.bcp.2018.08.027>.
 50. Hong, C. R.; Wilson, W. R.; Hicks, K. O. An intratumor pharmacokinetic/ pharmacodynamic model for the hypoxia-activated prodrug evofosfamide (TH-302): monotherapy activity is not dependent on a bystander effect. *Neoplasia* **2019**, *21* (2), 159–171. <https://doi.org/10.1016/j.neo.2018.11.009>.
 51. Li, Y.; Zhao, L.; Li, X. F. The hypoxia-activated prodrug TH-302: exploiting hypoxia in cancer therapy. *Front. Pharmacol.* **2021**, *12*, 636892. <https://doi.org/10.3389/fphar.2021.636892>.
- * Comprehensive review paper on TH-302.
52. Tap, W. D.; Papai, Z.; Van Tine, B. A. et al. Doxorubicin plus evofosfamide versus doxorubicin alone in locally advanced, unresectable or metastatic soft-tissue sarcoma (TH CR-406/SARC021): an international, multicentre, open-label, randomised phase 3 trial. *Lancet Oncol.* **2017**, *18* (8), 1089–1103. [https://doi.org/10.1016/S1470-2045\(17\)30381-9](https://doi.org/10.1016/S1470-2045(17)30381-9).

Chapter 2

53. Van Cutsem, E.; Lenz, H. J.; Furuse, J. et al. MAESTRO: a randomized, double-blind phase III study of evofosfamide (Evo) in combination with gemcitabine (Gem) in previously untreated patients (pts) with metastatic or locally advanced unresectable pancreatic ductal adenocarcinoma (PDAC). *J. Clin. Oncol.* **2016**, *34* (15), 4007. http://dx.doi.org/10.1200/JCO.2016.34.15_suppl.4007.
54. Smaill, J. B.; Patterson, A. V.; Denny, W. A. et al. Prodrug forms of kinase inhibitors and their use in therapy. WO2010104406A1, **2010**.
55. Smaill, J. B.; Patterson, A. V.; Lu, G. L. et al. Kinase inhibitors, prodrug forms thereof and their use in therapy. WO2011028135A1, **2011**.
56. Liu, S. V.; Villaruz, L. C.; Lee, V. H. F. et al. LBA61 First analysis of RAIN-701: study of tarloxotinib in patients with non-small cell lung cancer (NSCLC) EGFR Exon 20 insertion, HER2-activating mutations & other solid tumours with NRG1/ERBB gene fusions. *Ann. Oncol.* **2020**, *31* (4), S1189. <https://doi.org/10.1016/j.annonc.2020.08.2294>.
57. Nishino, M.; Suda, K.; Koga, T. et al. Activity of tarloxotinib-E in cells with EGFR exon-20 insertion mutations and mechanisms of acquired resistance. *Thorac. Cancer.* **2021**, *12* (10), 1511–1516. <https://doi.org/10.1111/1759-7714.13931>.
58. Estrada-Bernal, A.; Le, A. T.; Doak, A. E. et al. Tarloxotinib is a hypoxia-activated Pan-HER kinase inhibitor active against a broad range of HER-family oncogenes. *Clin. Cancer Res.* **2021**, *27* (5), 1463–1475. <https://doi.org/10.1158/1078-0432.ccr-20-3555>.
59. Xueying, S.; Zongxia, F.; Yanfang, G. et al. An m-nitroarylmethoxy camptothecin anoxic activation prodrug for antitumor drugs. CN102746316(A), **2012**.
60. Yinjie, H.; Wanhu, L.; Fang, Q. et al. Para-nitro aromatic methyl crizotinib hypoxia-activated prodrug for anticancer drugs. CN103570689A, **2014**.
61. Fei, L.; Dongyin, C.; Lei, Y. et al. Hypoxia-activated prodrug of lenvatinib and application of hypoxia activated prodrug. CN107513057A, **2017**.
62. Wei, L.; Chen, J.; Shuai, W. et al. Hypoxic activation prodrug based on 2,2-dimethyl-3-(2-nitroimidazolyl) propionic acid. CN107417672A, **2017**.
63. Qiumeng, Z.; Chen, J.; Yu, J. et al. Synthesis of new branched 2-nitroimidazole as a hypoxia sensitive linker for ligand-targeted drugs of paclitaxel. *ACS Omega* **2018**, *3* (8), 8813–8818. <https://doi.org/10.1021/acsomega.8b01208>.
64. Fei, L.; Xinji, Z.; Yi, Z. N-formate hypoxic activation prodrug of gemcitabine phosphate and application of prodrug. CN107698639A, **2018**.
65. Fei, L. Gemcitabine protide and application thereof. WO2018028494A1, **2018**.
66. Slusarczyk, M.; Lopez, M. H.; Balzarini, J. et al. Application of ProTide technology to gemcitabine: a successful approach to overcome the key cancer resistance mechanisms leads to a new agent (NUC-1031) in clinical development. *J. Med. Chem.* **2014**, *57* (4), 1531–1542. <https://doi.org/10.1021/jm401853a>.
67. Shiyong, L.; Xueyan, J.; Hong, C. et al. Hypoxia activation doxorubicin prodrug and preparation method thereof. CN108395460A, **2018**.
68. Guohui, S.; Weinan, X.; Xiaodong, S. et al. Inhibitor of low-oxygen targeted tumor cell DNA repair enzyme methylguanine methyl transferase (MGMT), and preparation method and application of inhibitor. CN109721603A, **2019**.
69. Guohui, S.; Yaxin, H.; Zhaoqi, H. et al. Nitrobenzene substituted O6-3-aminomethylbenzylguanine, and preparation method and application thereof. CN111925371A, **2020**.

70. Huang, X.; Sun, Z.; Zhuang, J. et al. Pyridinium-modified prodrug small molecule containing different nitroaromatic heterocycles. CN110437281A, **2019**.
71. Minchinton, A.; Kyle, A.; Evans, J. et al. DNA-PK inhibiting compounds. WO2021050059A1, **2021**.
72. Lindner, L. H. Hypoxia-activated prodrug: an appealing preclinical concept yet lost in clinical translation. *Lancet Oncol.* **2017**, *18* (8), 991–993. [https://doi.org/10.1016/s1470-2045\(17\)30401-1](https://doi.org/10.1016/s1470-2045(17)30401-1).
73. Spiegelberg, L.; Houben, R.; Niemans, R. et al. Hypoxia-activated prodrugs and (lack of) clinical progress: the need for hypoxia-based biomarker patient selection in phase III clinical trials. *Clin. Transl. Radiat. Oncol.* **2019**, *15*, 62–69. <https://doi.org/10.1016/j.ctro.2019.01.005>.
74. Yang, L.; West, C. M. L. Hypoxia gene expression signatures as predictive biomarkers for personalising radiotherapy. *Br. J. Radiol.* **2019**, *92*, 20180036. <https://doi.org/10.1259/bjr.20180036>.
75. Sanduleanu, S.; Jochems, A.; Upadhaya, T. et al. Non-invasive imaging prediction of tumor hypoxia: a novel developed and externally validated CT and FDG-PET-based radiomic signatures. *Radiother. Oncol.* **2020**, *153*, 97–105. <https://doi.org/10.1016/j.radonc.2020.10.016>.
76. Salem, A.; Asselin, M. C.; Reymen, B. et al. Targeting hypoxia to improve non-small cell lung cancer outcome. *J. Natl. Cancer Inst.* **2018**, *110*, (1), 14– 30. <https://doi.org/10.1093/jnci/djx160>.
77. Wang, B.; Zhao, Q.; Zhang, Y. et al. Targeting hypoxia in the tumor microenvironment: a potential strategy to improve cancer immunotherapy. *J. Exp. Clin. Cancer Res.* **2021**, *40* (1), 24. <https://doi.org/10.1186/s13046-020-01820-7>.
78. Fu, Z.; Mowday, A. M.; Smaill, J. B. et al. Tumour hypoxia-mediated immunosuppression: mechanisms and therapeutic approaches to improve cancer immunotherapy. *Cells.* **2021**, *10* (5), 1006. <https://doi.org/10.3390/cells10051006>.

Chapter 3

Hypoxia-activated prodrug derivatives of carbonic anhydrase inhibitors in benzenesulfonamide series: synthesis and biological evaluation

Emilie Anduran, Ashok Aspatwar, Nanda-Kumar Parvathaneni, Dennis Suylen, Silvia Bua, Alessio Nocentini, Seppo Parkkila, Claudiu T. Supuran, Ludwig Dubois, Philippe Lambin and Jean-Yves Winum.

Published in *Molecules* 2020, 25(10), 2347

Abstract

Hypoxia, a common feature of solid tumours microenvironment, is associated with an aggressive phenotype and is known to cause resistance to anticancer chemo- and radiotherapies. Tumour-associated carbonic anhydrases isoform IX (hCA IX), which is upregulated under hypoxia in many malignancies participating to the microenvironment acidosis, represents a valuable target for drug strategy against advanced solid tumours. To overcome cancer cell resistance and improve efficacy of therapeutics, the use of bio-reducible prodrugs also known as Hypoxia-activated prodrugs (HAPs), represents an interesting strategy to be applied to target hCA IX isozyme through the design of selective CA IX inhibitors (CAIs). Here we report the design, synthesis and biological evaluations including CA inhibition assays, toxicity assays on zebrafish and viability assays on human cell lines (HT29 and HCT116) of a new HAP-CAIs harboring different bio-reducible moieties in nitroaromatic series and a benzenesulfonamide warhead to target hCA IX. CA inhibition assays of this compound series showed a slight selectivity against hCA IX versus the cytosolic off-target hCA II and hCA I isozymes. Toxicity and viability assays have highlighted that the compound bearing the 2- nitroimidazole moiety possesses the lowest toxicity (LC₅₀ of 1400 µM) and shows interesting results on viability assays.

Introduction

Intratumoral heterogeneity, a main feature of solid tumors, is one of the causes of the intractability of cancers.¹ There are multiple mechanisms driving tumor heterogeneity including genetic, epigenetic and microenvironmental factors such as hypoxia.² The presence of oxygen deprivation areas (typically less than 1%), defined as hypoxic domains, and resulting from inadequate tumor vascularization, have been identified in a wide variety of human tumours.³ The adaptive cellular response to low oxygen tensions is coordinated by hypoxia inducible transcription factors HIF-1 which activate gene expression programs controlling multiple responses.⁴ Among them are found the change in glucose metabolism towards anaerobic glycolysis (Warburg effect), which causes a decrease of pH of the tumor microenvironment.⁵ Several key proteins and buffer systems,⁶ including monocarboxylate transporters (MCTs), isoforms of anion exchanger, $\text{Na}^+/\text{HCO}_3^-$ co-transporters, Na^+/H^+ exchangers, and carbonic anhydrases (CAs) isoforms IX and XII are involved in this pH regulatory process, to maintain a physiological intracellular pH accompanied with extracellular acidification.⁷ This acidosis strongly contributes to malignant progression, aggressive phenotype, and resistance to therapy (chemotherapy and radiation) of the cancer cells, leading to a poor prognosis regardless of treatment.⁸

The hypoxic microenvironment of solid tumors has attracted significant attention as a target which can be exploited in drug design for the development of novel anticancer or imaging agents.⁹

Two approaches have been considered in the literature: the first approach consists of the inhibition of molecular targets necessary for the survival of hypoxic cells, particularly carbonic anhydrase IX and XII. A wealth of research depicts hCA IX and hCA XII as biomarkers and therapeutic targets for various cancer types and both of these enzymes are associated with cancer progression, metastasis, and impaired therapeutic response. The development of small molecules as specific CA IX inhibitors represents a successful field with several potent inhibitors reported so far.¹⁰⁻¹³ The second approach is based on the exploitation of the redox potential, between hypoxic and normoxic areas for the development of prodrugs that activate selectively in a highly reducing hypoxic environment (Hypoxia Activated Prodrugs, HAP).¹⁴ HAPs are hypothesized to improve the therapeutic index of drugs that are ineffective against tumor cells in hypoxic microenvironments. The potential of HAPs is often evaluated clinically in combination with other cancer treatment (chemotherapy or radiotherapy) to affect both the normoxic and hypoxic fraction of the tumour.¹⁴⁻¹⁶

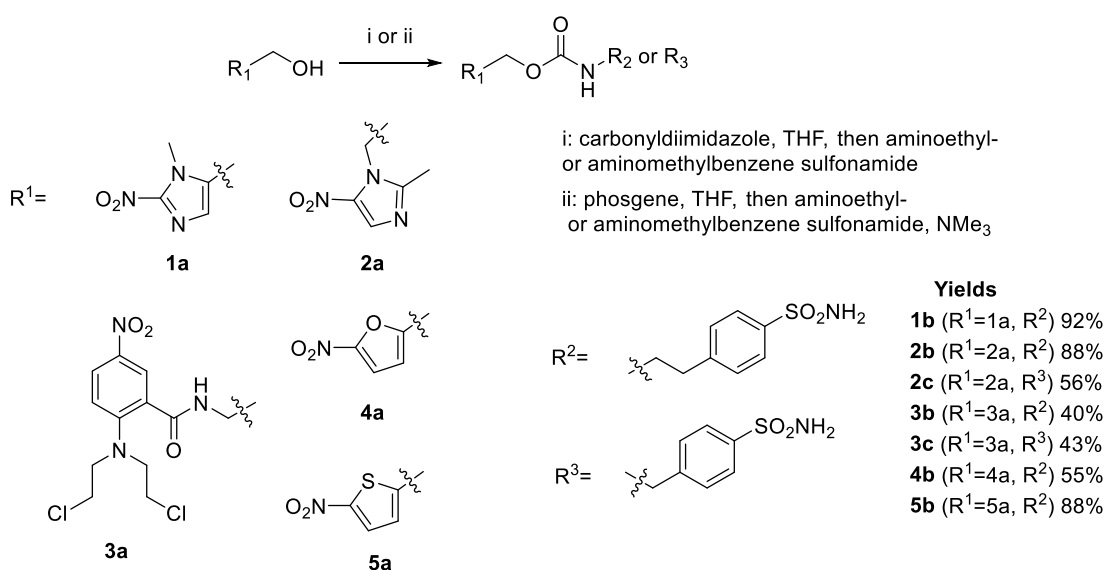
Over the last two decades, many HAPs have been documented.¹⁴ The molecular motifs used as cleavable entities are all susceptible to bioreduction, mainly by enzymatic processes (e.g. reductases) by a mono- or di-electronic process depending on the enzyme involved. The most frequently found in the literature are *N*-oxide, quinone, or nitroaromatic derivatives which have been the subject of in-depth studies up to the clinical stage.¹⁴⁻¹⁶ Nitroaromatic HAPs have been described for targets such as PARP inhibitors,¹⁷ PERK inhibitors,¹⁸ TK inhibitors¹⁹ and also for different types of nanosystems.²⁰⁻²¹ Few numbers of CA inhibitors (CAIs) have been designed using this HAP approach.²²⁻²⁶ As part of an effort to discover novel small-molecule inhibitors of hCA to enhance cancer therapy, we report herein a new class of 2- and, 5-nitroimidazole,

nitrofuran, nitrothiophene and nitrogen mustards (alkylating agents) based bio-reducible drugs harboring a benzenesulfonamide to target hCA IX.

Results

Chemistry

2-, 5- Nitroimidazole, nitrofuran, nitrothiophene and nitrogen mustard were conjugated with benzene sulfonamides using a carbamate linker. Because of the low reactivity observed, introduction of the carbamate linker proved to be challenging for some derivatives and two approaches were used to achieve the synthesis of these inhibitors starting from the nitroaromatic alcohols: (i) reaction with carbonyldiimidazole to access to the carbamoyl imidazole derivatives which reacted, in a one-pot reaction, with aminomethyl- or aminoethyl-benzenesulfonamide, or (ii) reaction with phosgene to yield to the chloroformates which were then reacted with aminomethyl- or aminoethyl- benzenesulfonamide in the presence of triethylamine (scheme 1).²⁷ Compounds **1b-5b** and **2c-3c** were isolated with yields ranging from 43% to 88% and characterized extensively by spectroscopic and spectrometric methods (see materials and methods part).



Scheme 1: Synthesis of HAP-CAIs **1b-4b** and **2c-3c**

Carbonic anhydrase inhibition assay

HAP-CAIs reported here were assayed using the CO₂ hydrase assay against three physiologically relevant human CA isoforms, the cytosolic hCA I and II and the transmembrane, tumor-associated hCA IX (Table 1).²⁸ The clinically used sulfonamide acetazolamide (**AZ**, 5-acetamido-1, 3, 4- thiazole-2-sulfonamide) has been taken along as standard in these measurements. All compounds acted as inhibitors against the three isoforms hCA I, II and IX, although with variable potency (Table 1). Against the abundant, cytosolic isoform hCA I compound **3c** showed a weak inhibition potency (2180 nM). Compound **1b** showed moderate inhibition activity towards hCA I

(166.7 nM) and hCA II (30.6 nM) isoforms and higher inhibition (7.6 nM) towards hCA IX, while compounds **2b** and **2c** strongly inhibited all CA isoforms (K_i ranging from 2.3 to 14.1 nM) with no differences observed in the selectivity ratios hCA II over hCA IX (**2b** = 0.35, **2c** = 0.28). Compounds **3b** and **3c** showed moderate inhibition of hCA IX, whilst compound **3b** binding to hCA II was very tight (3.1 nM). The large difference in binding capacity or selectivity ratios (**3b**= 0.09, **3c**= 0.94) of compounds from the same family (nitrogen mustard) supports the substitution effect on the carbamate linker. Compounds **4b** and **5b** showed moderate inhibition activity towards hCA I, respectively (84 nM) and (64.7 nM), while they strongly inhibited hCA II and hCA IX (K_i ranging from 5.7 to 19.8 nM). Nevertheless, considering the difficulty to obtain small compounds with a better affinity for the tumor-associated isozyme (hCA IX) over hCA II, the selectivity obtained for these series is comparable or better than that of the clinically used CA inhibitor acetazolamide **AAZ**.

Table 1: Inhibitory activity of compounds **1b-5b**, **2c-3c**, and the clinically used sulfonamide inhibitor acetazolamide (**AAZ**), against hCA I, hCA II, and hCA IX using a stopped flow CO₂ hydrase assay.

Compounds	K_i (nM) *			Selectivity ratio
	hCA I	hCA II	hCA IX	K_i hCA II/ K_i hCA IX
1b	166.7	30.6	7.6	1.19
2b	3.7	4.3	12.1	0.35
2c	2.3	4.0	14.1	0.28
3b	83.0	3.1	32.3	0.09
3c	2179.9	83.7	88.7	0.94
4b	83.8	15.5	5.7	2.72
5b	64.7	19.8	15.1	1.31
AAZ	250	12.0	25	0.48

* Mean from 3 different assays (errors in the range of \pm 5-10 % of the reported values).

Stability of carbamate linker under acidic conditions

Stability to chemical hydrolysis of compounds **1b-3c** was evaluated by measuring peak area or retention time of the compound after incubation at varying pH conditions up to 8 hours. No degradation was observed at any pH condition for all tested compounds, indicating significant stability. Additionally, all tested compounds were found to be stable for at least 8 h to harsh acid-catalyzed hydrolysis (pH = 2.0, 37 °C, data not shown). Literature studies have shown that the electron-withdrawing nitro group conjugated with the carbamate linker resulted in a remarkable decrease in stability, which may explain the apparent low inhibitory potency of these compounds toward FAAH, due to decomposition under the assay conditions.²⁹ Of all compounds (**1b-3c**), the nitro group was not in direct conjugation with the carbamate linker, thereby showing no stability loss when incubated under various pH conditions.

Biological assays

Cell viability and clonogenic assays

The cytotoxicity of all compounds (**1b-3c**) was determined in a panel of human tumor cell lines. Compound **1b** showed an IC_{50} of 204.5 μM ($p < 0.0001$) in HT29 cells under anoxia (IC_{50A}) and no detectable cytotoxicity ($IC_{50} >$ highest tested concentration) was observed under normoxia (Figure 1). Furthermore, in HCT116 cells compound **1b** resulted in an IC_{50} of 148.6 μM and 59.3 μM under normoxic and anoxic conditions respectively, resulting in a hypoxia selectivity cytotoxicity ratio (HCR) of 2.5 (Table 2). All other compounds, except compound **3b** in HCT116 cells, did not show any cytotoxicity at the tested concentrations. Compound **3b** resulted in a cell dependent cytotoxicity with HCR of 2.7 in HCT116 cells, while no cytotoxicity in HT29 cells was observed.

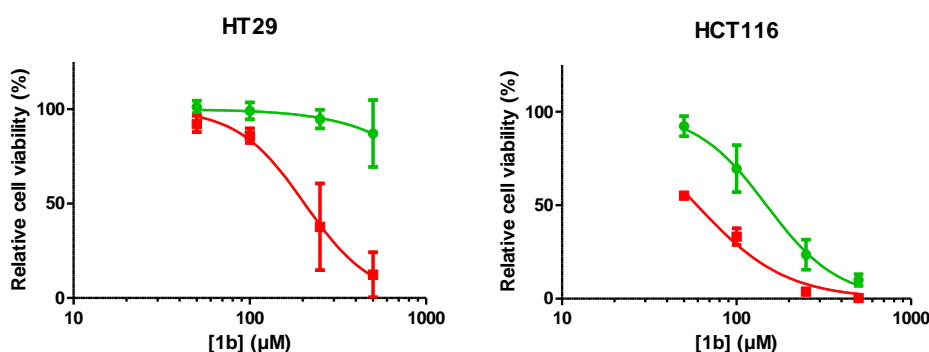


Figure 1: Relative cell viability (%) in HT29 and HCT116 cells exposed to increasing concentrations of the derivative **1b** under normoxic (green) and anoxic (red) conditions. Data represent the average \pm SEM of three independent biological repeats.

Based on its selective cytotoxicity under anoxia in both cell lines, compound **1b** was selected for further studies investigating its effects on cell survival. Compound **1b** did not reduce clonogenic cell survival under normoxia or anoxia at the tested concentrations (Figure 2). TH-302, a 2-nitroimidazole based hypoxia-activated prodrug-alkylating agent was used as positive control (data not shown).³⁰

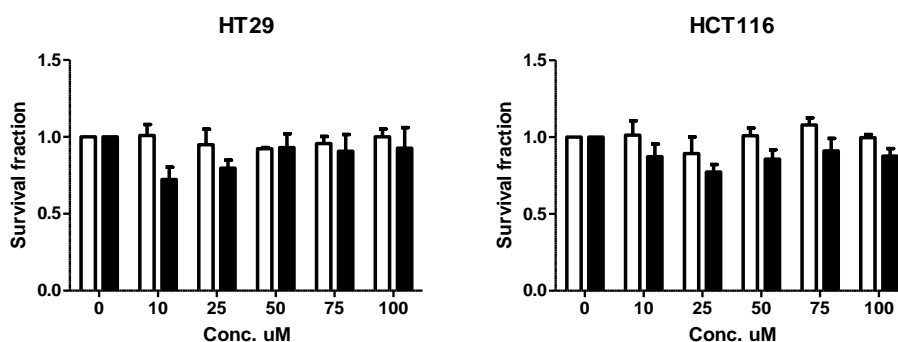


Figure 2: Clonogenic cell survival of HT29 and HCT116 cells during normoxia (white bars) and anoxia (black bars) when exposed to compound **1b**. Data represent the average \pm SEM of three independent biological repeats.

Table.2. HCR of all compounds IC₅₀N vs IC₅₀A

Compounds	HT29			HCT116		
	IC ₅₀ N	IC ₅₀ A	HCR (IC ₅₀ N/IC ₅₀ A)	IC ₅₀ N	IC ₅₀ A	HCR (IC ₅₀ N/IC ₅₀ A)
1b	> 500	204.5	>2.44	148.6	59.36	2.50
2b	>500	>500	-	>500	>500	-
2c	>500	>500	-	>500	>500	-
3b	>500	>500	-	267.1	97.27	2.74
3c	>500	>500	-	>500	>500	-

Abbreviations: IC₅₀: Concentration of an inhibitor where the response is reduced by half; Normoxia (N); Anoxia (A); Hypoxia selectivity cytotoxicity ratio (HCR).

Toxicity evaluation on zebrafish

During development, zebrafish embryos are easily affected by chemical compounds compared to adult zebrafish or other animal models or cell models, and therefore are suitable for assessing the subtle toxic effects of the chemicals.^{24,26} The toxicity of compound **1b**, **4b** and **5b** was determined by using 24-hours post fertilization zebrafish embryos.³¹ In these tests, the LC₅₀, zebrafish phenotypic parameters and the swim pattern were analyzed for each compound.

Determination of half maximal lethal concentration 50 (LC₅₀)

The lethality of **1b**, **4b** and **5b** on the developing zebrafish embryos was concentration dependent (Figure 3). Among the three compounds tested for the toxicity, **1b** was the less toxic and did not cause any mortality of the larvae, even at 1 mM concentration at the end of 5 day of exposure to the compound. However, the compound **4b** was more toxic compared to the other two compounds and caused significant mortality even at 500 μM concentration (Figure 3). The LC₅₀ values of the prodrugs at the end of the 5 days of exposure were 500 μM (**4b**), 1000 μM (**5b**) and 1400 μM (**1b**) as shown in the figure 1. The LC₅₀ concentration of the compounds were higher compared to the inhibitors that we screened in our earlier studies,^{28,29} suggesting that these compounds can be characterized further for developing as drugs.

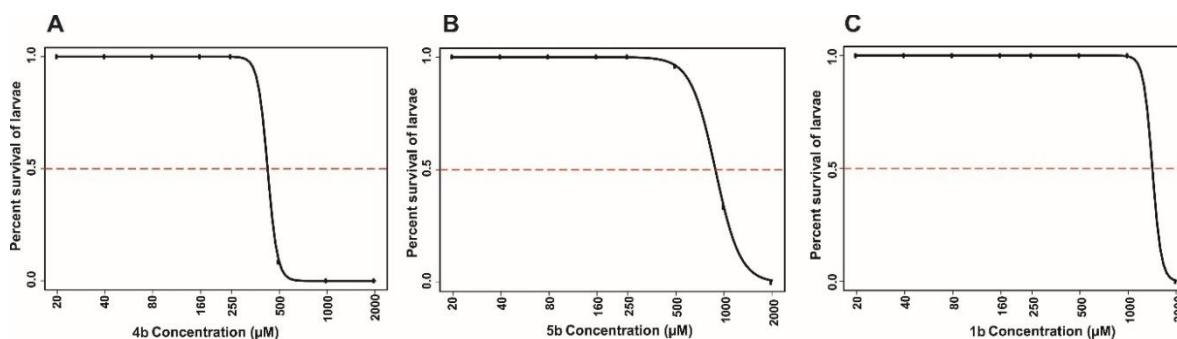


Figure 3: The LC₅₀ values of the prodrugs. The LC₅₀ doses of the compounds were calculated based on the 50% mortality of the developing larvae at the end of five days after the exposure of embryos to different concentrations of inhibitors. A) Shows the LC₅₀ value of compound **4b** (500μM concentration). B) The LC₅₀ for the compound **5b** was 1000 μM and C) The compound **1b** showed LC₅₀ value of 1400 μM. The LC₅₀ doses were determined after three independent experiments with similar experimental conditions (N=72).

Different phenotypic parameters were also analyzed (hatching, heartbeat, edema, swim bladder development, yolk sac utilization and body shape) from the developing larvae of 1-5 days, after exposure to the compounds. The figure 4 shows the representative images of larvae treated with the concentration which is considered as safe for further characterization. Among the compounds screened, the prodrug **1b** was found to be less toxic with no or minimal phenotypic abnormalities even at 1 mM. In our earlier study, compounds **1b-3c** also showed minimal or no phenotypic abnormalities at 1 mM concentrations. In the present study, compounds **4b** and **5b** showed phenotypic defects such as edema and absence of swim bladder (arrows) at lower concentrations compared to **1b**, as shown in figure 4.

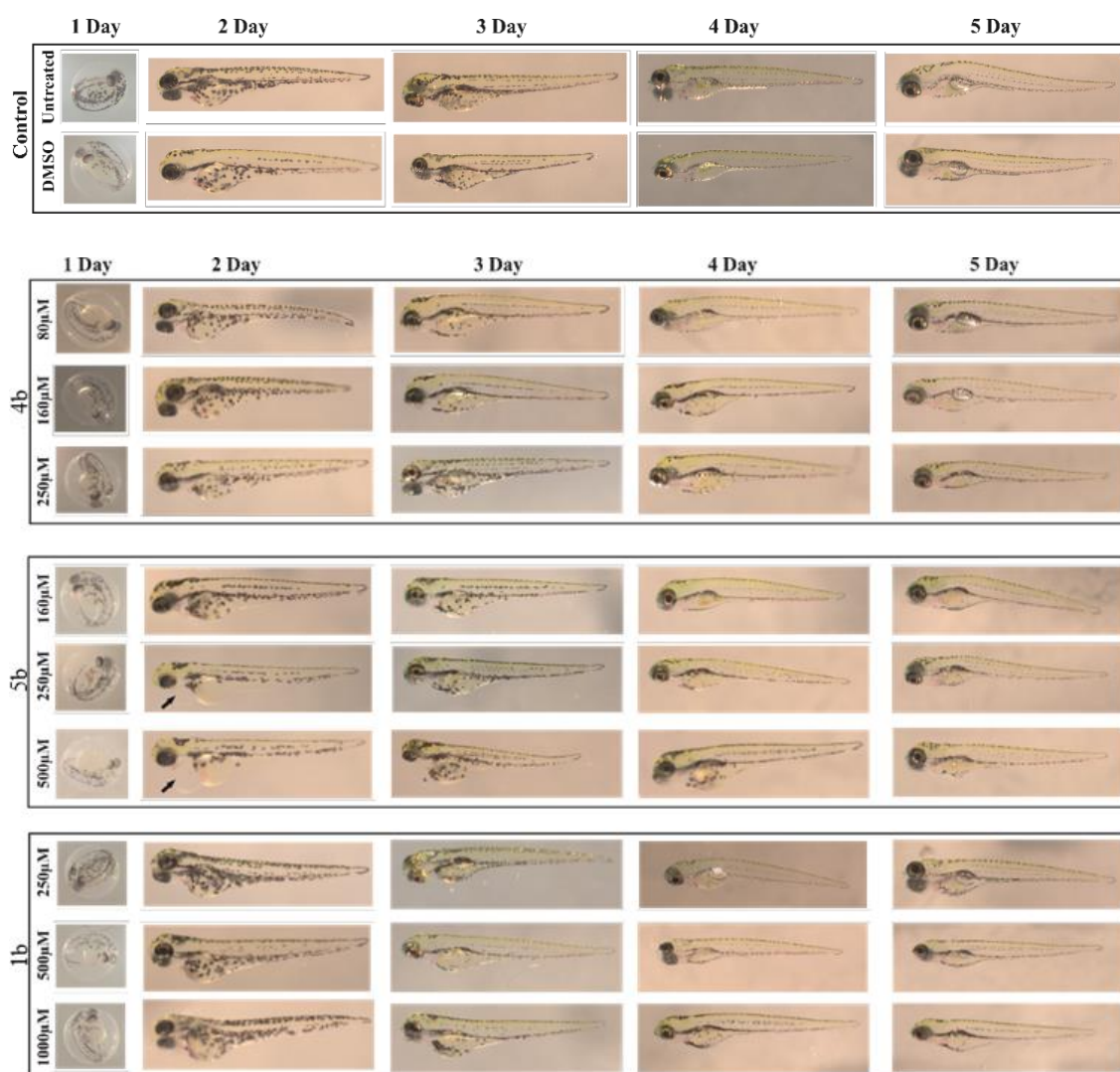


Figure 4: The images of zebrafish larvae in control and prodrug treated groups. Representative images of 2-5 dpf zebrafish larvae exposed to different concentrations (80 μM -1000 μM) of **1b**, **4b** and **5b**. The upper panel shows images normal development of zebrafish larvae in control group (not treated with inhibitors) and 1% DMSO treated group. The lower panel shows the larvae treated with concentration of the compounds at which they induced minimal or no phenotypic defects. Prodrug **4b** showed (arrow) absence of swim bladder at 250 μM concentration. Prodrug **5b** induced edema (arrow) as early as 2 days post exposure to the compound. The compound **1b** showed absence of swim bladder (arrow) at 1000 μM .

Further, the toxic effects of compounds across the concentrations (20 μM -2mM) were assessed on individual parameters of the 5 days post exposed zebrafish larvae. The figure 5 presents plot

graphs of dose-dependent effects of prodrugs on larvae. The results indicated that **1b** compound showed minimal or no adverse effect on the observable parameters of the larvae (figure 5 A-E). However, prodrugs **4b** and **5b** exhibited adverse effect on hatching, swim bladder development, utilization of yolk sac, and shape of the body and induced pericardial edema as shown in figure 5 A-E.

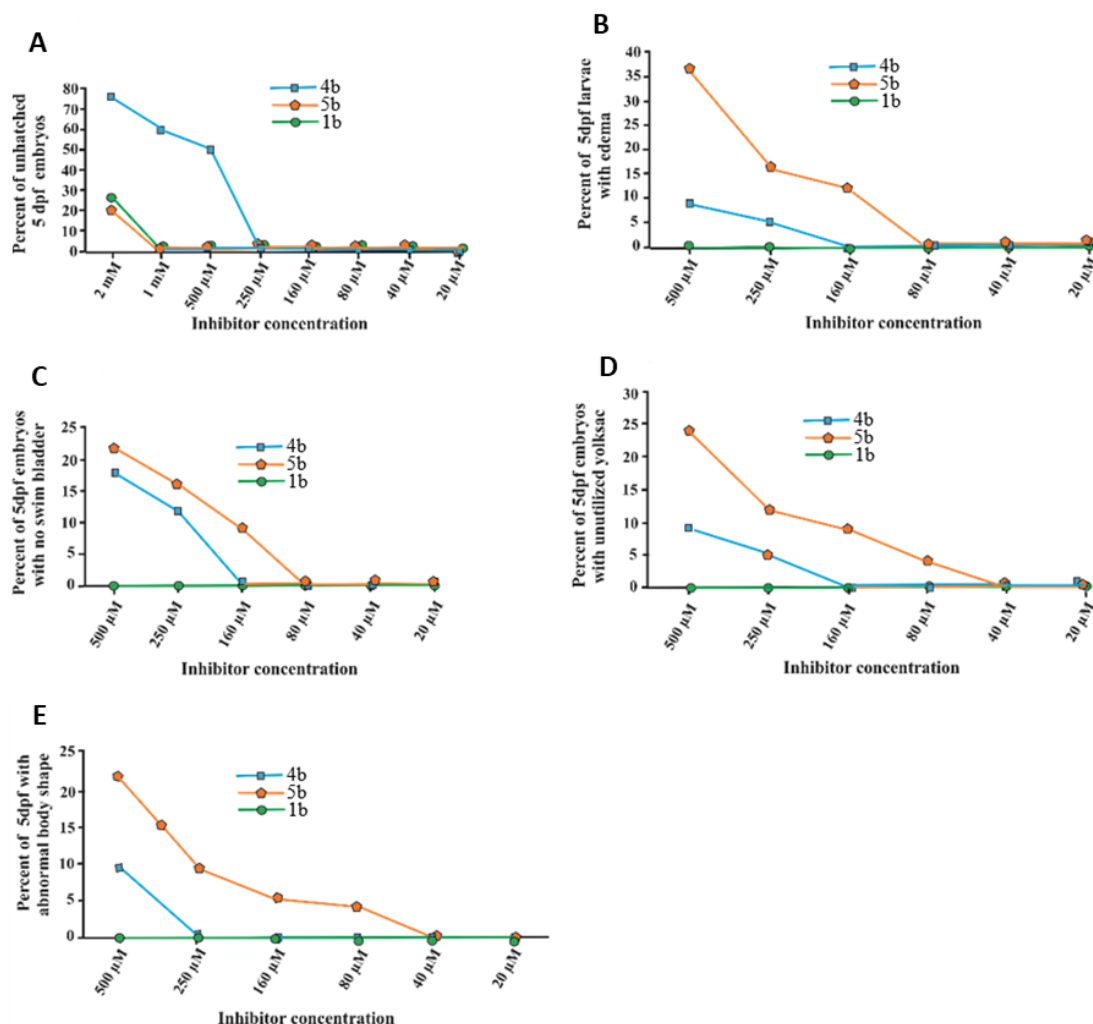


Figure 5: The effect of the prodrugs **4b**, **5b**, and **1b** on the phenotypic parameters of zebrafish larvae. The plot graphs show the phenotypic abnormalities in the zebrafish larvae after 5 days of exposure to compounds. A) hatching, B) edema, C) swim bladder development, D) yolk sac utilization and E) body shape, for each concentration, (N=72). * $p < 0.05$ by two-tailed Fisher's test.

Swim pattern analysis to assess the subtle toxic effects of the prodrugs

To assess the subtle toxic effects of the prodrugs on the swim patterns of the larvae, they were assessed at the end of 5 days of exposure to the compounds. The swim pattern analysis showed no abnormal or ataxic movement pattern in the larvae exposed to the concentration that did not induce any of the phenotypic defects and is considered as safe. In our earlier studies the nitroimidazole-based compounds DTP338 and DTP348, showed ataxic movement pattern even at 100 μ M concentration due to neurotoxicity.^{24,26} Therefore, the prodrugs screening in the

current study can be considered safe for further preclinical characterization and development as potential drugs.

Discussion

We developed here new HAPs incorporating a benzenesulfonamide through a carbamate linker, designed with different bio-reducible moieties for the selective delivery of anticancer drugs on hypoxic tumors. Through this study we demonstrated that these HAPs can selectively inhibit the hCA IX at the nanomolar level. In contrast to other nitroaromatic drugs, HAPs **1b–3c** did not show stability loss when incubated under various pH conditions as the nitro group was not in direct conjugation with the carbamate linker. Compound **1b**, harboring a 2- nitroimidazole as reducible moiety, showed the best cytotoxic action against HT29 and HCT116 cells (IC_{50} of 204.5 and 59.36 μ M under hypoxia) and an HCR of approximately 2.5. Our data also show that **1b** is the less toxic with no mortality observed on zebrafish larvae even at 1 mM concentration at the end of 5 day of exposure. Of note, the prodrug **1b** also did not induce phenotypic abnormalities in the larvae as well as abnormal or ataxic swim movement at the concentration that did not induce any of the phenotypic defects and is considered as safe. As other nitroimidazole derivatives, such as DTP338 and DTP348, induced a neurotoxic effect even at 100 μ M concentration (REF), the data gathered here suggest a potential for derivative **1b** to be optimized for the development of new safer HAPs.

Materials and Methods

Chemistry

General

All reagents and solvents were of commercial quality and used without further purification unless otherwise specified. All reactions were carried out under an inert atmosphere of nitrogen. TLC analyses were performed on silica gel 60 F254 plates (Merck Art. no. 1.05554). Spots were visualized under 254 nm UV illumination or by ninhydrin solution spraying. Melting points were determined on a Büchi Melting Point 510 and are uncorrected. ^1H and ^{13}C NMR spectra were recorded on a Bruker DRX-400 spectrometer using DMSO- d_6 as solvent and tetramethylsilane as internal standard. For ^1H and ^{13}C NMR spectra, chemical shifts are expressed in δ (ppm) downfield from tetramethylsilane, and coupling constants (J) are expressed in hertz. Electron ionization mass spectra were recorded in positive or negative mode on a Water MicroMass ZQ. All compounds that were tested in the biological assays were analyzed by high-resolution ESI mass spectra (HRMS) using a Q-ToF mass spectrometer fitted with an electrospray ion source in order to confirm the purity of >95%.

General procedure for preparation of chloroformate: The corresponding hydroxy starting compound (**1a**, **2a** and **3a**) (2 mmol) in tetrahydrofuran (10 mL) was added to phosgene (4 mL, 8

mmol) and THF (15 mL) at 0°C. The reaction was stirred for 16 h, then the solvent was removed in vacuo. The crude chloroformate was used without further purification.

General procedure for synthesis of 1b, 2b, 2c, 3b, and 3c: A suspension of chloroformate (23.4 mmol) in dry THF (100 ml) was treated with trimethylamine (50 mmol). The corresponding amine (23.4 mmol) was added afterwards and the reaction was stirred overnight at room temperature. The solvent was removed in vacuo. The residue was dissolved in chloroform and washed twice with 1.0 N sodium hydroxide and water. The organic phase was dried over sodium sulfate, filtered and concentrated under vacuum. The residue was purified by chromatography on silica gel using methylene chloride–methanol 98:2 as eluent.

General procedure for synthesis of 4b and 5b: To a suspension of carbonyl diimidazole CDI (0.31 mmol) in dry THF (5 mL) the corresponding hydroxy starting compound (4a and 5a) (0.28 mmol) was added. The reaction was stirred 3h at room temperature and the 4-(2-aminoethyl) benzene sulfonamide was added. The reaction mixture was stirred overnight at room temperature and concentrated under reduced pressure. The residue was dissolved in EtOAc (12.5 mL) and washed with water (2x7.5 mL) and brine (7.5 mL). The organic phase was dried over sodium sulfate, filtered and concentrated under vacuum. The residue was purified by chromatography on silica gel using cyclohexane-ethyl acetate 3:7 as eluent.

(1-methyl-2-nitro-1H-imidazol-5-yl) methyl (4-sulfamoylphenethyl) carbamate (**1b**): yield = 92%; ¹H NMR (400 MHz, DMSO-d₆) δ 7.73 (d, *J* = 8.3, 2H), 7.48 (t, *J* = 5.6, 1H), 7.38 (d, *J* = 8.3, 2H), 7.30 (s, 2H), 7.21 (s, 1H), 5.12 (s, 2H), 3.89 (s, 3H), 3.26 (dd, *J* = 13.2, 6.7, 2H), 2.79 (t, *J* = 7.1, 2H). ¹³C NMR (101 MHz, DMSO-d₆) δ 155.36, 145.99, 143.42, 142.09, 133.83, 129.17, 128.41, 125.68, 54.82, 48.62, 34.69, 34.16 – 33.11. HRMS (ESI+) [*M*+*H*]⁺ calculated for [C₁₄H₁₈N₅O₆S]⁺: 384.0978, found: 384.0982.

2-(2-methyl-5-nitro-1H-imidazol-1-yl) ethyl (4-sulfamoylphenethyl) carbamate (**2b**): yield = 88%; ¹H NMR (400 MHz, DMSO) δ 8.03 (s, 1H), 7.73 (d, *J* = 8.3, 2H), 7.38 – 7.32 (m, 3H), 7.31 (s, 2H), 4.48 (t, *J* = 4.9, 2H), 4.30 (t, *J* = 4.9, 2H), 3.17 (dd, *J* = 13.1, 6.7, 2H), 2.72 (t, *J* = 7.1, 2H), 2.39 (s, 3H). ¹³C NMR (101 MHz, DMSO) δ 155.69, 151.86, 143.61, 142.11, 138.56, 133.18, 129.26, 125.81, 61.93, 35.01, 14.02. HRMS (ESI+) [*M*+*H*]⁺ calculated for [C₁₅H₂₀N₅O₆S]⁺: 398.1134, found: 398.1136.

2-(2-methyl-5-nitro-1H-imidazol-1-yl) ethyl (4-sulfamoylbenzyl) carbamate (**2c**): yield = 56%; ¹H NMR (400 MHz, DMSO-d₆) δ 8.04 (s, 1H), 7.88 (t, *J* = 6.1, 1H), 7.76 (d, *J* = 8.4, 2H), 7.34 (d, *J* = 8.4, 2H), 7.32 (s, 2H), 4.54 (t, *J* = 5.0, 2H), 4.36 (t, *J* = 5.0, 2H), 4.19 (d, *J* = 6.1, 2H), 2.44 (s, 3H). ¹³C NMR (101 MHz, DMSO-d₆) δ 155.87, 151.72, 143.53, 142.68, 138.45, 133.07, 127.26, 125.65, 62.11, 45.52, 43.37, 13.98. HRMS (ESI+) [*M*+*H*]⁺ calculated for [C₁₄H₁₈N₅O₆S]⁺: 384.0978, found: 384.0972.

2-(2-(bis(2-chloroethyl)amino)-5-nitrobenzamido) ethyl (4-sulfamoylphenethyl) carbamate (**3b**): yield = 40%; ¹H NMR (400 MHz, DMSO-d₆) δ 8.72 (t, *J* = 5.3, 1H), 8.15 – 8.05 (m, 2H), 7.73 (d, *J* = 8.1, 2H), 7.39 (t, *J* = 6.9, 2H), 7.29 (s, 2H), 7.22 (d, *J* = 8.0, 1H), 4.11 (t, *J* = 5.4, 2H), 3.74 (dt, *J* = 9.9, 4.9, 8H), 3.46 (d, *J* = 5.4, 3H), 3.25 (dd, *J* = 13.8, 6.5, 2H), 2.80 (t, *J* = 7.3, 2H). ¹³C NMR (101 MHz, DMSO-d₆) δ 167.45, 156.11, 151.59, 143.54, 142.05, 138.21, 129.11, 126.33 – 123.92, 118.08,

62.04, 59.78, 53.12, 41.38, 34.44, 31.23, 30.39. HRMS (ESI+) $[M+H]^+$ calculated for $[C_{22}H_{28}Cl_2N_5O_7S]^+$: 575.1008, found: 575.1011.

2-(2-(bis(2-chloroethyl)amino)-5-nitrobenzamido) ethyl (4-sulfamoylbenzyl)carbamate (**3c**): yield = 43%; 1H NMR (400 MHz, DMSO) δ 8.75 (t, J = 5.5, 1H), 8.17 – 8.08 (m, 2H), 7.80 (dd, J = 12.0, 5.9, 1H), 7.76 (d, J = 8.2, 2H), 7.43 (d, J = 8.1, 2H), 7.31 (s, 2H), 7.23 (d, J = 9.1, 1H), 4.26 (t, J = 8.1, 2H), 4.15 (t, J = 5.2, 2H), 3.80 – 3.69 (m, 8H), 3.17 (s, 2H). ^{13}C NMR (101 MHz, DMSO) δ 167.56, 156.53, 151.68, 143.90, 142.68, 138.32, 127.41, 125.76, 117.97, 56.19, 53.22, 48.69, 41.33, 21.08. HRMS (ESI+) $[M+H]^+$ calculated for $[C_{21}H_{26}Cl_2N_5O_7S]^+$: 562.0930, found: 562.0935.

(5-nitrofuranyl)methyl (4-sulfamoylphenethyl) carbamate (**4b**): yield = 55%; 1H NMR (400 MHz, DMSO- d_6) δ 7.73 (d, J = 8.4, 2H), 7.71 (d, J = 4.2, 1H), 7.63 (t, J = 5.6 Hz, 1H), 7.39 (d, J = 8.4 Hz, 2H), 7.37 (s, 2H), 6.84 (d, J = 4.2 Hz, 1H), 5.08 (s, 2H), 3.25 (t, J = 7.1 Hz, 2H), 2.78 (t, J = 7.1 Hz, 2H). ^{13}C NMR (400 MHz, DMSO- d_6) δ 156.45, 155.10, 145.30, 142.26, 130.52, 127.00, 113.99, 113.78, 58.50, 42.62, 36.22. HRMS (ESI+) $[M+H]^+$ calculated for $[C_{14}H_{16}N_3O_7S]^+$: 370.0709, found: 370.0708.

(5-nitrothiophen-2-yl)methyl(4-sulfamoylphenethyl)carbamate (**5b**): yield = 88%; 1H NMR (400 MHz, DMSO- d_6) δ 8.05 (d, J = 4.2 Hz, 1H), 7.74 (d, J = 8.4 Hz, 2H), 7.63 (t, J = 5.6 Hz, 1H), 7.40 (d, J = 8.4 Hz, 2H), 7.33 (s, 2H), 7.22 (d, J = 4.2 Hz, 1H), 5.23 (s, 2H), 3.24 (t, J = 7.1 Hz, 2H), 2.82 (t, J = 7.1 Hz, 2H). ^{13}C NMR (400 MHz, DMSO- d_6) δ 156.66, 149.35, 145.27, 142.25, 130.53, 127.52, 126.99, 61.48, 42.59, 36.21. HRMS (ESI+) $[M+H]^+$ calculated for $[C_{14}H_{16}N_3O_6S_2]^+$: 386.0481, found: 386.0479.

Carbonic anhydrase inhibition assays

An Applied Photophysics stopped-flow instrument was used for assaying the CA catalysed CO_2 hydration activity. Phenol red (at a concentration of 0.2 mM) was used as indicator, working at the absorbance maximum of 557 nm, with 20 mM Hepes (pH 7.5) as buffer, and 20 mM Na_2SO_4 (for maintaining the constant ionic strength), following the initial rates of the CA-catalysed CO_2 hydration reaction for a period of 10–100 s. The CO_2 concentrations ranged from 1.7–17 mM for the determination of the kinetic parameters and inhibition constants. In particular, CO_2 was bubbled in distilled deionised water for 30 min so that the water was saturated (the concentration at a specific temperature is known from literature). In addition, a CO_2 assay kit (from Sigma) was used to measure the concentration in variously diluted solutions obtained from the saturated one (which was kept at the same temperature and a constant bubbling during the experiments). For each inhibitor at least six traces of the initial 5–10% of the reaction was used for determining the initial velocity.²⁸ The uncatalysed rates were determined in the same manner and subtracted from the total observed rates. Stock solutions of inhibitor (0.1 mM) were prepared in distilled-deionised water and dilutions up to 0.01 nM were done thereafter with distilled-deionised water. Inhibitor and enzyme solutions were pre-incubated together for 15 min–2 h (or longer, i.e. 4–6 h) at room temperature (at 4 °C for the incubation periods longer than 15 min) prior to assay, in order to allow for the formation of the E-I complex. The inhibition constants were obtained by non-linear least-squares methods using PRISM 3 and the Cheng-Prusoff equation, as reported earlier,³¹⁻³² and represent the mean from at least three different

determinations. hCA I was purchased by Sigma-Aldrich and used without further purification, whereas all the other hCA isoforms were recombinant ones obtained in-house as reported earlier.³³

In vitro chemical stability and analytical method

The chemical stability of the compounds **1b**, **2b**, **2c**, **3b** and **3c** at various pH (6.2, 6.6, 7.0 and 7.4) was measured on a Waters XEVO QTOF G2 Mass Spectrometer, with an Acquity H-class solvent manager, FTN-sample manager and TUV-detector. The system was equipped with a reversed phase C18-column (Waters, acquity PST 130A, 1.7 μ m 2.1 x 50mm i.d.), column temperature 40 degrees. Mobile phases consisted of 0.1% formic acid in water and 90% acetonitrile. FTN-purge solvent was 5% acetonitrile in water. Mobile phase gradient was maintained starting with 5% acetonitrile to 50% acetonitrile for 15 minutes at 220nm wavelength. Stock solutions of compounds were prepared in DMSO and each sample was incubated at a final concentration of 1–5 μ M in pre-thermostated buffered solution. The final DMSO concentration in the samples was kept at 1%. The samples were maintained at 37 °C in a temperature-controlled shaking water bath (60 rpm). At various time points, 100 μ L aliquots were removed and injected into the High-Performance Liquid Chromatography (HPLC) system for analysis. Mass was measured in positive sensitivity mode; mass range between 100 and 1000 Da.

Biological assays

Cells

Human colorectal HCT116 and HT29 carcinoma cells were cultured in DMEM (Lonza) supplemented with 10% fetal bovine serum and 1% PenStrep. Cells were exposed to anoxic conditions for 24 h in a hypoxic chamber (MACS VA500 microaerophilic workstation, Don Whitley Scientific, UK) with an atmosphere consisting of $\leq 0.02\%$ O₂, 5% CO₂ and residual N₂. Normoxic cells were grown in regular incubators with 21% O₂, 5% CO₂ at 37 °C.

Cell viability assays

The cytotoxic efficacy of the bio-reducible derivatives was determined based on cell viability assays using alamarBlue® (Invitrogen). In short, HT29 and HCT116 were seeded in 96-well plates and allowed to attach overnight. The next day plates were exposed to normoxia or anoxia and medium was replaced with pre-incubated normoxic or anoxic DMEM. Compounds were dissolved in DMSO (0.5%, Sigma-Aldrich) and final concentrations were made with pre-incubated anoxic or normoxic DMEM and added to the wells after 24 h of exposure. Cells were exposed to compounds for a total of 2 h, after which medium was washed off and replaced with fresh medium. Cells were allowed to grow for an additional 72 h under normoxic conditions prior to measurement. Cells were incubated with alamarBlue® for 2 h during normoxic conditions, which corresponds with their metabolic function, a measure for cell viability.

Chapter 3

Fluorescence was measured using plate reader (FLUOstar Omega, BMG LABTECH) using a fluorescence excitation wavelength of 540- 580 nm.

Clonogenic assays

Clonogenic survival of HT29 and HCT116 cells were seeded with high density for CA IX-dependent extracellular acidification.³⁴ Compound **1b** doses were selected from corresponding IC₅₀ (anoxic/normoxic) ranging from 10 to 100 µM for preliminary experiments. These cells were exposed to 23:30 h normoxic or anoxic conditions and 30 min to drugs after which cells were trypsinized and reseeded in triplicate with known cell numbers. Cells were allowed to grow for 9 (HCT116) and 14 (HT29) days to form colonies that were quantified after staining and fixation with 0.4% methylene blue in 70% ethanol. Surviving fractions were calculated and compared to control survival curves produced in the same experiment without compound treatment.

Statistical analyses

GraphPad Prism (version 5.03) was used for all statistical analyses. For the cytotoxic compounds IC₅₀ values were estimated with the curve of the log (inhibitor) vs. normalized response (Variable slope).

Toxicity assay

Preparation of inhibitor samples

The hypoxia-activated prodrugs were screened for their toxicity using 24-hours post fertilization zebrafish embryos as described earlier.¹ The compounds were either dissolved in Embryonic medium ([5.0 mM NaCl, 0.17 mM KCl, 0.33 mM CaCl₂, 0.33 mM MgSO₄, and 0.1% w/v Methylene Blue (Sigma-Aldrich, Germany)]) or in dimethyl sulfoxide (DMSO) (Sigma-Aldrich, St. Louis, MO) or in dimethyl sulfoxide (DMSO) (Sigma-Aldrich, St. Louis, MO) to prepare 100 mM stock solutions. Before start of each experiment, the series of dilutions were made from the above stock in the embryonic medium.

Maintenance of the zebrafish

The wild type adult zebrafish (AB strains) were maintained at 28.5°C in an incubator.³⁵ In each breeding tank, about embryos 3-5 pairs of male and female fish were set up overnight for collecting the embryos. Next morning, 1-2- hours post fertilization (hpf) embryos were collected in a sieve and rinsed with embryonic medium and kept the collected embryos in an incubator at 28.5°C overnight.³⁵ The toxicity evaluation studies of the compounds were performed using the fish that were 24-hpf. All the zebrafish experiments were performed at the zebrafish core facility, Tampere University, Finland and according to the protocol used in our laboratory.

Ethical statement. The research unit at Tampere University has an established zebrafish core facility authorized granted by the National Animal Experiment Board (ESAVI/7975/04.10.05/2016). The experiments using developing zebrafish embryos were performed according to the Provincial Government of Eastern Finland Province Social and Health Department Tampere Regional Service Unit protocol # LSLH-2007–7254/Ym-23.

Determination of half maximal lethal concentration 50 (LC₅₀).

The LC₅₀ values for all the three prodrugs were determined using 24-hpf embryos using 8-10 different concentrations for each compound. We used minimum of 30 zebrafish larvae for each concentration of the compound [24][26][36-37]. The 24-hpf larvae were exposed to different concentrations of the inhibitors that ranged from 20 μM to mM. Dose response curve (DRC) was calculated using DRM of the DRC R package [38]. The control group constituted an equal number of larvae not treated with any compound and the larvae that were treated with 1% of DMSO. Toxicological evaluation studies were performed in 24-well plates (Corning V R Costar V R cell culture plates). In each well, we placed 1-2 24-hpf embryos in 1 ml of embryonic medium containing a diluted inhibitor. For control groups, 1% DMSO diluted in either embryonic medium or embryonic medium with no chemical compound. A minimum of three sets of experiments were carried out for each prodrug. Mortality of the larvae was checked every 24 h until 5 days after exposure to the prodrugs.

Phenotypic analysis of the larvae

After exposure to the prodrugs, we evaluated the effects of these compound on the zebrafish larvae by analyzing eight phenotypic parameters such as: 1) mortality, 2) hatching 3) edema 4) swimming pattern, 5) yolk sack utilization, 6) heartbeat, 7) body shape, and 8) swim bladder development. The images of the developing larvae were taken using a Lumar V1.12 fluorescence microscope attached to a camera with a 1.5 lens (Carl Zeiss MicroImaging GmbH, Göttingen, Germany). The images were analyzed with AxioVision software versions 4.7 and 4.8 as described in our standard protocol for assessment of toxicity and safety of the chemical compounds.

Swim pattern analysis

The swim pattern of the zebrafish larvae was studied after 5 days of exposure to these compounds. For the analyses of swim pattern, about 15-20 zebrafish larvae after 5 days of exposure to the compounds were placed in a 35 mm x 15 mm petri dish containing embryonic medium and the larvae were allowed to settle in the petri dish for 1 minute. The movement of the zebrafish larvae was observed under the microscope for 1 minute. A short video of about 1 min was taken for each group of larvae that were treated with a concentration of the compound that did not show any phenotypic abnormalities. The swim patterns were compared with the control group zebrafish larvae that were not treated with any inhibitor.

References

- Ramón Y Cajal, S.; Sesé, M.; Capdevila, C.; Aasen, T.; De Mattos-Arruda, L.; Diaz-Cano, S. J.; Hernández-Losa, J.; Castellví, J. Clinical implications of intratumor heterogeneity: challenges and opportunities. *J. Mol. Med.* **2020**, *98* (2), 161-177. <https://doi.org/10.1007/s00109-020-01874-2>.
- Junttila, M. R.; de Sauvage, F. J. Influence of tumour micro-environment heterogeneity on therapeutic response. *Nature* **2013**, *501* (7467), 346-354. <https://doi.org/10.1038/nature12626>.
- Petrova, V.; Annicchiarico-Petruzzelli, M.; Melino, G.; Amelio, I. The hypoxic tumour microenvironment. *Oncogenesis* **2018**, *7* (1), 1-13. <https://doi.org/10.1038/s41389-017-0011-9>.
- Schito, L.; Semenza, G. L. Hypoxia-Inducible Factors: Master Regulators of Cancer Progression. *Trends in Cancer* **2016**, *2* (12), 758-770. <https://doi.org/10.1172/jci159839>.
- Parks, S. K.; Cormerais, Y.; Pouyssegur, J. Hypoxia and cellular metabolism in tumour pathophysiology. *J. Physiol.* **2017**, *595* (8), 2439-2450. <https://doi.org/10.1113/jp273309>.
- Corbet, C.; Feron, O. Tumour acidosis: from the passenger to the driver's seat. *Nat. Rev. Cancer.* **2017**, *17* (10), 577-593. <https://doi.org/10.1007/s10555-019-09799-0>.
- Pastorekova, S.; Gillies, R. J. The role of carbonic anhydrase IX in cancer development: links to hypoxia, acidosis, and beyond. *Cancer Metastasis Rev.* **2019**, *38* (1-2), 65-77. <https://doi.org/10.1007/s10555-019-09799-0>.
- van Kuijk, S.J.; Yaromina, A.; Houben, R.; Niemans, R.; Lambin, P.; Dubois, L.J. Prognostic Significance of Carbonic Anhydrase IX Expression in Cancer Patients: A Meta-Analysis. *Front. Oncol.* **2016**, *6*, 69. <https://doi.org/10.1371/journal.pone.0114096>.
- Dubois, L.J.; Niemans, R.; van Kuijk, S.J.; Panth, K.M.; Parvathaneni, N.K.; Peeters, S.G.; Zegers, C.M.; Rekers, N.H.; van Gisbergen, M.W.; Biemans, R.; Lieuwes, N.G.; Spiegelberg, L.; Yaromina, A.; Winum, J.Y.; Vooijs, M.; Lambin, P. New ways to image and target tumour hypoxia and its molecular responses. *Radiother. Oncol.* **2015**, *116* (3), 352-357. <https://doi.org/10.1016/j.radonc.2015.08.022>.
- Ilies, M.; Winum, J.-Y. Carbonic Anhydrase Inhibitors for The Treatment of Tumors: Therapeutic, Immunologic, And Diagnostic Tools Targeting Isoforms IX And XII. In *Carbonic Anhydrases. Biochemistry and Pharmacology of an Evergreen Pharmaceutical Target*, 1st ed.; Supuran, C. T., Nocentini, A., Eds.; Academic Press: Amsterdam, The Netherlands, **2019**; pp. 331-365.
- Supuran, C. T.; Alterio, V.; di Fiore, A.; d' Ambrosio, K.; Carta, F.; Monti, S. M.; de Simone, G. Inhibition of carbonic anhydrase IX targets primary tumors, metastases, and cancer stem cells: Three for the price of one. *Med. Res. Rev.* **2018**, *38* (6), 1799-1836. <https://doi.org/10.1002/med.21497>.
- Nocentini, A.; Supuran, C. T. Carbonic anhydrase inhibitors as antitumor/antimetastatic agents: a patent review (2008-2018). *Expert. Opin. Ther. Pat.* **2018**, *28* (10), 729-740. <https://doi.org/10.1080/13543776.2018.1508453>.
- Supuran, C. T. Carbonic anhydrase inhibitors as emerging agents for the treatment and imaging of hypoxic tumors. *Expert Opin. Investig. Drugs* **2018**, *27* (12), 963-970. <https://doi.org/10.1080/13543784.2018.1548608>.
- Sharma, A.; Arambula, J. F.; Koo, S.; Kumar, R.; Singh, H.; Sessler, J. L.; Kim, J. S. Hypoxia-targeted drug delivery. *Chem. Soc. Rev.* **2019**, *48* (3), 771-813. <https://doi.org/10.1039/c8cs00304a>.
- Su, M. X.; Zhang, L. L.; Huang, Z. J.; Shi, J. J.; Lu, J. J. Investigational Hypoxia-Activated Prodrugs: Making Sense of Future Development. *Curr. Drug Targets* **2019**, *20* (6), 668-678. <https://doi.org/10.2174/1389450120666181123122406>.
- Baran, N.; Konopleva, M. Molecular Pathways: Hypoxia-Activated Prodrugs in Cancer Therapy. *Clin. Cancer Res.* **2017**, *23* (10), 2382-2391. <https://doi.org/10.1158/1078-0432.ccr-16-0895>.
- Dickson, B. D.; Wong, W. W.; Wilson, W. R.; Hay, M. P. Studies Towards Hypoxia-Activated Prodrugs of PARP Inhibitors. *Molecules* **2019**, *24* (8), 1-20. <https://doi.org/10.3390/molecules24081559>.

18. Liew, L. P.; Singleton, D. C.; Wong, W. W.; Cheng, G. J.; Jamieson, S. M. F.; Hay, M. P. Hypoxia-Activated Prodrugs of PERK Inhibitors. *Chem. Asian J.* **2019**, *14* (8), 1238-1248. <https://doi.org/10.1002/asia.201801826>.
19. Bielec, B.; Schueffl, H.; Terenzi, A.; Berger, W.; Heffeter, P.; Keppler, B.; Kowol, C. R. Development and biological investigations of hypoxia-sensitive prodrugs of the tyrosine kinase inhibitor crizotinib. *Bioorg Chem.* **2020**, *99*, 103778. <https://doi.org/10.1016/j.bioorg.2020.103778>.
20. Zhou, M.; Xie, Y.; Xu, S.; Xin, J.; Wang, J.; Han, T.; Ting, R.; Zhang, J.; An, F. Hypoxia-activated nanomedicines for effective cancer therapy. *Eur. J. Med. Chem.* **2020**, *195*, 112274. <https://doi.org/10.1016/j.ejmech.2020.112274>.
21. Zeng, Y.; Ma, J.; Zhan, Y.; Xu, X.; Zeng, Q.; Liang, J.; Chen, X. Hypoxia-activated prodrugs and redox-responsive nanocarriers. *Int. J. Nanomedicine* **2018**, *13*, 6551-6574. <https://doi.org/10.2147/ijn.s173431>.
22. de Simone, G.; Vitale, R. M.; di Fiore, A.; Pedone, C.; Scozzafava, A.; Montero, J.-L.; Winum, J.-Y.; Supuran, C. T. Carbonic anhydrase inhibitors: Hypoxia-activatable sulfonamides incorporating disulfide bonds that target the tumor-associated isoform IX. *J. Med. Chem.* **2006**, *49* (18), 5544-51. <https://doi.org/10.1021/jm060531j>.
23. Nocentini, A.; Trallori, E.; Singh, S.; Lomelino, C. L.; Bartolucci, G.; di Cesare Mannelli, L.; Ghelardini, C.; McKenna, R.; Gratteri, P.; Supuran, C. T. 4-Hydroxy-3-nitro-5-ureido-benzenesulfonamides Selectively Target the Tumor-Associated Carbonic Anhydrase Isoforms IX and XII Showing Hypoxia-Enhanced Antiproliferative Profiles. *J. Med. Chem.* **2018**, *61* (23), 10860-10874. <https://doi.org/10.1021/acs.jmedchem.8b01504>.
24. Aspatwar, A.; Parvathaneni, N. K.; Barker, H.; Anduran, E.; Supuran, C. T.; Dubois, L.; Lambin, P.; Parkkila, S.; Winum, J. Y. Design, synthesis, in vitro inhibition and toxicological evaluation of human carbonic anhydrases I, II and IX inhibitors in 5-nitroimidazole series. *J. Enzyme Inhib. Med. Chem.* **2020**, *35* (1), 109-117. <https://doi.org/10.1080/14756366.2019.1685510>.
25. van Kuijk, S.J.A.; Parvathaneni, N.K.; Niemans, R.; van Gisbergen, M.W.; Carta, F.; Vullo, D.; Pastorekova, S.; Yaromina, A.; Supuran, C.T.; Dubois, L.J.; Winum, J.Y.; Lambin, P. New approach of delivering cytotoxic drugs towards CAIX expressing cells: A concept of dual-target drugs. *Eur. J. Med. Chem.* **2017**, *127*, 691-702. <https://doi.org/10.1016/j.ejmech.2016.10.037>.
26. Aspatwar, A.; Becker, H.M.; Parvathaneni, N.K.; Hammaren, M.; Svorjova, A.; Barker, H.; Supuran, C.T.; Dubois, L.; Lambin, P.; Parikka, M.; Parkkila, S.; Winum, J.Y. Nitroimidazole-based inhibitors DTP338 and DTP348 are safe for zebrafish embryos and efficiently inhibit the activity of human CA IX in *Xenopus* oocytes. *J. Enzyme Inhib. Med. Chem.* **2018**, *33* (1), 1064-1073. <https://doi.org/10.1080/14756366.2018.1482285>.
27. Musser, J. H.; Chakraborty, U.; Bailey, K.; Sciortino, S.; Whyzmuzis, C.; Amin, D.; Sutherland, C. A. Synthesis and Antipolytic Activities of Quinolyl Carbanilates and Related Analogues. *J. Med. Chem.* **1987**, *30* (1), 62-67. <https://doi.org/10.1021/jm00384a011>.
28. Khalifah, R. G. The Carbon Dioxide Hydration Activity of Carbonic Anhydrase. *J. Biol. Chem.* **1971**, *246* (8), 2561-2573. <https://doi.org/10.1073/jbipnas.70.7.1986>.
29. Tarzia, G.; Duranti, A.; Gatti, G.; Piersanti, G.; Tontini, A.; Rivara, S.; Lodola, A.; Plazzi, P. V.; Mor, M.; Kathuria, S.; et al. Synthesis and Structure-Activity Relationships of FAAH Inhibitors: Cyclohexylcarbamic Acid Biphenyl Esters with Chemical Modulation at the Proximal Phenyl Ring. *Chem. Med. Chem.* **2006**, *1* (1), 130-139. <https://doi.org/10.1002/cmdc.200500017>.
30. Meng, F.; Evans, J. W.; Bhupathi, D.; Banica, M.; Lan, L.; Lorente, G.; Duan, J. X.; Cai, X.; Mowday, A. M.; Guise, C. P.; et al. Molecular and Cellular Pharmacology of the Hypoxia-Activated Prodrug TH-302. *Mol. Cancer Ther.* **2012**, *11* (3), 740-751. <https://doi.org/10.1158/1535-7163.mct-11-0634>.
31. Sharma, A.; Tiwari, M.; Supuran, C.T. Novel coumarins and benzocoumarins acting as isoform-selective inhibitors against the tumor-associated carbonic anhydrase IX. *J. Enzyme Inhib. Med. Chem.* **2014**, *29*, 292-6. <https://doi.org/10.3109/14756366.2013.777334>.

Chapter 3

32. Durdagi, S.; Scozzafava, G.; Vullo, D.; Sahin, H.; Kolayli, S.; Supuran, C.T. Inhibition of mammalian carbonic anhydrases I-XIV with grayanotoxin III: solution and in silico studies. *J. Enzyme Inhib. Med. Chem.* **2014**, *29*, 469-75. <https://doi.org/10.3109/14756366.2013.804072>.
33. Alterio, V.; Hilvo, M.; Di Fiore, A.; Supuran, C.T.; Pan, P.; Parkkila, S.; Scaloni, A.; Pastorek, J.; Pastorekova, S.; Pedone, C.; Scozzafava, A.; Monti, S.M.; De Simone, G. Crystal structure of the catalytic domain of the tumor-associated human carbonic anhydrase IX. *Proc. Natl. Acad. Sci. USA* **2009**, *106*, 16233-16238. <https://doi.org/10.1073/pnas.0908301106>.
34. Ditte, P.; Dequiedt, F.; Svastova, E.; Hulikova, A.; Ohradanova-Repic, A.; Zatovicova, M.; Csaderova, L.; Kopacek, J.; Supuran, C.T.; Pastorekova, S.; Pastorek, J. Phosphorylation of carbonic anhydrase IX controls its ability to mediate extracellular acidification in hypoxic tumors. *Cancer Res.* **2011**, *71* (24), 7558-7567. <https://doi.org/10.1158/0008-5472.can-11-2520>.
35. Aspatwar, A.; Hammaren, M. M.; Parikka, M.; Parkkila, S. Rapid Evaluation of Toxicity of Chemical Compounds Using Zebrafish Embryos. *J. Vis. Exp.* **2019**, *2019* (150), 1-7. <https://doi.org/10.3791/59315>.
36. Aspatwar, A.; Hammarén, M.; Koskinen, S.; Luukinen, B.; Barker, H.; Carta, F.; Supuran, C. T.; Parikka, M.; Parkkila, S. β -CA-Specific Inhibitor Dithiocarbamate Fc14–584B: A Novel Antimycobacterial Agent with Potential to Treat Drug-Resistant Tuberculosis. *J. Enzyme Inhib. Med. Chem.* **2017**, *32* (1), 832-840. <https://doi.org/10.1080/14756366.2017.1332056>.
37. Gourmelon, A.; Delrue, N. Validation in Support of Internationally Harmonised OECD Test Guidelines for Assessing the Safety of Chemicals. *Adv. Exp. Med. Biol.* **2016**, *856*, 9-32. https://doi.org/10.1007/978-3-319-33826-2_2.
38. Ritz, C.; Baty, F.; Streibig, J.C.; Gerhard, D. Dose-Response Analysis Using R. *Plos One* **2015**, *10* (12), e0146021. <https://doi.org/10.1371/journal.pone.0146021>.

Chapter 4

Design, synthesis and biological evaluations of toll-like receptor 7 & 8 agonist HAP (Imiquimod / Resiquimod) and Bruton's tyrosine kinase inhibitor HAPs (ibrutinib)

Emilie Anduran, Ying Cong, Rianne Biemans, Dennis Suylen, Ingrid Dijkgraaf, Philippe Lambin, Ludwig J. Dubois and Jean-Yves Winum.

In preparation

Abstract

Nowadays, Immunotherapy is becoming a powerful strategy in cancer treatment by reactivating the immune system to fight against tumour cells through a natural process, evaded during the tumour progression. Hypoxia, a common feature of solid tumour, is associated to an aggressive phenotype, tumour cell proliferation and is involved in the suppression of anti-tumour immune responses, thus causing immunotherapy resistance leading to a poor patient prognosis. Therefore, the hypoxic microenvironment represents today, an extremely valuable target for cancer therapy. Indeed, numerous therapeutic strategies have been developed to counteract this hypoxic phenotype, such as hypoxia activated prodrugs (HAPs) allowing the delivery of a cytotoxic payload by targeting the hypoxic tumour environment. Here, we proposed the design, synthesis and biological evaluations of a series of HAP analogues allowing the release of a cytotoxic payload in the hypoxic tumour microenvironment. These HAPs comprise a hypoxic trigger connected *via* a carbamate link to a toll-like receptor agonist or an inhibitor of Bruton's tyrosine kinase, with the idea to release the drug undergoing an enzymatic activation in hypoxic tumour. We designed and synthesized these HAPs combining a nitroimidazole, a nitrofurane and a nitrothiophene as hypoxia trigger, two toll-like receptor agonists, Imiquimod and Resiquimod and an inhibitor of Bruton's tyrosine kinase, Ibrutinib as payloads. One of the Resiquimod analogues was the only prodrug to show efficacy in anoxic condition compared to normoxia despite some stability issues. This suggests that these HAPs, based on the same coupling synthesis are able to release their cytotoxic payload under anoxia but the complexity of the synthesis makes them difficult to study. The purpose of this work was to study the ability of the HAPs to be reduced and to release immunotherapeutics on tumour cells under anoxic conditions.

Introduction

The human immune system operates through two types of immune responses. The innate immune response corresponds to a less specific, but rapid action of immune cells such as macrophages, natural killers, dendritic cells, monocytes and neutrophils. They represent the first line of defence of the human organism against abnormal cells and pathogens. These innate immune cells use pattern recognition receptors to be able to detect pathogen-associated molecular patterns (PAMPs) or damaged-associated molecular pattern (DAMPs) which will allow the secretion of inflammatory cytokines in order to kill cancer cells. The second type of immunity is the adaptive immune response. T cells and B cells act with high specificity recognition against abnormal cells and pathogens, neutralizing them with T cells and by producing specific antibodies.¹⁻³

Cancer immunotherapy is becoming, nowadays, a powerful strategy in anticancer treatment as it is based on the reactivation of the immune system to attack cancer cells through a natural process which is evaded during the tumour progression.⁴⁻⁸ During the anticancer immune response, antigen-presenting cells (APC) take up tumour antigens on tumour tissue to carry them to the lymph nodes. There, the APCs stimulate naïve T cells to proliferate and to differentiate in *e.g.* cytotoxic T cells, which then migrate back to the tumour to kill cancer cells.⁹⁻¹²

Toll-like receptors (TLRs) are one of the most important families of pattern-recognition receptors expressed on immune cells that recognize PAMPs and DAMPs.^{3,5,10} Their activation allows the production of cytokines which induce the antitumour immune response.^{11,13,14} TLRs can also be expressed by tumour cells to cause a direct cytotoxic effect after activation.⁴ The human genome possesses ten functional TLRs, among them TLRs 1, 2, 4, 5, 6 and 10 corresponding to transmembrane receptors and TLRs 3, 7, 8 and 9 to endosomal receptors.¹⁵ TLRs 7 and 8 can be activated by the binding of small molecule agonists such as imidazoquinolines.¹⁶ Among this family of compounds, imiquimod and resiquimod, respectively TLR7 and TLR7/8 agonists, are two analogous drugs which have been commercialized as topical treatment of basal cell carcinoma but have shown side-effects.^{13,15,17}

Bruton's tyrosine kinase (BTK) is a cytosolic kinase from the TEC family of kinases playing an important role in the immune system as a target against B cells malignancies.¹⁸ Ibrutinib is the first BTK inhibitor to have been commercialized but it has shown, like imidazoquinolines agonists, some side-effects.¹⁹

Hypoxia, nowadays known as a common feature of solid tumours, has been shown to be involved in the suppression of anti-tumour immune response in cancer cells and thus cause immunotherapy resistance.²⁰ Indeed, tumours can evade immune recognition and destruction by cytotoxic T-cells via several mechanisms, including the generation of an immunosuppressive environment. This immunosuppressive environment manifests through the recruitment of immunosuppressive cells such as regulatory T-cells and myeloid derived suppressor cells, which suppress the effector function of cytotoxic T-cells.

In order to improve immunotherapy strategy within a hypoxic tumour microenvironment and to overcome the side-effects observed after the use of immunotherapeutics, we have designed

new hypoxia activated prodrugs (HAPs) enabling the targeting and the release of these drugs in the hypoxic tumour environment.

Results and discussion

Two toll-like receptor agonists, Imiquimod and Resiquimod and a Bruton's tyrosine kinase inhibitor, Ibrutinib, were coupled to three bioreducible moieties, the 2-nitroimidazol-, nitrofuran- and nitrothiophene-based groups (Figure 1).

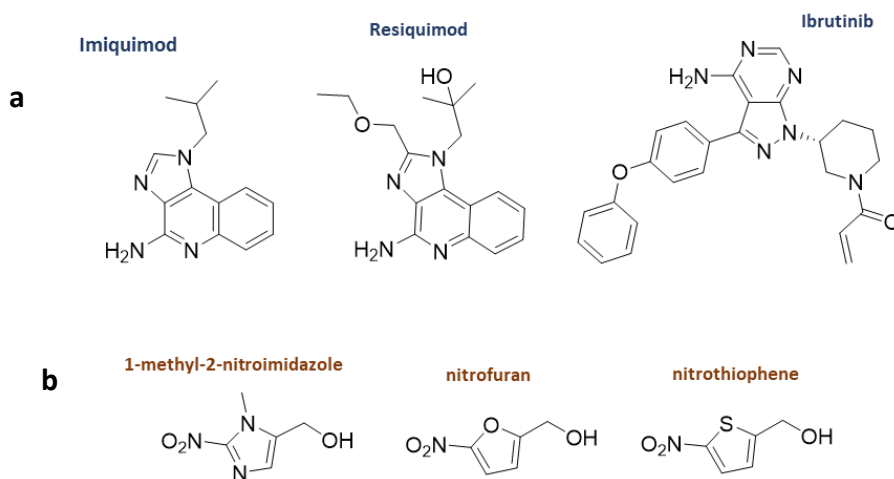
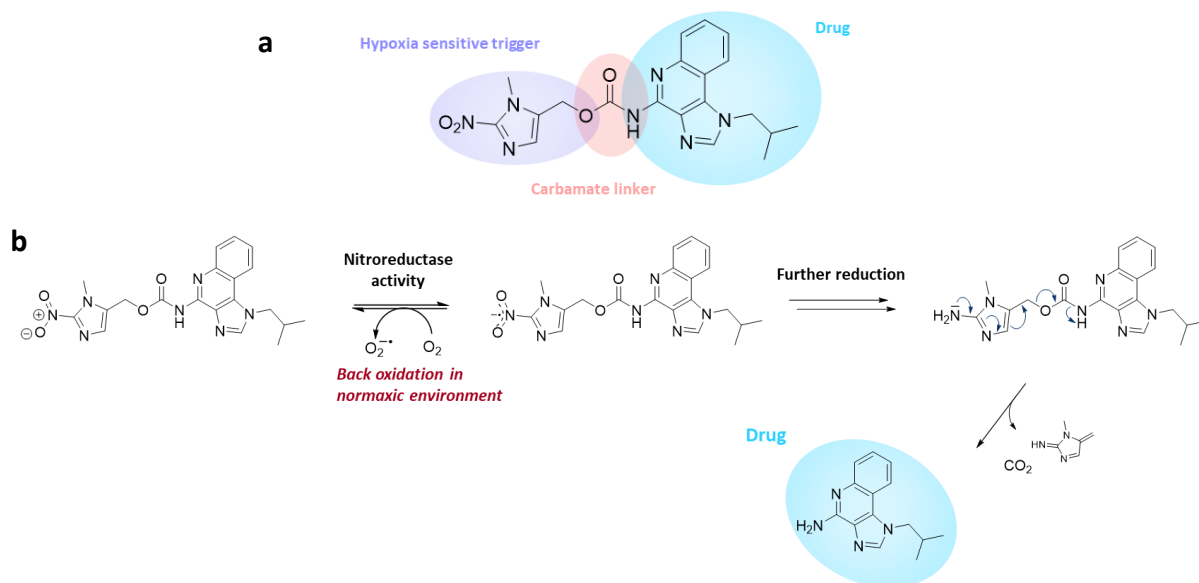


Figure 1: (a) structures of drugs. (b) bioreducible moieties.

These nitro compounds were used as a hypoxia sensitive trigger in order to improve the targeting of these drugs and to allow their release by undergoing a bioreduction reaction depending on the oxygen level in the tumour microenvironment (Scheme 1).²¹

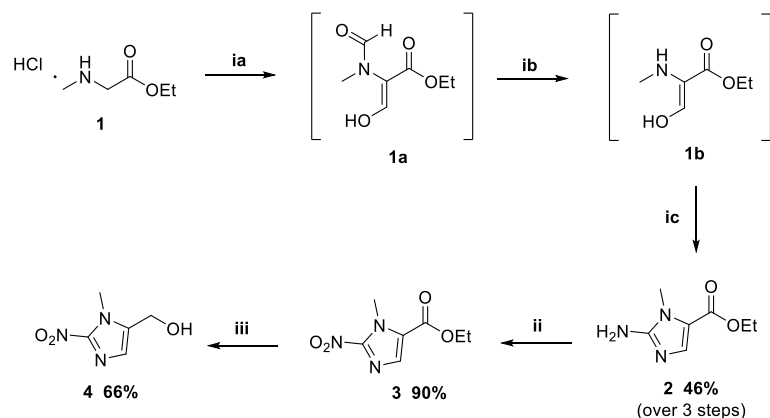
In this study we decided to use the 1-methyl-2-nitroimidazole, the nitrofuran and the nitrothiophene groups based on their varying reduction potential in the hypoxic environment with the idea to observe differences during the drug release.²² These three nitro-based compounds bear a hydroxyl function essential to couple them to the amine function of the drugs by forming a carbamate linker.^{23,24} This linker plays an important role in the control of the drug activity by inhibiting the activity of the imiquimod, resiquimod and ibrutinib amines until their release in the tumour environment.²⁵



Scheme 1: (a) structure of HAP compound combining the 2-nitroimidazole and Imiquimod. (b) mechanism of drug release.

Only nitroimidazole was available from commercial sources. The synthesis of the 2-nitroimidazole and the formation of the nitrothiophene alcohol from the commercially available aldehyde have been achieved in our laboratory. The 1-methyl-2-nitroimidazole group was synthesized in three steps following procedures already described in the literature (scheme 2).^{22,26,27} The first step, *via* two intermediates, resulted in the formation of the 2-aminoimidazole using the sarcosine ethyl ester as starting material. The use of the ethyl ester instead of the methyl ester has been described as an improvement of the original procedure preventing low reproducibility and solubility issues in the reaction mixture.²⁶ The first intermediate **1a**, was furnished by the treatment of the sarcosine ethyl ester with sodium hydride and ethyl formate as a diformylation step. Then the N-deformylation step occurred in acidic conditions by using concentrated hydrochloric acid to form **1b**. The imidazole ring was formed through a Marckwald cyclisation using cyanamide with an overall yield of 46%.²⁸

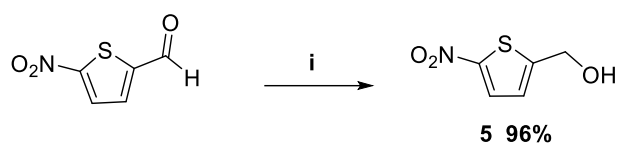
The second step of this synthesis pathway corresponded to the introduction of the nitro group through a diazotation reaction of the amine **2** using sodium nitrite. The alcohol **4** was obtained by a reduction step on **3** using NaBH₄ as reducing agent with a yield of 66% (Scheme 2).



Scheme 2: Reagents and conditions: (ia) NaH, EtOCHO, THF, rt, 18h; (ib) conc. HCl, EtOH, rt, 2h; (ic) NH₂CN, EtOH, H₂O, reflux, 1.5h; (ii) NaNO₂, AcOH, rt, 5h; (iii) NaBH₄, THF/MeOH 6/0.5, 0°C, 45min to rt, 1h.

Chapter 4

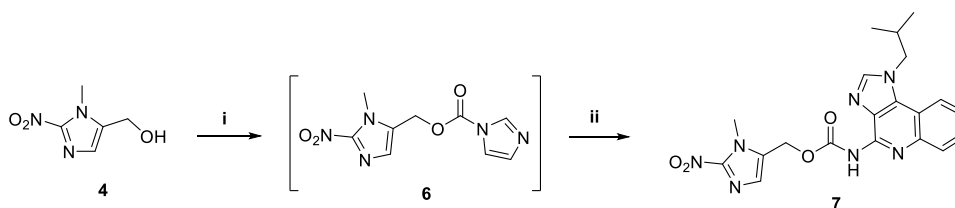
In order to enable the coupling of the nitrothiophene-based group to the drugs, it was necessary to achieve a reduction step on the commercially available aldehyde compound to afford the alcohol (Scheme 3).²⁴



Scheme 3: reagents and conditions: (i) NaBH₄, MeOH, from 0°C to rt, 2h.

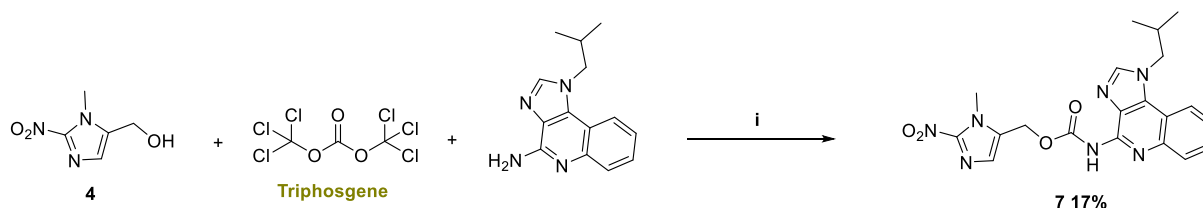
To enable the formation of the expected HAP, different reaction conditions were tested starting by the coupling of the 2-nitroimidazole with Imiquimod in a one-step reaction (Scheme 4). The synthesis of this compound was tested first by using the same procedure employed previously in the lab for the formation of other HAPs.²⁹ Due to the extremely low reactivity of the Imiquimod amine induced by the electron-withdrawing effect of the nitrogen in position 1, reaction conditions were adapted for microwave heating.

Carbonyl diimidazole was used as a coupling agent in the presence of the alcohol **4** in THF to first activate the hydroxyl group forming the intermediate **6**. Then Imiquimod was added and the reaction mixture was stirred in a microwave using conditions already described in the literature.^{1,13} However, we didn't observe the formation of the carbamate at the end of the reaction. Therefore, different coupling agents responsible for the activation of the alcohol/amine were tested as well as stirring at room temperature instead of using a microwave.



Scheme 4: Coupling reaction between the 2-nitroimidazole alcohol and the Imiquimod amine. Reagents and conditions: (i) CDI, THF, rt, 3h; (ii) Imiquimod, DIEA, MW.

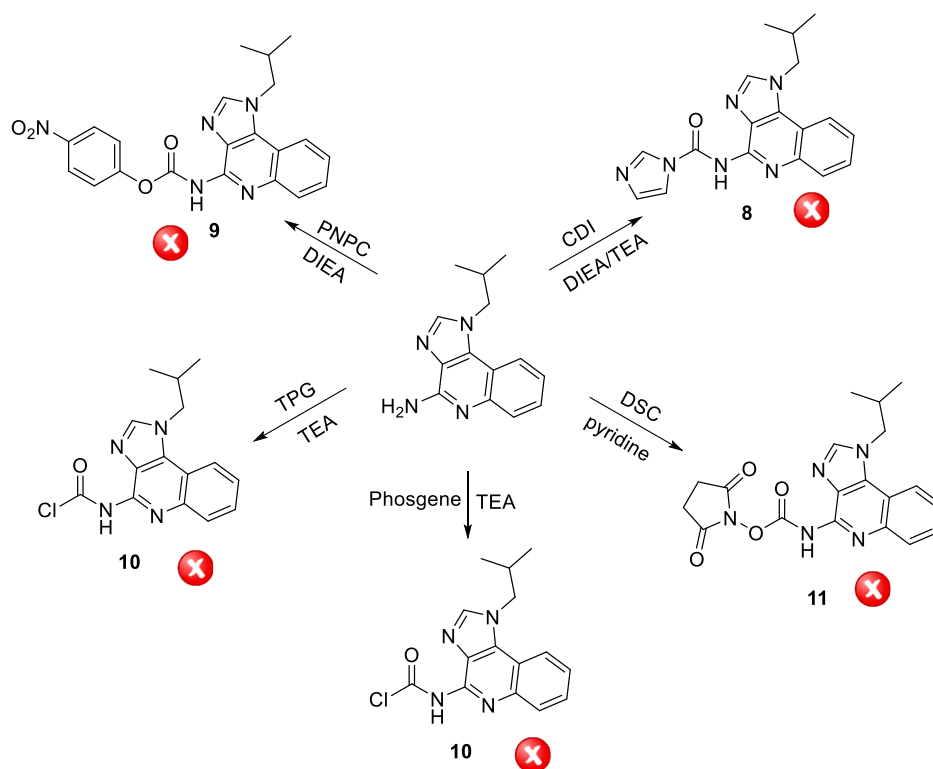
The formation of the compound **7** was observed for the first time when using triphosgen as activating agent and by stirring the reaction at room temperature (Scheme 5), but **7** was only obtained in a very low yield (17%).



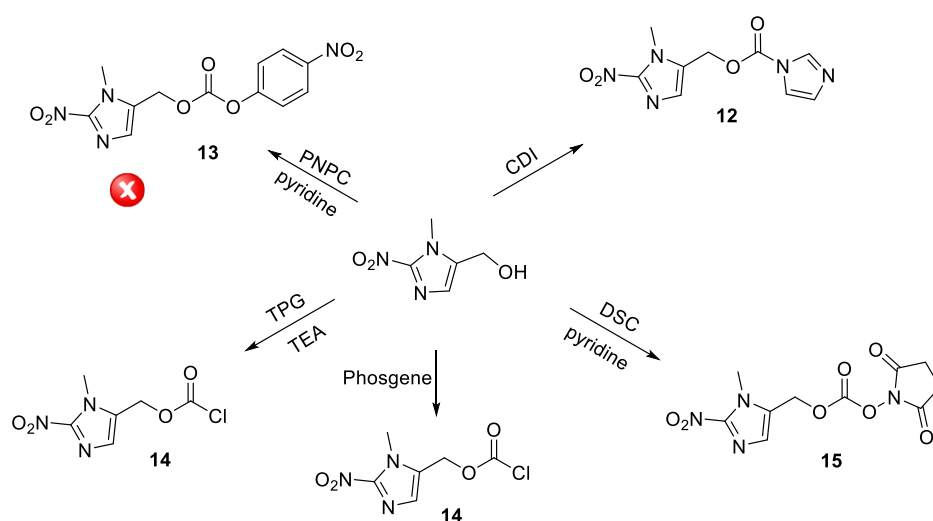
Scheme 5: Coupling reaction using triphosgen. Reagents and conditions: (i) DIEA, DCM, rt, 3h.

In order to improve this reaction yield and to better control the formation of **7**, a different strategy was applied to first form and isolate the activated intermediate either on the alcohol or

on the amine and in a second step, to achieve the coupling. We wanted to determine which coupling agent would be efficient enough to react on the total amount of the alcohol or amine and if the intermediate formed would be sufficiently activated to allow the coupling of the drug in the second step. Different coupling agents were tested to activate both Imiquimod (scheme 6) and 2-nitroimidazole (scheme 7) using carbonyldiimidazole, *p*-nitrophenyl chloroformate, triphosgen, phosgen or disuccinimidyl carbonate. Facing solubility issues during the Imiquimod activation, different techniques were used to obtain the desired intermediate such as microwave^{1,13} or a ball-milling procedure.^{30,31}



Scheme 6: Reaction conditions to activate the Imiquimod



Scheme 7: Reaction conditions to activate 2-nitroimidazole

After several activation tests on imiquimod (Scheme 6) and 2-nitroimidazole (Scheme 7), we demonstrated that the 2-nitroimidazole was easier to activate compared to Imiquimod. Therefore, we decided to start with the formation of the activated alcohol intermediate and in a second step to couple the amine. We first started with the isolation of the intermediate **12** obtained by activation with carbonyldiimidazole. A total conversion was observed by TLC, but the crude compound was not stable enough to be purified by silica chromatography. As the crude product was clean on TLC and on NMR, no purification has been done and it was used directly in the coupling step with Imiquimod. We didn't observe any formation of the expected final compound. Therefore, we tried to activate the alcohol in a different manner by using *p*-nitrophenyl chloroformate as described by Burt et al.^{32,33} In this case, however, we didn't succeed to form the carbonate intermediate **13**. Harder conditions were tested using triphosgene and phosgene to form a chloroformate intermediate **14**.³⁴ As in the case of the activation with CDI, a total conversion was observed by TLC and the crude product was directly used in the following step, but again we didn't observe the formation of the expected compound from the coupling between the chloroformate nitroimidazole and the amine of imiquimod. This activation was done as well on the nitrofuran and nitrothiophene alcohol, however with same results as for the Imiquimod coupling with the nitroimidazole. Disuccinimidyl carbonate was tested as an alternative coupling agent with the aim to couple Imiquimod with the bio-reducible moieties. As described earlier, the alcohol activation was successfully achieved on the nitroimidazole and then Imiquimod was coupled on the activated intermediate **15** (Scheme 7). This time, the formation of the expected compound was observed, however, these activating conditions didn't improve the yield of the coupling step. These reaction conditions, then, were applied to the other alcohol and amines to obtain the other HAP compounds.

Because of constraints related to the low drug reactivity and the poor water and solvent solubility of Imiquimod and Ibrutinib, the coupling reactions were not reproducible with the same yield, thereby it has not been possible to isolate all the 9 compounds. Resiquimod showed a better solubility and a higher reactivity than the two other drugs. Furthermore, log *P* calculations were performed in order to estimate the solubility of the prodrugs, we observed that all compounds showed a profile more lipophilic than hydrophilic as all the calculation values were positives. For each compound family, the nitro-based compound seemed to be more soluble compared to the nitrofuran- and nitrothiophene-based prodrugs and were easier to synthesize. The coupling of the nitrofuran showed extremely low yield in the three cases, therefore, it was not possible to isolate compounds **16** and **22** after purification (Table 1, in grey). The Resiquimod family showed the lowest log *P* values, indicative for a higher water solubility compared to the other compounds.

Solubility tests were performed on Imiquimod, Resiquimod, Ibrutinib alone and on each prodrug derivative using cell culture medium containing different DMSO concentrations with the aim to select the compounds to be tested for efficiency on cells. It was observed that only the Resiquimod and Resiquimod HAPs were soluble in culture medium at a maximum concentration of 1mM with 1% DMSO final concentration. Solubility tests for the nitrofuran-based compound **19** could not be performed as we did not succeed to obtain sufficient large amounts for further testing.

Table 1: Structures of the 9 HAP compound analogues

REFERENCES	STRUCTURE	MW (g/mol)	LogP = $\log\left(\frac{[C]_{oct.}}{[C]_{w.}}\right)^*$	SOLUBILITY (1% DMSO in medium)
IMIQUIMOD		423.43	3.05	✗
		409.40	3.81	-
		425.46	4.46	✗
TLR agonist / BTK inhibitor HAPs RESIQUIMOD		497.51	2.54	✓
		483.48	3.31	?
		499.54	3.95	✓
IBRUTINIB		623.63	3.90	✗
		609.60	4.66	-
		625.66	5.31	✗

* Log P calculated using Molinspiration calculation website

Viability assays on the Resiquimod analogues were performed in order to evaluate the cytotoxicity of the prodrugs **18** and **20**. LC-MS analysis has been done on **18** and **20** prior the viability assay to validate the purity of compounds. We observed the presence of residual Resiquimod with **18**, showing a degradation by decoupling of the payload of approximately 40% (Figure 1). **20** showed a degradation around 70-75% (Figure 2S). Cytotoxicity of the two prodrugs was evaluated under normoxic and anoxic (<0.01% O₂) conditions in order to evaluate the ability of the prodrugs to release the payload on anoxia. The assay has been done using two different cell lines, CT26, a murine colon carcinoma cell line and PC3, a human prostate cancer cell line by using 500 μM as highest concentrations.

In CT26 compound **18** showed an IC₅₀ of 404.2 μM under normoxia and 29.35 μM under anoxia. The effect observed in normoxic conditions could be related to the residual Resiquimod present with the prodrug while in anoxic conditions a higher effect can be observed due to the enzymatic activation of the prodrug resulting in the intracellular release of resiquimod. Resiquimod alone showed, in normoxic and anoxic conditions, IC₅₀ of respectively 65.03 μM and higher than the maximal concentration tested (578 μM). This low cytotoxic effect observed in anoxic conditions could be explained because of the upregulation of tumour cell efflux pumps.

These efflux pumps are membrane proteins able to actively pump various drugs out of the cells under hypoxia, reducing the cytotoxic efficacy of these drugs.^{35,36}

The same profile was observed in PC3 cell line, **18** showed IC₅₀ of 111,4 μM and 16,05 μM in normoxic and anoxic conditions, respectively, explained by the activation of **18** inside the intracellular environment of cells under anoxia. Resiquimod showed an IC₅₀ of 56.45 μM in normoxia and 462.7 μM in anoxia. Due to the same efflux pump mechanisms explained above, we observed, here as well, a lower cytotoxic effect under anoxia (Figure 2a).

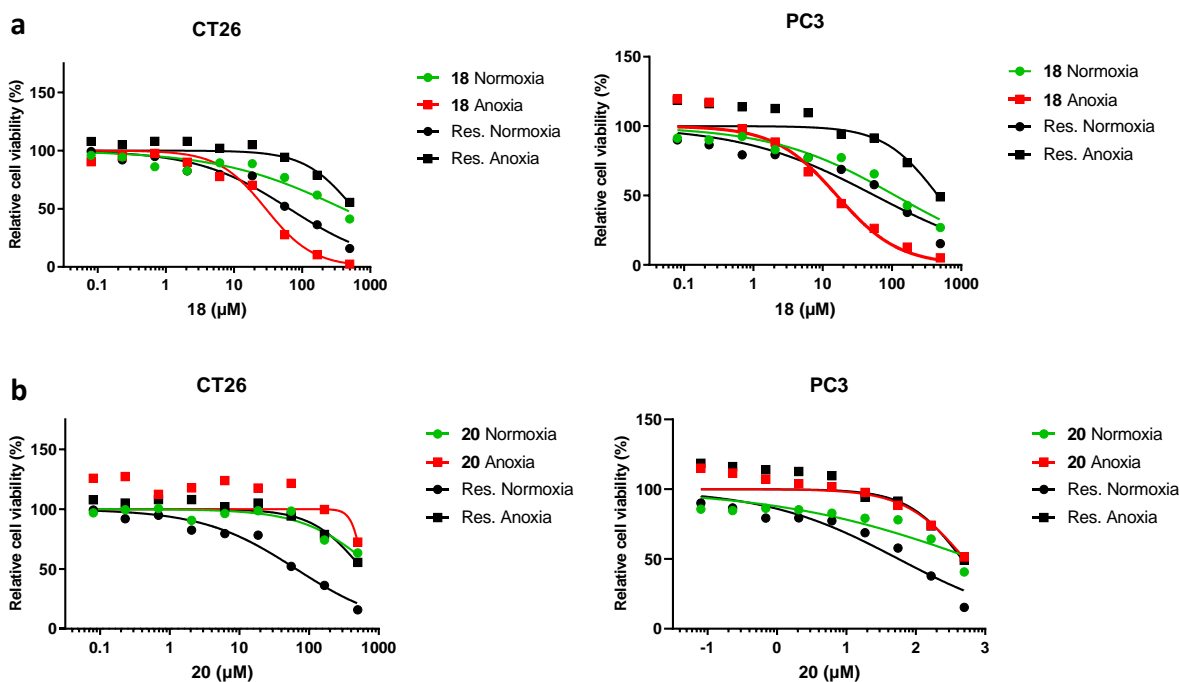


Figure 2: Relative cell viability (%) in CT26 and PC3 cells exposed to increasing concentrations of the derivatives (a) **18** and (b) **20** under normoxic (green) and anoxic (red) conditions compared to Resiquimod (black).

We did not obtain relevant cytotoxicity results after testing **20** due to a too pronounced degradation, confirmed by LC-MS analysis (Figure 2S). Indeed, in CT26 we have observed a relatively high IC₅₀, higher than the maximal concentration tested; 873.7 μM and 600.7 μM in normoxic and anoxic conditions respectively, showing a similar effect of the prodrug on cells likely caused by the presence of residual Resiquimod in a too large quantity. These effects could be compared to the one of Resiquimod alone in anoxic conditions with a IC₅₀ of 578.7 μM, which showed a very low cytotoxicity on cells explained by the efflux pump effect. Only Resiquimod in normoxic conditions showed a higher cytotoxicity with an IC₅₀ of 65.03 μM.

Comparable results have been observed in the PC3 cell line. **20** showed low cytotoxicity in normoxia and anoxia with an IC₅₀ of 690.8 μM and 510.7 μM respectively, similar as Resiquimod in anoxic conditions (IC₅₀ of 462.7 μM). Only the drug alone showed, here as well, a higher effect under normoxia with an IC₅₀ of 56.45 μM (Figure 2b).

Conclusion

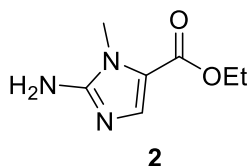
Immunotherapy is becoming, today, a powerful strategy in cancer treatment by reactivating the immune system to fight against tumour cells through a natural process which is evaded during the tumour progression. We described here the design, synthesis and biological evaluation of several HAP analogues allowing the release of a cytotoxic payload in the hypoxic tumour microenvironment. We designed and synthesized these HAPs combining a nitroimidazole, a nitrofurane and a nitrothiophene as hypoxia trigger, two toll-like receptor agonist, Imiquimod and Resiquimod and an inhibitor of Bruton's tyrosine kinase, Ibrutinib as payloads. These two moieties have been connected using a carbamate linker to enable the release of the drug under hypoxia, forming a molecule of carbon dioxide as by-product. Solubility and reactivity issues have been encountered during the synthesis of these HAPs linked to the three payloads, preventing the formation of some of the expected HAPs. Biological evaluations have been performed using viability assay on **18** and **20**, two Resiquimod-based prodrugs, soluble in the cell medium. **18** showed a higher cytotoxicity in anoxic conditions than in normoxia explained by the release of the drug under anoxia, as expected. Unfortunately, **20** did not show any positive results likely due to a too high degradation. These first results suggest that these HAPs, based on the same coupling synthesis are able to release their cytotoxic payload under anoxia but the complexity of the synthesis makes them difficult to study.

Experimental section

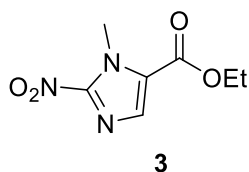
Chemistry

General

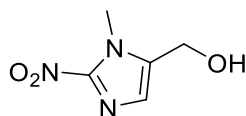
All reagents and solvents were of commercial quality and used without further purification unless otherwise specified. All reactions were carried out under an inert atmosphere of argon. TLC analyses were performed on silica gel 60 F254 plates (Merck Art. no. 1.05554). Spots were visualized under 254 nm UV illumination or by ninhydrin solution spraying. ^1H and ^{13}C NMR spectra were recorded on a Bruker DRX-400 spectrometer using $\text{CDCl}_3\text{-d}_6$, MeOD-d_6 or DMSO-d_6 as solvent and tetramethylsilane as internal standard. For ^1H and ^{13}C NMR spectra, chemical shifts are expressed in δ (ppm) downfield from tetramethylsilane, and coupling constants (J) are expressed in hertz. Electron ionization mass analysis were performed in positive or negative mode on a Waters acquity UPLC. All compounds that were tested in the biological assays were analyzed by high-resolution ESI mass spectra (HRMS) using a Bruker microTOF-Q II mass spectrometer fitted with an electrospray ion source in order to confirm the purity of >95%.

ethyl 2-amino-1-methyl-1H-imidazole-5-carboxylate (2)

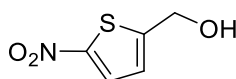
To a suspension of ethyl *N*-methylglycine hydrochloride (85.4 mmol, 1 eq) in dry THF (60 mL) and dry absolute ethanol (7mL) was added ethyl formate (37 mL). The mixture was cooled to 0 °C and sodium hydride 60 % (13.6 g, 4 eq) was added portion wise. Once gas evolution had ceased, the reaction mixture was warmed to rt and stirred for 18h. the reaction was quenched by addition of wet diethyl ether and filtered. The collected solid were washed with diethyl ether then dried under vacuum. The solid was then suspended in ethanol (250 mL) and concentrated hydrochloric acid (50 mL) was slowly added to the suspension. The suspension was stirred at rt for 2h then filtered to remove salt. The resulting solution was concentrated under vacuum then dissolved in ethanol (350 mL) and water (150 mL) and pH was adjusted to 3 by using aqueous sodium hydroxide 2 M. Cyanamide (130.2 mmol, 2 eq) was added to the solution and the reaction mixture was heated to 100 °C for 2h then cooled to rt and concentrated *in vacuo*. The residue was dissolved in ethyl acetate and saturated aqueous potassium carbonate solution and was extracted with ethyl acetate. The combined organic fractions were washed with brine, dried over sodium sulfate, filtered and concentrated under vacuum. The crude was purified by trituration in dichloromethane to afford **2** (6.7 g, 46 % yield). ¹H NMR (400 MHz, CD₃OD) δ 7.32 (s, 1H), 4.23 (q, *J* = 7.1 Hz, 2H), 3.62 (s, 3H), 1.31 (t, *J* = 7.1 Hz, 3H). ¹³C NMR (400 MHz, CD₃OD) δ 161.99, 155.26, 135.87, 119.28, 60.89, 30.91, 14.69.

ethyl 1-methyl-2-nitro-1H-imidazole-5-carboxylate (3)

To an aqueous solution of sodium nitrite (32 mL, 25.37 g, 367.70 mmol, 10 eq), was added **1** (36.77 mmol, 1 eq) in acetic acid (35 mL) drop wise. The reaction mixture was stirred at rt for 5h until gas evolution ceased. The organic fraction was extracted with CH₂Cl₂, washed with brine and saturated solution of Na₂SO₃, dried over Na₂SO₄ and filtered. The filtrate was concentrated under vacuum to give **3** (6.59 g, 90 % yield). ¹H NMR (400 MHz, CD₃OD) δ 7.72 (s, 1H), 4.39 (q, *J* = 7.2 Hz, 2H), 4.30 (s, 3H), 1.39 (t, *J* = 7.1 Hz, 4H). ¹³C NMR (400 MHz, CD₃OD) δ 160.34, 137.03, 134.65, 127.93, 62.75, 35.93, 14.44.

(1-methyl-2-nitro-1H-imidazol-5-yl)methanol (4)**4**

To a solution of **2** (24.10 mmol, 1 eq) in dry THF (125 mL) and MeOH (10 mL) was added NaBH₄ (72,30 mmol, 3 eq) portion wise at 0 °C. the reaction was stirred at 0 °C for 45 min, then at rt for 1h. the reaction mixture was cooled to 0 °C, quenched by addition of ice and pH was adjusted to 7 using a 1 M HCl aqueous solution. The aqueous solution was saturated with NaCl, and the organic fraction was extracted with EtOAc, washed with saturated aqueous NaHCO₃, dried over Na₂SO₄ and the solvent was removed under reduced pressure. The crude was triturated with DCM and the solid was filtered to afford **4** as a yellow solid. ¹H NMR (400 MHz, CD₃OD) δ 7.10 (s, 1H), 4.66 (s, 2H), 4.04 (s, 3H). ¹³C NMR (400 MHz, CD₃OD) δ 139.32, 137.02, 127.41, 54.52, 34.81.

(5-nitrothiophen-2-yl)methanol (5)**5**

To a solution of 5-nitrothiophene-2-carbaldehyde (1.91 mmol, 1 eq) in dry methanol (8 mL) was added NaBH₄ (2.29 mmol, 1.2 eq) portion wise at 0 °C and the reaction mixture was stirred 2h at 0 °C. The reaction mixture was quenched by addition of ice and pH was adjusted to 7 using 2 M HCl aqueous solution. The organic fraction was extracted with EtOAc, dried over Na₂SO₄ and concentrated under vacuum. Purification by flash chromatography on silica gel (methanol/dichloromethane 0.5/9.5) afford **5** (229 mg, 75 % yield). ¹H NMR (400 MHz, CDCl₃) δ 7.81 (d, *J* = 4.1 Hz, 1H), 6.93 (dt, *J* = 4.1, 1.0 Hz, 1H), 4.88 (s, 2H). ¹³C NMR (400 MHz, CDCl₃) δ 153.30, 151.13, 128.84, 123.57, 60.47. [M-H]⁻ calculated for [C₅H₄NO₃S]⁻: 157.9917 found: 157.9914.

General procedure for alcohol activation:

To a solution of disuccinimidyl carbonate (2.39 mmol, 1.5 eq) in dichloromethane (7 mL) was added dropwise at 0°C a solution of the corresponding hydroxy starting compound (1.59 mmol, 1 eq) and pyridine (1.91 mmol, 1.2 eq) in dichloromethane (8 mL). The reaction mixture was stirred at room temperature (rt) for 2h and the solvent was removed under vacuum. The crude carbonate was used at the following step without further purification.

General procedure for drug coupling 7, 17, 18, 19, 20, 21, 22 and 23:

To a solution of carbonate (0.31 mmol, 1 eq) in dichloromethane (1 mL) was added at rt a solution of the corresponding amine (0.31 mmol, 1 eq) and triethylamine (0.62 mmol, 2 eq) in dichloromethane (2mL). The reaction mixture was stirred overnight and the solvent was removed under vacuum. The residue was purified by flash chromatography on C18 gel column (CH₃CN 45% /H₂O).

(1-methyl-2-nitro-1H-imidazol-5-yl)methyl (1-isobutyl-1H-imidazo[4,5-c]quinolin-4-yl)carbamate (7)

¹H NMR (400 MHz, CD₃OD) δ 8.24 (s, 1H), 8.21 (d, *J* = 8.3 Hz, 1H), 8.10 (d, *J* = 7.8 Hz, 1H), 7.67 (ddd, *J* = 8.4, 6.8, 1.1 Hz, 1H), 7.61 (ddd, *J* = 8.2, 7.1, 1.3 Hz, 1H), 7.31 (s, 1H), 5.43 (s, 2H), 4.49 (d, *J* = 7.5 Hz, 2H), 4.12 (s, 3H), 2.36 – 2.25 (m, 1H), 1.01 (d, *J* = 6.7 Hz, 6H). MS (ESI⁺) *m/z* 424.40 [M+H]⁺, 869.15 [M+2]⁺. HRMS (ESI⁺) [M+H]⁺ calculated for [C₂₀H₂₂N₇O₄]⁺: 424.1728 found: 424.1757.

(5-nitrothiophen-2-yl)methyl (1-isobutyl-1H-imidazo[4,5-c]quinolin-4-yl)carbamate (17)

HRMS (ESI⁺) [M+H]⁺ calculated for [C₂₀H₂₀N₅O₄S]⁺: 426.1231 found: 426.1217.

(1-methyl-2-nitro-1H-imidazol-5-yl)methyl (2-(ethoxymethyl)-1-(2-hydroxy-2-methylpropyl)-1H-imidazo[4,5-c]quinolin-4-yl)carbamate (18)

¹H NMR (400 MHz, CD₃OD) δ 8.73 (dd, *J* = 8.5, 0.8 Hz, 1H), 8.24 (dd, *J* = 8.5, 1.0 Hz, 1H), 7.91 (ddd, *J* = 8.5, 7.2, 1.2 Hz, 1H), 7.81 (ddd, *J* = 8.4, 7.2, 1.2 Hz, 1H), 7.39 (s, 1H), 5.62 (s, 2H), 5.11 (s, 2H), 4.93 (s, 2H), 4.14 (s, 3H), 3.66 (q, *J* = 7.0 Hz, 2H), 1.32 (s, 6H), 1.25 (t, *J* = 7.0 Hz, 3H). ¹³C NMR (400 MHz, CD₃OD) δ 157.85, 154.98, 144.99, 141.64, 131.96, 130.53, 128.38, 126.31, 124.49, 122.23, 116.49, 72.34, 67.81, 66.45, 58.90, 56.99, 49.00, 35.08, 34.89, 28.00, 15.36. MS (ESI⁺) *m/z* 498.45 [M+H]⁺.

(5-nitrofuran-2-yl)methyl (2-(ethoxymethyl)-1-(2-hydroxy-2-methylpropyl)-1H-imidazo[4,5-c]quinolin-4-yl)carbamate (19)

¹H NMR (400 MHz, CDCl₃) δ 8.29 (dd, *J* = 8.1, 1.6 Hz, 1H), 8.11 – 8.07 (m, 1H), 7.69 – 7.59 (m, 2H), 7.29 (d, *J* = 3.7 Hz, 1H), 6.19 (d, *J* = 5.6 Hz, 1H), 5.31 (s, 2H), 4.84 (d, *J* = 10.1 Hz, 2H), 4.75 (d, *J* = 10.2 Hz, 2H), 3.65 (tt, *J* = 6.6, 3.2 Hz, 2H), 1.35 (s, 6H), 1.24 (t, *J* = 7.0 Hz, 3H). ¹³C NMR (400 MHz, CDCl₃) δ 154.01, 152.09, 148.73, 143.53, 140.40, 137.92, 131.27, 127.93, 127.13, 126.92, 121.10, 120.39, 118.39, 98.28, 71.59, 70.58, 66.78, 65.41, 56.48. HRMS (ESI⁺) [M-H]⁻ calculated for [C₂₃H₂₄N₅O₇]⁻: 482.1681 found: 482.1670.

(5-nitrothiophen-2-yl)methyl (2-(ethoxymethyl)-1-(2-hydroxy-2-methylpropyl)-1H-imidazo[4,5-c]quinolin-4-yl)carbamate (20)

^1H NMR (400 MHz, CDCl_3) δ 8.39 (d, J = 3.8 Hz, 1H), 8.21 (d, J = 9.6 Hz, 1H), 8.16 (d, J = 8.6 Hz, 1H), 7.83 (d, J = 4.2 Hz, 1H), 7.67 – 7.59 (m, 1H), 7.55 – 7.47 (m, 1H), 7.14 (d, J = 3.9 Hz, 1H), 5.44 (s, 2H), 4.92 (s, 3H), 4.80 (s, 2H), 3.67 (dd, J = 13.6, 6.3 Hz, 2H), 3.03 (s, 1H), 1.33 (s, 6H), 1.26 (t, J = 6.8 Hz, 5H). ^{13}C NMR (400 MHz, CDCl_3) δ 150.90, 146.22, 144.53, 143.62, 135.67, 130.65, 128.45, 127.80, 127.08, 125.01, 123.52, 122.33, 120.20, 119.96, 117.02, 71.62, 66.92, 65.06, 61.37, 56.55, 28.04, 15.07. MS (ESI⁺) m/z 500.45 [M+H]⁺.

(1-methyl-2-nitro-1H-imidazol-5-yl)methyl (R)-(1-(1-acryloylpiperidin-3-yl)-3-(4-phenoxyphenyl)-1H-pyrazolo[3,4-d]pyrimidin-4-yl)carbamate (21)

MS (ESI⁺) m/z 624.22 [M+H]⁺.

(5-nitrothiophen-2-yl)methyl (R)-(1-(1-acryloylpiperidin-3-yl)-3-(4-phenoxyphenyl)-1H-pyrazolo[3,4-d]pyrimidin-4-yl)carbamate (23)

^1H NMR (400 MHz, CD_3OD) δ 8.64 (d, J = 4.9 Hz, 1H), 7.90 (d, J = 4.2 Hz, 2H), 7.86 (d, J = 4.2 Hz, 1H), 7.38 – 7.32 (m, 2H), 7.04 (d, J = 4.2 Hz, 1H), 7.02 – 6.97 (m, 3H), 6.83 (dd, J = 16.7, 10.6 Hz, 1H), 6.67 (dd, J = 16.8, 10.7 Hz, 1H), 6.26 – 6.09 (m, 1H), 5.77 (d, J = 10.6 Hz, 1H), 5.63 (d, J = 10.4 Hz, 1H), 5.38 (d, J = 0.7 Hz, 2H), 5.08 (d, J = 6.1 Hz, 1H), 4.69 – 4.60 (m, 1H), 4.31 – 4.21 (m, 1H), 4.12 (dd, J = 12.6, 6.2 Hz, 1H), 3.93 (dd, J = 13.6, 9.0 Hz, 1H), 2.52 – 2.34 (m, 1H), 2.33 – 2.21 (m, 1H), 2.17 – 2.05 (m, 1H), 1.85 – 1.65 (m, 2H). MS (ESI⁺) m/z 626.05 [M+H]⁺.

Biological assays

Cells

Murine colon carcinoma CT26 and human prostate cancer PC3 cells were cultured in DMEM (Sigma-Aldrich) and RPMI (Sigma-Aldrich), respectively, supplemented with 10% fetal bovine serum. Cells were exposed to anoxic conditions for 24 h in an anoxic chamber (Whitley MG500, anoxic workstation, Don Whitley Scientific, UK) with an atmosphere consisting of 5% CO_2 , 10% H_2 , and residual N_2 at 37 °C. Normoxic cells were grown in a cell culture incubator (HERAcell® 150 CO_2 Incubator, Thermo Fisher Scientific, Heraeus) with 21% O_2 , 5% CO_2 at 37 °C.

Cell viability assays

The cytotoxic efficacy of the bioreducible derivatives was determined based on cell viability assays using alamarBlue® (Invitrogen). In short, CT26 and PC3 were seeded in 96-well plates and allowed to attach overnight. The next day, plates were exposed to normoxia or anoxia. Compounds were dissolved in DMSO (50mM, Sigma-Aldrich) and final concentrations were made with pre-incubated anoxic or normoxic DMEM and RPMI and added to the wells after 24 h

Chapter 4

of exposure. Cells were exposed to compounds for 4h in anoxic conditions and normoxic conditions, after which they were allowed to grow for an additional 72 h under normoxic conditions prior to the measurement. Cells were incubated with alamarBlue® for 2 h in normoxic conditions, which corresponds with their metabolic function, a measure for cell viability. Fluorescence was measured using plate reader (SpectraMax® ID3, Molecular Devices) using a fluorescence excitation wavelength of 545 - 585 nm.

References

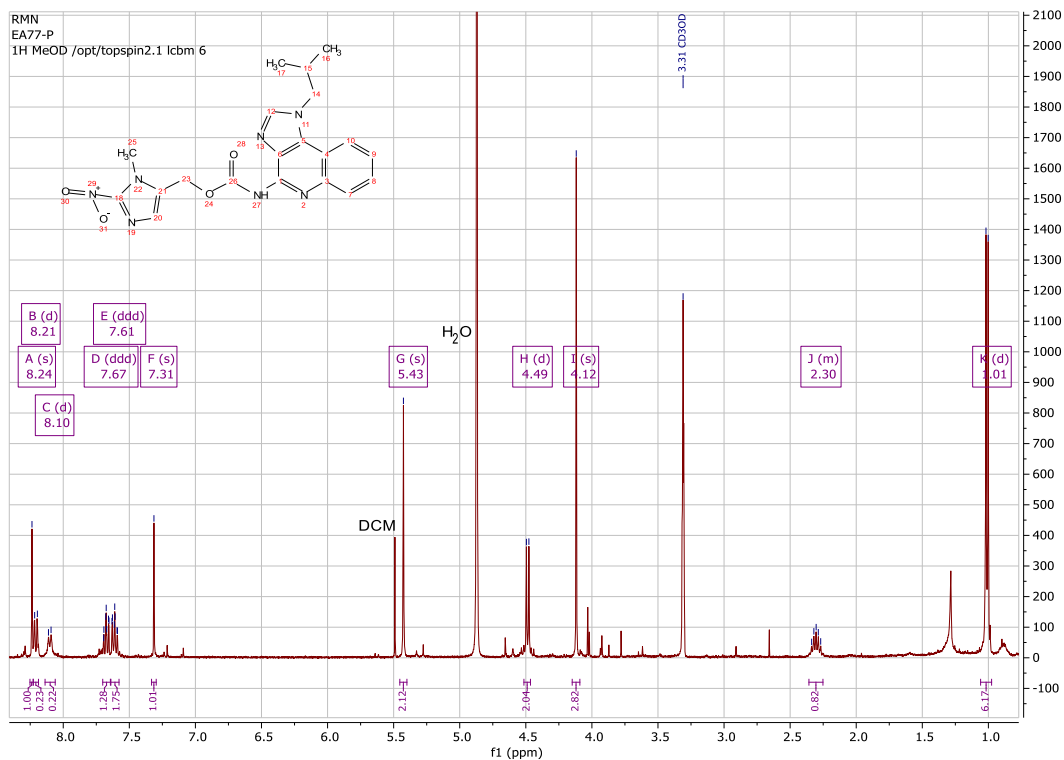
1. Keen, N.; McDonnell, K.; Park, P. U.; Mudd, G. E.; Ivanova-Berndt, G. Bicyclic Peptide Ligand PRR-A Conjugates and Uses Thereof. WO2019034868A1, **2019**.
2. Dong, H.; Markovic, S. N. *The Basics of Cancer Immunotherapy*. 1st ed.; Springer, **2018**.
<https://doi.org/10.1007/978-3-319-70622-1>.
3. Dajon, M.; Iribarren, K.; Cremer, I. Toll-like Receptor Stimulation in Cancer: A pro- and Anti-Tumor Double-Edged Sword. *Immunobiology* **2017**, *222* (1), 89–100. <https://doi.org/10.1016/j.imbio.2016.06.009>.
4. Galon, J.; Bruni, D. Approaches to Treat Immune Hot, Altered and Cold Tumours with Combination Immunotherapies. *Nature Reviews Drug Discovery* **2019**, *18*, 197–218. <https://doi.org/10.1038/s41573-018-0007-y>.
5. Huck, B. R.; Kçtzner, L.; Urbahns, K. Small Molecules Drive Big Improvements in Immuno- Oncology Therapies Angewandte. *Angewandte Chemie* **2018**, *57*, 4412–4428. <https://doi.org/10.1002/anie.201707816>.
6. Chen, S.; Song, Z.; Zhang, A. Small-Molecule Immuno-Oncology Therapy: Advances, Challenges and New Directions. *Current Topics in Medicinal Chemistry* **2019**, *19* (3), 180–185.
<https://doi.org/10.2174/1568026619666190308131805>.
7. Mpekris, F.; Voutouri, C.; Baish, J. W.; Duda, D. G.; Munn, L. L.; Stylianopoulos, T.; Jain, R. K. Combining Microenvironment Normalization Strategies to Improve Cancer Immunotherapy. *PNAS* **2020**, *117* (7), 3728–3737. <https://doi.org/10.1073/pnas.1919764117/-/DCSupplemental>.
8. Geng, Q.; Rohondia, S. O.; Khan, H. J.; Jiao, P.; Dou, Q. P. Small Molecules as Antagonists of Co-Inhibitory Pathways for Cancer Immunotherapy: A Patent Review (2018-2019). *Expert Opinion on Therapeutic Patents* **2020**, *30* (9), 677–694. <https://doi.org/10.1080/13543776.2020.1801640>.
9. Riley, R. S.; June, C. H.; Langer, R.; Mitchell, M. J. Delivery Technologies for Cancer Immunotherapy. *Nature Reviews Drug Discovery* **2019**, *18*, 175–196. <https://doi.org/10.1038/s41573-018-0006-z>.
10. Thauvin, C.; Widmer, J.; Mottas, I.; Hocevar, S.; Allémann, E.; Bourquin, C.; Delie, F. Development of Resiquimod-Loaded Modified PLA-Based Nanoparticles for Cancer Immunotherapy: A Kinetic Study. *European Journal of Pharmaceutics and Biopharmaceutics* **2019**, *139*, 253–261. <https://doi.org/10.1016/j.ejpb.2019.04.007>.
11. Kerr, W. G.; Chisholm, J. D. The Next Generation of Immunotherapy for Cancer: Small Molecules Could Make Big Waves. *The Journal of Immunology* **2019**, *202* (1), 11–19. <https://doi.org/10.4049/jimmunol.1800991>.
12. Michaelis, K. A.; Norgard, M. A.; Zhu, X.; Lévasseur, P. R.; Sivagnanam, S.; Liudahl, S. M.; Burfeind, K. G.; Olson, B.; Pelz, K. R.; Angeles Ramos, D. M.; Maurer, H. C.; Olive, K. P.; Coussens, L. M.; Morgan, T. K.; Marks, D. L. The TLR7/8 Agonist R848 Remodels Tumor and Host Responses to Promote Survival in Pancreatic Cancer. *Nature Communications* **2019**, *10* (1). <https://doi.org/10.1038/s41467-019-12657-w>.
13. Ryu, K. A.; Stutts, L.; Tom, J. K.; Mancini, R. J.; Esser-Kahn, A. P. Stimulation of Innate Immune Cells by Light-Activated TLR7/8 Agonists. *J. Am. Chem. Soc.* **2014**, *136* (31), 10823–10825. <https://doi.org/10.1021/ja412314j>.
14. Wang, Z.; Gao, Y.; He, L.; Sun, S.; Xia, T.; Hu, L.; Yao, L.; Wang, L.; Li, D.; Shi, H.; Liao, X. Structure-Based Design of Highly Potent Toll-like Receptor 7/8 Dual Agonists for Cancer Immunotherapy. *Journal of Medicinal Chemistry* **2021**, *64* (11), 7507–7532. <https://doi.org/10.1021/acs.jmedchem.1c00179>.
15. Kaushik, D.; Kaur, A.; Petrovsky, N.; Salunke, D. B. Structural Evolution of Toll-like Receptor 7/8 Agonists from Imidazoquinolines to Imidazoles. *RSC Medicinal Chemistry* **2021**, *12*, 1065–1120.
<https://doi.org/10.1039/d1md00031d>.
16. Zhu, H.; Li, Y. Small-Molecule Targets in Tumor Immunotherapy. *Natural Products and Bioprospecting* **2018**, *8* (4), 297–301. <https://doi.org/10.1007/s13659-018-0177-7>.

Chapter 4

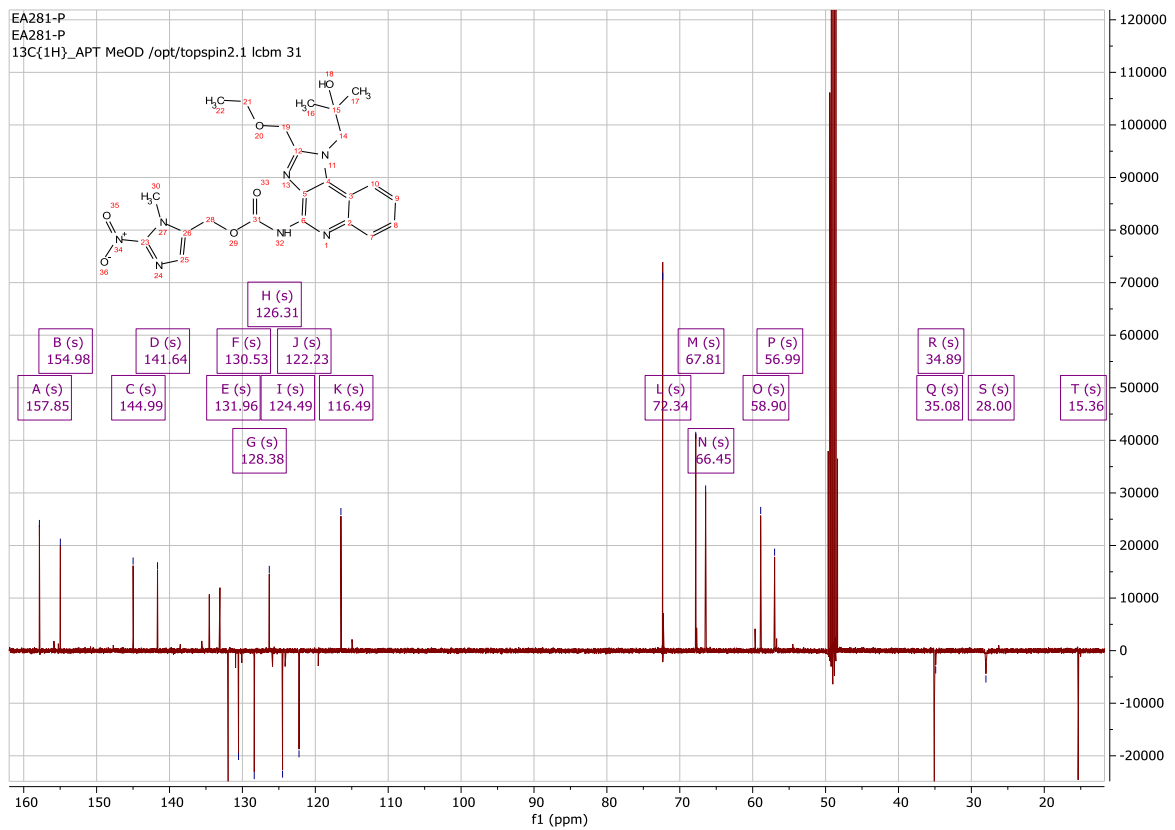
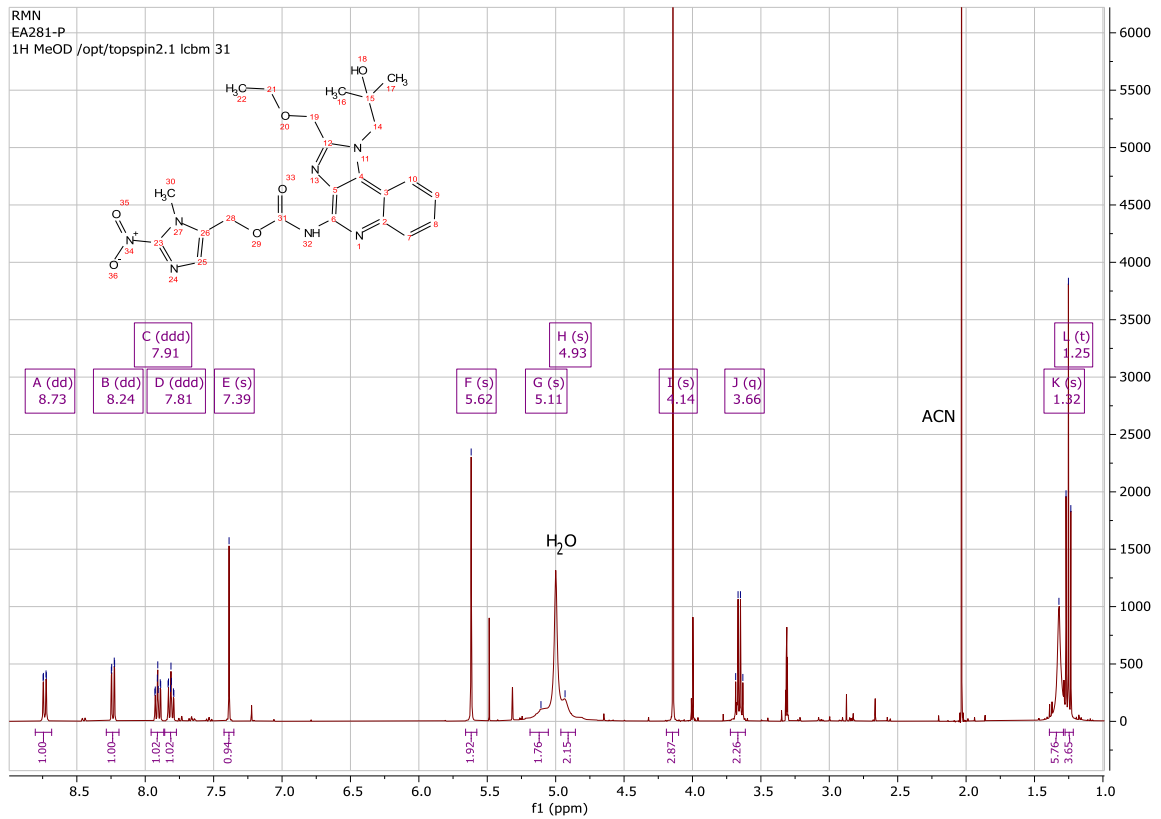
17. Yin, T.; He, S.; Wang, Y. Toll-like Receptor 7/8 Agonist, R848, Exhibits Antitumoral Effects in a Breast Cancer Model. *Molecular Medicine Reports* **2015**, *12* (3), 3515–3520. <https://doi.org/10.3892/mmr.2015.3885>.
18. Wen, T.; Wang, J.; Shi, Y.; Qian, H.; Liu, P. Inhibitors Targeting Bruton's Tyrosine Kinase in Cancers: Drug Development Advances. *Leukemia* **2021**, *35*, 312–332. <https://doi.org/10.1038/s41375-020-01072-6>.
19. Suskil, M. von; Sultana, K. N.; Elbezanti, W. O.; Al-Odat, O. S.; Chitren, R.; Tiwari, A. K.; Challagundla, K. B.; Srivastava, S. K.; Jonnalagadda, S. C.; Budak-Alpdogan, T.; Pandey, M. K. Bruton's Tyrosine Kinase Targeting in Multiple Myeloma. *International Journal of Molecular Sciences* **2021**, *22* (11), 5707. <https://doi.org/10.3390/ijms22115707>.
20. Fu, Z.; Mowday, A. M.; Smaill, J. B.; Hermans, I. F.; Patterson, A. v. Tumour Hypoxia-Mediated Immunosuppression: Mechanisms and Therapeutic Approaches to Improve Cancer Immunotherapy. *Cells* **2021**, *10* (5), 1006. <https://doi.org/10.3390/cells10051006>.
21. Mistry, I. N.; Thomas, M.; Calder, E. D. D.; Conway, S. J.; Hammond, E. M. Clinical Advances of Hypoxia-Activated Prodrugs in Combination With Radiation Therapy. *Radiation Oncology Biology* **2017**, *98* (5), 1183–1196. <https://doi.org/10.1016/j.ijrobp.2017.03.024>.
22. O'Connor, L. J.; Cazares-Körner, C.; Saha, J.; Evans, C. N. G.; Stratford, M. R. L.; Hammond, E. M.; Conway, S. J. Design, Synthesis and Evaluation of Molecularly Targeted Hypoxia-Activated Prodrugs. *Nature Protocols* **2016**, *11* (4), 781–794. <https://doi.org/10.1038/nprot.2016.034>.
23. Duan, J. X.; Jiao, H.; Kaizerman, J.; Stanton, T.; Evans, J. W.; Lan, L.; Lorente, G.; Banica, M.; Jung, D.; Wang, J.; Ma, H.; Li, X.; Yang, Z.; Hoffman, R. M.; Ammons, W. S.; Hart, C. P.; Matteucci, M. Potent and Highly Selective Hypoxia-Activated Achiral Phosphoramidate Mustards as Anticancer Drugs. *Journal of Medicinal Chemistry* **2008**, *51* (8), 2412–2420. <https://doi.org/10.1021/jm701028q>.
24. Winn, B. A.; Shi, Z.; Carlson, G. J.; Wang, Y.; Nguyen, B. L.; Kelly, E. M.; Ross, R. D.; Hamel, E.; Chaplin, D. J.; Trawick, M. L.; Pinney, K. G. Bioreductively Activatable Prodrug Conjugates of Phenstatin Designed to Target Tumor Hypoxia. *Bioorganic and Medicinal Chemistry Letters* **2017**, *27* (3), 636–641. <https://doi.org/10.1016/j.bmcl.2016.11.093>.
25. Ryu, K. A.; Stutts, L.; Tom, J. K.; Mancini, R. J.; Esser-kahn, A. P. Stimulation of Innate Immune Cells by Light-Activated TLR7/8 Agonists. *J Am Chem Soc* **2014**, *136*, 10823–10825. <https://doi.org/10.1021/ja412314j>.
26. O'Connor, L. J.; Cazares-Körner, C.; Saha, J.; Evans, C. N. G.; Stratford, M. R. L.; Hammond, E. M.; Conway, S. J. Efficient Synthesis of 2-Nitroimidazole Derivatives and the Bioreductive Clinical Candidate Evofosfamide (TH-302). *Organic Chemistry Frontiers* **2015**, *2* (9), 1026–1029. <https://doi.org/10.1039/c5qo00211g>.
27. Ghedira, D.; Voissière, A.; Peyrode, C.; Kraiem, J.; Gerard, Y.; Maubert, E.; Vivier, M.; Miot-Noirault, E.; Chezal, J. M.; Farhat, F.; Weber, V. Structure-Activity Relationship Study of Hypoxia-Activated Prodrugs for Proteoglycan-Targeted Chemotherapy in Chondrosarcoma. *European Journal of Medicinal Chemistry* **2018**, *158*, 51–67. <https://doi.org/10.1016/j.ejmech.2018.08.060>.
28. Gerard, Y. Synthèse de Prodrogues Bispécifiques Activables En Milieu Hypoxique: Application Au Traitement Du Chondrosarcome et Nouvelles Perspectives Dans Le Cadre Du Cancer de La Prostate. Ph. D. Dissertation, Université Clermont Auvergne, **2018**. <https://tel.archives-ouvertes.fr/tel-02316014>
29. Anduran, E.; Aspatwar, A.; Parvathaneni, N. K.; Suylen, D.; Bua, S.; Nocentini, A.; Parkkila, S.; Supuran, C. T.; Dubois, L.; Lambin, P.; Winum, J. Y. Hypoxia-Activated Prodrug Derivatives of Carbonic Anhydrase Inhibitors in Benzenesulfonamide Series: Synthesis and Biological Evaluation. *Molecules* **2020**, *25* (10), 2347. <https://doi.org/10.3390/molecules25102347>.
30. Lanzillotto, M.; Konnert, L.; Lamaty, F.; Martinez, J.; Colacino, E. Mechanochemical 1,1'-Carbonyldiimidazole-Mediated Synthesis of Carbamates. *ACS Sustainable Chemistry and Engineering* **2015**, *3* (11), 2882–2889. <https://doi.org/10.1021/acssuschemeng.5b00819>.

31. Thomas-Xavier Métro, T. X.; Martinez, J. and Lamaty, F. 1,1'-Carbonyldiimidazole and Mechanochemistry: A Shining Green Combination. *ACS Sustainable Chem. Eng.* **2017**, 5, 11, 9599–9602. <https://doi.org/10.1021/acssuschemeng.7b03260>.
32. Burt, A. J.; Hantho, J. D.; Nielsen, A. E.; Mancini, R. J. An Enzyme-Directed Imidazoquinoline Activated by Drug Resistance. *Biochemistry* **2018**, 57 (15), 2184–2188. <https://doi.org/10.1021/acs.biochem.8b00095>.
33. Hay, M. P.; Anderson, R. F.; Ferry, D. M.; Wilson, W. R.; Denny, W. A. Synthesis and Evaluation of Nitroheterocyclic Carbamate Prodrugs for Use with Nitroreductase-Mediated Gene-Directed Enzyme Prodrug Therapy. *Journal of Medicinal Chemistry* **2003**, 46 (25), 5533–5545. <https://doi.org/10.1021/jm030308b>.
34. Venkatesh, Y.; Nandi, S.; Shee, M.; Saha, B.; Anoop, A.; Pradeep Singh, N. D. Bis-Acetyl Carbazole: A Photoremovable Protecting Group for Sequential Release of Two Different Functional Groups and Its Application in Therapeutic Release. *European Journal of Organic Chemistry* **2017**, 2017 (41), 6121–6130. <https://doi.org/10.1002/ejoc.201701253>.
35. Thews, O.; Gassner, B.; Kelleher, D. K.; Gekle, M. Activity of Drug Efflux Transporters in Tumor Cells Under Hypoxic Conditions. *Adv Exp Med Biol.* **2008**, 614, 157-164. https://doi.org/10.1007/978-0-387-74911-2_19
36. Schaible, B.; Taylor, C. T.; Schaffer, K. Hypoxia Increases Antibiotic Resistance in *Pseudomonas Aeruginosa* through Altering the Composition of Multidrug Efflux Pumps. *Antimicrobial Agents and Chemotherapy* **2012**, 56 (4), 2114–2118. <https://doi.org/10.1128/AAC.05574-11>.

Supplementary data

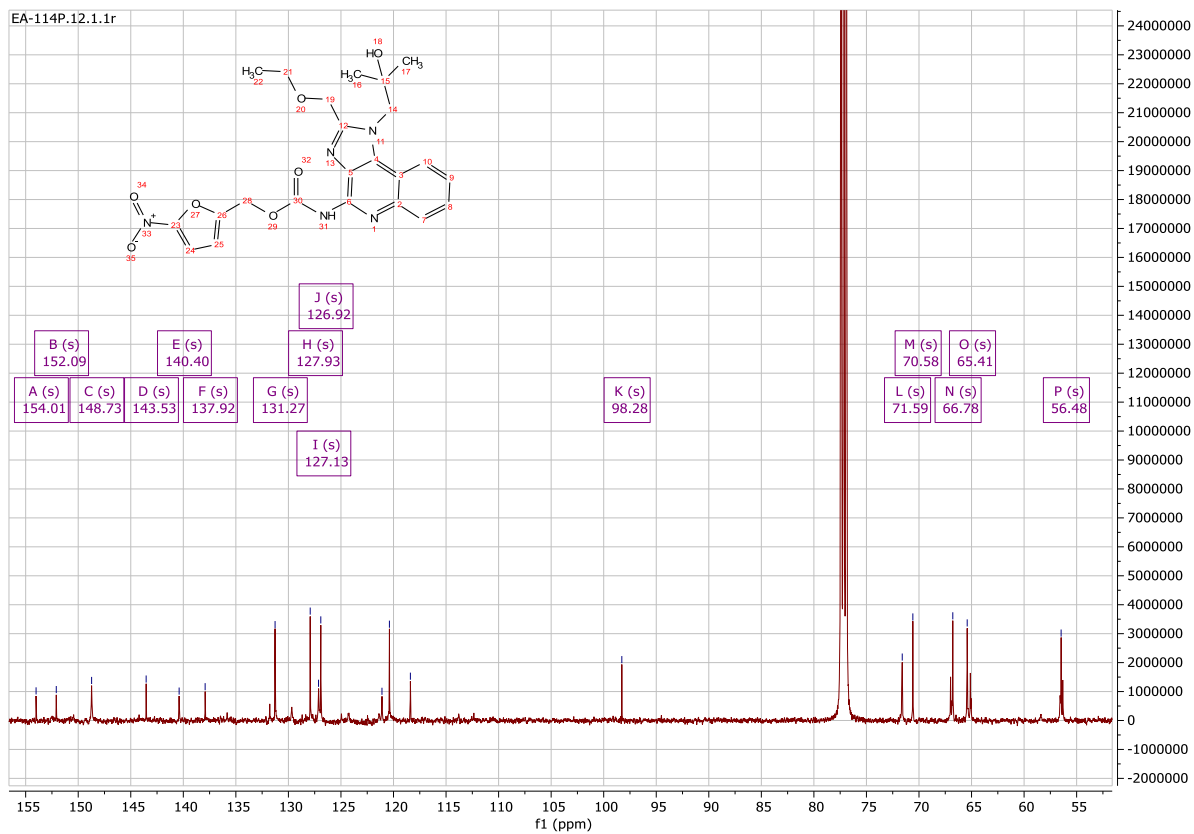
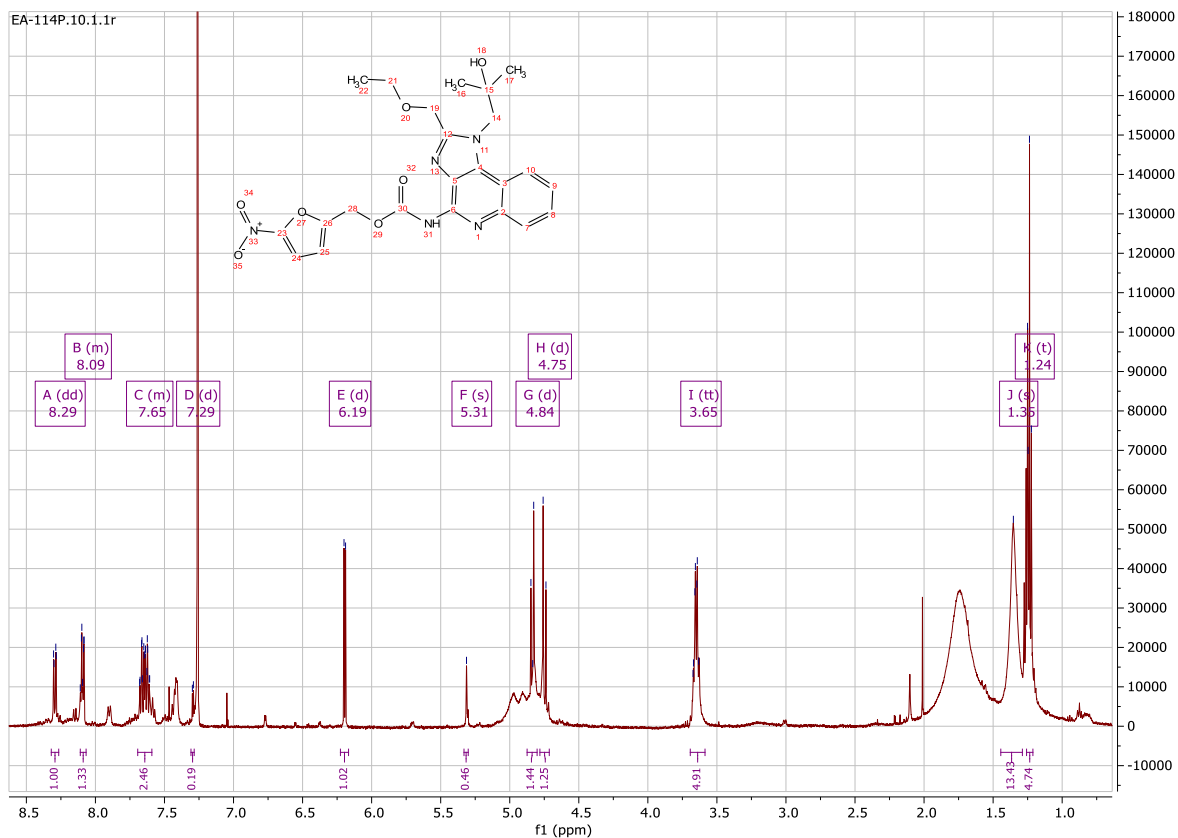
NMR spectra ^1H : (1-methyl-2-nitro-1H-imidazol-5-yl)methyl (1-isobutyl-1H-imidazo[4,5-c]quinolin-4-yl)carbamate (7).

NMR spectra ^1H & ^{13}C : (1-methyl-2-nitro-1H-imidazol-5-yl)methyl (2-(ethoxymethyl)-1-(2-hydroxy-2-methylpropyl)-1H-imidazo[4,5-c]quinolin-4-yl)carbamate (**18**).

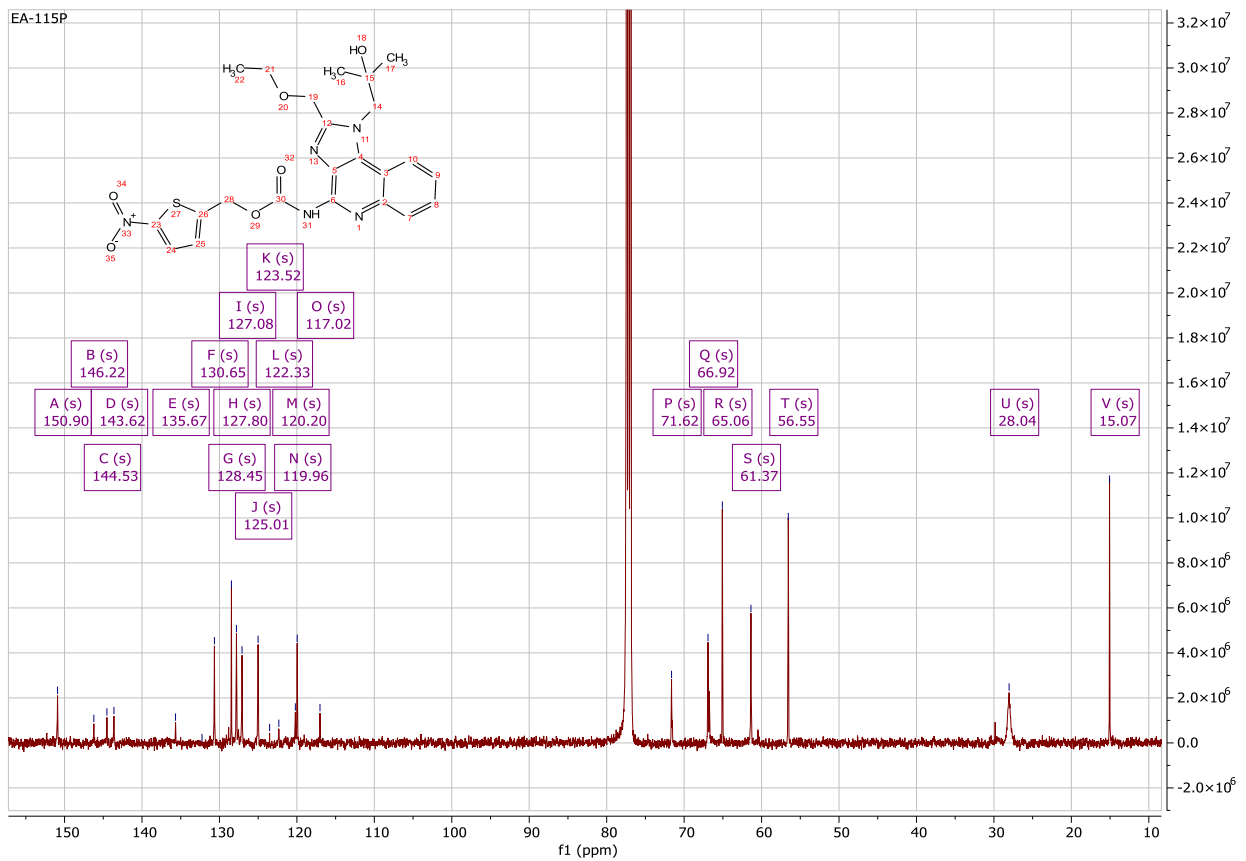
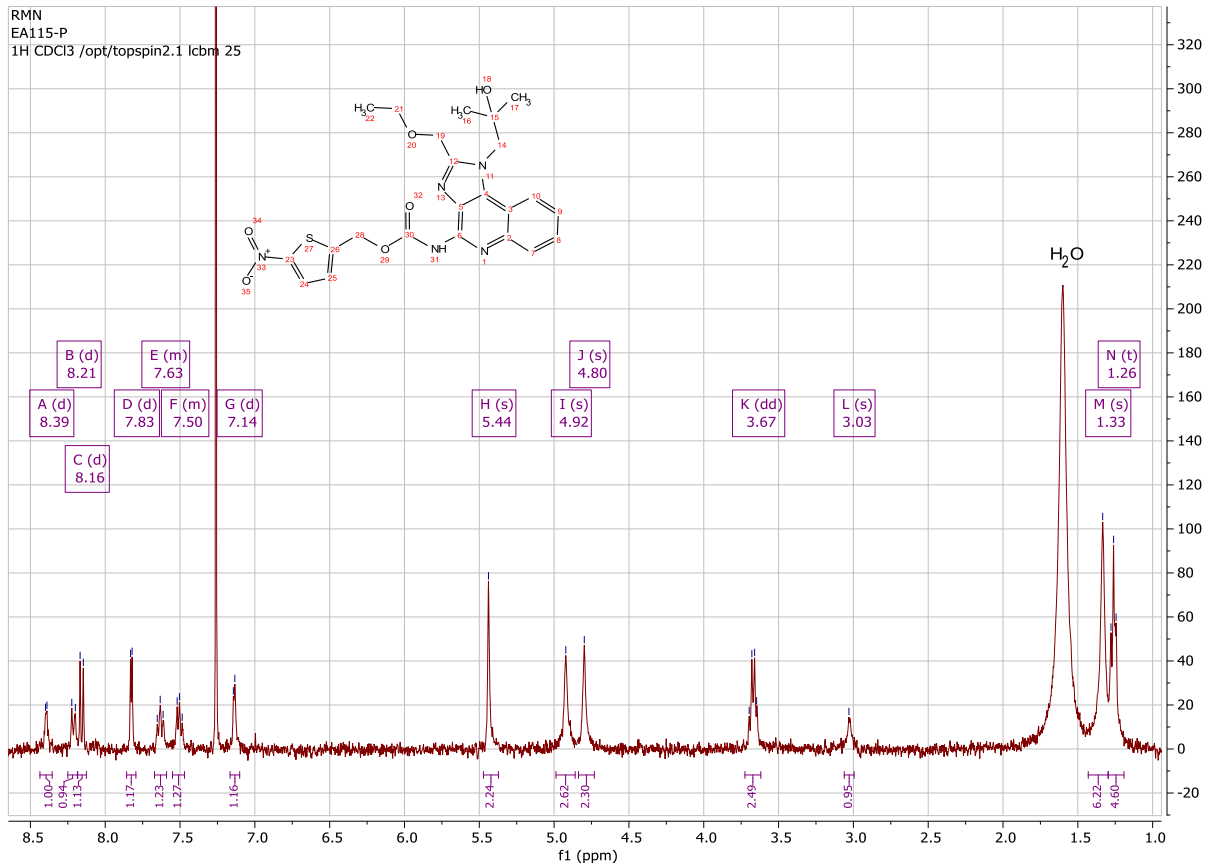


Chapter 4

NMR spectra ^1H & ^{13}C : (5-nitrofuran-2-yl)methyl (2-(ethoxymethyl)-1-(2-hydroxy-2-methylpropyl)-1H-imidazo[4,5-c]quinolin-4-yl)carbamate (**19**).



NMR spectra 4 ¹H & ¹³C: (5-nitrothiophen-2-yl)methyl (2-(ethoxymethyl)-1-(2-hydroxy-2-methylpropyl)-1H-imidazo[4,5-c]quinolin-4-yl)carbamate (**20**).



Chapter 4

NMR spectra 5 ¹H: (5-nitrothiophen-2-yl)methyl (R)-1-(1-acryloylpiperidin-3-yl)-3-(4-phenoxyphenyl)-1H-pyrazolo[3,4-d]pyrimidin-4-yl)carbamate (**23**).

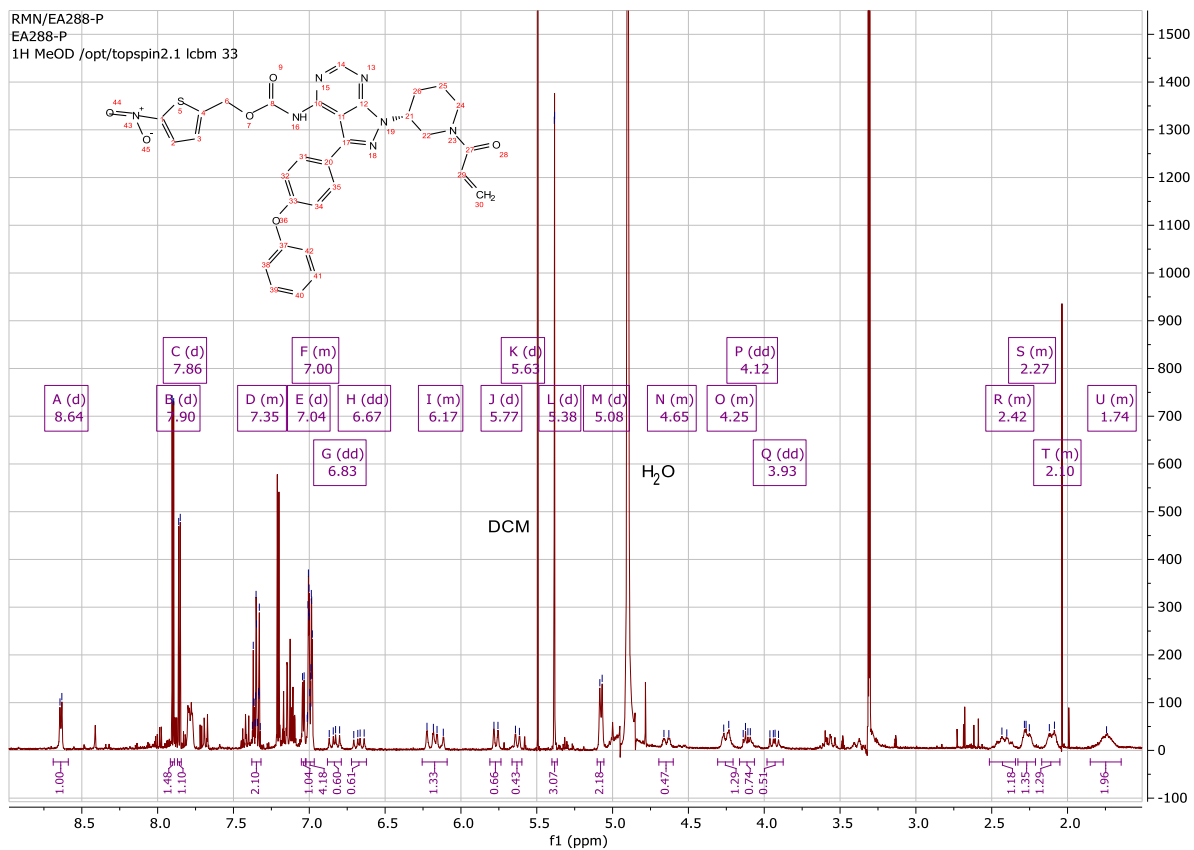


Figure 1S: LC-MS analysis of **18** showing degradation of the compound by Resiquimod decoupling. Mass on the top part, UV on the bottom part.

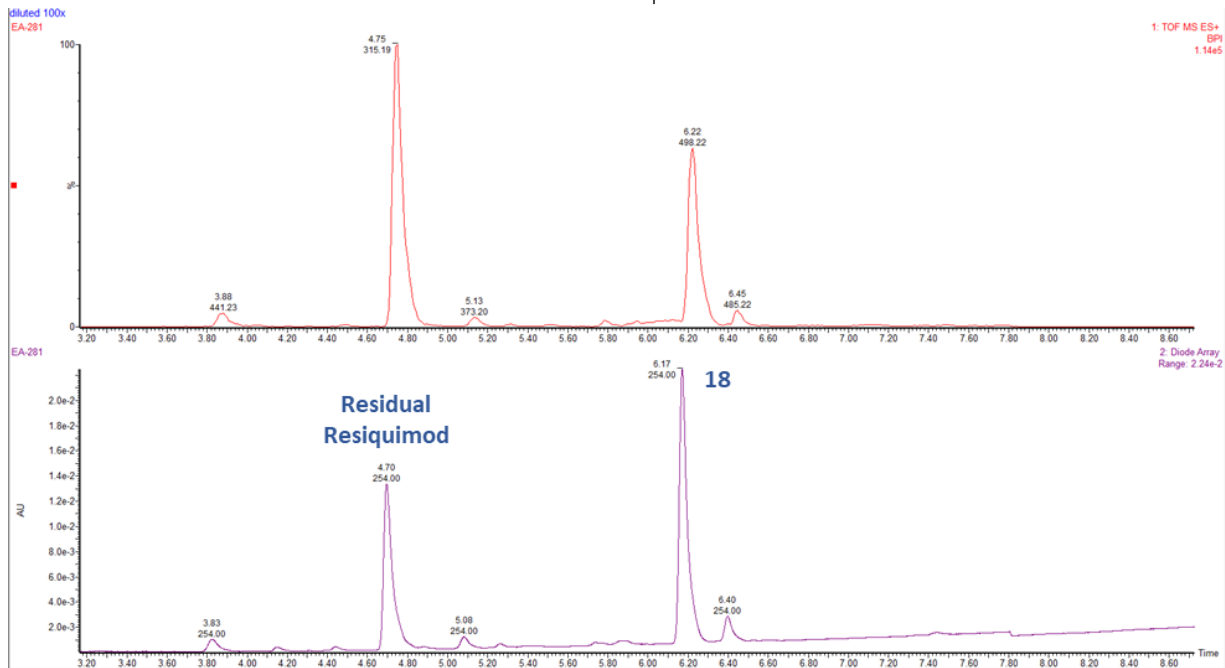
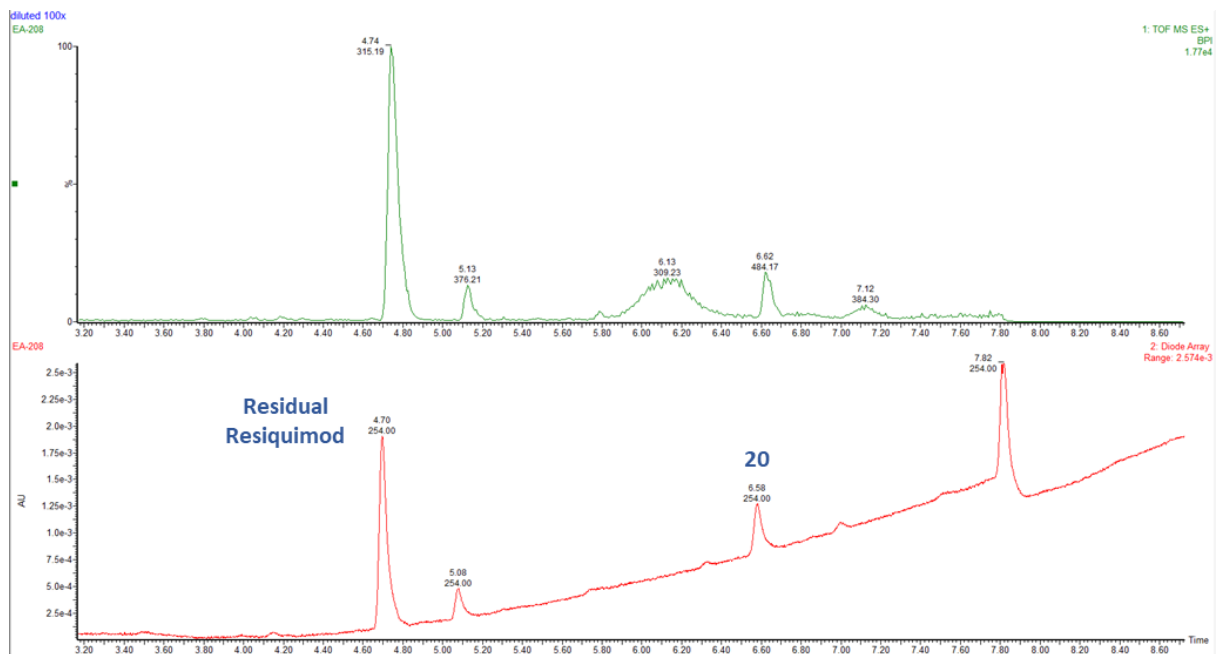


Figure 2S: LC-MS analysis of **20** showing degradation of the compound by Resiquimod decoupling. Mass on the top part, UV on the bottom part.



Chapter 5

Design and synthesis of new hypoxia-activated prodrug antibody-conjugated derivative of the toll-like receptor agonist Resiquimod: a proof-of-concept study to increase tumour uptake

Emilie Anduran, Ying Cong, Dennis Suylen, Rianne Bieman Ingrid Dijkgraaf, Philippe Lambin, Ludwig J. Dubois and Jean-Yves Winum.

In preparation

Abstract

Nowadays antibody-drug conjugation (ADC) is a promising therapeutic strategy intensively studied enabling the use of highly potent drugs combined with a tumour specific antibody, thereby enhancing the efficacy of therapeutics and preventing adverse effects. Hypoxia is a characteristic feature of solid tumour, associated to a more aggressive phenotype, tumour cell proliferation and resistance to traditional chemo- and radiotherapy-based treatments, leading to a poor patient prognosis. Therefore, the hypoxic environment represents today, an extremely valuable target for cancer therapy. Indeed, numerous therapeutic strategies have been developed to counteract this hypoxic phenotype, such as hypoxia activated prodrugs (HAPs) allowing the delivery of cytotoxic payload by targeting the hypoxic tumour environment. Here, we report the design and the synthesis of a new ADC prodrug combining a toll-like receptor agonist, Resiquimod, as payload released after enzymatic bioactivation in hypoxic tumours and Cetuximab, a chimeric monoclonal antibody inhibiting the human epidermal growth factor receptor, highly expressed in cancer cells. The purpose of this antibody-prodrug conjugate is to allow a higher tumour targeting by combining an antibody having a high specificity to a cancer cell characteristic and a HAP targeting tumour hypoxia environment for drug delivery upon activation.

Introduction

In the past four decades, antibody-drug conjugates (ADCs) have been intensively studied as promising biotherapeutic strategies to specifically target cancer cells, allowing the release of highly potent drugs otherwise too toxic for healthy tissues, directly in tumour environment, minimizing adverse effects.¹⁻⁴ To date, 12 ADCs have been approved by the Food and Drug Administration (FDA), while more than 80 are currently in development.⁵ ADCs generally comprise out of 3 components, a monoclonal antibody, a linker and a payload covalently connected.⁶⁻⁹ The major role of the antibody is to target specifically highly expressed antigens on tumour cells or in the tumour microenvironment.¹⁰ Therefore, the choice of the antibody represents an important consideration to allow proper tumour targeting as such that the release of the cytotoxic payload can be done avoiding off-target toxicity on healthy cells. Some antigens are now well known to be an appropriate target because of their high expression in tumour tissues, such as the human epidermal growth factor receptor 2 (HER2) which is more than 100 times overexpressed in the tumour microenvironment.^{7,11,12} The most common conjugation method to connect the payload to the antibody is to couple the linker using the amino group of lysine or the thiol group of cysteine residues.^{13,14} However, ADCs are synthesized most of the time by random conjugation of the linker, resulting in a heterogenous product. It still remains challenging to afford control on drug-to-antibody ratio (DAR) in order to improve the homogeneity of conjugation.

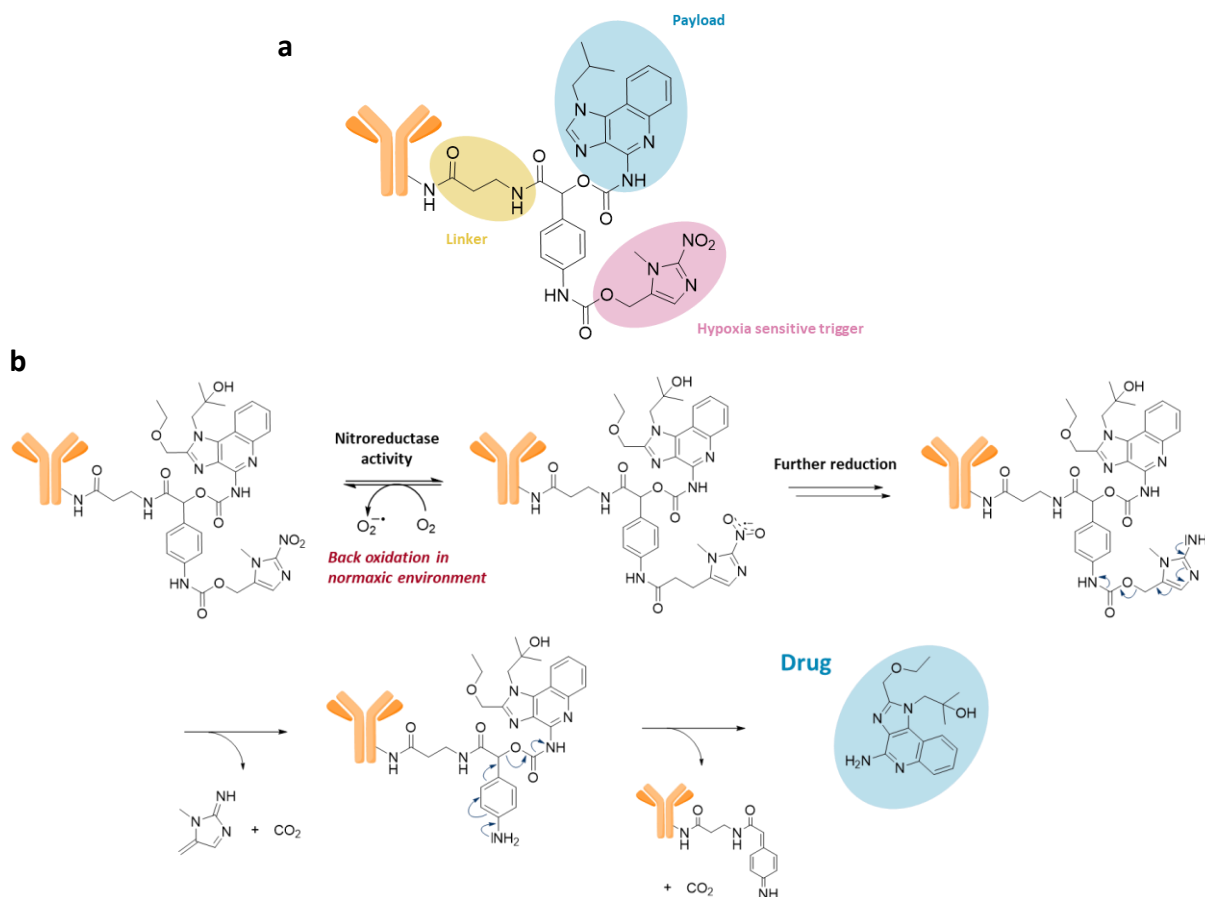
Hypoxia is common feature in the majority of solid tumours and is characterised by low oxygen supply and associated to a more aggressive phenotype and to resistance to traditional chemo- and radiotherapy-based treatments, leading to poor patient prognosis.¹⁵⁻¹⁷ Nowadays, as hypoxia represents a valuable target to treat cancer, several strategies to counteract this hypoxic phenotype have been developed such as hypoxia-activated prodrugs (HAPs).^{18,19} HAPs are therapeutic agents designed to penetrate in hypoxic regions to release, only under low oxygen tension, a cytotoxic compound induced by enzymatic reduction bioactivation.^{20,21}

Here we described the design and the synthesis of a new antibody-HAP conjugate comprising a toll-like receptor agonist as payload, released after activation in the hypoxic tumour environment. In this proof-of-concept, the antibody Cetuximab, a chimeric monoclonal antibody inhibiting the epidermal growth factor receptor, was utilized in this ADC approach as it is highly expressed on cancer cells. The purpose of this antibody-prodrug conjugate is to allow a higher tumour targeting by combining an antibody having a high specificity to a cancer cell characteristic and a HAP targeting the tumour hypoxia environment for the drug delivery upon activation.

Results and discussion

Two HAPs, **8** and **17**, were designed combining several moieties all connected to a central platform obtained after one reaction step from a *p*-nitrophenyl ketone. Each having different roles, such as Resiquimod as the payload, 1-methyl-2-nitroimidazole as a hypoxia sensitive

trigger and a linker, using a β -alanine (here in yellow) to conjugate the prodrug to an antibody (Scheme 1a).



Scheme 1: (a) Structure of HAP compound. (b) Proposed mechanism of drug release.

The different moieties are connected via a carbamate linker to allow the drug release through a self-immolative mechanism.^{22–24} These cascade disassembling reactions must occur in a hypoxic tumour environment thanks to the action of electron oxidoreductase enzymes leading, after several reductions, to the drug release (Scheme 1b). In the presence of oxygen the prodrug is back oxidized, preventing the release of the drug in normoxic tissues and the subsequent killing of healthy cells. In hypoxic tissues, the prodrug can undergo further reduction reactions to allow the hypoxia selective release of the payload either after further reduction or by fragmentation of the prodrug, resulting in enhanced cell death.²⁵

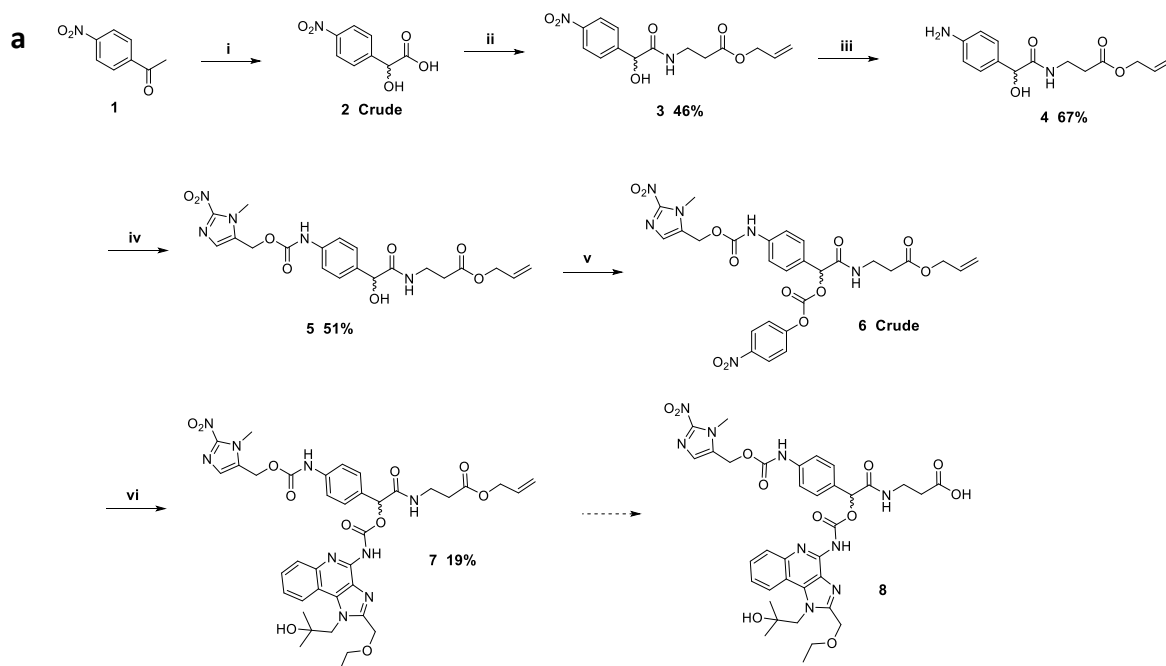
In order to synthesize this HAP-antibody combination, first it was necessary to assemble the carboxylic acid compound to enable, afterwards, the coupling to the antibody. The 1-methyl-2-nitroimidazole, showing promising results in previous work, has been selected as hypoxia sensitive trigger.²⁶ Two toll-like receptor agonists, Imiquimod and Resiquimod were considered as active drug as they have demonstrated highly potent activity as immunotherapeutics.²⁷ Considering reactivity and solubility issues encountered in the past, only Resiquimod was used for the synthesis described in this chapter.

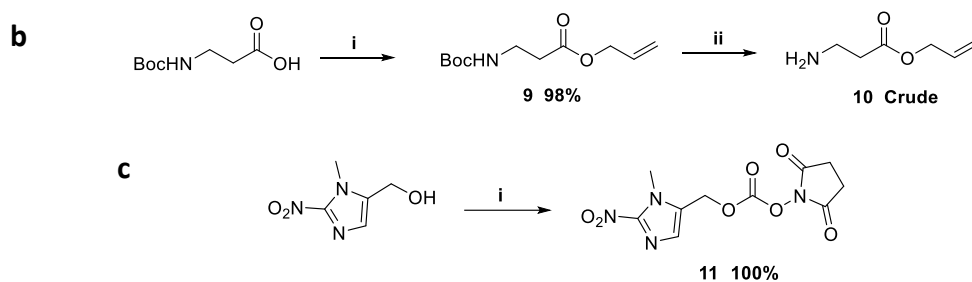
To synthesize **8**, a multistep synthesis including 7 steps was necessary (Scheme 2a) starting by an oxidation-Cannizzaro reaction on the aryl methyl ketone to form an α -hydroxy-arylacetic acid

using SeO_2 and catalysed by the ytterbium triflate.²⁸ **3** was obtained after coupling the linker **10** on the carboxylic acid group of **2** by forming an amide bond. To enable this coupling, it was necessary to activate the carboxylic acid group of the substrate during the coupling step. Two activating agents, the *N*'-ethylcarbodiimide (EDC)²⁹ and the hexafluorophosphate azabenzotriazole tetramethyl uranium (HATU) were tested. HATU was preferred, allowing the connection of the linker at a higher yield. The linker **10** was formed through a two-step synthesis (Scheme 2b), starting by the allyl-protection of the carboxylic acid group of a Boc- β -alanine, followed by the deprotection of the amine to allow the coupling.

Next, the nitro group on the *para* position of the aromatic ring of **3** was reduced in primary amine in the 4th step, allowing in the next step, the coupling of the hypoxia sensitive trigger using **11** (Scheme 2c) to form **5**. This coupling step was preceded by an activation of the hydroxyl group of the 1-methyl-2-nitroimidazole to form a carbonate compound using the disuccinimidyl carbodiimide (DSC).

Next, another activation step was performed on the hydroxyl group of **5** using the *para*-nitrophenyl chloroformate (PNPC) as activating agent in order to couple Resiquimod to **6**. In parallel, this activation was performed as well on Resiquimod. We observed the formation of the expected activated compound, however the following coupling step on **5** did not allow the formation of **6** as much as by doing the activation on **5**. After isolation of **7**, residual Resiquimod was observed in the presence of the compound by TLC, showing a degradation by decoupling of the drug directly after purification. As **7** was not stable enough to continue further the synthesis, we were not able to isolate the final compound **8** normally afforded after a deprotection step of the allyl ester.

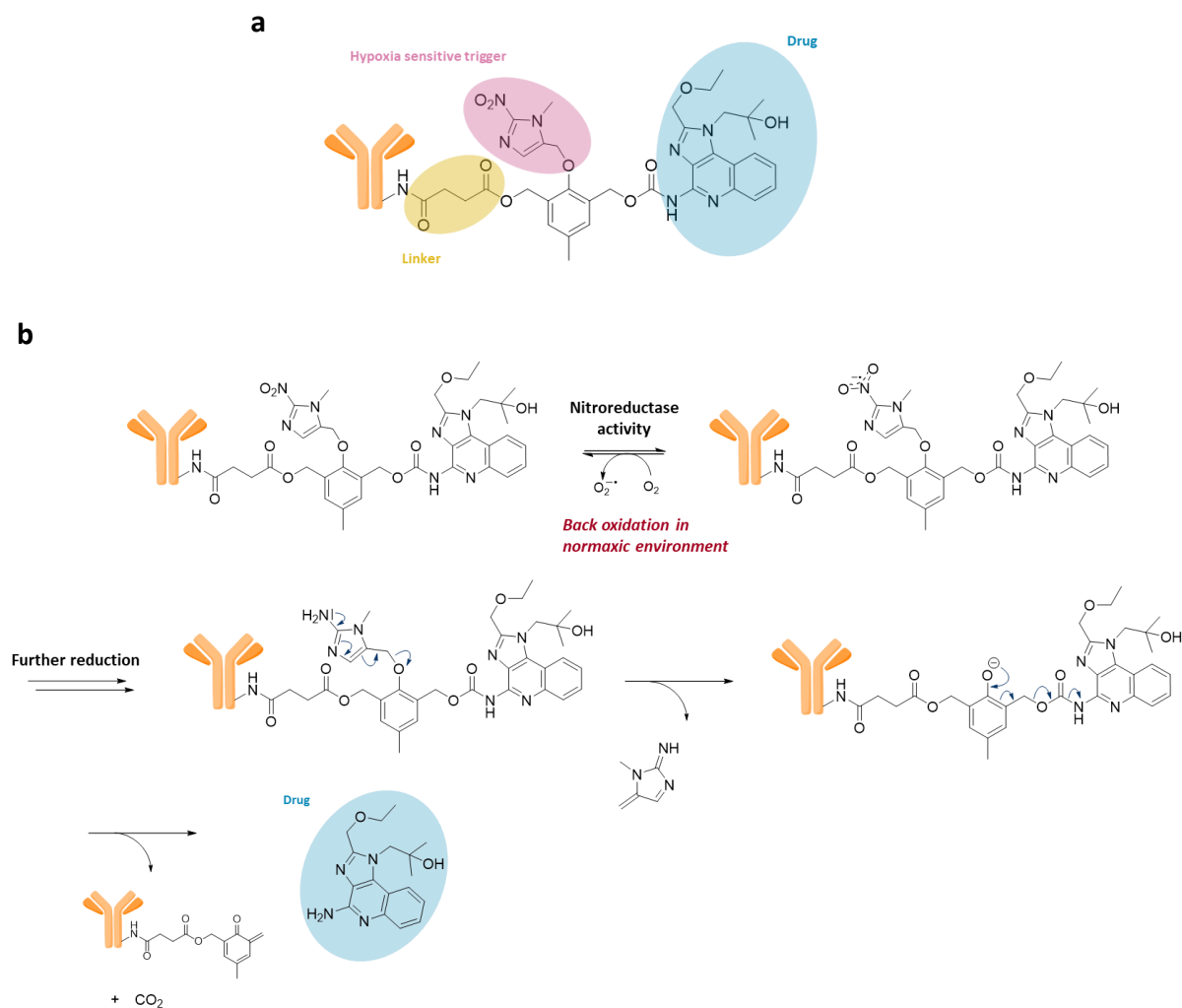




Scheme 2: (a) Synthesis pathway to form the carboxylic acid HAP **8**.

Reagents and conditions: (i) Yb(OTf)₃, SeO₂, dioxane/H₂O, 98°C, 18h; (ii) **10**, HATU, DIEA, DMA, rt, overnight; (iii) AcOH, Zn, THF, rt, 2h; (iv) **11**, pyridine, DCM, rt, 4h; (v) PNPC, pyridine, DCM, 40°C, 4h; (vi) Resiquimod, DIEA, EtOAc, M-W, 45min, 87°C, 90 W. **(b)** Synthesis pathway of linker **10**. (i) allyl bromide, K₂CO₃, DMF, rt, overnight; (ii) TFA, DCM, rt, 2h. **(c)** Activation step of the 1-methyl-2-nitroimidazole. (i) DSC, pyridine, DCM, rt, overnight.

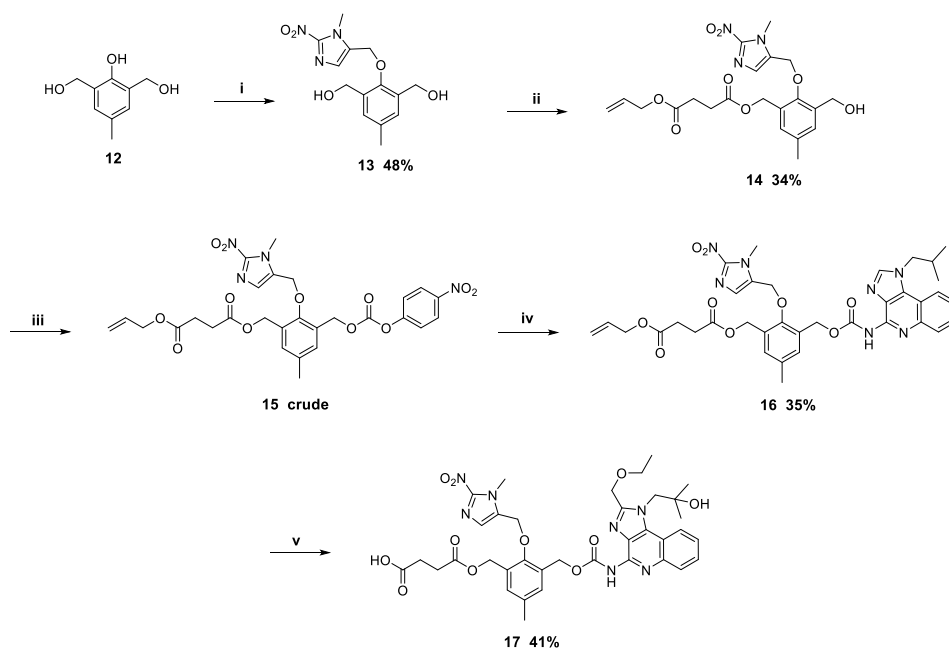
Based on the same idea as for the previous prodrug, we have decided to synthesize in parallel a second HAP to be conjugated to an antibody, comprising the same three moieties connected to a Bis(hydroxymethyl)-*p*-cresol central platform (Scheme 3).



Scheme 3: (a) Structure of HAP compound. (b) Proposed mechanism of drug release.

As previously, to form this second antibody-prodrug, it was first necessary to synthesize the carboxylic acid compound, to connect it, afterwards, to the antibody. **17** was obtained through a five-step synthesis pathway (Scheme 4).

Initially, this synthesis was comprising two steps more, a protection step on **13**, to protect one of the two hydroxyl groups with the aim to have only one reacting position to achieve the coupling of the linker on the next step and then a deprotection step to continue the synthesis on the second hydroxyl. After having tried this protection step on **13** using 4,4'-dimethoxytrityl chloride as protecting group as described in the literature on the same type of substrate³⁰, it was observed that the protected compound was not stable enough. Indeed, we observed that the compound started to deprotect after purification. We decided then to try to form **14** without these two steps with the aim to obtain the final compound through a shorter synthesis pathway.

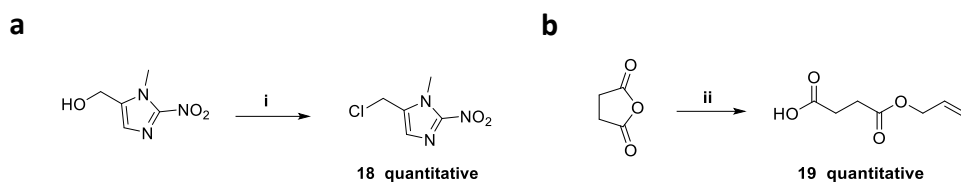


Scheme 4: Synthesis pathway to form the carboxylic acid HAP **17**

Reagents and conditions: (i) **18**, K₂CO₃, acetone, 60°C, overnight; (ii) **19**, EDC, HOBT, DMF, rt, 10h; (iii) PNPC, DIEA, DCM, 40°C, 4h; (iv) Resiquimod, DIEA, EtOAc, rt, 3h; (v) Pd(PPh₃)₄, PhSiH₃, THF, rt, 4h.

The final compound **17** was formed starting first by the coupling the hypoxia sensitive trigger on the central platform. To this end, it was necessary to first activate the alcohol of the 1-methyl-2-nitroimidazole using mesyl chloride in basic conditions to form **18** (schema 5a).³¹ Then, **18** was coupled on the phenol group of **12** in basic conditions. On the following step, the objective was to couple the linker **19** only on one hydroxyl position. Before that, **19** was obtained after reaction between succinic anhydride and allyl alcohol in the presence of DMAP (schema 5b).³² To enable the formation of **14** it was necessary to find the best conditions to control the reaction promoting the formation of the mono coupling compound. To this end, the carboxylic acid function of the linker was activated first by EDC/HOBT before initiating the reaction with **14** at low temperature. The second hydroxyl group was activated next to obtain **15**, using PNPC similar as for the previous HAP compound synthesis, in order to couple Resiquimod. The drug was coupled in basic conditions on the following step to form **16**. As observed with **7**, the same stability issue was noted on **16**. After isolation of **16**, the presence of

Resiquimod has been observed with the compound by TLC. However, the decoupling of Resiquimod seemed minimal compared to **7**, which allowed us to achieve the final step, the deprotection of the allyl ester to afford the carboxylic acid compound **17**.



Scheme 5: (a) Synthesis pathway of liker 10. (b) Activation step of the 1-nethyl-2-nitroimidazole. Reagents and conditions: (i) MsCl, DIEA, THF, rt, 4h; (ii) allyl alcohol, DMAP, toluene, 110°C, 5h.

After isolation of **17**, solubility and stability tests were performed because of the partial decoupling of the drug (Figure 1S). A DMSO stock solution of the compound was diluted in cell culture medium at different concentrations, showing that **17** was soluble at a maximum concentration of 500 μ M with 1% DMSO. Stability of **17** was measured at 37°C by HPLC at different time points on a sample presenting already a small amount of residual Resiquimod. Areas of **17** and residual Resiquimod peaks were measured, a low increasement of Resiquimod peak was observed at the beginning of the measurement (t.0 – t.1h) when the sample was incubated at 37°C. Then, the compound remains relatively stable (Table 1).

Table 1: Stability measurements of **17**

Time points	0	1h	2h	3h	4h	5h	6h	7h	8h	24h	28h	48h
17 area (%)	76	74	74	74	73	73	73	73	73	73	73	72
Res. area (%)	24	26	26	26	27	27	27	27	27	27	27	28

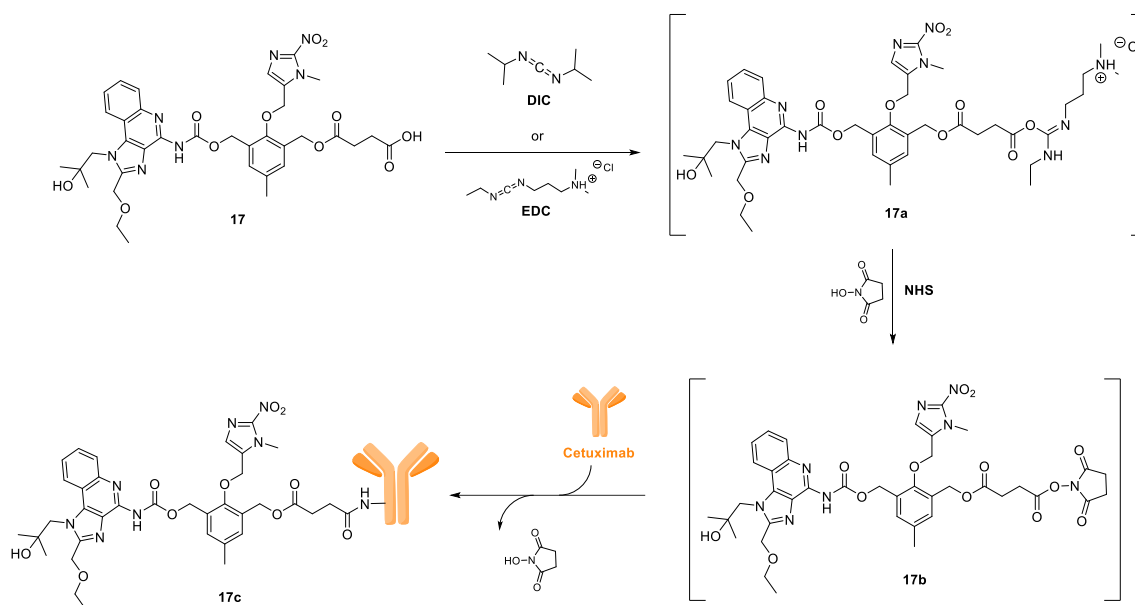
* t.0 at rt, from t.1h at 37°C

To achieve the antibody conjugation on **17**, we decided to follow 2 steps, a first one to activate the carboxylic acid function of **17**, followed by the coupling with the antibody as 2nd step. Cetuximab, a chimeric monoclonal antibody was selected to perform this conjugation by coupling **17** to the amine group of a lysine residue, as previously described.³³ The Cetuximab antibody blocks the ligand-binding domain of the endothelial growth factor receptor (EGFR), a receptor highly expressed in aggressive tumours and associated to treatment resistance.³⁴

In order to enable an homogeneous coupling and to afford a better control on the DAR, we first tried to achieve the conjugation in an equimolar ratio, starting by the activation step of the carboxylic acid group of **17**. Diisopropylcarbodiimide (DIC) was used as activating agent to couple the *N*-hydroxysuccinimide (NHS), forming an activated ester function. DIC was selected because of its miscibility with DMSO, as **17** was already in stock solution in DMSO. After this activation step, the reaction mixture was directly added to the antibody aqueous buffer and one hour later, the coupling mixture was analysed by MALDI-TOF mass spectrometry to monitor the

formation of the ADC as described in our previous study.³³ Unfortunately, we did not observe the formation of the expected conjugate.

The coupling was repeated, but increasing the equivalent of **17**. After DIC/NHS activation, the reaction mixture was analysed by LC-MS after 1 hour stirring. Only **17** was observed, as the intermediate ester **17b** is unstable, we could not guarantee to be able to observe it by LC-MS analysis. Thus, the antibody coupling was achieved then without observing the formation of the conjugation product. **17b** reaction mixture was added to the Cetuximab buffer solution and stirred for 1 additional hour before to do mass measurement. The formation of the conjugated product was not observed, we did another mass measurement after overnight stirring without observing the formation of **17c**. Thereby, new conditions were tested in order to activate **17** (Scheme 6).



Scheme 6: Antibody conjugation mechanism.

Abbreviations: Diisopropylcarbodiimide (DIC), ethyl dimethylaminopropyl carbodiimide

Next, the activation was performed using ethyl dimethylaminopropyl carbodiimide (EDC) as activating agent followed by the addition of NHS as described in the literature.³⁵ After 1 hour stirring, the reaction mixture was added to the antibody buffer solution and was stirred 1 hour more. The formation of the expected conjugated product was not observed after mass analysis using these coupling conditions.

Conclusion

Nowadays antibody-drug conjugation is a promising therapeutic strategy comprising several therapeutics approved by the FDA and even more currently in development. Indeed, they allow the delivery of highly potent cytotoxic payloads, otherwise too toxic for healthy tissues, by targeting tumour cells. We proposed here to design two antibody-prodrug conjugates combining a HAP, enabling the targeting and the release of a toll-like receptor agonist, Resiquimod, in the tumour hypoxic environment to Cetuximab, an EGFR antibody, highly

expressed in tumour cells. We encountered stability issues during the synthesis of the first HAP **8**, after the coupling step of Resiquimod, which has prevented obtaining of the final compound. Indeed, after isolation of **7**, a partial degradation by decoupling of the Resiquimod has been observed, preventing the last synthesis step, the deprotection of the allyl ester. We observed degradation as well during the synthesis of the second HAP **17**, also after the Resiquimod coupling, but we succeeded to isolate it. We decided then to continue by performing the antibody conjugation on carboxylic acid group of **17**. Cetuximab has been selected as antibody because of this specificity with the human epidermal growth factor receptor, highly expressed in cancer cells and because of its use in different ADC studies.^{35,36} Till now, we have tested different conjugation conditions by first activating the carboxylic acid function and couple the antibody but we didn't observe the formation of the desired conjugate. These first results indicate that **17** cannot be activated and suggest that we could try to first active the lysine residue of Cetuximab and then couple **17** on it.

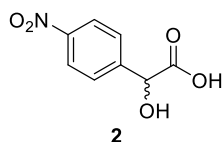
Experimental section

Chemistry

General

All reagents and solvents were of commercial quality and used without further purification unless otherwise specified. All reactions were carried out under an inert atmosphere of argon. TLC analyses were performed on silica gel 60 F254 plates (Merck Art. no. 1.05554). Spots were visualized under 254 nm UV illumination or by ninhydrin solution spraying. ¹H and ¹³C NMR spectra were recorded on a Bruker DRX-400 spectrometer using CHCl₃-d₆, MeOD-d₆ or DMSO-d₆ as solvent and tetramethylsilane as internal standard. For ¹H and ¹³C NMR spectra, chemical shifts are expressed in δ (ppm) downfield from tetramethylsilane, and coupling constants (*J*) are expressed in hertz. Electron Ionization mass analysis were performed in positive or negative mode on a Waters acquity UPLC. All compounds that were tested in the biological assays were analyzed by high-resolution ESI mass spectra (HRMS) using a Bruker microTOF-Q II mass spectrometer fitted with an electrospray ion source in order to confirm the purity of >95%.

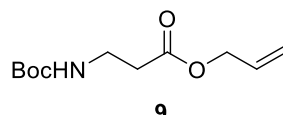
2-hydroxy-2-(4-nitrophenyl)acetic acid (**2**)



To a solution of ketone (30.28 mmol, 1 eq) in a 3:1 mixture dioxane/H₂O (120 mL), SeO₂ (60.55 mmol, 2 eq) and Yb(OTf)₃ (3.03 mmol, 0.1 eq) were added and the resulting suspension was stirred at 90°C for 18h. The mixture was filtered through a short pad of Celite®, the filtrate diluted with 1% aq. NaOH (300 mL) and extracted with CH₂Cl₂ (2 x 300 mL). The aqueous

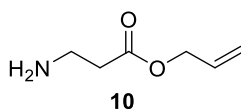
solution was acidified to pH 1 with 10% aq. HCl and extracted with EtOAc (3 x 300 mL). The combined organic phases were dried on Na₂SO₄, the solvent removed under reduced pressure yielding the desired α -hydroxy aryl acetic acid **1**. The crude product was directly used without further purification. ¹H NMR (400 MHz, CD₃OD) δ 8.23 (d, *J* = 8.8 Hz, 1H), 7.74 (dd, *J* = 9.0, 0.6 Hz, 1H), 5.31 (s, 1H). ¹³C NMR (400 MHz, CD₃OD) δ 174.87, 148.23, 128.82, 124.42, 73.28, 49.00.

Allyl 3-((tert-butoxycarbonyl)amino)propanoate (**9**)



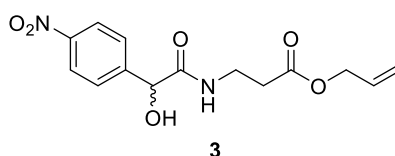
To a solution of compound **2a** (21.14 mmol, 1 eq) in 40 mL DMF, K₂CO₃ (25.37 mmol, 1.2 eq) was added at 0 °C. Then allyl bromide (25.37 mmol, 1.2 eq) was added and the reaction mixture was stirred overnight at room temperature. Most of DMF was removed in vacuo. The residue was redissolved in EtOAc and washed with water, brine, dried over anhydrous Na₂SO₄ and concentrated under vacuum to afford the crude product **2b**. ¹H NMR (400 MHz, CDCl₃) δ 5.90 (ddt, *J* = 17.2, 10.4, 5.8 Hz, 1H), 5.35 – 5.19 (m, 2H), 5.02 (s, 1H), 4.59 (dt, *J* = 5.8, 1.4 Hz, 2H), 3.44 – 3.33 (m, 2H), 2.55 (t, *J* = 6.1 Hz, 2H), 1.42 (s, 9H). ¹³C NMR (400 MHz, CDCl₃) δ 172.26, 155.88, 132.05, 118.60, 79.52, 77.16, 65.44, 36.18, 34.70, 28.50.

Allyl 3-((tert-butoxycarbonyl)amino)propanoate (**10**)



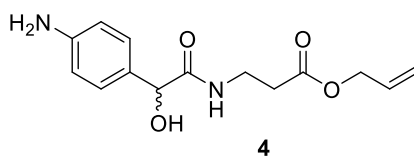
Compound **2b** (19.31 mmol, 1eq) was vigorously stirred in 20% TFA/DCM solution for 2 hours. The reaction mixture was concentrated and dried *in vacuo* to afford compound **2c**. The crude product was directly used without further purification. ¹H NMR (400 MHz, CDCl₃) δ 7.82 (s, 3H), 5.99 – 5.77 (m, 1H), 5.39 – 5.18 (m, 2H), 4.62 (d, *J* = 5.9 Hz, 2H), 3.42 – 3.20 (m, 2H), 2.80 (t, *J* = 5.8 Hz, 2H). ¹³C NMR (400 MHz, CDCl₃) δ 171.75, 131.21, 119.41, 77.16, 66.45, 36.01, 30.61.

Allyl 3-(2-hydroxy-2-(4-nitrophenyl)acetamido)propanoate (**3**)



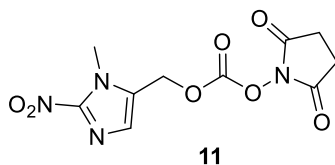
To a solution of compound **1** (10.14 mmol, 1 eq) in 20 mL of DMA, a solution of **2c** (12.17 mmol, 1.2 eq) and DIEA (30.43 mmol, 3 eq) in 20 mL of DMA was added under an argon atmosphere and 1-[Bis(dimethylamino)methylene]-1H-1,2,3-triazolo[4,5-b]pyridinium 3-oxide hexafluorophosphate (HATU) (12.17 mmol, 1.2 eq) was added at 0°C. Then the reaction mixture was stirred at room temperature overnight. The mixture was diluted by DCM and washed with 1 M HCl, water and brine, dried over anhydrous Na₂SO₄. Purification by column chromatography on silica gel (hexane/EtOAc 2/3) gave **3** (1.43 g, 46% yield). ¹H NMR (400 MHz, CDCl₃) δ 8.21 (d, *J* = 8.8 Hz, 4H), 7.64 (d, *J* = 8.7 Hz, 4H), 7.02 (s, 2H), 5.87 (ddd, *J* = 16.2, 11.0, 5.8 Hz, 2H), 5.34 – 5.21 (m, 5H), 5.17 (s, 2H), 4.57 (d, *J* = 5.8 Hz, 4H), 3.54 (dd, *J* = 12.0, 6.1 Hz, 4H), 2.54 (t, *J* = 6.0 Hz, 4H). ¹³C NMR (400 MHz, CDCl₃) δ 172.17, 170.94, 149.20, 146.55, 131.76, 127.47, 123.95, 118.91, 77.16, 73.29, 65.70, 35.11, 33.75.

Allyl 3-(2-(4-aminophenyl)-2-hydroxyacetamido)propanoate (**4**)

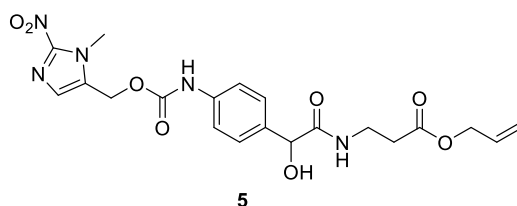


To a solution of **3** (3.08 mmol, 1 eq) were added acetic acid (15.38 mmol, 5 eq) and zinc (30.75 mmol, 10 eq) under an argon atmosphere. Then the reaction mixture was stirred at room temperature for 2h. The mixture was filtered through a pad of celite and the filtrate was washed with a saturated solution of NaHCO₃, with brine, dried over Na₂SO₄ and concentrated under vacuum to afford the crude product **4** directly used at the following step. ¹H NMR (400 MHz, CDCl₃) δ 7.12 (d, *J* = 8.3 Hz, 2H), 6.68 (s, 1H), 6.63 (d, *J* = 8.0 Hz, 2H), 5.88 (ddd, *J* = 22.9, 10.9, 5.7 Hz, 1H), 5.27 (ddd, *J* = 14.1, 11.0, 0.7 Hz, 2H), 4.87 (s, 1H), 4.56 (d, *J* = 5.6 Hz, 2H), 3.65 – 3.44 (m, 3H), 2.54 (t, *J* = 6.1 Hz, 2H). ¹³C NMR (400 MHz, CDCl₃) δ 172.95, 172.00, 147.01, 131.99, 129.46, 128.32, 118.75, 115.45, 77.16, 74.09, 65.58, 35.19, 34.07.

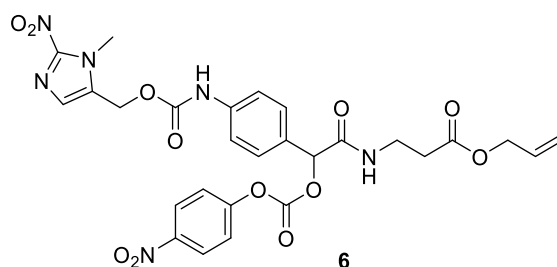
2,5-dioxopyrrolidin-1-yl ((1-methyl-2-nitro-1H-imidazol-5-yl)methyl) carbonate (**11**)



To a solution of disuccinimidyl carbonate (6.68 mmol, 1.5 eq) in DCM (38 mL), pyridine (5.35 mmol, 1.2 eq) was added at 0°C and (1-methyl-2-nitro-1H-imidazol-5-yl)methanol was added slowly. The reaction mixture was stirred overnight at room temperature. Then solvent was removed under reduced pressure to obtain **5** directly used at the following step. ¹H NMR (400 MHz, CD₃OD) δ 7.33 (s, 1H), 5.55 (s, 2H), 4.06 (s, 3H), 2.84 (s, 4H).

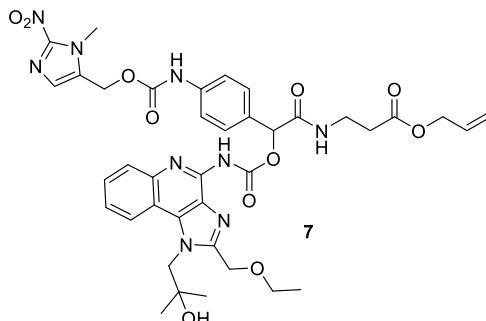
Allyl 3-(2-hydroxy-2-(4-(((1-methyl-2-nitro-1H-imidazol-5-yl)methoxy)carbonyl)amino)phenyl)acetamido)propanoate (5)

To a solution of compound **4** (1.98 mmol, 1 eq) in 8 mL of DCM, pyridine (2.96 mmol, 1.5 eq) was added. Then a solution of **5** (2.17 mmol, 1.1 eq) in 8 mL of DCM was added dropwise at room temperature under an argon atmosphere. The reaction mixture was stirred at room temperature for 4h, until disappearance of the starting material **4**. The mixture was diluted by DCM and washed with 10% CuSO₄ solution, brine, dried over anhydrous Na₂SO₄ and concentrated un vacuum. The pure compound **6** was obtained after flash chromatography (Ethyl Acetate/Cyclohexane 4/1) (376 mg, 41,3%). ¹H NMR (400 MHz, CD₃OD) δ 7.42 (d, *J* = 8.6 Hz, 2H), 7.34 (d, *J* = 8.5 Hz, 2H), 7.26 (s, 2H), 5.91 (ddt, *J* = 17.2, 10.5, 5.7 Hz, 2H), 5.29 (s, 2H), 5.25 (ddq, *J* = 32.7, 10.5, 1.4 Hz, 6H), 4.94 (s, 1H), 4.56 (ddd, *J* = 5.7, 2.7, 1.2 Hz, 3H), 4.07 (s, 3H), 3.50 (td, *J* = 6.6, 4.0 Hz, 2H), 2.57 (t, *J* = 6.6 Hz, 3H). ¹³C NMR (400 MHz, (CD₃)₂SO) δ 172.12, 170.99, 152.67, 137.92, 135.64, 135.58, 133.32, 132.60, 129.84, 128.76, 127.08, 117.76, 73.00, 64.43, 55.12, 39.52, 34.24, 34.21, 33.59. MS (ESI⁺) *m/z* 462.00 [M+H]⁺.

Allyl 3-(2-(4-(((1-methyl-2-nitro-1H-imidazol-5-yl)methoxy)carbonyl)amino)phenyl)-2-(((4-nitrophenoxy)carbonyl)oxy)acetamido)propanoate (6)

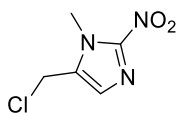
To a solution of **6** (0.22 mmol, 1 eq) in 10 mL of DCM, 4-nitrophenyl carbonochloridate (0.50 mmol, 2.3 eq) and pyridine (0.54 mmol, 2.5 eq) were added and the reaction mixture was refluxed 1h. Then the reaction was quenched by addition of water. The aqueous layer was extracted with DCM and the combined organic layers were dried over anhydrous Na₂SO₄ and concentrated under pressure to obtain **7** directly used at the following step. ¹H NMR (400 MHz, CDCl₃) δ 8.31 – 8.25 (m, 2H), 7.44 (s, 2H), 7.42 – 7.37 (m, 2H), 7.27 (s, 2H), 6.86 (t, *J* = 6.1 Hz, 1H), 6.77 (s, 1H), 5.94 (s, 1H), 5.93 – 5.84 (m, 1H), 5.28 (ddq, *J* = 20.1, 10.4, 1.4 Hz, 2H), 5.25 (s, 2H), 4.59 (d, *J* = 5.7 Hz, 2H), 4.07 (s, 3H), 3.61 (dd, *J* = 11.9, 6.1 Hz, 2H), 2.64 – 2.58 (m, 2H).

Allyl 3-(2-(((2-(ethoxymethyl)-1-(2-hydroxy-2-methylpropyl)-1H-imidazo[4,5-c]quinolin-4-yl)carbamoyl)oxy)-2-(4-(((1-methyl-2-nitro-1H-imidazol-5-yl)methoxy)carbonyl)amino)phenyl) acetamido)propanoate (7)



To a solution of compound **7** (0.50 mmol, 1 eq) in 30 mL of EtOAc, Resiquimod was added (0.59 mmol, 1.2 eq) and DIEA (1.24 mmol, 2.5 eq). Then the reaction mixture was stirred at room temperature for overnight and solvent was removed under pressure. Purification by column chromatography on silica gel (cyclohexane/EtOAc 3/7) gave **8** (10 mg, 4% yield). ¹H NMR (400 MHz, CDCl₃) δ 8.20 (d, J = 8.5 Hz, 1H), 7.92 (s, 1H), 7.65 – 7.55 (m, 1H), 7.54 – 7.42 (m, 1H), 7.35 (d, J = 8.3 Hz, 1H), 7.28 (d, J = 5.8 Hz, 1H), 7.08 (s, 1H), 6.10 (s, 1H), 5.81 (ddd, J = 23.0, 10.4, 5.8 Hz, 1H), 5.18 (dddd, J = 14.1, 10.5, 2.7, 1.3 Hz, 2H), 5.12 (s, 2H), 4.91 (s, 2H), 4.77 (s, 2H), 4.48 (dt, J = 5.7 Hz, 2H), 3.94 (s, 3H), 3.74 – 3.48 (m, 2H), 3.60 (q, J = 14.0, 7.1 Hz, 2H), 2.62 (t, J = 6.7 Hz, 2H), 1.33 (s, 6H), 1.21 (t, J = 7.0 Hz, 3H). MS (ESI⁺) m/z 762.28 [M+H]⁺.

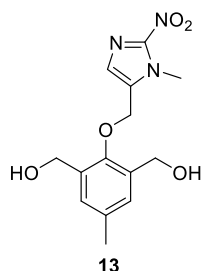
5-(chloromethyl)-1-methyl-2-nitro-1H-imidazole (18)



18

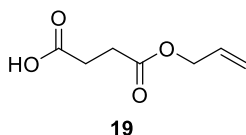
To a solution of (1-methyl-2-nitro-1H-imidazol-5-yl)methanol (3.18 mmol, 1 eq) in THF (5 mL) was added DIEA (3.82 mmol, 1.2 eq) and MsCl (3.82 mmol, 1.2 eq). The reaction mixture was stirred at rt for 4h. The mixture was diluted with EtOAc, wash with 1M HCl solution, brine and dried over anhydrous Na₂SO₄. Compound **1** was directly used at the following step. ¹H NMR (400 MHz, CD₃OD) δ 7.23 (s, 1H), 4.87 (s, 2H), 4.05 (s, 3H). ¹³C NMR (400 MHz, CD₃OD) δ 135.63, 128.62, 128.60, 34.79, 34.77.

(5-methyl-2-((1-methyl-2-nitro-1H-imidazol-5-yl)methoxy)-1,3-phenylene)dimethanol (13)



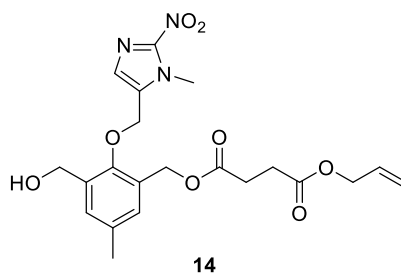
To a solution of (2-hydroxy-5-methyl-1,3-phenylene)dimethanol (5.98 mmol, 1 eq) in acetone (30 mL) was added a solution of **1** (5.98 mmol, 1 eq) in acetone (30 mL) and K_2CO_3 (29.9 mmol, 5 eq). the reaction was stirred at reflux overnight. The reaction mixture was filtered off and the filtrate concentrated under vacuum to afford **2** directly used at the following step. 1H NMR (400 MHz, $CDCl_3$) δ 7.22 (s, 1H), 7.19 (s, 2H), 5.13 (s, 2H), 4.66 (s, 4H), 4.18 (s, 3H), 2.35 (s, 3H). ^{13}C NMR (400 MHz, $CDCl_3$) δ 152.94, 147.76, 135.38, 133.98, 133.83, 133.83, 130.84, 130.84, 129.04, 66.22, 61.20, 34.57, 34.57, 20.93.

4-(allyloxy)-4-oxobutanoic acid (19)



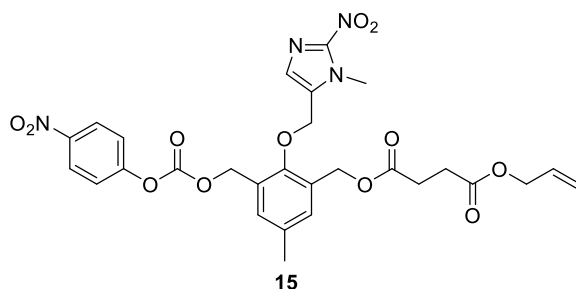
To a solution of succinic anhydride (5 mmol, 1 eq) in toluene (11 mL) was added DMAP (0.5 mmol ; 0.1 eq) and allyl alcohol (5 mmol, 1 eq). The reaction was stirred at reflux for 5h then toluene was evaporated under vacuum to obtain **3** directly used at the following step. 1H NMR (400 MHz, $CDCl_3$) δ 5.91 (ddt, $J = 17.2, 10.5, 5.7$ Hz, 1H), 5.28 (ddq, $J = 28.6, 10.4, 1.4$ Hz, 2H), 4.60 (dt, $J = 5.7, 1.4$ Hz, 2H), 2.77 – 2.59 (m, 4H). ^{13}C NMR (400 MHz, $CDCl_3$) δ 177.97, 172.01, 132.07, 118.53, 65.62, 29.08, 29.00.

Allyl (3-(hydroxymethyl)-5-methyl-2-((1-methyl-2-nitro-1H-imidazol-5-yl)methoxy)benzyl) succinate (14)



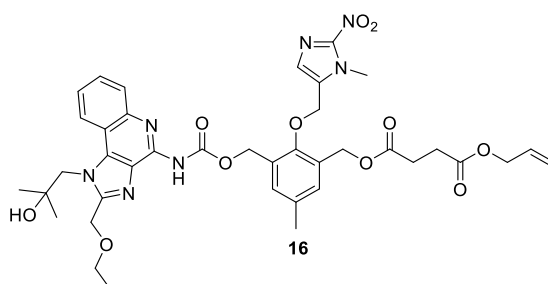
To a solution of **2** (0.33 mmol, 1 eq) in DMF (2.5 mL) was added a solution of **3** (0.49 mmol, 1.5 eq) with EDC.HCl (0.59 mmol, 1.8 eq) and HOBT.H₂O (0.59 mmol, 1.8 eq) in DMF (2.5 mL) dropwise at 0°C. The reaction was stirred at rt for 10h. The reaction mixture was washed with water and dried over anhydrous Na₂SO₄. Purification by flash chromatography on silica gel (hexane/EtOAc 1/1) gave **4** (50 mg, 34% yield). ¹H NMR (400 MHz, CDCl₃) δ 7.22 (s, 1H), 7.20 (s, 1H), 7.17 (s, 1H), 5.86 (ddt, *J* = 17.1, 10.4, 5.7 Hz, 1H), 5.24 (dddd, *J* = 10.4, 3.8, 2.8, 1.4 Hz, 2H), 5.10 (s, 2H), 5.06 (s, 2H), 4.63 (s, 2H), 4.54 (dt, *J* = 5.7, 1.4 Hz, 2H), 4.14 (s, 3H), 2.68 – 2.63 (m, 4H), 2.33 (s, 3H). ¹³C NMR (400 MHz, CDCl₃) δ 172.22, 172.05, 153.11, 135.38, 133.83, 133.76, 132.04, 131.69, 131.59, 129.08, 129.06, 118.51, 66.22, 65.60, 61.80, 61.10, 34.62, 29.24, 29.06, 20.92. HRMS (ESI⁺) [M+H]⁺ calculated for [C₂₁H₂₅N₃O₈]⁺: 448.1714, found: 448.1712.

Allyl (5-methyl-2-((1-methyl-2-nitro-1H-imidazol-5-yl)methoxy)-3-(((4-nitrophenoxy)carbonyl)oxy)methyl)benzyl) succinate (15)



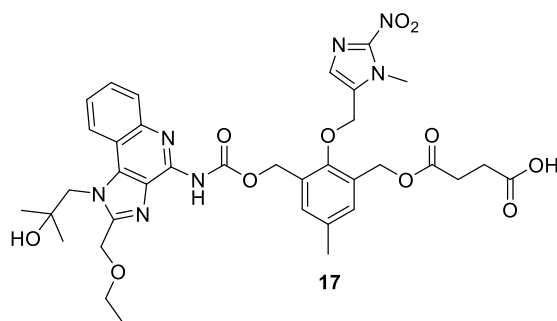
To a solution of **4** (0.17 mmol, 1 eq) in DCM (11 mL) was added 4-Nitrophenyl chloroformate (0.35 mmol; 2 eq) and DIEA (0.87 mmol, 5 eq). The reaction was stirred at reflux for 4h. The reaction mixture was washed with water, dried over anhydrous Na₂SO₄ and concentrated under vacuum to afford **5**, directly used at the following step. ¹H NMR (400 MHz, CDCl₃) δ 8.30 – 8.27 (m, 2H), 7.42 – 7.37 (m, 2H), 7.31 – 7.30 (m, *J* = 1.4 Hz, 2H), 7.23 (s, 1H), 5.87 (ddt, *J* = 17.2, 10.4, 5.7 Hz, 1H), 5.32 – 5.20 (m, 2H), 5.20 (s, 2H), 5.17 (s, 2H), 5.09 (s, 2H), 4.59 – 4.53 (m, 2H), 4.14 (s, 3H), 2.69 (dq, *J* = 4.8, 2.4 Hz, 4H), 2.37 (s, 3H).

Allyl (3-(((2-(ethoxymethyl)-1-(2-hydroxy-2-methylpropyl)-1H-imidazo[4,5-c]quinolin-4-yl)carbamoyl)oxy)methyl)-5-methyl-2-((1-methyl-2-nitro-1H-imidazol-5-yl)methoxy)benzyl) succinate (16)



To a solution of **5** (0.14 mmol, 1 eq) in EtOAc (40 mL) was added Resiquimod (0.17 mmol, 1.2 eq) and DIEA (0.34 mmol, 2.5 eq). The reaction mixture was stirred at rt for 3h and the reaction mixture was concentrated under vacuum. Purification by flash chromatography on silica gel (hexane/EtOAc 3/7) gave **6** (36 mg, 35% yield). ¹H NMR (400 MHz, CDCl₃) δ 8.18 (d, J = 7.4 Hz, 1H), 8.06 (d, J = 8.0 Hz, 1H), 7.61 (ddd, J = 8.4, 7.2, 1.3 Hz, 1H), 7.50 (ddd, J = 8.5, 5.1, 1.7 Hz, 1H), 7.40 (d, J = 2.2 Hz, 1H), 7.24 (s, 1H), 7.22 (d, J = 2.1 Hz, 1H), 5.87 (ddt, J = 17.2, 10.4, 5.7 Hz, 1H), 5.32 (s, 2H), 5.25 (dddd, 2H), 5.16 (s, 2H), 5.11 (s, 2H), 4.92 (s, 2H), 4.79 (s, 2H), 4.58 – 4.52 (m, 2H), 3.65 (q, J = 7.0 Hz, 2H), 2.73 – 2.63 (m, 4H), 2.35 (s, 3H), 1.34 (s, 6H), 1.25 (t, J = 7.0 Hz, 3H). ¹³C NMR (400 MHz, CDCl₃) δ 172.17, 172.00, 153.56, 153.29, 151.24, 150.81, 150.53, 146.40, 135.75, 135.33, 133.68, 132.60, 132.24, 132.04, 129.48, 129.02, 129.02, 129.01, 127.63, 124.90, 124.76, 120.28, 120.02, 118.47, 118.24, 71.62, 66.83, 66.28, 65.56, 65.16, 62.56, 61.71, 56.41, 34.68, 29.22, 29.06, 20.90, 15.03, 14.61, 14.32. MS (ESI⁺) m/z 788.34 [M+H]⁺. HRMS (ESI⁺) [M+H]⁺ calculated for [C₃₉H₄₅N₇O₁₁]⁺: 788.3250, found: 788.3253.

4-(((3-(((2-(ethoxymethyl)-1-(2-hydroxy-2-methylpropyl)-1H-imidazo[4,5-c]quinolin-4-yl)carbamoyl)oxy)methyl)-5-methyl-2-((1-methyl-2-nitro-1H-imidazol-5-yl)methoxy)benzyl)oxy)-4-oxobutanoic acid (17**)**



To a solution of **6** (0.01 mmol, 1 eq) in THF (5 mL) was added PhSiH₃ (0.02 mmol, 2 eq) and Pd(PPh₃)₄ (5 wt %). The reaction was stirred at rt for 4h and the reaction was concentrated under vacuum. Purification by flash chromatography on silica gel (hexane/EtOAc 3/7) gave **7** (31 mg, 41% yield). ¹H NMR (400 MHz, CDCl₃) δ 8.17 (d, J = 8.4 Hz, 1H), 8.01 (d, J = 8.4 Hz, 1H), 7.57 (t, J = 7.7 Hz, 1H), 7.46 (t, J = 7.6 Hz, 1H), 7.34 (d, J = 2.0 Hz, 1H), 7.20 (d, J = 1.2 Hz, 1H), 7.04 (s, 1H), 5.22 (s, 1H), 5.08 (s, 3H), 4.90 (s, 2H), 4.76 (s, 2H), 4.04 (s, 2H), 3.57 (dd, J = 14.1, 7.1 Hz, 2H), 2.62 (s, 3H), 2.30 (s, 2H), 1.34 (d, J = 16.0 Hz, 6H), 1.18 (dd, J = 7.7, 6.3 Hz, 4H). ¹³C NMR (400 MHz, CDCl₃) δ 176.24, 172.47, 153.81, 151.55, 149.83, 146.00, 136.87, 136.14, 135.13, 133.97, 132.95, 132.89, 129.52, 129.52, 129.03, 128.73, 128.39, 128.03, 127.96, 124.91, 120.51, 116.61, 71.64, 66.77, 66.20, 65.03, 62.88, 62.04, 56.37, 34.68, 29.61, 29.50, 28.19, 28.14, 20.84, 15.02. MS (ESI⁻) m/z 746.31 [M-H]⁻, 1493.62 [2M-1]⁻. HRMS (ESI⁻) [M-H]⁻ calculated for [C₃₆H₄₁N₇O₁₁]⁻: 746.2791, found: 746.2793.

References

- Greene, M. K.; Chen, T.; Robinson, E.; Straubinger, N. L.; Minx, C.; Chan, D. K. W.; Wang, J.; Burrows, J. F.; van Schaeysbroeck, S.; Baker, J. R.; Caddick, S.; Longley, D. B.; Mager, D. E.; Straubinger, R. M.; Chudasama, V.; Scott, C. J. Controlled Coupling of an Ultrapotent Auristatin Warhead to Cetuximab Yields a Next-Generation Antibody-Drug Conjugate for EGFR-Targeted Therapy of KRAS Mutant Pancreatic Cancer. *British Journal of Cancer* **2020**, *123* (10), 1502–1512. <https://doi.org/10.1038/s41416-020-01046-6>.
- Mohamed Amar, I. A.; Huvelle, S.; Douez, E.; Letast, S.; Henrion, S.; Viaud-Massuard, M. C.; Aubrey, N.; Allard-Vannier, E.; Joubert, N.; Denevault-Sabourin, C. Dual Intra- and Extracellular Release of Monomethyl Auristatin E from a Neutrophil Elastase-Sensitive Antibody-Drug Conjugate. *European Journal of Medicinal Chemistry* **2022**, *229*, 1–11. <https://doi.org/10.1016/j.ejmech.2021.114063>.
- Tsuchikama, K.; An, Z. Antibody-Drug Conjugates: Recent Advances in Conjugation and Linker Chemistries. *Protein and Cell* **2018**, *33*–46. <https://doi.org/10.1007/s13238-016-0323-0>.
- Rossin, R.; Versteegen, R. M.; Wu, J.; Khasanov, A.; Wessels, H. J.; Steenbergen, E. J.; ten Hoeve, W.; Janssen, H. M.; van Onzen, A. H. A. M.; Hudson, P. J.; Robillard, M. S. Chemically Triggered Drug Release from an Antibody-Drug Conjugate Leads to Potent Antitumour Activity in Mice. *Nature Communications* **2018**, *9*, 1065–1120. <https://doi.org/10.1038/s41467-018-03880-y>.
- Shi, W.; Li, W.; Zhang, J.; Li, T.; Song, Y.; Zeng, Y.; Dong, Q.; Lin, Z.; Gong, L.; Fan, S.; Tang, F.; Huang, W. One-Step Synthesis of Site-Specific Antibody–Drug Conjugates by Reprogramming IgG Glycoengineering with LacNAc-Based Substrates. *Acta Pharmaceutica Sinica B* **2022**, Article ASAP. <https://doi.org/10.1016/j.apsb.2021.12.013>.
- Birrer, M. J.; Moore, K. N.; Betella, I.; Bates, R. C. Antibody-Drug Conjugate-Based Therapeutics: State of the Science. *J Natl Cancer Inst* **2019**, *111* (6), 538–549. <https://doi.org/10.1093/jnci/djz035>.
- Ponziani, S.; di Vittorio, G.; Pitari, G.; Cimini, A. M.; Ardini, M.; Gentile, R.; Iacobelli, S.; Sala, G.; Capone, E.; Flavell, D. J.; Ippoliti, R.; Giansanti, F. Antibody-Drug Conjugates: The New Frontier of Chemotherapy. *International Journal of Molecular Sciences* **2020**, *21* (15), 1–28. <https://doi.org/10.3390/ijms21155510>.
- Faust, A.; Bäumer, N.; Schlütermann, A.; Becht, M.; Greune, L.; Geyer, C.; Rüter, C.; Margeta, R.; Wittmann, L.; Dersch, P.; Lenz, G.; Berdel, W. E.; Bäumer, S. Tumor-Cell-Specific Targeting of Ibrutinib: Introducing Electrostatic Antibody-Inhibitor Conjugates (AiCs). *Angew. Chem. Int. Ed.* **2022**, *61*, 1–11. <https://doi.org/10.1002/anie.202109769>.
- Matsuda, Y.; Mendelsohn, B. A. An Overview of Process Development for Antibody-Drug Conjugates Produced by Chemical Conjugation Technology. *Expert Opinion on Biological Therapy* **2021**, *21* (7), 963–975. <https://doi.org/10.1080/14712598.2021.1846714>.
- Jain, N.; Smith, S. W.; Ghone, S.; Tomczuk, B. Current ADC Linker Chemistry. *Pharmaceutical Research* **2015**, *32*, 3526–3540. <https://doi.org/10.1007/s11095-015-1657-7>.
- Hasan, M. M.; Laws, M.; Jin, P.; Rahman, K. M. Factors Influencing the Choice of Monoclonal Antibodies for Antibody–Drug Conjugates. *Drug Discovery Today* **2022**, *27* (1), 354–361. <https://doi.org/10.1016/j.drudis.2021.09.015>.
- Thomas, A.; Teicher, B. A.; Hassan, R. Antibody-Drug Conjugates for Cancer Therapy. *Lancet Oncol.* **2016**, *17* (6), 254–262. <https://doi.org/10.1016/j.apsb.2021.12.013>
- Matsuda, Y. Current Approaches for the Purification of Antibody–Drug Conjugates. *Journal of Separation Science* **2022**, *45* (1), 27–37. <https://doi.org/10.1002/jssc.202100575>.
- Cao, Y. J.; Yu, C.; Wu, K. L.; Wang, X.; Liu, D.; Tian, Z.; Zhao, L.; Qi, X.; Loreda, A.; Chung, A.; Xiao, H. Synthesis of Precision Antibody Conjugates Using Proximity-Induced Chemistry. *Theranostics* **2021**, *11* (18), 9107–9117. <https://doi.org/10.7150/thno.62444>.

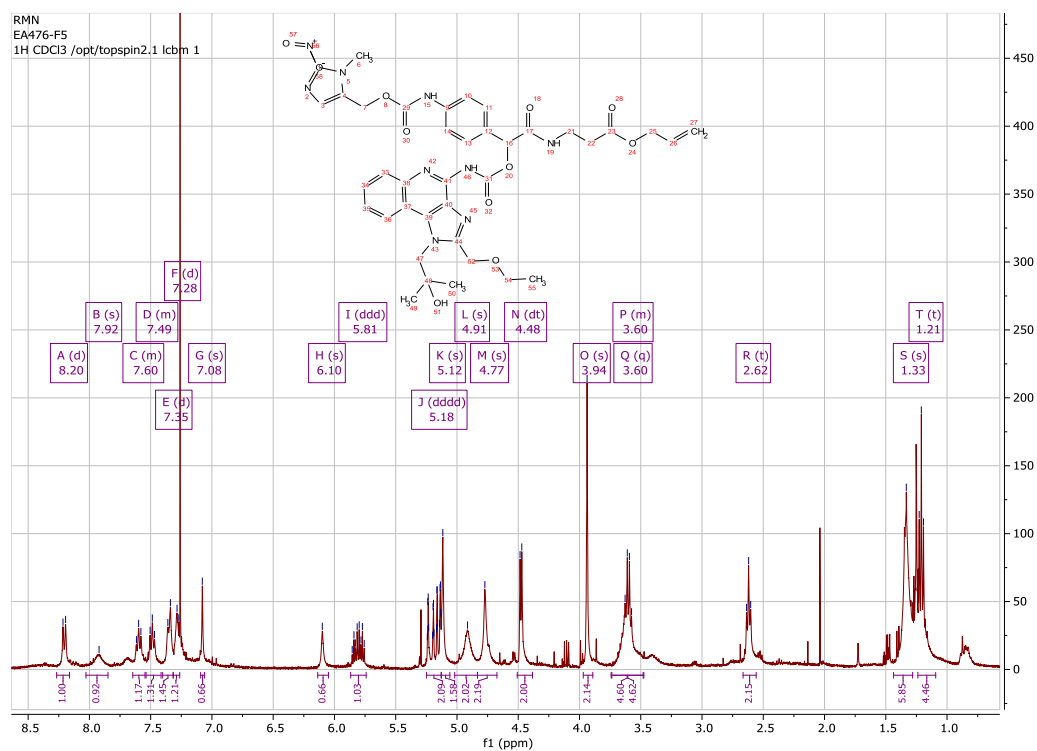
15. van der Wiel, A. M. A.; Jackson-Patel, V.; Niemans, R.; Yaromina, A.; Liu, E.; Marcus, D.; Mowday, A. M.; Lieuwes, N. G.; Biemans, R.; Lin, X.; Fu, Z.; Kumara, S.; Jochems, A.; Ashoorzadeh, A.; Anderson, R. F.; Hicks, K. O.; Bull, M. R.; Abbattista, M. R.; Guise, C. P.; Deschoemaeker, S.; Thiollay, S.; Heyerick, A.; Solivio, M. J.; Balbo, S.; Smaill, J. B.; Theys, J.; Dubois, L. J.; Patterson, A. v.; Lambin, P. Selectively Targeting Tumor Hypoxia with the Hypoxia-Activated Prodrug CP-506. *Molecular Cancer Therapeutics* **2021**, *20* (12), 2372–2383. <https://doi.org/10.1158/1535-7163.MCT-21-0406>.
16. Baran, N.; Konopleva, M. Molecular Pathways: Hypoxia-Activated Prodrugs in Cancer Therapy. *Clinical Cancer Research* **2017**, *23* (10), 2382–2391. <https://doi.org/10.1158/1078-0432.CCR-16-0895>.
17. Mistry, I. N.; Thomas, M.; Calder, E. D. D.; Conway, S. J.; Hammond, E. M. Clinical Advances of Hypoxia-Activated Prodrugs in Combination With Radiation Therapy. *Radiation Oncology Biology* **2017**, *98* (5), 1183–1196. <https://doi.org/10.1016/j.ijrobp.2017.03.024>.
18. Sun, Z.; Zhang, H.; Zhang, H.; Wu, J.; Gao, F.; Zhang, C.; Hu, X.; Liu, Q.; Wei, Y.; Wei, Y.; Zhuang, J.; Zhuang, J.; Huang, X. A Novel Model System for Understanding Anticancer Activity of Hypoxia-Activated Prodrugs. *Molecular Pharmaceutics* **2020**, *17* (6), 2072–2082. <https://doi.org/10.1021/acs.molpharmaceut.0c00232>.
19. Anduran, E.; Dubois, L. J.; Lambin, P.; Winum, J. Y. Hypoxia-Activated Prodrug Derivatives of Anti-Cancer Drugs: A Patent Review 2006–2021. *Expert Opinion on Therapeutic Patents* **2022**, *32* (1), 1–12. <https://doi.org/10.1080/13543776.2021.1954617>.
20. Hunter, F. W.; Wouters, B. G.; Wilson, W. R. Hypoxia-Activated Prodrugs: Paths Forward in the Era of Personalised Medicine. *British Journal of Cancer* **2016**, *114*, 1071–1077. <https://doi.org/10.1038/bjc.2016.79>.
21. Lindsay, D.; Garvey, C. M.; Mumenthaler, S. M.; Foo, J. Leveraging Hypoxia-Activated Prodrugs to Prevent Drug Resistance in Solid Tumors. **2016**, 1–25. <https://doi.org/10.1371/journal.pcbi.1005077>.
22. Alouane, A.; Saux, T. le; Schmidt, F.; Jullien, L. Self-Immolative Spacers: Kinetic Aspects, Structure – Property Relationships, and Applications. *Angewandte Chemie* **2015**, *54*, 7492–7509. <https://doi.org/10.1002/anie.201500088>.
23. Wang, Z.; Wu, H.; Liu, P.; Zeng, F.; Wu, S. A Self-Immolative Prodrug Nanosystem Capable of Releasing a Drug and a NIR Reporter for in Vivo Imaging and Therapy. *Biomaterials* **2017**, *139*, 139–150. <https://doi.org/10.1016/j.biomaterials.2017.06.002>.
24. Gonzaga, R. V.; do Nascimento, L. A.; Santos, S. S.; Machado Sanches, B. A.; Giarolla, J.; Ferreira, E. I. Perspectives About Self-Immolative Drug Delivery Systems. *Journal of Pharmaceutical Sciences* **2020**, *109*, 3262–3281. <https://doi.org/10.1016/j.xphs.2020.08.014>.
25. Wilson, W. R.; Hay, M. P. Targeting Hypoxia in Cancer Therapy. *Nature Reviews Cancer*. **2011**, *11*, 393–410. <https://doi.org/10.1038/nrc3064>.
26. Anduran, E.; Aspatwar, A.; Parvathaneni, N. K.; Suylen, D.; Bua, S.; Nocentini, A.; Parkkila, S.; Supuran, C. T.; Dubois, L.; Lambin, P.; Winum, J. Y. Hypoxia-Activated Prodrug Derivatives of Carbonic Anhydrase Inhibitors in Benzenesulfonamide Series: Synthesis and Biological Evaluation. *Molecules* **2020**, *25* (10), 2347. <https://doi.org/10.3390/molecules25102347>.
27. Kaushik, D.; Kaur, A.; Petrovsky, N.; Salunke, D. B. Structural Evolution of Toll-like Receptor 7/8 Agonists from Imidazoquinolines to Imidazoles. *RSC Medicinal Chemistry* **2021**, *12* (7), 1065–1120. <https://doi.org/10.1039/d1md00031d>.
28. Curini, M.; Epifano, F.; Genovese, S.; Marcotullio, M. C.; Rosati, O. Ytterbium Triflate-Promoted Tandem One-Pot Oxidation-Cannizzaro Reaction of Aryl Methyl Ketones. *Organic Letters* **2005**, *7* (7), 1331–1333. <https://doi.org/10.1021/ol050125e>.
29. Hu, M.; Li, L.; Wu, H.; Su, Y.; Yang, P. Y.; Uttamchandani, M.; Xu, Q. H.; Yao, S. Q. Multicolor, One- and Two-Photon Imaging of Enzymatic Activities in Live Cells with Fluorescently Quenched Activity-Based Probes (QABPs). *J Am Chem Soc* **2011**, *133* (31), 12009–12020. <https://doi.org/10.1021/ja200808y>.

Chapter 5

30. Kumar, R.; Kim, E. J.; Han, J.; Lee, H.; Shin, W. S.; Kim, H. M.; Bhuniya, S.; Kim, J. S.; Hong, K. S. Hypoxia-Directed and Activated Theranostic Agent: Imaging and Treatment of Solid Tumor. *Biomaterials* **2016**, *104*, 119–128. <https://doi.org/10.1016/j.biomaterials.2016.07.010>.
31. Liew, L. P.; Singleton, D. C.; Wong, W. W.; Cheng, G. J.; Jamieson, S. M. F.; Hay, M. P. Hypoxia-Activated Prodrugs of PERK Inhibitors. *Chemistry - An Asian Journal* **2019**, *14* (8), 1238–1248. <https://doi.org/10.1002/asia.201801826>.
32. Catry, M. A.; Madder, A. Molecules Synthesis of Functionalised Nucleosides for Incorporation into Nucleic Acid-Based Serine Protease Mimics; *Molecules* **2007**, *12* (1), 114–129. <https://doi.org/10.3390/12010114>
33. Aerts, H. J. W. L.; Dubois, L.; Hackeng, T. M.; Straathof, R.; Chiu, R. K.; Lieuwes, N. G.; Jutten, B.; Wepler, S. A.; Lammering, G.; Wouters, B. G.; Lambin, P. Development and Evaluation of a Cetuximab-Based Imaging Probe to Target EGFR and EGFRvIII. *Radiotherapy and Oncology* **2007**, *83* (3), 326–332. <https://doi.org/10.1016/j.radonc.2007.04.030>.
34. Zeng, D.; Guo, Y.; White, A. G.; Cai, Z.; Modi, J.; Ferdani, R.; Anderson, C. J. Comparison of Conjugation Strategies of Cross-Bridged Macrocyclic Chelators with Cetuximab for Copper-64 Radiolabeling and PET Imaging of EGFR in Colorectal Tumor-Bearing Mice. *Molecular Pharmaceutics* **2014**, *11* (11), 3980–3987. <https://doi.org/10.1021/mp500004m>.
35. Sabra, R.; Billa, N.; Roberts, C. J. Cetuximab-Conjugated Chitosan-Pectinate (Modified) Composite Nanoparticles for Targeting Colon Cancer. *International Journal of Pharmaceutics* **2019**, *572*, 1–11. <https://doi.org/10.1016/j.ijpharm.2019.118775>.
36. Huang, H. C.; Pigula, M.; Fang, Y.; Hasan, T. Immobilization of Photo-Immunoconjugates on Nanoparticles Leads to Enhanced Light-Activated Biological Effects. *Small* **2018**, *14* (31), 1800236. <https://doi.org/10.1002/smll.201800236>.

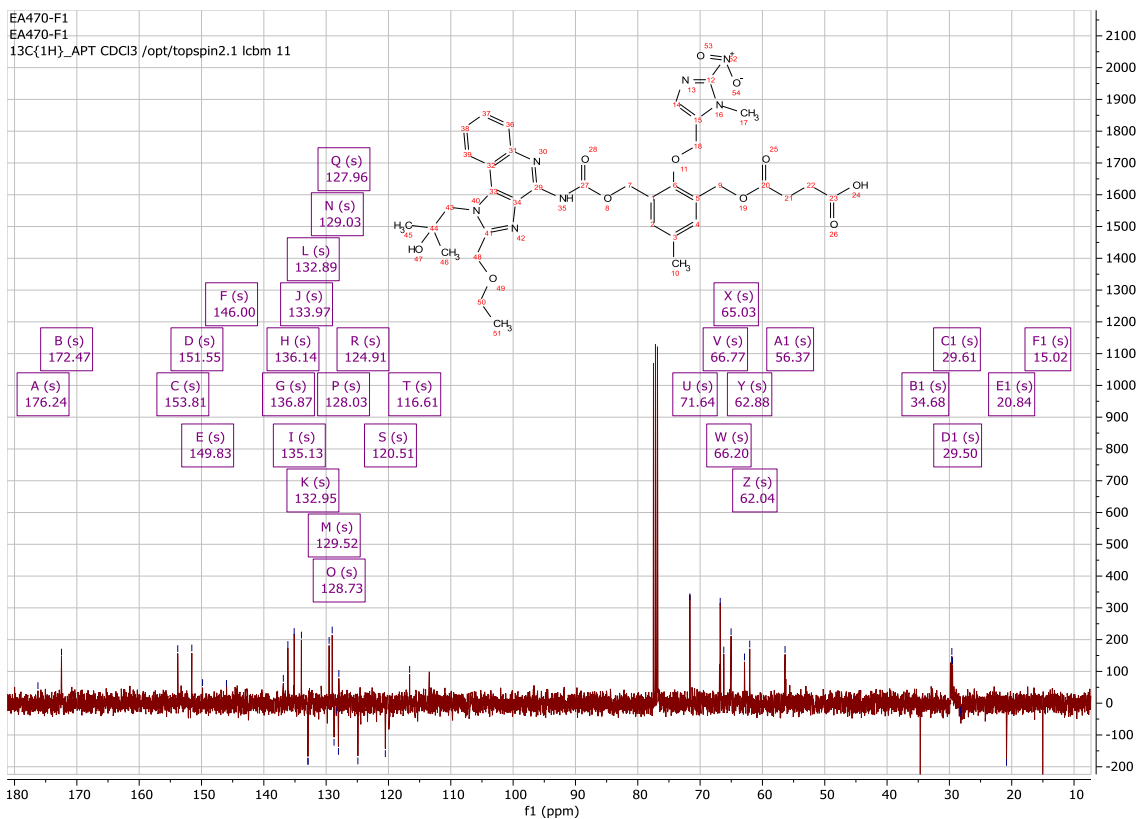
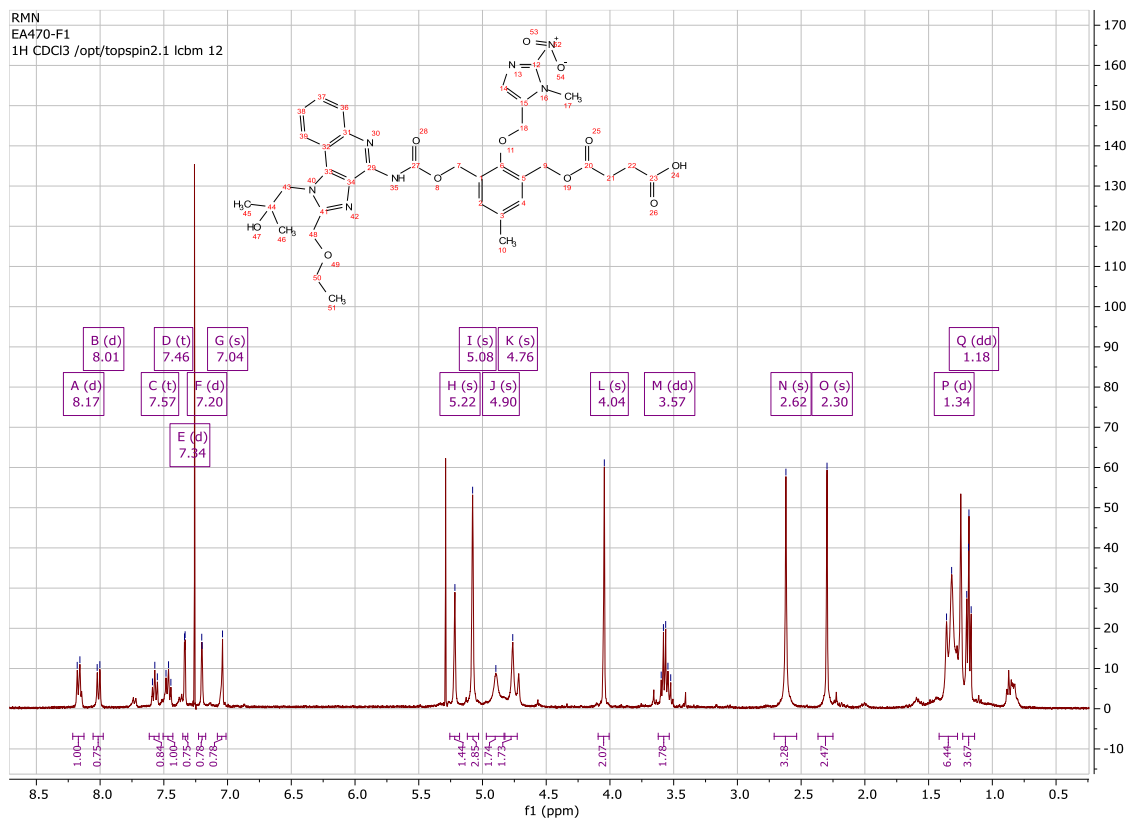
Supplementary data

NMR spectra 1 ¹H: Allyl 3-(2-(((2-(ethoxymethyl)-1-(2-hydroxy-2-methylpropyl)-1H-imidazo[4,5-c]quinolin-4-yl)carbamoyl)oxy)-2-(4-((((1-methyl-2-nitro-1H-imidazol-5-yl)methoxy)carbonyl)amino)phenyl) acetamido)propanoate (7)



Chapter 5

NMR spectra ^1H & ^{13}C : 4-((3-(((2-(ethoxymethyl)-1-(2-hydroxy-2-methylpropyl)-1H-imidazo[4,5c]quinolin-4-yl)carbamoyl)oxy)methyl)-5-methyl-2-((1-methyl-2-nitro-1H-imidazol-5-yl)methoxy)benzyl)oxy)-4-oxobutanoic acid (**17**)



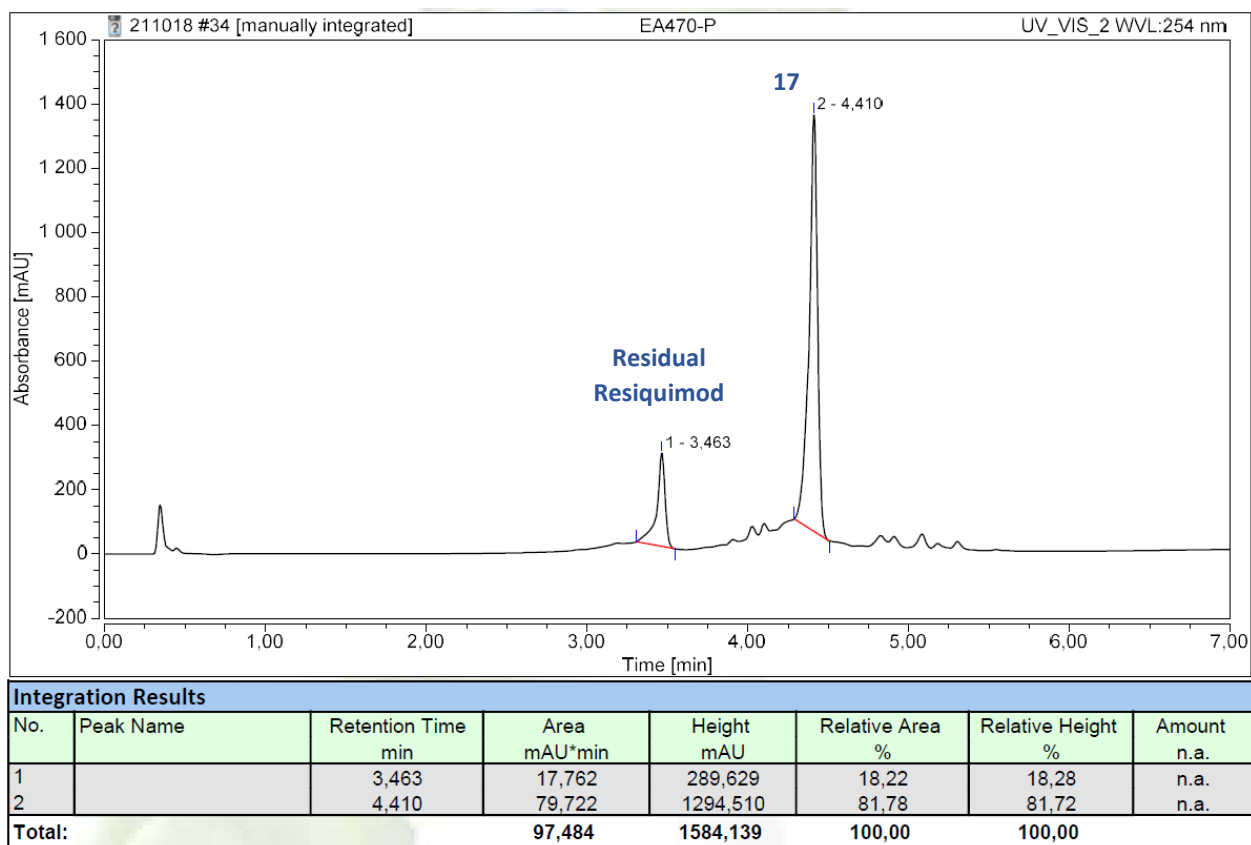


Figure 1S: Purity analysis of 17 by HPLC showing a decoupling about 18 % of Resiquimod.

Chapter 6

General Discussion and future perspectives

Solid tumours are associated, nowadays, to a harsh metabolic microenvironment resulting in an imbalance of positive and negative regulators of processes in activating and deregulating angiogenesis, desmoplasia, and inflammation.¹ This enables tumour progression and resistance to conventional therapies. Hypoxia is a well-known characteristic of solid tumours, which affects tumour cells through a high scale adaptative reprogramming by modifying the glycolytic energy metabolism and angiogenesis amongst others, making tumours more aggressive, proliferative and resistant to conventional treatments.²⁻⁷ Therefore, hypoxia is an extremely valuable target to be exploited for certain anti-cancer therapy strategies.⁸

HYPOXIA-ACTIVATED PRODRUGS

In the last 30 years, researchers have shown interest in the hypoxia tumour environment in order to take advantage of the difference of oxygen concentration between hypoxic tumours and healthy tissues which represents a unique phenotype of cancer cells. Hypoxia-activated prodrugs (HAPs) have been developed to exploit the hypoxic tumour microenvironment for personalized cancer medicine. The selectivity of HAPs with regard to hypoxia relies on a preferential activation in hypoxic *versus* well-oxygenated tissues, an easy diffusion within the hypoxic tumour areas, and the release or activation of a cytotoxic effector which diffuses partially back into the aerobic fraction of the tumour to produce a cytotoxic effect on rapidly proliferating cells, creating a bystander effect.⁹⁻¹² Numerous HAPs have been developed during the last decades, they are in majority composed of a cytotoxic payload connected via a linker to a hypoxia sensitive trigger to undergo enzymatic bioreduction in the hypoxic tumour environment to activate the prodrug, enabling drug release.^{13,14} Two approaches have been described in the literature, the first one is based on the exploitation of the redox potential between normoxic and hypoxic tissues in order to allow the selective activation of prodrugs directly in the hypoxic tumour environment. One of the most studied HAPs so far is TH-302, also known as Evofosfamide, which has reached phase 3 trials. TH-302 is a 2-nitroimidazole-based nitrogen mustard prodrug enabling the release of a DNA cross-linking agent through one-electron enzymatic reduction mechanisms. This compound has shown promising results in combination with other anti-cancer agents and therapies but as well in monotherapy.¹⁵⁻¹⁷ TH-4000, also called Tarloxotinib bromide, is the second HAP which has reached clinical trials. TH-4000 consists of a kinase inhibitor connected to a nitroimidazole bioreducible trigger and its mechanism of activation follows the one-electron bioreduction pathway. Another HAP showing promising results in *in vitro* and *in vivo* studies is CP-506, which recently entered a first-in-human clinical safety trial. CP-506 is the next generation of the pre-prodrug PR-104 which is resistant to aldo-keto reductase 1C3 activation in normal tissues. This prodrug contains a nitrogen mustard and can be metabolised by undergoing a one-electron bioreduction to release, after further reduction, cytotoxic metabolites.^{18,19} In the large number of HAP compounds described, the nitro (hetero)aromatic triggers are always considered as the best structural feature to achieve bioreductive properties. Today, a limited series of HAPs has been evaluated in clinical trials, including porfiromycin, banoxantrone, tirapazamine, evofosfamide, PR-104 and tarloxotinib, among them, evofosfamide, tarloxotinib and CP-506 are the only HAP derivatives currently in clinical trials.¹

HAPS TARGETING CAIX FOR SOLID TUMOUR THERAPY

The second strategy for hypoxia anti-cancer therapy consists to target its molecular response, by targeting proteins regulated by the hypoxia-inducible factor (HIF) and involved in hypoxic tumour cell metabolism which is at the origin of cancer progression, metastasis, and impaired therapeutic response. One of these proteins, highly expressed in hypoxic cells is the carbonic anhydrase IX (CAIX). This enzyme has been described as an adverse prognostic biomarker and therapeutic target for various cancer types.^{20,21} For this reason, it has been suggested that CAIX represents a promising target for anticancer treatment.^{22,23} The development of small molecules as CAIX inhibitors represents a successful field with several potent inhibitors reported so far.^{24,25} Nevertheless, the main problem encountered with these inhibitors was the lack of selectivity to target hypoxic tumoural CAIX, resulting in systemic toxicity. Till date, a benzenesulfonamide CAIX inhibitor, named SLC-0111, showed a promising anticancer action and progressed into clinical trials.²³ Few numbers of CAIX inhibitors have been designed using the HAP approach, therefore novel HAP CAIX inhibitors were designed, synthesized and biologically evaluated in this thesis work, as described in Chapter 3. The rationale to design this HAP CAIX inhibitor derivatives is to increase the tumour specificity of the payload and potentially decrease toxicity on normoxic tissues. Seven compounds were designed, composed of two moieties connected to each other using a carbamate link, combining bio-reducible hypoxia triggers and sulfonamide moieties, already known as potent CA inhibitors. Five different bio-reducible moieties were coupled to benzenesulfonamides in order to evaluate their different reduction potential and their ability to deliver the cytotoxic payload in the hypoxic tumour. All the HAPs showed a selective inhibition toward CAIX, however, only one of the seven synthesized derivatives was effective on HT29 cells. Indeed, the compound harbouring the nitroimidazole hypoxia trigger showed a potent selective inhibition of CAIX in anoxic condition with no activity under normoxia. Despite these positive results, this prodrug did not show anti-proliferative effect on cancer cells. In addition, studies performed on zebrafish larvae suggest this compound could be studied further in combination with other therapeutics or anticancer treatment modalities. Furthermore, this compound has been evaluated for its toxic effects on healthy cells, using Zebrafish as a model and did not show any toxicity on larvae with no mortality or no phenotypic abnormality observed, suggesting that this prodrug could be considered as safe.²⁶

IMMUNOTHERAPY FOR SOLID TUMOUR TREATMENTS

A different family of anticancer drugs is becoming, nowadays, a powerful strategy against cancer, the immunotherapeutics. Indeed, immunotherapy is the most rapidly growing treatment class and has a major impact in oncology. Contrarily to chemotherapy, immunotherapy is based on reactivation of the immune system to attack cancer cells through a natural process which is evaded during the tumour progression.²⁷⁻³¹ The immune system is able to recognise cancer cells but needs to receive a second confirmation before to initiate cancer cell death. This confirmatory signal is mediated by a variety of co-stimulatory and inhibitory receptors referred as check-points which induce cancer cell death *via* T-cell action. However, tumour cells are capable to deregulate the expression of checkpoint proteins in order to adapt and survive. Rather than influencing the metabolism of tumour cells, immunotherapy harnesses the power of

immune cells. The immune system is known to provide a rich source of targets for therapeutic intervention such as programmed cell death protein 1 (PD-1), programmed death ligand 1 (PD-L1) or cytotoxic T-lymphocyte associated protein 4 (CTLA-4). Enormous efforts have been made in the search for more potent and specific checkpoint inhibitors, leading to over ten immune check-point antibodies targeting CTLA-4 and PD-1/PD-L1 and over thousands are under active clinical trials.²⁸ Recent years showed a huge advance in small-molecule immunotherapy targeting for example, the PD-1/PD-L1 complex, indoleamine 2,3-dioxygenase (IDO), a stimulator of interferon genes (STING) or the toll-like receptor (TLR) with some compounds already in clinical trials.³¹⁻³³ Imiquimod and Resiquimod, respectively TLR7 and TLR7/8 agonists, are two analogous drugs which have shown promising results as topical treatment of basal cell carcinoma and have been approved by the food and drug administration (FDA). Ibrutinib, an irreversible inhibitor of Bruton's tyrosine kinase (BTK), as well as other kinases, has been approved for use against leukemia, mantle cell lymphoma, and Waldenstrom macroglobulinaemia.³⁴ Furthermore, Ibrutinib showed in preclinical studies improved benefits in combination therapy with an anti-PD-L1 antibody compared to monotherapy treatment.³⁵ With the aim to improve the hypoxic tumour targeting properties of these promising drugs and to decrease adverse effects encountered, we have designed and synthesized nine hypoxia-activated prodrugs as described in Chapter 4. These derivatives have been obtained by coupling three nitro-aromatic bio-reducible hypoxia triggers, the 2-nitroimidazole, nitrofuran and nitrothiophene to the three drugs Imiquimod, Resiquimod and Ibrutinib. The compounds were synthesized by connecting the two moieties with a carbamate linker. However, during the synthesis, the three drugs did not show a high reactivity, preventing the formation of the expected compounds in good and reproducible yield. Furthermore, it has been observed that the compounds were not soluble in aqueous conditions except the Resiquimod analogues. Therefore, only those derivatives progressed into biological testing. Only one of prodrugs demonstrated interesting cytotoxicity activity in anoxia compared to normoxic conditions despite partial degradation. Indeed, a viability assay on the nitroimidazole-based Resiquimod analogue showed effective cytotoxicity on CT26 and PC3 cancer cells, suggesting an efficient drug release in anoxic conditions as expected. This encouraging result could lead to the design and synthesis of other HAP-immunotherapeutics.

Immunotherapy is a promising research field for cancer therapy allowing to provide treatments aiming at the activation/stimulation of the human immune system to specifically kill cancer cells, with less adverse effects. This therapy class could therefore lead to a decrease of the adverse effects generally observed in conventional chemotherapy treatment. However, a better understanding of the immune response mechanisms involved in the tumour environment remains crucial. In the same way, the influence of hypoxia on the biology of immune cells still needs to be understood in more detail.³⁶ Studies have suggested that reversing tumour hypoxia by reoxygenation could alleviate immune suppression and lead to a better efficiency of immunotherapeutics.¹ The design of hypoxia-activated prodrugs containing immunotherapeutic payloads could enhance the efficiency of such therapeutics for the treatment of solid tumour. Despite all the preclinical and clinical evaluations currently ongoing, the next challenge will be to anticipate the reasons why in certain patients the immune intervention does not offer a durable

response compared to others. In addition, the improvement of *in vitro* conditions compared to *in vivo* could lead to more successful preclinical and clinical evaluations.

ANTIBODY CONJUGATES FOR SOLID TUMOUR TARGETING

In the last decades antibody-drug conjugates (ADCs) have gained interest because they offer, contrarily to traditional chemotherapeutics, an increased therapeutic window related to the cell-targeting properties of the antibodies. Indeed, ADCs are generally consisting of a potent cytotoxic payload covalently coupled through a linker to an antibody which allows a specific targeting and delivery of the payload directly in the tumour environment, minimizing adverse-effects.³⁷⁻⁴⁰ The selection of the antibody is highly important because it will play at the same time the role of the payload carrier and the one of targeting component⁴¹, therefore, antibodies must possess specific affinity towards tumour-associated antigens compared to normal tissue by targeting over-expressed antigens on the surface of tumour cells. For this reason, several ADCs have been designed to target the human epidermal growth factor receptor 2 (HER2). A receptor expressed more than 100 times in cancer cells, resulting in 2 million receptors expressed on the surface of tumour cells. However, the synthesis of such conjugates remains complex. Commonly, payloads are connected to antibodies using lysine or cysteine residues. The cysteines present the advantage of providing a better control on the drug-antibody ratio (DAR), as the attachment site is more predictable. Because lysines are more present on antibodies, it makes it difficult to control the payload conjugation and it can result on heterogenous coupling with a risk of hindering the antigen-binding region or toxicity if a large amount of payload was coupled on the same antibody.⁴² It still remains challenging to afford control on drug-to-antibody ratio (DAR) in order to improve the homogeneity of conjugation, but in recent years improvements have been achieved through the use of site-specific conjugation technology.

In this thesis, in order to improve the targeting of immunotherapeutics towards the tumour, we first designed and synthesized a HAP compound consisting of a Resiquimod payload as immunotherapeutic and a 2-nitroimidazole hypoxia bio-reducible trigger which has been selected according to the results obtained previously, described in Chapter 3 and 4. This HAP was also harbouring a linker with the aim to connect a tumour-specific antibody. This complex molecule has been designed to allow the drug release through a self-immolative mechanism initiated, as commonly in HAPs activation, by enzymatic bio-reduction in hypoxic tumour environment. Despite stability issues, the prodrug has been used for the antibody conjugation step on Cetuximab lysine residues to determine appropriate coupling conditions. We decided to use lysine coupling based on previous experience with coupling Oregon Green to Cetuximab.⁴³ However, first attempts by performing an activation step on the prodrug before the addition of the antibody did not show effective coupling, suggesting that another approach by activating first the antibody needs to be tested. The latter strategy has shown promising results in literature and might be preferred.⁴³

To date, 12 ADCs have been approved by the Food and Drug Administration (FDA), while more than 90 are currently in clinical development.⁴⁴ This as a result of recent efforts invested in the optimisation of various antibody properties such as antigen binding, immunogenicity tolerance

or solid tumour distribution and penetration.⁴¹ In addition, in future few years, the ADC research will explore the suitability of replacing the whole antibody with designed antibody fragments in order to optimise the size of the therapeutic carrier, one of the main drawbacks of the current approved ADC treatments. Likewise, the combination of antibodies with hypoxia-activated prodrugs could increase the efficacy of therapeutic payload for the treatment of solid tumours.

FUTURE DIRECTIONS

The development of hypoxia-activated prodrugs is an interesting therapeutic strategy to overcome the resistance issues encountered with the conventional therapies used for the treatment of solid tumours. This therapeutic approach is expanding every day through the design and synthesis of different prodrugs belonging to various family of compounds, but remains a complex research field and needs further improvement. The idea of combining a hypoxia sensitive trigger with a cytotoxic payload has been improved by the targeting of triggers directly involved in the hypoxic tumour metabolism such as CAIX. Among the CAIX targeting HAPs synthesized during this thesis, one prodrug showed interesting preliminary results which could justify to continue further study. Moreover, immunotherapy represents today a promising cancer therapy based on the stimulation of the immune system and the development of hypoxia-activated immunotherapeutics could improve the treatment selectivity towards tumour cells. Unfortunately, the immunotherapeutic HAPs synthesized in this thesis work has shown important water solubility and stability issues, preventing further biological evaluation. Another promising strategy in anticancer treatments is the antibody-drug conjugation. This rapidly growing class of therapeutics allows a specific targeting of tumour cells by using antibody recognition of overexpressed cancer antigens. This therapeutic class counts today several approved treatments which are actively studied for improvement. The antibody conjugation of the HAP compound designed and synthesized in this work still needs to be achieved in order to enable further potential biological evaluations. Today, the field of cancer therapy evolves thanks to several innovative strategies aiming the specific targeting of tumours to provide safety treatments compared to traditional therapies.

References

1. Fu, Z.; Mowday, A. M.; Smaill, J. B.; Hermans, I. F.; Patterson, A. v. Tumour Hypoxia-Mediated Immunosuppression: Mechanisms and Therapeutic Approaches to Improve Cancer Immunotherapy. *Cells* **2021**, *10* (5), 1006. <https://doi.org/10.3390/cells10051006>.
2. Wilson, W. R.; Hay, M. P. Targeting Hypoxia in Cancer Therapy. *Nature Reviews Cancer* **2011**, *11*, 393–410. <https://doi.org/10.1038/nrc3064>.
3. Peng, X.; Gao, J.; Yuan, Y.; Liu, H.; Lei, W.; Li, S.; Zhang, J.; Wang, S. Hypoxia-Activated and Indomethacin-Mediated Theranostic Prodrug Releasing Drug On-Demand for Tumor Imaging and Therapy. *Bioconjugate Chemistry* **2019**, *30* (11), 2828–2843. <https://doi.org/10.1021/acs.bioconjchem.9b00564>.
4. Liu, J. N.; Bu, W.; Shi, J. Chemical Design and Synthesis of Functionalized Probes for Imaging and Treating Tumor Hypoxia. *Chemical Reviews* **2017**, *117* (9), 6160–6224. <https://doi.org/10.1021/acs.chemrev.6b00525>.
5. Vilaplana-Lopera, N.; Besh, M.; Moon, E. J. Targeting Hypoxia: Revival of Old Remedies. *Biomolecules* **2021**, *11* (11), 1604. <https://doi.org/10.3390/biom11111604>.
6. Lindsay, D.; Garvey, C. M.; Mumenthaler, S. M.; Foo, J. Leveraging Hypoxia-Activated Prodrugs to Prevent Drug Resistance in Solid Tumors. *PLoS Comput Biol* **2016**, *12* (8), 1–25. <https://doi.org/10.1371/journal.pcbi.1005077>.
7. Kang, D.; Cheung, S. T.; Wong-Rolle, A.; Kim, J. Enamine N-Oxides: Synthesis and Application to Hypoxia-Responsive Prodrugs and Imaging Agents. *ACS Central Science* **2021**, *7* (4), 631–640. <https://doi.org/10.1021/acscentsci.0c01586>.
8. Sun, Z.; Zhang, H.; Zhang, H.; Wu, J.; Gao, F.; Zhang, C.; Hu, X.; Liu, Q.; Wei, Y.; Wei, Y.; Zhuang, J.; Zhuang, J.; Huang, X. A Novel Model System for Understanding Anticancer Activity of Hypoxia-Activated Prodrugs. *Molecular Pharmaceutics* **2020**, *17* (6), 2072–2082. <https://doi.org/10.1021/acs.molpharmaceut.0c00232>.
9. Anduran, E.; Dubois, L. J.; Lambin, P.; Winum, J. Y. Hypoxia-Activated Prodrug Derivatives of Anti-Cancer Drugs: A Patent Review 2006–2021. *Expert Opinion on Therapeutic Patents* **2022**, *32* (1), 1–12. <https://doi.org/10.1080/13543776.2021.1954617>.
10. Hunter, F. W.; Wouters, B. G.; Wilson, W. R. Hypoxia-Activated Prodrugs: Paths Forward in the Era of Personalised Medicine. *British Journal of Cancer* **2016**, *144*, 1071–1077. <https://doi.org/10.1038/bjc.2016.79>.
11. Petrova, V.; Annicchiarico-Petruzzelli, M.; Melino, G.; Amelio, I. The Hypoxic Tumour Microenvironment. *Oncogenesis* **2018**, *7* (10), 1–13. <https://doi.org/10.1038/s41389-017-0011-9>.
12. Ward, R. A.; Fawell, S.; Floc'H, N.; Flemington, V.; McKerrecher, D.; Smith, P. D. Challenges and Opportunities in Cancer Drug Resistance. *Chemical Reviews* **2021**, *121* (6), 3297–3351. <https://doi.org/10.1021/acs.chemrev.0c00383>.
13. Sharma, A.; Arambula, J. F.; Koo, S.; Kumar, R.; Singh, H.; Sessler, J. L.; Kim, J. S. Hypoxia-Targeted Drug Delivery. *Chemical Society Reviews* **2019**, *48* (3), 771–813. <https://doi.org/10.1039/c8cs00304a>.
14. Phillips, R. M. Targeting the Hypoxic Fraction of Tumours Using Hypoxia-Activated Prodrugs Cytotoxic Reviews Godefridus J. Peters and Eric Raymond. *Cancer Chemotherapy and Pharmacology* **2016**, *77*, 441–457. <https://doi.org/10.1007/s00280-015-2920-7>.
15. Meng, F.; Bhupathi, D.; Sun, J. D.; Liu, Q.; Ahluwalia, D.; Wang, Y.; Matteucci, M. D.; Hart, C. P. Enhancement of Hypoxia-Activated Prodrug TH-302 Anti-Tumor Activity by Chk1 Inhibition. *BMC Cancer* **2015**, *15* (422), 1–17. <https://doi.org/10.1186/s12885-015-1387-6>.
16. Peeters, S. G. J. A.; Zegers, C. M. L.; Biemans, R.; Lieuwes, N. G.; van Stiphout, R. G. P. M.; Yaromina, A.; Sun, J. D.; Hart, C. P.; Windhorst, A. D.; van Elmpt, W.; Dubois, L. J.; Lambin, P. TH-302 in Combination with Radiotherapy Enhances the Therapeutic Outcome and Is Associated with Pretreatment [18F]HX4 Hypoxia PET Imaging. *Clinical Cancer Research* **2015**, *21* (13), 2984–2992. <https://doi.org/10.1158/1078-0432.CCR-15-0018>.

Chapter 6

17. Liapis, V.; Labrinidis, A.; Zinonos, I.; Hay, S.; Ponomarev, V.; Panagopoulos, V.; DeNichilo, M.; Ingman, W.; Atkins, G. J.; Findlay, D. M.; Zannettino, A. C. W.; Evdokiou, A. Hypoxia-Activated pro-Drug TH-302 Exhibits Potent Tumor Suppressive Activity and Cooperates with Chemotherapy against Osteosarcoma. *Cancer Letters* **2015**, *357* (1), 160–169. <https://doi.org/10.1016/j.canlet.2014.11.020>.
18. van der Wiel, A. M. A.; Jackson-Patel, V.; Niemans, R.; Yaromina, A.; Liu, E.; Marcus, D.; Mowday, A. M.; Lieuwes, N. G.; Biemans, R.; Lin, X.; Fu, Z.; Kumara, S.; Jochems, A.; Ashoorzadeh, A.; Anderson, R. F.; Hicks, K. O.; Bull, M. R.; Abbattista, M. R.; Guise, C. P.; Deschoemaeker, S.; Thiolloy, S.; Heyerick, A.; Solivio, M. J.; Balbo, S.; Smaill, J. B.; Theys, J.; Dubois, L. J.; Patterson, A. v.; Lambin, P. Selectively Targeting Tumor Hypoxia with the Hypoxia-Activated Prodrug CP-506. *Molecular Cancer Therapeutics* **2021**, *20* (12), 2372–2383. <https://doi.org/10.1158/1535-7163.MCT-21-0406>.
19. Jackson-Patel, V.; Liu, E.; Bull, M. R.; Ashoorzadeh, A.; Bogle, G.; Wolfram, A.; Hicks, K. O.; Smaill, J. B.; Patterson, A. v. Tissue Pharmacokinetic Properties and Bystander Potential of Hypoxia-Activated Prodrug CP-506 by Agent-Based Modelling. *Frontiers in Pharmacology* **2022**, *13*, 1–17. <https://doi.org/10.3389/fphar.2022.803602>.
20. Eckert, A. W.; Horter, S.; Bethmann, D.; Kotrba, J.; Kaune, T.; Rot, S.; Bache, M.; Bilkenroth, U.; Reich, W.; Greither, T.; Wickenhauser, C.; Vordermark, D.; Taubert, H.; Kappler, M. Investigation of the Prognostic Role of Carbonic Anhydrase 9 (CAIX) of the Cellular mRNA/Protein Level or Soluble CAIX Protein in Patients with Oral Squamous Cell Carcinoma. *International Journal of Molecular Sciences Article Int. J. Mol. Sci* **2019**, *20*, 375. <https://doi.org/10.3390/ijms20020375>.
21. Pérez-Sayáns, M.; Suárez-Peñaranda, J. M.; Pilar, G. D.; Barros-Angueira, F.; Gándara-Rey, J. M.; García-García, A. Hypoxia-Inducible Factors in OSCC. *Cancer Letters* **2011**, *313* (1), 1–8. <https://doi.org/10.1016/j.canlet.2011.08.017>.
22. Supuran, C. T. Experimental Carbonic Anhydrase Inhibitors for the Treatment of Hypoxic Tumors. *Journal of Experimental Pharmacology* **2020**, *2020* (12), 603–617. <https://doi.org/10.2147/JEP.S265620>.
23. Ilies, M. A.; Winum, J. Y. *Carbonic Anhydrase Inhibitors for the Treatment of Tumors: Therapeutic, Immunologic, and Diagnostic Tools Targeting Isoforms IX and XII*, 1st ed.; Carbonic Anhydrases: Biochemistry and Pharmacology of an Evergreen Pharmaceutical Target, Vol. 16; Elsevier, 2019; pp 331–365. <https://doi.org/10.1016/B978-0-12-816476-1.00016-2>.
24. Supuran, C. T. Carbonic Anhydrase Inhibitors as Emerging Agents for the Treatment and Imaging of Hypoxic Tumors. *Expert Opinion on Investigational Drugs* **2018**, *27* (12), 963–970. <https://doi.org/10.1080/13543784.2018.1548608>.
25. Nocentini, A.; Supuran, C. T. Carbonic Anhydrase Inhibitors as Antitumor/Antimetastatic Agents: A Patent Review (2008–2018). *Expert Opinion on Therapeutic Patents* **2018**, *28* (10), 729–740. <https://doi.org/10.1080/13543776.2018.1508453>.
26. Anduran, E.; Aspatwar, A.; Parvathaneni, N. K.; Suylen, D.; Bua, S.; Nocentini, A.; Parkkila, S.; Supuran, C. T.; Dubois, L.; Lambin, P.; Winum, J. Y. Hypoxia-Activated Prodrug Derivatives of Carbonic Anhydrase Inhibitors in Benzenesulfonamide Series: Synthesis and Biological Evaluation. *Molecules* **2020**, *25* (10), 2347. <https://doi.org/10.3390/molecules25102347>.
27. Galon, J.; Bruni, D. Approaches to Treat Immune Hot, Altered and Cold Tumours with Combination Immunotherapies. *Nature Reviews Drug Discovery* **2019**, *18*, 197–218. <https://doi.org/10.1038/s41573-018-0007-y>.
28. Huck, B. R.; Kçtznler, L.; Urbahns, K. Small Molecules Drive Big Improvements in Immuno- Oncology Therapies Angewandte. *Angewandte Chemie* **2018**, *57*, 4412–4428. <https://doi.org/10.1002/anie.201707816>.
29. Chen, S.; Song, Z.; Zhang, A. Small-Molecule Immuno-Oncology Therapy: Advances, Challenges and New Directions. *Current Topics in Medicinal Chemistry* **2019**, *19* (3), 180–185. <https://doi.org/10.2174/1568026619666190308131805>.

30. Mpekris, F.; Voutouri, C.; Baish, J. W.; Duda, D. G.; Munn, L. L.; Stylianopoulos, T.; Jain, R. K. Combining Microenvironment Normalization Strategies to Improve Cancer Immunotherapy. *PNAS* **2020**, *117* (7), 3728–3737. <https://doi.org/10.1073/pnas.1919764117>.
31. Geng, Q.; Rohondia, S. O.; Khan, H. J.; Jiao, P.; Dou, Q. P. Small Molecules as Antagonists of Co-Inhibitory Pathways for Cancer Immunotherapy: A Patent Review (2018–2019). *Expert Opinion on Therapeutic Patents* **2020**, *30* (9), 677–694. <https://doi.org/10.1080/13543776.2020.1801640>.
32. Hu, M.; Yang, C.; Luo, Y.; Chen, F.; Yang, F.; Yang, S.; Chen, H.; Cheng, Z.; Li, K.; Xie, Y. A Hypoxia-Specific and Mitochondria-Targeted Anticancer Theranostic Agent with High Selectivity for Cancer Cells. *Journal of Materials Chemistry B* **2018**, *6* (16), 2413–2416. <https://doi.org/10.1039/c8tb00546j>.
33. Riley, R. S.; June, C. H.; Langer, R.; Mitchell, M. J. Delivery Technologies for Cancer Immunotherapy. *Nature Reviews Drug Discovery* **2019**, *18*, 175–196. <https://doi.org/10.1038/s41573-018-0006-z>.
34. Faust, A.; Bäumer, N.; Schlütermann, A.; Becht, M.; Greune, L.; Geyer, C.; Rüter, C.; Margeta, R.; Wittmann, L.; Dersch, P.; Lenz, G.; Berdel, W. E.; Bäumer, S. Tumor-Cell-Specific Targeting of Ibrutinib: Introducing Electrostatic Antibody-Inhibitor Conjugates (AiCs). *Angewandte Chemie - International Edition* **2022**, *61* (1), 1–11. <https://doi.org/10.1002/anie.202109769>.
35. Suskil, M. von; Sultana, K. N.; Elbezanti, W. O.; Al-Odat, O. S.; Chitren, R.; Tiwari, A. K.; Challagundla, K. B.; Srivastava, S. K.; Jonnalagadda, S. C.; Budak-Alpdogan, T.; Pandey, M. K. Bruton's Tyrosine Kinase Targeting in Multiple Myeloma. *International Journal of Molecular Sciences* **2021**, *22* (11), 5707. <https://doi.org/10.3390/ijms22115707>.
36. Riera-Domingo, C.; Audigé, A.; Granja, S.; Cheng, W. C.; Ho, P. C.; Baltazar, F.; Stockmann, C.; Mazzone, M. Immunity, Hypoxia, and Metabolism—the Ménage à Trois of Cancer: Implications for Immunotherapy. *Physiological Reviews* **2020**, *100* (1), 1–102. <https://doi.org/10.1152/physrev.00018.2019>.
37. Greene, M. K.; Chen, T.; Robinson, E.; Straubinger, N. L.; Minx, C.; Chan, D. K. W.; Wang, J.; Burrows, J. F.; van Schaeybroeck, S.; Baker, J. R.; Caddick, S.; Longley, D. B.; Mager, D. E.; Straubinger, R. M.; Chudasama, V.; Scott, C. J. Controlled Coupling of an Ultrapotent Auristatin Warhead to Cetuximab Yields a Next-Generation Antibody-Drug Conjugate for EGFR-Targeted Therapy of KRAS Mutant Pancreatic Cancer. *British Journal of Cancer* **2020**, *123* (10), 1502–1512. <https://doi.org/10.1038/s41416-020-01046-6>.
38. Mohamed Amar, I. A.; Huvelle, S.; Douez, E.; Letast, S.; Henrion, S.; Viaud-Massuard, M. C.; Aubrey, N.; Allard-Vannier, E.; Joubert, N.; Denevault-Sabourin, C. Dual Intra- and Extracellular Release of Monomethyl Auristatin E from a Neutrophil Elastase-Sensitive Antibody-Drug Conjugate. *European Journal of Medicinal Chemistry* **2022**, *229*, 1–11. <https://doi.org/10.1016/j.ejmech.2021.114063>.
39. Tsuchikama, K.; An, Z. Antibody-Drug Conjugates: Recent Advances in Conjugation and Linker Chemistries. *Protein and Cell* **2018**, *9*, 33–46. <https://doi.org/10.1007/s13238-016-0323-0>.
40. Rossin, R.; Versteegen, R. M.; Wu, J.; Khasanov, A.; Wessels, H. J.; Steenbergen, E. J.; ten Hoeve, W.; Janssen, H. M.; van Onzen, A. H. A. M.; Hudson, P. J.; Robillard, M. S. Chemically Triggered Drug Release from an Antibody-Drug Conjugate Leads to Potent Antitumour Activity in Mice. *Nature Communications* **2018**, *9* (1484), 1–11. <https://doi.org/10.1038/s41467-018-03880-y>.
41. Thomas, A.; Teicher, B. A.; Hassan, R. Antibody-Drug Conjugates for Cancer Therapy. *Lancet Oncol.* **2016**, *17* (6), 254–262. https://jamanetwork.com/journals/jama/fullarticle/10.1001/jamaoncol.2019.3552?utm_campaign=articlePDF%26utm_medium=articlePDFlink%26utm_source=articlePDF%26utm_content=jamaoncol.2019.3552
42. de Cecco, M.; Galbraith, D. N.; McDermott, L. L. What Makes a Good Antibody–Drug Conjugate? *Expert Opinion on Biological Therapy* **2021**, *21* (7), 841–847. <https://doi.org/10.1080/14712598.2021.1880562>.
43. Aerts, H. J. W. L.; Dubois, L.; Hackeng, T. M.; Straathof, R.; Chiu, R. K.; Lieuwes, N. G.; Jutten, B.; Weppler, S. A.; Lammering, G.; Wouters, B. G.; Lambin, P. Development and Evaluation of a Cetuximab-Based Imaging Probe

Chapter 6

to Target EGFR and EGFRvIII. *Radiotherapy and Oncology* **2007**, *83* (3), 326–332.
<https://doi.org/10.1016/j.radonc.2007.04.030>.

44. Shi, W.; Li, W.; Zhang, J.; Li, T.; Song, Y.; Zeng, Y.; Dong, Q.; Lin, Z.; Gong, L.; Fan, S.; Tang, F.; Huang, W. One-Step Synthesis of Site-Specific Antibody–Drug Conjugates by Reprogramming IgG Glycoengineering with LacNAc-Based Substrates. *Acta Pharmaceutica Sinica B* **2022**, Article ASAP.
<https://doi.org/10.1016/j.apsb.2021.12.013>.

Summary

Summary

Cancer is one of the main causes of mortality worldwide and today, cancer incidence is still rising. Cancer is a result from the transformation of normal cells through a multi-step process due to genetic mutations occurring during DNA replication each time that a cell divides. The accumulation of these mutations allows these abnormal cells to become aggressive and to develop the ability to adapt to harsh conditions. The different conventional anti-cancer treatment options currently used are surgery, chemotherapy, radiation therapy or hormonal therapy. However, nowadays, cancer research focuses on more specific targeted treatments and immunotherapy with the purpose to reduce adverse effects of the conventional therapies.

Hypoxia is a common feature of solid tumours and is characterised by a very low oxygen content, typically less than 1%. This poor oxygen level contributes to a harsher tumour environment and is associated with poor patient prognosis. Additionally, hypoxia is also known to induce tumour progression and resistance to conventional therapies. Therefore, hypoxia represents an extremely valuable target to be exploited for certain anti-cancer therapy strategies by combining therapeutic payloads with hypoxia trigger moieties in order to allow the drug delivery specifically in the hypoxic tumour environment.

One way of exploiting tumour hypoxia in anti-cancer treatments is to target the hypoxia responsive pathway. HIF-1 α plays a key role in the hypoxic tumour microenvironment. Upon hypoxia HIF-1 α is stabilized, not degraded anymore by ubiquitylation and accumulates therefore in the cell nucleus. This results in the transcription of several genes having a hypoxia responsive element, involved in different mechanisms helping the cells to survive in the hypoxic environment, one of them being carbonic anhydrase IX (CAIX). CAIX is a transmembrane enzyme which catalyses the reversible hydration reaction of carbon dioxide into bicarbonate and a proton. This enzyme is overexpressed in tumours and is associated to an aggressive cancer cell phenotype, to metastasis formation and to poor patient prognosis, which makes CAIX an attractive target for anti-cancer treatment development. So far, only one CAIX inhibitor, SLC-0111, showed promising anti-cancer actions and progressed into clinical trials.

Another way of exploiting tumour hypoxia in anti-cancer therapy is by using hypoxia-activated prodrugs (HAPs). HAPs are mainly composed of a cytotoxic agent coupled to a hypoxia sensitive trigger via a linker. The HAP purpose is to deliver the active drug selectively in the hypoxic environment by undergoing an enzymatic bioactivation in hypoxic tumour cells and to enable the drug diffusion into the surrounding aerobic areas resulting in a bystander effect. Several HAPs have been developed but only few of them reached clinical trials. To date, no HAP compounds have been commercialized yet but several molecules, such as TH-4000 and CP-506 show promising results and are currently being investigated in clinical trials.

In Chapter 3, we describe the design, synthesis and biological evaluations of novel HAP derivatives of benzenesulfonamide CAIX inhibitors. These compounds have been synthesized by combining different hypoxia sensitive bioreducible moieties with two CAIX inhibitors. However, from all tested compounds, only one derivative was efficient in cell viability assays upon anoxic conditions. No cytotoxicity was observed under ambient air, therefore demonstrating a hypoxia selective cytotoxicity. Furthermore, this compound did not show any toxicity or adverse effects in zebrafish toxicity assays. Further biological evaluations on these compounds have not been continued, however, the general HAP strategy described in this work remains of interest for the design and synthesis of other new HAPs.

In Chapter 4, we propose the design and synthesis of nine HAP analogues comprising nitro aromatic groups as hypoxia sensitive trigger and immunotherapeutics as active drug. The poor

water-solubility of certain compounds did not allow biological evaluations, however, viability assessment of one soluble derivative demonstrated that a higher cytotoxicity upon anoxic conditions as compared to normoxic conditions. This, explained by the release of the drug under anoxia, demonstrates the ability of this compound to deliver the drug in hypoxic environment. In order to further improve the hypoxic tumour microenvironment targeting of our HAPs, we describe in Chapter 5 the design of two novel antibody-HAP conjugates. The purpose of this work was to connect to a central molecule, i) a drug, ii) a hypoxia sensitive trigger and iii) a linker to couple a tumour-specific antibody, allowing the targeting and the release of the active drug in the hypoxic tumour environment. We succeeded to synthesize one of the two proposed HAPs and, therefore, we have selected a nitroimidazole group as hypoxia bio-reducible moiety, an immunotherapeutic used previously as drug and a chimeric monoclonal antibody inhibiting the human epidermal growth factor receptor as hypoxia-specific antibody. Unfortunately, despite the different conditions tested to couple the antibody to the HAP, we did not observe antibody conjugation, thus, preventing biological evaluation of the compound.

In conclusion, the results described in this thesis confirm that tumour hypoxia represents an interesting and promising target to be exploited for anti-cancer treatment. The HAP concept aiming to combine an anti-cancer agent with a hypoxia bio-reducible moiety to form a prodrug demonstrated in this work encouraging results to target hypoxia. Furthermore, it remains crucial to select appropriate hypoxia sensitive triggers and drugs depending on important parameters which can impact the final HAP properties, such as its solubility, stability or toxicity. In general, the HAPs currently investigated in clinical trials already showed promising results and may improve anti-cancer therapies and decrease adverse effects of actual treatments.

Résumé

Résumé

Le cancer fait partie des principales causes de mortalité à travers le monde et de nos jours, l'incidence liée au cancer est toujours en hausse. Le cancer résulte de la transformation de cellules saines à travers un procédé comportant plusieurs étapes, causé par des mutations génétiques ayant lieu lors de la division cellulaire, lorsque l'ADN se duplique. L'accumulation de ces mutations permet aux cellules anormales d'adopter un caractère agressif et de développer la capacité de s'adapter à des conditions difficiles. Les traitements anticancéreux conventionnels employés actuellement sont la chirurgie, la chimiothérapie, la radiothérapie ou l'hormonothérapie. Cependant, de nos jours, la recherche contre le cancer se concentre sur l'immunothérapie et le développement de traitements ciblés ayant pour but de réduire les effets secondaires des traitements traditionnels.

L'hypoxie représente une des caractéristiques prédominantes des tumeurs solides directement liée à un faible taux d'oxygène, typiquement inférieur à 1%. Ce faible taux d'oxygène contribue à la formation d'un environnement tumoral complexe et est également associé à un mauvais pronostic chez le patient. Additionnellement, l'hypoxie est aussi liée à la résistance des cellules tumorales ainsi qu'à leur progression face aux thérapies conventionnelles. C'est pour cela que l'hypoxie représente une cible ayant une valeur importante à exploiter pour certaines stratégies thérapeutiques contre le cancer en combinant un agent thérapeutique avec une partie ciblant l'hypoxie afin de permettre la libération de l'agent actif spécifiquement dans l'environnement tumoral hypoxique.

Une des méthodes permettant d'exploiter l'hypoxie dans les traitements contre le cancer vise à cibler les mécanismes de réponse à l'hypoxie. Le facteur HIF-1 α joue un rôle clé dans l'environnement tumoral hypoxique. Sous hypoxie ce facteur est stabilisé, il n'est plus dégradé par ubiquitination et donc s'accumule dans le noyau cellulaire. Cela résulte en la transcription de plusieurs gènes comportant des éléments de réponse à l'hypoxie, impliqués dans différents mécanismes permettant aux cellules de survivre en milieu hypoxique, l'un d'entre eux étant l'anhydrase carbonique IX (CAIX). CAIX est une enzyme transmembranaire qui catalyse la réaction d'hydratation réversible du dioxyde de carbone en bicarbonate et un proton. Cette enzyme est surexprimée au sein des tumeurs et est également associée à un phénotype cellulaire agressif, à la formation de métastases et à un mauvais pronostic chez les patients, ce qui fait de CAIX une cible attractive pour le développement de traitements anticancéreux. Jusqu'à présent, seulement un inhibiteur de CAIX, SLC-0111, a montré des résultats prometteurs en essais cliniques.

Une autre méthode permettant d'exploiter l'hypoxie tumorale dans les thérapies contre le cancer vise à utiliser des prodrogues activables sous hypoxie (HAPs). Les HAPs sont composés majoritairement d'un agent cytotoxique couplé à une molécule sensible en milieu hypoxique via un espaceur. L'objectif d'une HAP est de délivrer sélectivement l'agent actif dans l'environnement hypoxique après avoir subi une bioactivation enzymatique au sein des cellules tumorales hypoxiques, ainsi que de permettre la diffusion de l'agent thérapeutique vers la zone normoxique entourant la tumeur, cela résultant en un effet « bystander ». Plusieurs HAPs ont été développées mais seulement quelques unes d'entre elles ont atteint les essais cliniques. A ce jour, aucune HAP n'a été commercialisée mais différents composés, comme par exemple TH-4000 and CP-506 montrent des résultats prometteurs et sont actuellement évalués en clinique.

Dans nos travaux (Chapitre 3) nous décrivons le design, la synthèse et les évaluations biologiques de nouveaux HAPs inhibiteurs de CAIX dérivés de benzenesulfonamide. Ces composés ont été synthétisés en combinant différentes parties bioréductives sensibles à

l'hypoxie avec deux inhibiteurs de CAIX. Cependant, parmi les composés testés, seulement un dérivé s'est montré efficace en test de viabilité sur cellules sous conditions anoxiques. Aucune cytotoxicité n'a été observée en conditions normoxiques, démontrant une cytotoxicité sélective en hypoxie. De plus, ce composé n'a montré aucune toxicité ou effet secondaire lors de test de toxicité sur zebrafish. Ce composé n'a pas subi d'évaluations biologiques supplémentaires, cependant, la stratégie de synthèse décrite pour former ces HAPs a montré de l'intérêt pour le design et la synthèse de nouvelles prodrogues.

Dans nos travaux (Chapitre 4), nous proposons le design et la synthèse de neuf HAPs comprenant des groupes nitro-aromatiques en tant que partie bioréductible et des agents immunothérapeutiques en tant que drogue. La faible solubilité en milieu aqueux de certains de ces composés n'a pas permis leur évaluation biologique, cependant, les tests de viabilité réalisés sur un des analogues, soluble a démontré une cytotoxicité plus élevée en conditions anoxiques comparée aux conditions normoxiques. Ceci, en conséquence de la libération de la drogue sous anoxie, démontre le potentiel de ce composé à délivrer l'agent actif dans un environnement hypoxique. En vue de continuer à améliorer le ciblage spécifique de l'environnement tumoral hypoxique de nos HAPs, nous décrivons dans le Chapitre 5 le design de deux nouveaux HAPs conjugués à un anticorps. L'objectif de ce travail était de connecter à une molécule centrale, i) un agent actif, ii) une partie bioréductible sous hypoxie et iii) un espaceur afin de coupler un anticorps tumeur-spécifique, permettant le ciblage et le relargage de la drogue dans l'environnement tumoral hypoxique. Nous avons effectué la synthèse d'une des deux HAPs proposées, pour cela nous avons sélectionné un groupe nitroimidazole en tant que partie bioréductible, un agent immunothérapeutique utilisé précédemment comme agent actif, ainsi qu'un anticorps monoclonal chimérique inhibant le récepteur du facteur de croissance épidermique comme anticorps spécifique à l'hypoxie. Malheureusement, malgré les différentes conditions testées afin de coupler l'anticorps à l'HAP, nous pas observé de conjugaison, cela empêchant la réalisation d'évaluation biologique.

Pour conclure, les résultats décrits dans ces travaux de thèse confirment que l'hypoxie tumorale représente une cible intéressante et prometteuse à exploiter en thérapie contre le cancer. Le concept de HAP visant à combiner un agent anticancéreux avec une molécule bioréductible sensible à l'hypoxie afin de former une prodrogue a démontré, dans ces travaux, des résultats encourageants dans le ciblage de l'hypoxie. Additionnellement, il reste crucial de sélectionner des parties bioréductibles et des agents thérapeutiques appropriés dépendant de paramètres importants qui peuvent avoir un impact sur les propriétés du composé final, comme par exemple sa solubilité, sa stabilité ou encore sa toxicité. En général, les HAPs actuellement évaluées en essais cliniques ont déjà montré des résultats prometteurs et pourraient améliorer les thérapies contre le cancer ainsi que diminuer les effets secondaires liés aux traitements actuels.

Impact paragraph

Impact Paragraph

This thesis describes the potential of increasing the efficiency of anticancer treatments such as chemotherapy or immunotherapy, by targeting these therapies specifically towards solid hypoxic tumours. The main purpose of this thesis was to design, synthesize and evaluate the action of therapeutic compounds targeting the hypoxic tumour microenvironment, named hypoxia-activated prodrugs (HAPs), to allow decreasing the adverse effects on normal tissues, the main drawback of currently clinically used anticancer therapeutics. Each year, millions of people die from cancer and its incidence keeps rising, therefore the development of personalized, taking into account the heterogeneity of the disease, anticancer therapies, remains challenging. Nevertheless, the increasing cancer incidence has also severe socio-economic impacts, therefore, the development of novel anticancer treatments remains essential. This impact paragraph will discuss on the novelty, value and relevance for society of the work described in this thesis.

CLINICAL RELEVANCE

Nowadays, cancer therapy is progressing into personalized treatments. Characterisation of the hypoxic tumour microenvironment enables the identification of new biomarkers allowing a better stratification of patients based on their sensitivity to a certain treatment, thus in order to provide a tailored treatment for patients. Carbonic anhydrase IX (CAIX), known to be highly expressed in hypoxic tumours, might be considered, today, as a valuable tumour-specific biomarker associated to poor prognosis for cancer patients. The CAIX inhibitors described in this thesis (Chapter 3) will unlikely be implemented in clinical practice due to limited efficacy. Although the clinical benefits of using CAIX inhibitors for cancer treatment in patients remains to be investigated, so far, only the CAIX inhibitor SLC-0111 progressed into clinical trials for the treatment of advanced, metastatic hypoxic tumours and showed promising preclinical anticancer action.

In addition, the hypoxic tumour microenvironment represents a target for anticancer therapy due to its very low level of oxygen which can be used to selectively activate therapeutics in solid tumours. Hypoxia-activated prodrugs (HAPs) are inactive compounds composed mainly of a therapeutic agent and a hypoxia trigger moiety allowing the release of the therapeutic agent in the (hypoxic) tumour environment. The use of HAPs for anticancer therapy represents a very innovative treatment strategy against solid tumours aiming to specifically target tumour tissues, to increase drug concentration only in tumour and potentially to decrease adverse effects on normal tissues of currently used chemotherapeutic agents (Chapter 2).

Immunotherapy is a promising research field for cancer therapy and, as well, a powerful therapeutic strategy to decrease adverse effects based on the reactivation of the immune system to attack cancer cells through a natural process which is evaded during the tumour progression (Chapter 4 and 5). The immune system is known to provide a rich source of targets for anticancer treatments, however, a better understanding of the patient immune response remains to be investigated in clinical setting.

GAIN FOR SOCIETY

The improvement of anticancer treatment efficacy by targeting hypoxic solid tumours will be beneficial for society in general as the very low level of oxygen is specific to solid tumours. First, since hypoxic tumours show resistance to conventional therapies such as chemo- and radiotherapy, the use of HAPs therapeutics targeting solid tumours for drug delivery can increase the efficacy of anticancer treatments. Secondary, it can allow, as well, a significant decrease of cancer therapy related adverse effects by delivering the active drug only in cancer tissues. Finally, the general treatment costs may also decrease when normal tissue adverse effects caused by standard treatment can be reduced. In general, any benefit in cancer treatment has the potential to be a gain for society.

IMPROVEMENT IN HEALTH CARE

Hypoxia is a characteristic feature present mainly in cancer tissues. This atypical absence of oxygen helps as a specific target of solid tumours for therapy purposes to improve health care as patients will experience less toxic side-effects. During last decades, a large variety of HAPs have been designed and synthesized (Chapter 2, 3 and 4), many of them reached clinical trials and few showed promising results in combination with other anti-cancer agents but definitive conclusions regarding the efficacy of a single treatment can only be drawn after completing clinical trials. This approach can potentially increase the therapeutic window of the anti-cancer therapy and thereby result in an improvement in health care.

Immunotherapy, today, is the most rapidly growing treatment class and has a major impact in oncology (Chapter 4). The idea to use therapeutics to reactivate the immune system in order to fight against tumours represents another therapeutic strategy which aims to decrease treatment side-effects and may show a higher potential combined with HAPs. In the same way, the conjugation of such therapeutics with a tumour-specific antibody would enable a better decrease of normal tissues adverse effects (Chapter 5).

NOVELTY OF THE CONCEPT

The targeting of hypoxic tumour by using HAPs is not a novel concept but it is a growing treatment class which gained a lot of interest by researchers in the last decades. Hypoxia is a potential strategy to target solid tumours due to its specific presence in tumours. Hypoxic solid tumours are characterized an abnormal blood vascularisation development and thereby a very low oxygen content which leads to the inefficiency of conventional chemo- and radiotherapy. By using HAPs therapeutics combining an anti-cancer agent and a hypoxia trigger moiety, targeting specifically hypoxic tumours, the efficacy of conventional treatments may increase (Chapter 3 and 4).

Although HAPs therapeutics targeting specifically hypoxic tumours have been developed for many years, this thesis described a novel dual targeting method based on the antibody-drug conjugation (ADC) (Chapter 5). However, the antibody conjugation described in this thesis did

Impact Paragraph

not work successfully, further exploration on this dual targeting agents may help to design more potent approaches to deliver cytotoxic drugs on hypoxic tumours. Such therapeutic compounds combining a HAP and a tumour specific antibody may improve the tumour targeting and thereby reduce more patient normal tissue adverse-effects.

ROAD TO THE MARKET

The targeting of hypoxia for anti-cancer treatment is a very interesting therapeutic strategy and its expression in solid tumours may be promising for the future market. The research described in this thesis demonstrates promising initial results in the development of HAPs for anti-cancer therapy. Unfortunately, the majority of the therapeutics developed here did not show enough stability to continue towards clinical trials, however, as the HAP concept consisting to connect hypoxia trigger moiety with therapeutic agent showed early promising results, various active drugs could be used following this process in order to obtain different types of HAP having a better stability, suitable to enter into clinicals. To date, no HAPs are on the market yet, but several candidates have been reported so far and are currently investigated in clinical trials.

In general, targeting tumour hypoxia may be clinically relevant, improve health care and provide gain for society. Several approaches have been described in this thesis to improve the targeting of hypoxic tumours with the aim to decrease adverse-effects observed till now with conventional chemotherapy. In addition, the identification of alternative therapeutic targets in cancer remains essential and requires preclinical and clinical research in order to evaluate the influence on health care and estimate a gain for society.

Acknowledgements / Remerciements

Acknowledgements

To my promotion team

Firstly, I would like to thank my promotors. Philippe, thank you for giving me the opportunity to work on this project in collaboration between Montpellier and Maastricht and for giving me the chance to learn and develop new skills in biology. Thank you also for your advices during this PhD.

Jean-Yves, je tiens également à vous remercier pour m'avoir donné l'opportunité de travailler sur ce projet très enrichissant, merci pour votre encadrement et pour m'avoir guidé tout au long de cette thèse.

Ludwig, I didn't spend so much time in Maastricht during my PhD but thank you for your supervision during these 6 months. Thank you for having teaching me how to do biology, for all your explanations in detail about how to set up experiments, for your optimism and positivity and also for your encouragement and advices during the writing period.

To my reading committee

I would like to thank now the members of my assessment committee, prof. Tilman Hackeng, prof. Sébastien Clément, prof. Guido Haenen, prof. Sébastien Thibaudeau and prof. Raivis Zalubovsky for the time to read and assess my thesis.

To the group in Montpellier

Je tiens tout d'abord à remercier le professeur Alberto Marra pour m'avoir accueilli dans son équipe. Je vous remercie pour votre disponibilité, pour vos conseils et bien sûr pour votre patience. Je remercie les docteurs Sébastien Ulrich et Marie Lopez pour les conseils qu'ils m'ont apportés. Merci également à Yannick Bessin et Magalie Lefeuvre pour votre investissement au labo ainsi que pour la bonne ambiance au labo, et merci Magalie de t'être occupée tant de fois de la LCMS. Karine, merci pour ton aide au niveau administratif ainsi que pour la gestion de toutes nos commandes.

Un grand merci aussi aux trois doctorantes avec qui j'ai commencé la thèse et qui m'ont accompagnées tout du long, Alexandra, Maëva et Irene, merci pour votre soutien dans les bons comme dans les mauvais moments. Alexandra, ma voisine de bureau, merci pour ta bonne humeur, pour ton aide quand j'avais besoin de conseils et bien sûr pour tes gâteaux. Maëva, merci pour la bonne ambiance que tu mettais au labo et aussi pour tes gâteaux ! Irene, merci également pour ta bonne humeur et pour tes leçons d'italien au labo.

Je remercie également les post-doc qui se sont succédaient durant ces 3 ans et demi de thèse, Arnaud, Santiago, Esteban, Francesco. Merci pour votre soutien, votre aide mais aussi votre bonne humeur.

Merci à Dandan, Chandramouli, ainsi qu'à tous les étudiants rencontrés pendant ma thèse pour les bons moments partagés au labo et en dehors.

To the group in Maastricht

I would like to thank everyone for the great working atmosphere and your welcome when I arrived, for your inputs and for helping me when I needed advices.

Ala, thank you for your advices and your help sometimes in the lab.

Rianne, thanks a lot for your help in the lab, your time, for having showing me how to do clonogenics and how to use the hypoxic chamber. Natasja, thank you to have been always available when I needed help from you. Thanks also to Kim and Jolanda.

Now I would like to thank all the PhDs of the lab: Jella, Alex, Elia, Joël, Annemarie, Lydie, Anais, Linde, Josselien, Ying, Hester, Shaowen, Yinzhe, Rui and Yanchao. Many thanks to all of you for your welcome in the group and your help in general and in the lab during my stay. It was completely new for me to work in biology, I learned a lot and I really enjoyed to work with you. I wish you the best for your PhD.

Merci à toi Cassandre pour ton aide et tes conseils au labo et aussi en période de rédaction. C'était sympa de discuter avec toi, je te souhaite bonne chance pour la suite. Lorena, thank you advices, it was also nice to discuss with you. Thank you also to the other postdocs for your help.

I would like to thank the students, especially Lesley for your help in the lab and with the hypoxic chamber. Thanks also Carlijn and Vera for the good atmosphere in the lab.

Many thanks also to Ingrid Dijkgraaf, Dennis Suylen and Hans Ippel from the Department of Biochemistry for their inputs in this project. Dennis, thank you for your time and all the analysis you have done for me.

I would like to thank all co-authors of the papers included here for their contributions and in general, all the person which have contributed to this work.

Enfin je voudrais remercier également ma famille, mes amies Mélanie, Céline, Gaelle et Audrey ainsi que tous ceux qui m'ont apporté leur soutien durant ces trois ans et demi de thèse.

Curriculum vitae



Emilie Anduran was born on March 15th 1993 in Auch, France, where she also grew up. After finishing pre-university education in 2011 at the Garros High school in Auch, she started to study chemistry by doing a two year technical degree at the University Institute of Technology of the University of Poitiers (France). There, she obtained her first scientific research experience during an internship at the Institute of Molecular Chemistry of the University of Bourgogne in Dijon (France). In 2015, she completed her bachelor in chemistry at the University of Bordeaux (France) which led to an internship at the Institute of Molecular Sciences of Bordeaux. In 2017, she graduated with a Master degree of Molecular and Macromolecular Chemistry with a specialization in health chemistry, from the same university. She further developed her research skills during two internships, at the School of Chemistry of the University of Manchester (UK) and at the Institute of Molecular Sciences of Bordeaux. Her interest in medicinal chemistry research prompted her to pursue in PhD program in collaboration between the Max Mousseron Biomolecular Institute of the University of Montpellier (France) and the School for Oncology and Reproduction of the University of Maastricht (The Netherlands). Her PhD research focused on the development of hypoxia-activated prodrugs as anti-cancer treatments targeting the hypoxic tumour environment, and these results are described in this thesis.

List of Publications

Anduran E, Cong Y, Suylen D, Dijkgraaf I, Lambin P, Dubois LJ, Winum JY.

Design and synthesis of new hypoxia-activated prodrug antibody-conjugated derivative of the toll-like receptor agonist Resiquimod: a proof-of-concept study to increase tumour uptake.

In preparation

Anduran E, Suylen D, Dijkgraaf I, Lambin P, Dubois LJ, Winum JY.

Design, synthesis and biological evaluations of toll-like receptor 7 & 8 agonist HAP (Imiquimod / Resiquimod) and Bruton's tyrosine kinase inhibitor HAPs (ibrutinib).

In preparation

Anduran E, Dubois L, Lambin P, Winum JY.

Hypoxia-activated prodrug derivatives of anti-cancer drugs: a patent review 2006 – 2020. *Expert Opinion on Therapeutic Patents* 2022, 32 (1), 1-12

Anduran E, Aspatwar A, Parvathaneni NK, Suylen D, Bua S, Nocentini A, Parkkila S, Supuran, CT, Dubois L, Lambin P, Winum JY.

Hypoxia-Activated Prodrug Derivatives of Carbonic Anhydrase Inhibitors in Benzenesulfonamide Series: Synthesis and Biological Evaluation.

Molecules 2020, 25, 2347

Aspatwar A, Parvathaneni NK, Barker H, **Anduran E**, Supuran CT, Dubois L, Lambin P, Parkkila S, Winum JY.

Design, synthesis, in vitro inhibition and toxicological evaluation of human carbonic anhydrases I, II and IX inhibitors in 5-nitroimidazole series.

Journal of Enzyme Inhibition and Medicinal Chemistry 2020, 35 (1), 109-1

